Doctoral Programme

in

Drug Research and Innovative Treatments

Curriculum in Pharmaceutical Sciences

COURSE XXXII

Coordinator Prof. **Elisabetta Teodori**

Settore Scientifico Disciplinare CHIM/08

PhD Candidate
Niccolò Chiaramonte

Supervisor
Prof. ***Maria Novella Romanelli***

Coordinator
Prof. ***Elisabetta Teodori***

Years 2016/2019

"Design, synthesis and preliminary biological evaluation of modulators of metalloenzymes"

Abstract

The present PhD thesis is focused on the chemical applied to synthesize new molecules as modulators of two metalloenzymes: the Carbonic Anhydrases and the Histone Deacetylases. The thesis reports the design, the preparation, the enzymatic activity and, for selected compounds, the in-vivo characterizations of the new molecules, together with the computational and crystallographic studies performed to investigate their binding modes.

The Carbonic Anhydrases (CAs), one of the most efficient enzyme known in nature, evolved in eight genetically different families (α-ι). A large number of isoforms are described among the different organisms, their presence being crucial for pH regulation, secretion of electrolytes and for other essential physiological or pathological processes. For these reasons, CAs are important targets for drugs that can be used for different pathologies, providing that it could be possible to exploit the existent differences between families or isoforms to achieve a selective activity. This may not be an easy task, since the catalytic sites are well conserved, at least among the sixteen human α isoforms (I-XVI); however, variability can be found in hydrophilic and lipophilic accessory sites close to the Zn-binding domain.

The Histone Deacetylases (HDACs) is an enzyme family that plays an important role in epigenetic regulation by removing the acetyl groups from the ε-amino moieties of the lysine side chains either in histones, affecting the DNA superhelix, or in non-histone proteins. Based on their homology, the 18 human HDAC isoforms were divided into four major classes (I-IV): three of them (I, II and IV) are classical, zinc-dependent HDACs whereas class III, called sirtuins, require NAD^+ to function. By removing the acetyl moieties, the HDACs regulate the gene expression mediated by nuclear receptors; an altered control of this process could therefore lead to an abnormal DNA transcription and the manifestation of several diseases such as neurodegenerative pathologies, viral infections and tumors.

Both the inhibition and the activation of some relevant human CA isoforms was investigated in this work of thesis. In particular, from a first series of zinc binders (series I) characterized by a chiral benzylpiperazine scaffold [N. Chiaramonte et al. Eur. J. Med. Chem. (2018), 151, 363-375], two related generations of piperazine-based Carbonic Anhydrases Inhibitors (CAIs) were developed and studied (series II-III) [N. Chiaramonte et al. Bioorg. Chem. (2019), 91, 103130]. As a result of the collaboration with Prof. Bernhard Wünsch of the University of Münster (GE), the preparation of the III series was carried out mainly in Germany.

General structures of the three series of CAs inhibitors

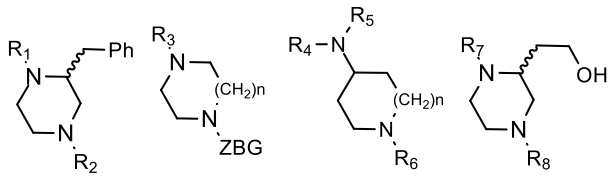

I-A,B series **II-A series** **II-B,C series** **III-A,B series**

ZBG= 4-$COC_6H_4SO_2NH_2$

For the meaning of the R groups, see the second chapter

As far as Carbonic Anhydrase activators (CAAs) are concerned, structural modifications of histamine, the first CAA reported in the literature, and Clonidine led to the generation of two series (V-VI) of positive modulators of this enzyme. Additionally, the CA activation profile of a set of commercially available piperazines (series VII) was also assessed [A. Angeli et al. J. Enz. Inhib. & Med. Chem. (2018), 33,1, 303-308].

General structures of the three series of CAs activators

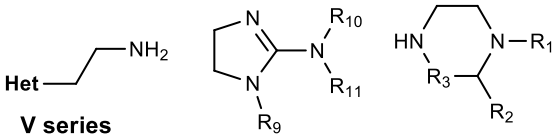

V series **VI series** **VII series**

Het: aromatic 5 membered heterocycle

For the meaning of the R groups, see the second chapter

Through a poly-pharmacological approach, the inhibition of both the CAs and the HDACs was investigated by hybridizing a coumarin moiety (CA inhibitor) with the pan-HDAC inhibitor SAHA (series IV). The contemporary inhibition of these targets could be beneficial in the treatment of several diseases, among which tumors. The biological characterization of these derivatives on some human CAs is described and discussed in this thesis, while the assays against the HDACs are still ongoing.

General structure of the hybrids

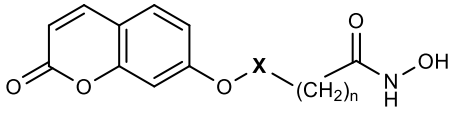

IV series

X= linker, see the second chapter

Summary

1. Introduction 1
1.1 The Carbonic Anhydrases 1
1.2 Human Carbonic Anhydrases 3
1.3 Carbonic Anhydrase Inhibitors 5
1.3.1 Zinc Binders 6
1.3.2 Compounds occluding the entrance of the active site 7
1.4 Therapeutic use of the Carbonic Anhydrase Inhibitors 8
1.4.1 Carbonic Anhydrases Inhibitors as diuretics 9
1.4.2 Carbonic Anhydrases Inhibitors as Antiepileptics 9
1.4.3 Carbonic Anhydrases Inhibitors as anti-glaucoma agents 10
1.4.4 Carbonic Anhydrases Inhibitors as Anticancer 11
1.5 Carbonic Anhydrases Activators 12
1.6 The Histone Deacetylases 13
2. Background and Aim of the Work 16
2.1 Piperazine and Aminopiperidine derivatives as CAs Inhibitors 16
2.2 CAIs-HDACIs hybrids 18
2.3 CAs Activators 19
3. Chemistry 22
3.1 Synthesis of Piperazine and Aminopiperidine derivatives 22
3.2 Synthesis of CA-HDAC hybrids 31
3.3 Synthesis of CA Activators 33
4. Results 37
4.1 Carbonic Anhydrase Inhibition 37
4.1.1 Benzylpiperazines, I-A and I-B series 37
4.1.2 Piperazine and aminopiperidine, II-A, II-B and II-C series 40
4.1.3 Hydroxyethylpiperazines, III-A and III-B series 42
4.1.4 CA-HDAC hybrids 44
4.2 Carbonic Anhydrases Activation 46
4.2.1 Histamine analogues 46
4.2.2 Clonidine analogues 49
4.2.3 Piperazine derivatives 52
4.3 Pharmacological Results 54
5. Computational and X-Ray Analysis 55
5.1 X-ray analysis, I-A and I-B series 55
5.2 Computational studies, I-A and I-B series 57

5.3 X-ray analysis, series II 59
6. Conclusions 63
6.1 Piperazine and Aminopiperdine derivatives 63
6.2 CAIs-HDACs Hybrids 63
6.3 Carbonic Anhydrase Activators 63
7. Experimental Part 64
7.1 Benzylpiperazines, I-A and I-B Series 65
7.2 Piperazines and Aminopiperidine II-A, II-B and II-C Series 72
7.3 Hydroxyethylpiperazines, III-A and III-B Series 79
7.4 CAIs-HDACI Hybrids, IV Series 85
7.5. Carbonic Anhydrase Activators 96
7.5.1 Histamine Analogues, V Series 96
7.5.2 Clonidine Analogues, VI Series 98
8. Bibliography 106

1. Introduction

1.1 The Carbonic Anhydrases

The Carbonic Anhydrases (CAs) are a superfamily of metalloenzymes widespread in all life kingdoms[1,2]. By analysing the sequence of these proteins, CAs were divided into seven phylogenetically different families (α-θ)[3,4] and only recently the eighth ι class was identified in marine phytoplankton[5]. A bivalent metal ion is located in the active site; its presence is fundamental for the catalytic activity as the apoenzyme is devoid of activity, and its nature is variating from family to family[6] (**Table 1.1**).

Table 1.1: distribution and nature of the metal ion among the different CAs families[1]

Family	Distribution	Metal Ion
α	Vertebrates/green plants	Zn^{2+}
β	Fungi/Plants	Zn^{2+}
γ	Bacteria/Archea	$Zn^{2+}/Fe^{2+}/Co^{2+}$
δ	Phytoplankton	Co^{2+}
ζ	Diatoms	Zn^{2+}/Cd^{2+}
η	P. Falciparum	Zn^{2+}
θ	Diatoms	Zn^{2+}
ι	Phytoplankton	Mn^{2+}

The CAs catalyse the simple but at the same time essential reversible hydration of carbonic anhydride (CO_2) to bicarbonate (HCO_3^-) and proton (H^+)[3,7] (**Equation 1.1**). CO_2 is the final oxidized product of almost all the metabolic pathways[8] and, since its uncatalyzed conversion to HCO_3^- is too slow, the Carbonic Anhydrase activity is essential to fulfil the metabolic needs connected to this equilibrium[9]. The optimal balance between these ions is fundamental for the successful flow of several biochemical processes[10] and this is ensured by the extremely efficient activity of the CAs, enzymes with a turnover number (K_{cat}) that can reach the value of 10^6 s^{-1} [11].

Equation 1.1

$$CO_2 + H_2O \overset{CA}{\rightleftharpoons} HCO_3^- + H^+$$

Despite the genetic differences, the active site cavity is similar among the families. The catalytic metal ion is located at the bottom of this cavity and it is kept in the optimal position by the coordination of three amino acid residues[1,3]. The coordination bonds are completed by a water molecule and the four interactions are structured in a tetrahedral geometry. Three histidine (His) residues are coordinating the zinc ion in α-, γ-, δ-CAs; one His and two

cysteine (Cys) in β-, ζ-CAs; one His, one glutamine (Gln) and two His in η-CAs[12]; one His, one Cys and one aspartate (Asp) in θ-*CAs*[13] while is still not well understood the architecture of ι-CAs[5]. All the existing families follow a two-steps catalytic mechanism in which the coordinated water molecule, "activated" as hydroxide anion, attacks the CO_2 molecule bound in a small hydrophobic pocket located closely[14]. Using the α-CAs active site as example, the catalytic cycle is reported in **figure 1.1:** the catalytically active hydroxide ion **[A]** behaves as strong nucleophile on the carbonic anhydride molecule **[B]** leading to the bicarbonate-bound transition state **[C]**. A water molecule is then displacing the HCO_3^- leading to the catalytically inactive form of the enzyme **[D]** that is then reactivated through the proton transfer[1–3]. The regeneration of the hydroxide ion (reported as step **(d)** in **figure 1.1** is the rate limiting one[15] and the proton transfer to the external buffer is mediated by a cluster of histidine residues among which His64 is playing central role[16] (the residues are numbered taking hCA II as reference). This is residue is indeed called the "proton shuttle" providing an efficient pathway for the transfer of protons between the active site and the external medium, the site specific mutagenesis of this residue is leading to kinetic defect mutants[15,16].

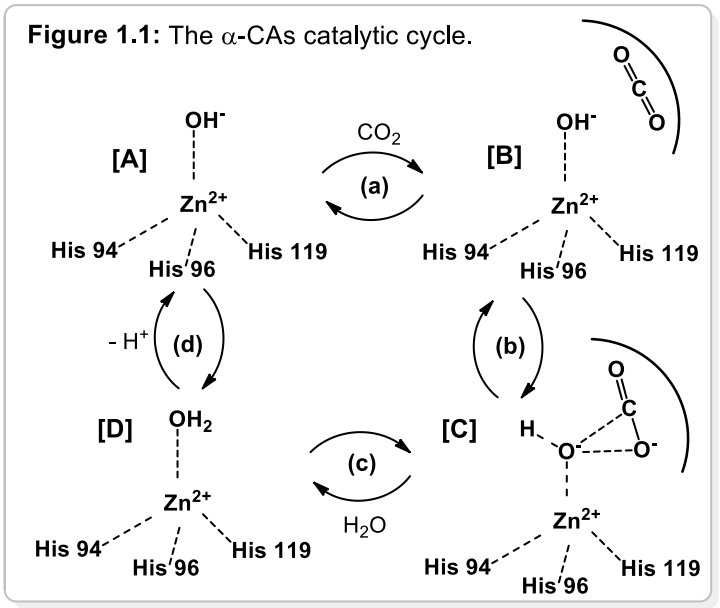

The convergent evolution of these enzymes led to another fundamental common characteristics, the "bipolar" nature of the active site[17]. By maintaining the balance among the slightly hydrophobic gas CO_2 and the two highly soluble ions HCO_3^- and H^+, the Carbonic Anhydrases developed a catalytic site divided in two halves of opposite nature: a hydrophilic and a hydrophobic one[1,17] (**Figure 1.2**)[18]. The widest accepted hypothesis is that the lipophilic portion is needed to entrap and stabilize the carbonic anhydride molecules while the other one is fundamental to solvate and release the hydrated products.

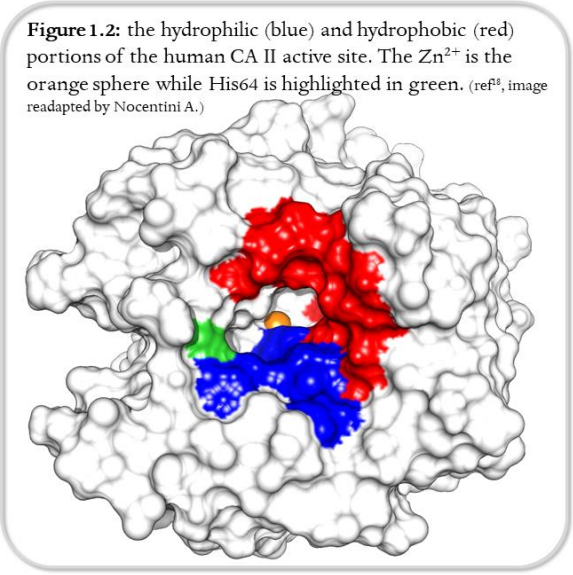

Figure 1.2: the hydrophilic (blue) and hydrophobic (red) portions of the human CA II active site. The Zn^{2+} is the orange sphere while His64 is highlighted in green. (ref[8], image readapted by Nocentini A.)

1.2 Human Carbonic Anhydrases

The human Carbonic Anhydrases (hCAs) belong to the α-family and fifteen isoforms were isolated so far[9]. The hCAs are indicated with roman numbers (I-XV) and substantial differences in efficiency were reported for the 12 are catalytically active isozymes (**Table 1.2**). The various isoforms are expressed in different body tissues where are deeply involved in several homeostatic processes[10].

Table 1.2: distribution and principal characteristics of the hCAs[1]

Isoform	Catalytic activity	Organ/Tissue	Subcellular localization	Structural Features
hCA I	Low	Erythrocytes, Eye	Cytosol	Monomeric
hCA II	High	Widespread		
hCA III	Very Low	Skeletal muscles, adipocytes		
hCA IV	Medium	Kidney, brain, eye	Membrane-associated	
hCA VA	Low	Liver	Mitochondrion	
hCA VB	High	Heart, kidney, pancreas		
hCA VI	Low	Salivary and mammal glands	Milk/saliva	Dimeric
hCA VII	High	Brain	Cytosol	Monomeric
hCA IX	High	Tumors, intestinal mucosa	Membrane-associated	Dimeric
hCA XII	Low	Tumors, reproductive epithelia		
hCA XIII	Low	Kidney, brain, lung	Cytosol	Monomeric
hCA XIV	Low	Brain, liver, eye	Membrane-associated	

Beside the differences of catalytic efficiency, the active site architecture is very well conserved among the isoforms. His94, His96 and His 119 are always the three Zn^{2+}-

coordinating residues and the metal bound water molecule is kept in the optimal position by an important interaction with threonine 199 (Thr) and an additional one with another water molecule, called Deep Water (**DP** in **figure 1.3**)[9,11,19]. The lipophilic pocket, delimitated by valine (Val) 121 and 143, leucine (Leu) 198 and tryptophan (Trp) 209, is highly conserved too and another well-maintained key residue is phenylalanine (Phe) 131, a bulky lipophilic amino acid placed in the middle the hydrophobic cavity[3].

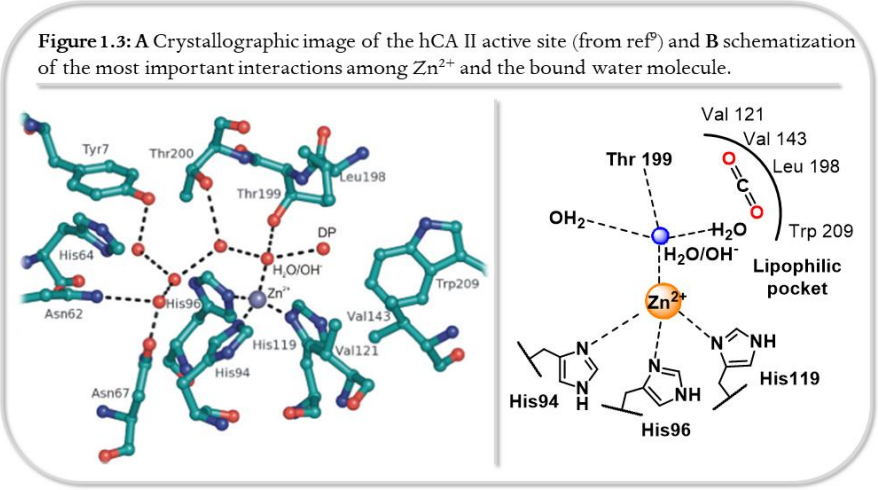

Figure 1.3: A Crystallographic image of the hCA II active site (from ref[9]) and **B** schematization of the most important interactions among Zn^{2+} and the bound water molecule.

Due to their wide abundance and to the important equilibrium they are regulating, the human isozymes are actively participating to several physiological processes and biosynthetic reactions[9,10]:

- the pH regulation, providing the bicarbonate and protons fundamental for the pH homeostasis;
- the electrolyte transportation, providing the H^+ used by the sym/antiporter or pumps;
- the CO_2 excretion in lungs;
- the aqueous humour secretion in eyes, rich of bicarbonate;
- the secretion of gastric fluid, cerebrospinal liquid and pancreatic juice
- the lipogenesis, the novo gluconeogenesis and the urea biosynthesis.

An altered functionality or expression of these enzymes could therefore lead to the outbreak of pathologic conditions, some of them will be mentioned in the following chapters.

1.3 Carbonic Anhydrase Inhibitors

The inhibitory modulation of the Carbonic Anhydrases it is nowadays a well-known process and several advances were done since Acetazolamide came into medical use in 1952[20]. The Carbonic Anhydrases Inhibitors (CAIs) belong to several different chemical classes and can be divided into five categories according to their inhibition mechanism[21]:

a) **Zinc binders**, i.e. compounds that chelate the bivalent metal ion of the active site, interrupting the coordination of the water molecule/hydroxide ion and consequently the enzymatic activity[21–23]. The mechanism is schematized in **figure 1.5A** and the crystallographic image of one of our inhibitor in reported in **figure 1.5B**[24]. The scaffold of these molecules may interact with one or both halves of the active site, stabilizing the interaction with the ion in a tetrahedral geometry. This is the most important class of inhibitors, to which belongs sulfonamides and their isosteres (sulfamates or sulfamides), dithiocarbamates, hydroxamate, etc[1,21]. Sulfonamides are the most studied CAIs with at least 20 compounds in clinical use for decades[21]. Some examples (Acetazolamide, Brinzolamide and Dorzolamide) are shown in **figure 1.4**.

b) Compounds that **anchor to the zinc-coordinated water molecule/hydroxide ion**, such as phenols and polyamines[1,21,25].

c) Compounds **occluding the entrance of the active site** (coumarins and their isosters) [1,21,26].

d) Compounds that **bind out of the active site**, such as 2-(benzylsulfonyl)benzoic acid [21,27].

e) CAIs acting **without a known mechanism**; such as secondary/tertiary sulfonamides, imatinib,etc[1,21].

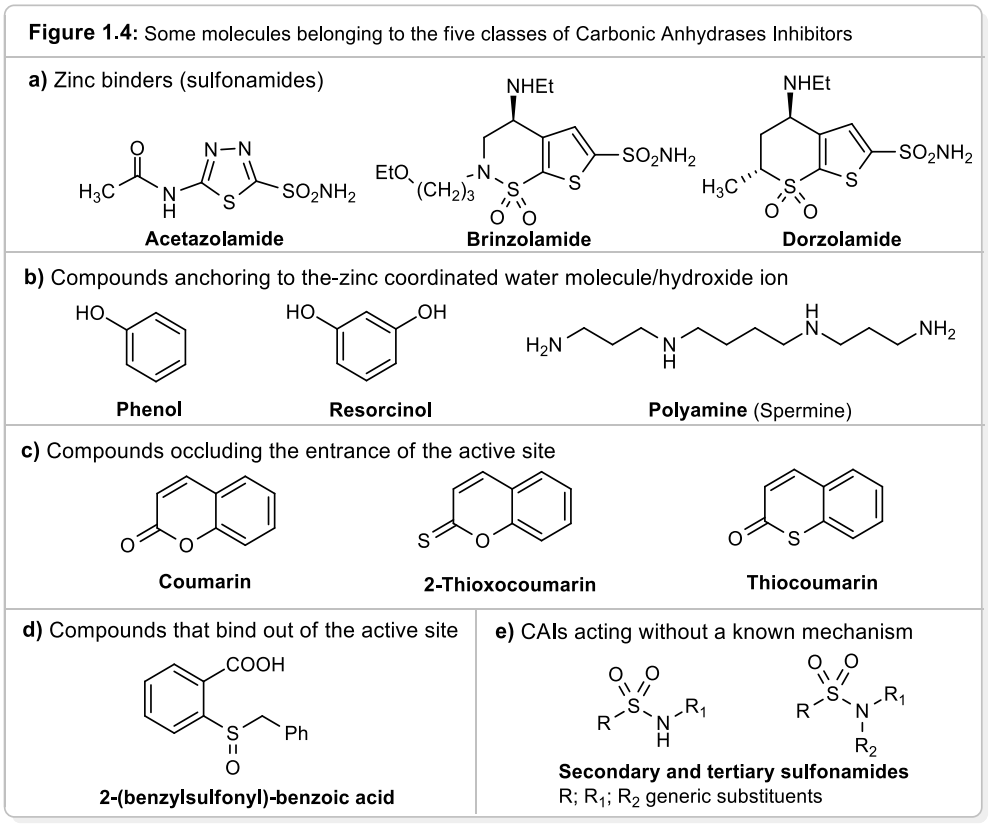

For their prominent role in this thesis, the following two sections will be only focused on **Zinc Binders** and on **Compounds that occlude the entrance of the active site**.

1.3.1 Zinc Binders

Sulfonamides and their isosters are the most important class of zinc-chelating agents and they include compounds in clinical use for decades with several different therapeutic applications[28]. This class of inhibitor is characterized by the presence of a chemical moiety, called Zinc Binding Group (ZBG), able to chelate the metal ion with a tetrahedral geometry, substituting the bound water molecule[1,21]. The ZBG is usually a weak acid that is normally deprotonated at physiological pH, therefore performing the metal chelation as anion. Several crystallographic images of zinc binders in CAs active site are nowadays available[29,30] and sulfonamides are without any doubt the widest studied class. As is possible to appreciate from the schematization reported in **figure 1.5A**, the tetrahedral geometry of the adduct is further stabilized by two additional hydrogen bonds among the deprotonated sulfonamide and two maintained amino acid: Thr 199 and glutamate (Glu) 106. These two residues are called "*gate keepers*" for their importance in controlling the access to the active site[21]. **Figure 1.5B** reports the test compound *(S)* **I-B4** bound into hCA I active site; the tetrahedral binding

geometry among the zinc (grey sphere) and the sulfonamide reported in yellow could be noticed in the centre of the image.

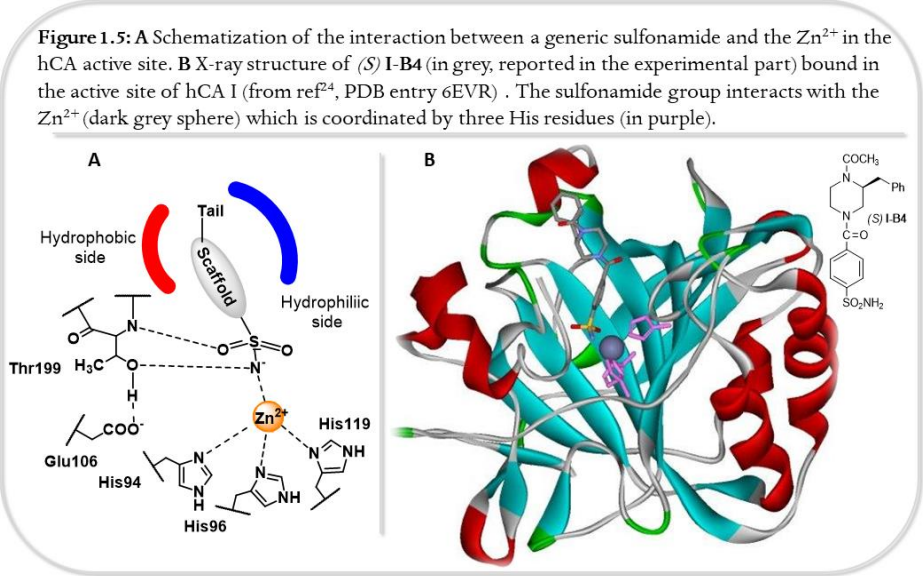

Figure 1.5: A Schematization of the interaction between a generic sulfonamide and the Zn^{2+} in the hCA active site. **B** X-ray structure of *(S)* **I-B4** (in grey, reported in the experimental part) bound in the active site of hCA I (from ref[24], PDB entry 6EVR) . The sulfonamide group interacts with the Zn^{2+} (dark grey sphere) which is coordinated by three His residues (in purple).

Zinc binders are usually potent inhibitors but, since the architecture of the catalytic site is very well conserved among the human isozymes, they are not able to discriminate between the hCAs isoforms, leading to the main drawback of this class of inhibitors: a general lack of selectivity[17,31]. Importantly, the ZBG could also be able to interact with all the metal factor of several other proteins: i.e. aminopeptidase, matrix metalloproteinase, etc… Several strategies were investigated in order to try to overcome these issues and one of the most studied is the so called "tail approach"[21–23,32]. This strategy is based on the structural modification of a portion on the inhibitor (**Tail** in **figure 1.5A**), usually in a position not fundamental for the Zn-chelating activity, that could potentially interact with the regions surrounding the active site, where the amino acids variability is higher. In particular, the chemical characteristics of the tail or even of some portions of the scaffold could be modulated to take advantage of potential accessories interactions with one of the halves of the catalytic site. Another usual problem of the zinc binders is the low water solubility[21], a fundamental property to reach the therapeutic concentrations and consequently the target. The "tail approach" was again used to overcome this issue by adding water solubilizing moieties like amino acids[33] or sugars to the inhibitor scaffold.

1.3.2 Compounds occluding the entrance of the active site

The discovery of this class of compounds started in 2008 from then screening of a series of natural products on bovine CAs[34]. Surprisingly, Vu H. et al. noticed that some coumarin derivatives were inhibiting the enzyme. As coumarins obviously lack the ZBG of classical CAs inhibitors, further investigations begun in order to understand the action mechanism. In two related papers Maresca A. et al.[26,35] deciphered the "mystery" demonstrating the non-classical action of these products. The research group demonstrated that through its weak esterase activity[1,3], the Carbonic Anhydrase was hydrolysing the coumarin lactone to Z-2-hydroxycinnamic acid, afterwards in equilibrium with its E isomer (**Figure 1.6**), the responsible for the inhibitory activity. Coumarins and their isosters are therefore prodrugs directly activated by the enzyme[35]. Through x-ray analysis (**Figure 1.7B**), Maresca's group observed that after the hydrolysis the cinnamic derivative was binding almost at the entrance of the active without any direct interaction with the zinc ion (schematization in **figure 1.7A**). An important characteristic of this inhibition mechanism is that the entrance of the cavity is one of the most variable region among the different human isoforms, coumarins could therefore overcome the selectivity issues of the zinc binders[21] and, interestingly, these derivatives showed a preferential inhibition of the two membrane associated and cancer-related isoforms hCA IX and XII[8].

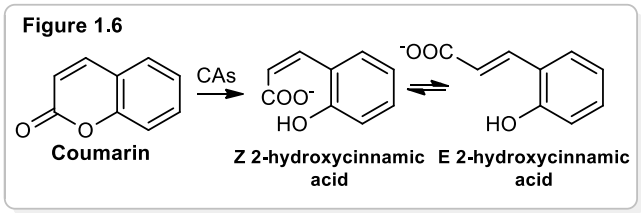

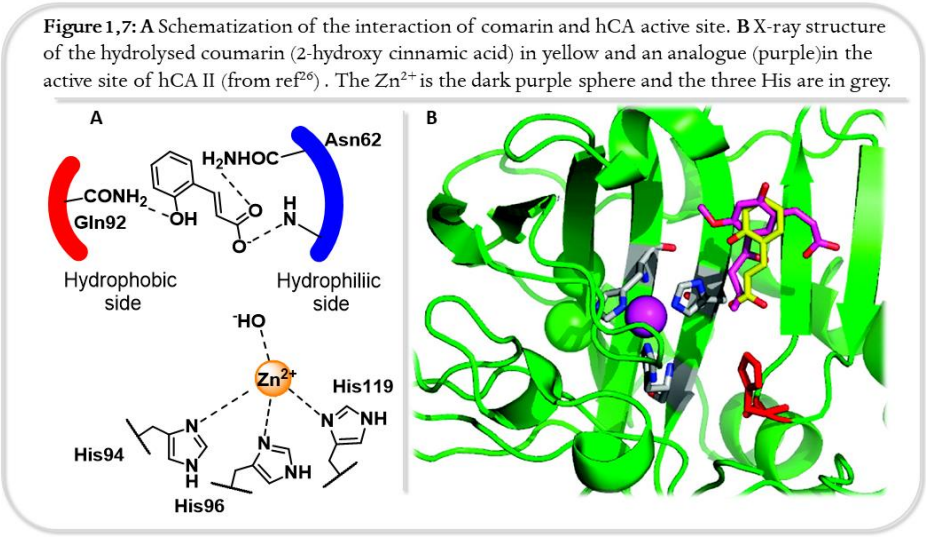

Figure 1,7: A Schematization of the interaction of comarin and hCA active site. **B** X-ray structure of the hydrolysed coumarin (2-hydroxy cinnamic acid) in yellow and an analogue (purple)in the active site of hCA II (from ref[26]) . The Zn^{2+} is the dark purple sphere and the three His are in grey.

1.4 Therapeutic use of the Carbonic Anhydrase Inhibitors

In this paragraph some of the pharmacological uses of the CAIs as well as some of the more promising potential future applications will be analysed. Some other potential applications of CAs Inhibitors are: as anti-obesity drugs, anti-osteoporosis agents and in the treatment of altitude sickness.

1.4.1 Carbonic Anhydrases Inhibitors as diuretics

The six renal identified isoforms (i.e. hCA II, IV, VB, IX, XII and XIV)[1,6,36] are strictly involved in some crucial processes, such as:

- the proton excretion in the proximal tubule;
- the bicarbonate reabsorption in the proximal and distal tubules;
- the urea excretion in the distal tubule and in the collecting duct.

Acetazolamide (**Figure 1.4**), as well as other related analogue like methazolamide and ethoxzolamide (**Figure 1.8**), was among the first non-mercurial diuretics used in therapy[6] but nowadays better drugs like the thiazides are available for this therapeutic application. The use of CAIs as diuretics is now limited to treat oedema, caused by heart failure or drugs[6,37]. As a matter of fact, the administration of CAIs leads to an alkalinisation of the urine caused by a decreased bicarbonate reabsorption and a progressive metabolic acidosis which is detrimental for the activity of the CAIs itself.

Figure 1.8

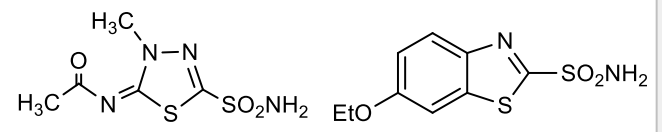

Methazolamide **Ethoxzolamide**

The discovery of the diuretic activity of CAIs was undoubtedly a key step for this class of pharmacological agents since from their structure manipulation derived many effective drugs. Nowadays, due to the development of several safer and more effective agents the use of CAIs as diuretics is limited to particular cases.

1.4.2 Carbonic Anhydrases Inhibitors as Antiepileptics

Seizures constitutes one of the most common neurological disorders in clinical medicine and one of the identified etiologic factors is the rapid change in ionic composition due to altered regulations in neurons[38]. Dysfunctions in excitatory/inhibitory receptors like the glutamatergic or GABAergic or in ion channels (Na^+, Ca^{2+}) is indeed leading to electrolyte unbalances and consequently to distorted excitability in the central nervous system. Additionally, decreased CO_2 concentrations in the brain were also linked to an altered neuron firing and seizure propensity[39]. The anticonvulsant effect of CAIs was noticed in the early 1960 with Acetazolamide and Methazolamide and intensively studied[39,40]. A decreased excitability in neurons was associated with the administration of these drugs but, unluckily, they did not provide a long-term effect in patient with epilepsy. Nowadays, Acetazolamide is still used only in some epileptic forms resistant to other drugs. On the other hand, two other CAIs Topiramate and Zonisamide (**Figure 1.9**) are highly effective and therefore widely used in therapy. Topiramate is a strong pan-hCAs inhibitors with K_i values in the nanomolar range while Zonisamide is a weaker inhibitor.

These drugs have a broad activity spectrum since they are able to potentiate also the GABAergic transmission, to inhibit the Na^+ and Ca^{2+} channels and interact with the pre-synaptic release of glutamate. The inhibition of the central hCAs could therefore give a contribution to the anticonvulsant effect but, surely, it is not the only mechanism[41,42].

Figure 1.9

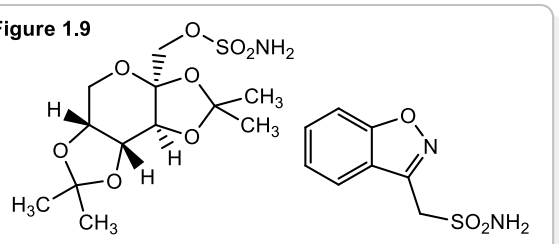

Topiramate Zonisamide

1.4.3 Carbonic Anhydrases Inhibitors as anti-glaucoma agents

Glaucoma is a group of multifactorial diseases involving the optic nerve that could lead from a progressive peripheral visual field loss to complete blindess[43]. The only known treatment that retard its development is the Intra Ocular Pressure (IOP) lowering. Two of the processes that, when altered, could give a contribution to the IOP increment are a massive aqueous humour secretion by epithelial cells or a poor outflow through the Schlemm's canal[43]. The hCAs isoforms II, IV and XII are the main actors in the bicarbonate production, the main constituent of aqueous humour[44]. The anti-glaucoma agents are usually topically administered as eye drops and they include prostaglandin analogues, β-adrenoreceptors antagonist, α- adrenoreceptors agonists, cholinergic agonists, Carbonic Anhydrase Inhibitors and the recently approved class of drugs: the Rho-kinase inhibitors[45]. CAIs, that could be rarely administered systemically, are among the first therapeutic choices and pharmaceutic preparations based on salts of Dorzolamide (Trusopt®) or Brinzolamide (Azopt®) are among the most used (**Figure 1.10**). By inhibiting the ocular hCAs, these drugs actively reduce the aqueous humour formation and consequently the IOP. Several new potential anti-glaucoma agents were studied in the last years and the main challenges were related to the typical low water solubility of sulfonamides. In addition, many efforts were done to overcome the drawback of the rapid clearance from the ocular surface that is leading to multiple daily administration but most of them were focused on the development of new formulations of the already approved drugs Dorzolamide and Brinzolamide[44].

Due to the complex etiology of this ocular disease and the different ways in which it could develop, the therapy with CAIs is only one of the effective available treatments. The efficacy they showed is anyway an encouraging starting point to develop new CAIs endowed with better pharmacokinetic properties or higher potency.

Figure 1.10

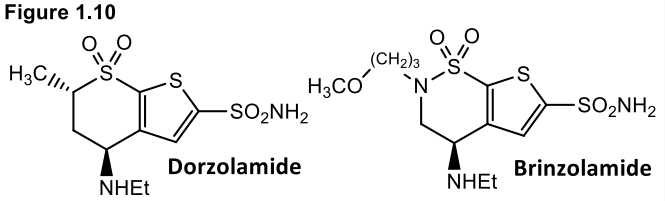

1.4.4 Carbonic Anhydrases Inhibitors as Anticancer

One of the most investigated potential application of the Carbonic Anhydrase Inhibitors is undoubtedly as antitumor drugs. The rationale behind that, is the demonstrated overexpression of the two membrane-associated hCA IX and XII in some types of cancer[46]. In particular, a massive presence of these two isoforms was noticed in hypoxic tumors[8]. Hypoxia is originated from insufficient oxygen supply by the vasculature that, due to the abnormal growing process of cancer cells, is unable to fulfil the O_2 demand[47]. Hypoxia is a key component in cancer progression and is often associated with a more aggressive tumor phenotype because hypoxic cells are more resistant to ionizing radiation and chemotherapy, leading to a more probable therapeutic failure. The hypoxia-inducible factor (HIF) is the main transcriptional effector of this cancer adaptive response that, by activating a intracellular cascade[48], is then increasing the expression of proteins like the transporters for glucose, lactate and ions, glycolytic enzymes, pro-angiogenic growth factors and even some receptors[47]. Importantly, the massive proliferation of cancer cells is always associated with an increased need of energy and nutrients that is therefore leading to an altered metabolism and an overproduction of acid metabolites, such as lactate, protons and CO_2. These molecules could be accumulated inside the cancer cells, leading to pH lowering and intracellular acidosis. The preventing process that tumor cells are carrying out, mainly through HIF cascade, includes the activation of ion-exchangers (pump and transporters), among which the one for bicarbonate[49]. This mechanism re-establish a slightly alkaline intracellular pH while, on the contrary, results in a extracellular acidosis that is even harmful for the proximal healthy cells[47] (**Figure 1.11**).

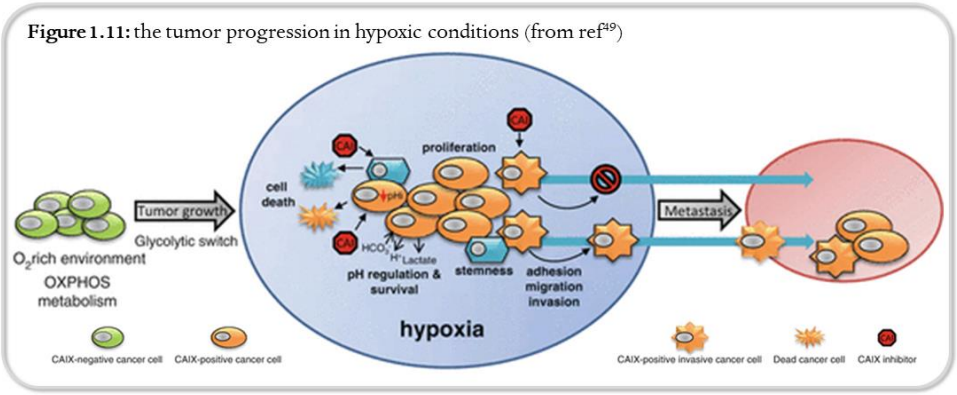

Figure 1.11: the tumor progression in hypoxic conditions (from ref[49])

In the management of acidosis by cancer cells, a central role is also played by hCA IX and hCA XII. These dimeric isoforms are among the most efficient and possess an extracellular catalytic site[8,50]. As a matter of fact, by actively hydrating CO_2, the hCA IX and XII generate

the bicarbonate ions that will be transported inside the cells to balance acidosis[51], their pivotal role in this process was demonstrated by Pastorekova S. et al.[52]. Therefore, the development of small molecules that selectively inhibit these two isoforms is extremely interesting and many efforts were done in the last decades. Several classical zinc binders were synthesized and some of them were designed with the tail approach but, despite some derivatives achieved a good selectivity[51] against these isoforms, there is still only one sulfonamide in the clinical trials: SLC-0111[53,54] (**Figure 1.12**). Although they showed very interesting preliminary results, neither coumarins led to approved drugs. Their inhibition preference for hCA IX and XII strongly encouraged the development of new derivatives and new classes of CAIs were detected starting from this investigation[55] (some of them are reported in **figure 1.12**). Another relatively new approach to target these isoforms is the development of specific monoclonal antibodies, a strategy that already showed promising results[51,53].

The overexpression of hCA IX and XII and their preeminent role of in cancer progression is nowadays extensively recognised. The inhibition of these isozymes could therefore represent a key strategy in the treatment of some aggressive cancer types or to improve the efficacy of other co-administered chemotherapeutics. The bullet to appropriately hit these targets is still undiscovered but the promising indications already obtained are encouraging its research.

Figure 1.12

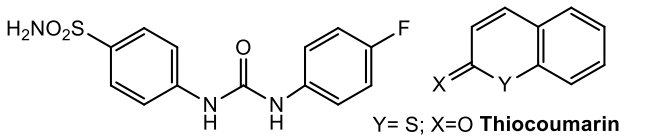

SLC-0111

Y= S; X=O **Thiocoumarin**
Y=O; XS; **2-Thioxocoumarin**
Y=S; X=S **Dithiocoumarin**

1.5 Carbonic Anhydrases Activators

If CAs inhibitors are widely used in therapy and many information were collected since decades, on the contrary the possibility to activate these enzymes was first reported in 1940 by Leiner[56] and demonstrated only recently[15,16]. The activator binds in a different region of the catalytic site with respect to the inhibitors but, thanks to the formation of a quite stable complex with the enzyme, is able to increase its turnover number (k_{cat}). Most of the compounds with activator properties are small polar molecules that create a pattern of hydrogen bonds with some protic residues of the active site that are actively participating in the rate-determining step of the catalytic cycle: the proton removal from the coordinated water molecule. In such a way, Carbonic Anhydrase Activators (CAAs) are able to increase the efficacy of the proton transfer behaving like the natural proton shuttle residue His64. The schematized mechanism is reported in **equation 1.2** and the steps in parenthesis represent the formation of the complex with the enzyme and the proton transfer to the activator[15].

Equation 1.2

$$Zn^{2+}\text{-}OH_2 + A \rightleftharpoons [Zn^{2+}\text{-}OH_2\text{-}A] \rightleftharpoons [Zn^{2+}\text{-}OH^-\text{-}AH^+] \rightleftharpoons Zn^{2+}\text{-}OH^- + AH^+$$

Zn^{2+}: catalytic zinc; A: activator

Interestingly, the activator-binding site was precisely localized in a region quite far from His64 but strictly connected to this residue through a network of water molecules. Histamine (HST) was the first molecule with activator properties discovered and its framework of interactions in the CAs active site will be discussed in the "Background and Aim of the Work" part of this thesis (chapter 2). Many other molecules were then studied and activator effects were then reported for several amines, amino acids and other bioactive molecules like dopamine or adrenaline[57] (**Figure 1.13**).

Figure 1.13: some of the natural molecule with CAs activator properties

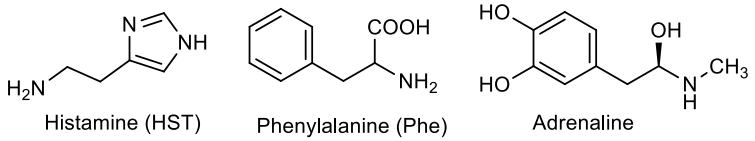

Histamine (HST) Phenylalanine (Phe) Adrenaline

Since the Carbonic Anhydrases are very efficient enzymes, their activation was initially considered the result of an experimental artifact[58] and anyway "not so important". But since deficiencies of some human isozymes were observed in several pathologic conditions (retinal problems, hyperammonemia, …[15]), the interest on CAAs grew intensively. The few information we still have about the role played by the hCAs in these diseases are affecting the application of CAAs as therapeutic agents but many ongoing projects are focused on this problem. Some other potential applications will be discussed in chapter two again.

The interest on the therapeutic applications of the Carbonic Anhydrase Activators grew a lot in the last years but, beside the encouraging preliminary results, many efforts will be needed to further investigate the utility of these molecules as pharmacological agents.

1.6 The Histone Deacetylases

The Histone Deacetylases (HDACs) is an enzyme family that plays an important role in epigenetic regulation. Their main role is to remove the acetyl groups from the ε-amino moieties of the lysine (Lys) side chains in histones.

Histones are alkaline proteins widespread in eukaryotic nuclei whose presence is fundamental for the DNA packaging[59]. Histones are the central core for the so called "nucleosome", the first level of chromatin organization composed by eight histone units that are constituting the backbone for the DNA, wrapped around it[60]. Histones are directly affecting the DNA superhelix and from their interaction depend the DNA folding[61]. Importantly, these proteins are rich of basic lysine and arginine residues whose side chains

are able to create salt bridges and hydrogen bonds with the phosphate oxygens of DNA, compacting the deoxyribonucleic acid. An increased DNA-histone binding is therefore leading to a condensed structure that is preventing the activity of the polymerases and the DNA-transcription. The histones contain a high number of sites that can be subjected to post- translational modifications, such as acetylation, methylation or phosphorylation, that influence the charge of the amino acid tails and affect the chromatin through electrostatic interactions[62]. The acetylation of the Lys residues is an essential part of gene regulation. By masking the positive charge of the Lys side chains, the acetylation is resulting in a relaxed chromatin and an increased DNA transcription.

Based on their homology, the 18 human HDAC isoforms were divided into four major classes (I-IV): three of them (I, II and IV) are called classical Histone Deacetylases and are zinc-dependent enzymes whereas class III HDACs are called sirtuins and require NAD^+ to function[63]. The class I includes HDAC 1,2,3 and 8; the class IIA includes HDAC 4,5,7 and 9; the class IIB is composed by HDAC 6 and 10 and finally class IV comprises only HDAC 11. Most of them are only distributed in the nucleus while others are able to move in and out the nucleus itself to activate intracellular cascades. By removing the acetyl moieties, the HDACs regulate the gene expression mediated by nuclear receptors. An altered control of this process could therefore lead to an abnormal DNA transcription and an overexpression of these enzymes was associated with the development or manifestation of several diseases: neurodegenerative pathologies, viral infections among which HIV, and tumors[64].

Histone Deacetylase Inhibitors (HDACIs) are considered to be among the most promising drugs to be developed for cancer therapy due to the main role of these enzymes in tumorigenesis[65]: the treatment of several tumor cell-lines with HDACIs results in growth arrest, differentiation and apoptosis. The first non-selective HDACI Suberoylanilidine Hydroxamic Acid (SAHA) was approved in 2006, then three other HDAC-targeting anticancer agents came into therapy (**Figure 1.14**) for the treatment of various cancers (i.e. leukemia, lymphomas). Unfortunately, these pan-HDACIs are not able to discriminate among the isoforms and could therefore produce serious side effects that limits their utility. The development of isoform selective HDACIs to enhance tolerability will be a priority in the next years.

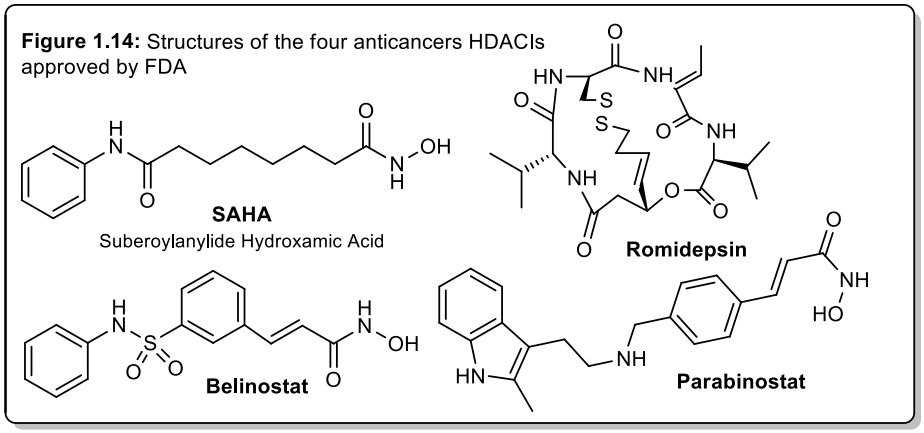

Figure 1.14: Structures of the four anticancers HDACIs approved by FDA

From a structural point of view, the HDACs Inhibitors are generally characterised by three portions:

- a Zinc Binding Group that is chelating the Zn^{2+} ion;
- an aromatic portion called "Cap";
- a linker connecting the two parts together

The three portions are highlighted in **figure 1.15** using the **SAHA** structure as example.

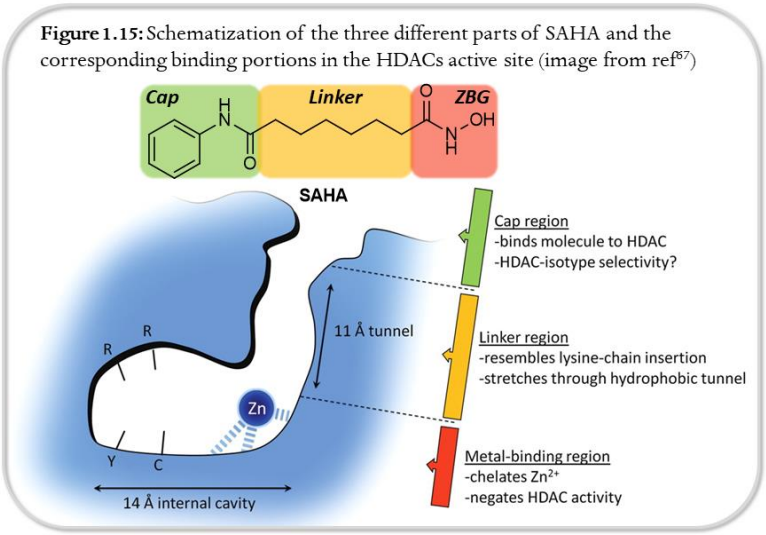

Figure 1.15: Schematization of the three different parts of SAHA and the corresponding binding portions in the HDACs active site (image from ref[67])

While the pharmacophore ZBG is interacting with the bivalent metal, the two other portions are binding to side regions of the active site that stabilize the interaction. These accessories bonds were deeply analysed in order to investigate if they may be able to affect the isoform selectivity, interestingly a high amino acid variability among the isozymes was individuated in the Cap-binding site (**Figure 1.15**[66]). For this reason, both the capping group and the length and the polarity of the linker were extensively variated in the research of selective inhibitors[67]. The most studied ZBG is the hydroxamic acid and three of the four approved inhibitors possess this moiety[68]. Various related groups or isosters were also investigated, leading in some instances to isoform-selective compounds such as Entinostat (MS-275)[69] or to Chidamide[70], approved in China for relapsed or refractory peripheral T-cell lymphoma. The inability of this group to discriminate among other metalloproteins such as aminopeptidases, matrix metalloproteinases, and carbonic anhydrases could be the cause of the side effects typical of this class of inhibitors[71,72].

The strong interest on this superfamily of enzymes and the good therapeutic activity of the approved inhibitors, confirmed that HDACs is a validated target for the treatment of several diseases among which tumors. The development of isoform selective modulating agents probably represents the key strategy to be pursued in the next years to discover new HDACIs endowed with better properties and less side effects.

2. Background and Aim of the Work

2.1 Piperazine and Aminopiperidine derivatives as CAs Inhibitors

Several molecules are known to be inhibitory modulators of the Carbonic Anhydrase and, according to their action mechanism, four different categories were identified[21]. Although a wide number of compounds belonging to diverse chemical classes have been discovered, an isoform-selective inhibitor is still lacking[73].

The piperazine ring is a widely used scaffold in medicinal chemistry[74]. The two nitrogen could be easily functionalised and several chemically different derivatives can be obtained. The advantages connected to the physicochemical or reactivity properties will not be analysed in this thesis, but just mentioning that more than 200 therapeutically approved drugs[74] contain at least a piperazine moiety could be enough to understand their importance.

The research group in which I performed my PhD work was several times involved in the synthesis of piperazines[75,76] or structurally related analogues[77]. We took advantage of this expertise in the first aim of my PhD project, deciding to investigate how this fascinating heterocycle would have affected the properties of a new designed series of CAIs. Our idea was to prepare a set of chiral derivatives based on a carbon-functionalized piperazine scaffold, as summarized in **figure 2.1**. We decided to develop zinc-binders, to provide the inhibitory activity against the Carbonic Anhydrases, we therefore decorated one of the nitrogen with a sulfonamide moiety while we rationally modified the other one with different substituents.

Figure 2.1

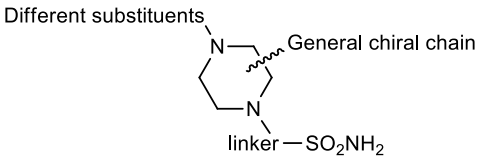

Figure 2.2

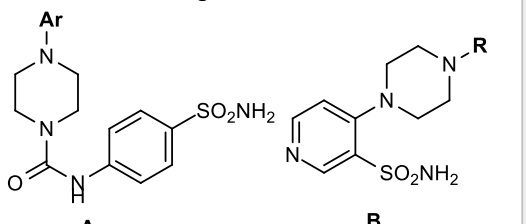

The piperazine ring has been used several times for designing Carbonic Anhydrases inhibitors; in **figure 2.2** two series of derivatives (**A** and **B**) are shown as examples: they consist of N-aryl-piperazines carrying an arylsulfonamide moiety as zinc binding group (ZBG), linked to the piperazine N-atom directly (**B**)[78] or through an urea moiety (**A**)[79]. Both the series of molecules were tested on hCA I, II, IX and XII and while the compounds with general formula **A** showed good potency (K_i in the low nanomolar), the compounds with general formula **B** were weaker inhibitors (K_i in the high nanomolar).

Other examples of piperazine-based CAs inhibitors can be found in the literature[80,81], but to our knowledge, no C-substituted piperazine were published when we started the project.

As a starting point we identified L or D phenylalanine as chiral building block that would have led to the obtainment of a piperazine scaffold bearing a lipophilic benzyl group on the stereogenic centre (**Figure 2.3**). We selected the easily available 4-sulfamoylbenzoic acid as zinc binding group, known to be a good pharmacophore and, by modulating the position of the sulfonamide moiety on the heterocycle and functionalizing the opposite nitrogen with different residues, we synthesized two isomeric series of compounds (**I-A** and **I-B** in **figure 2.3**). The benzyl group connected to the carbon backbone is generating two enantiomers for each product and the **R** group is directly affecting the nature of the test-compounds leading to amines, amides or sulfonamides[24].

Figure 2.3

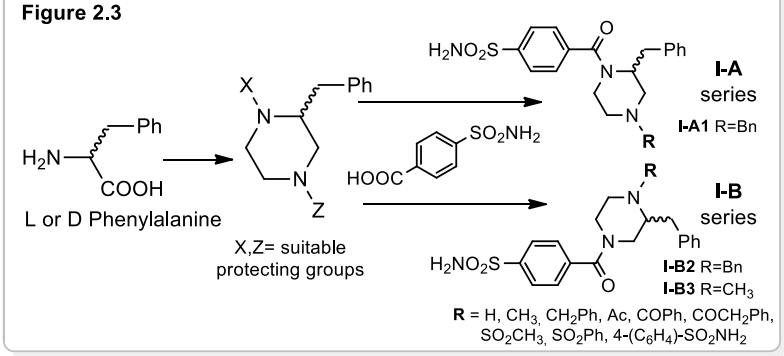

Based on the probable action mechanism of these derivatives, schematized in **figure 2.4**, the interactions with the enzyme made by the **R** groups, the absolute configuration of the stereogenic centre and even the piperazine ring conformation could be different for each compound. These degrees of variations represent a part of our strategy to look for selectivity: the modulation of these characteristics could affect the binding mode and drive to a tighter interaction with an enzyme isoform.

Aiming to further investigate the structure-activity relationships of these compounds we afterwards prepared some structural analogues. By selecting the piperazine scaffold itself as first point of modification, we performed a contemporary scaffold-homologation and simplification.

Figure 2.4

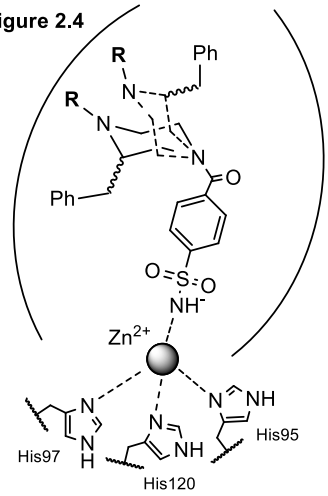

Figure 2.5: Ring-modified derivatives

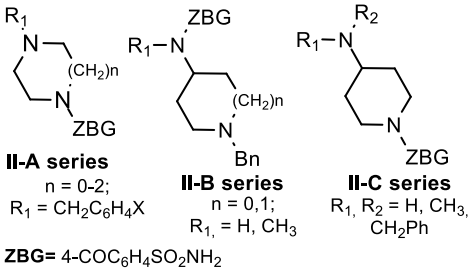

The **II-A**, **B** and **C** series (**Figure 2.5**) were indeed designed and synthesized[82]. We simplified the structure by removing the C-linked side chain and therefore the chirality but keeping anyway in the designed compounds both a N-benzyl moiety and the 4-sulfamoylbenzoic amide as zinc binding group. By modulating the ring size, we aimed to observe the effect on activity caused by

the restriction or the enlargement of the six-membered scaffold. We additionally performed the extrusion of one nitrogen atom, obtaining two series of amino-piperidine (**II-B** and **II-C**) that were mainly differing for the amide position. In addition, we also decided to study the effect of the aromatic substitution on the N-benzyl group on activity and selectivity by preparing some phenyl substituted analogues.

Beside the ring, we were also extremely interested in the side-chain modification. The benzyl moiety represents a bulky lipophilic substituent that could even become detrimental for the activity if directed toward a hindered portion of the enzyme. We therefore modified this residue inserting the hydroxyethyl chain, a polar and flexible group able to accept or donate hydrogen bonds and obtaining the **III-A** and **III-B** series, reported in **figure 2.6**. The OH group could additionally represent a point of further chemical modification or derivatization. Since the hydrochloric salts of the two basic amines **I-A1** and **I-B3** showed promising results as Intra Ocular Pressure (IOP) reducing agents in animal models of glaucoma, we limited the series only to amino-derivatives. As a matter of fact, potential anti-glaucoma molecules have to be endowed with a good water solubility and the HCl salts of the two compounds **I-A1** and **I-B3** already showed this property. Finally, we decided to keep the 4-sulfamoylbenzoic moiety as ZBG in order to maintain constant the point of interaction with the metal ion.

Figure 2.6 *Side chain modified piperazines*

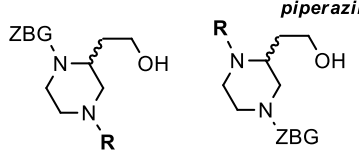

III-A series **III-B series**

R = H, CH_3, CH_2Ph

ZBG= 4-$COC_6H_4SO_2NH_2$

2.2 CAIs-HDACIs hybrids

The Carbonic Anhydrases were also targeted in the second part of my project together with another metalloenzyme family: the Histone Deacetylases. Using a poly pharmacology approach, we designed potential dual inhibitors of these Zinc proteins, aiming to contemporary modulate their activity. We combined the **7-hydroxycoumarin** moiety, potent and selective blocker of hCA-IX[9], with the structure of **SAHA**, the first clinically approved HDACs inhibitor[65], generating the hybrids with general structure **IV** in **figure 2.7**. Since the CA IX, XII and HDAC 1,2 8 isoforms are overexpressed in some cancer cell lines[64], new bivalent inhibitors of these

Figure 2.7

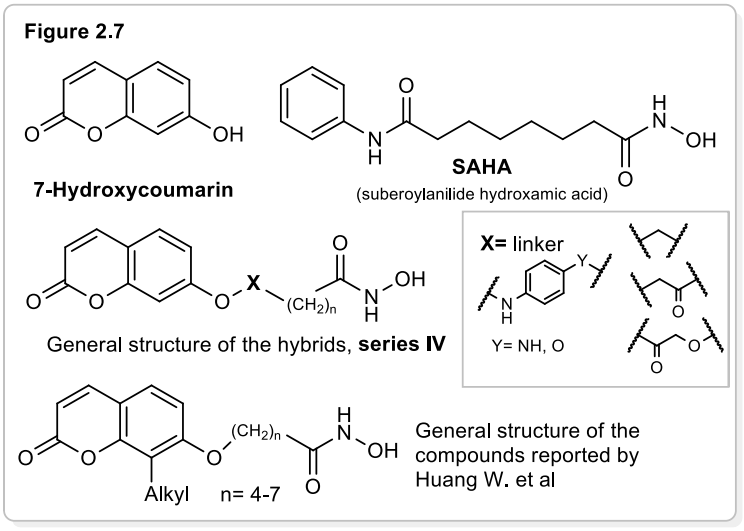

isozymes could represent an important tool to hit the tumor progression. While, as mentioned, coumarin represents a preferential hCA IX and XII targeting-pharmacophore, **SAHA** is a pan-HDAC inhibitor unable to discriminate the different isoforms. We anyway decided to use the **SAHA** as starting point mainly due to the simplicity of its structure and to its well-known inhibitory efficacy, very important to evaluate the potentiality of our new hybrids. In addition, we were encouraged by a work published by Huang W. et al.[83] in which the promising HDAC inhibitory activity of some hydroxamates capped with coumarin derivatives was reported (**Figure 2.7**); the authors did not investigate the potential activity of the compounds against the Carbonic Anhydrase isoforms.

To keep the structure analogy with the **SAHA** portion and for synthetic reasons too, we initially selected a small set of linkers to connect the pharmacophores: the p-phenylenediamine/p-aminophenol or the acetyl group.

Data taken from the literature suggests that the association of inhibitors of these two enzymes could enhance the activity of the single agents. In 2015 Ledaki et al. have found that SAHA treatment significantly reduced the number of MCF-7 cells colonies CA IX-positive, downregulating the expression of this isoform[84]. Later, Mokhtari et al. demonstrated that the expected downregulation of stemness genes (OCT4, SOX2 and Nanog) after treatment of Neuroblastoma cells with the HDACI MS-275 was further enhanced by co-treatment[85] with acetazolamide. As already mentioned in the introduction, MS-275 is an inhibitor selective for Class I HDAC, while Acetazolamide is a pan CA blocker; however, Ledaki's data would suggest that our idea to combine a hCA IX-selective portion with a moiety deriving from a pan HDAC inhibitor could be successful. Indeed, the synergic activity of the co-administration of SAHA and the hCA IX-selective inhibitor FC16 has been recently demonstrated (*Lido Calorini, personal communication*). However, it must be taken into account that hCA IX is placed on the cell membrane, while HDACs are mainly in the nucleus; therefore, the optimization of the physicochemical and pharmacokinetic properties of molecules combining hCA IX and HDAC inhibitory properties could be challenging.

2.3 CAs Activators

While the Carbonic Anhydrase inhibition is a well-known and deeply investigated process, on the opposite side there are not so many information about the activation of this enzyme. Based on the evidence that some small polar molecules like amines and amino acids are able to increase the catalytic activity of this enzyme[15,16] and since genetic deficiencies of several isoforms were associated to the outbreak of pathologic conditions[86,87], the interest of the scientific community on Carbonic Anhydrase activators is raising fast. Histamine (HST) is one of the most studied activator[88,89] and several structure modification were performed to enhance its potency or selectivity. Since x-ray crystallographic adducts[19] showed that the aliphatic amino moiety of HST is not interacting with the enzyme (**Figure 2.8B**[90]), this

functional group was one of the first extensively modified, giving the products with general structure **C**[91–93] reported in **figure 2.9.** In particular, some interesting compounds were found in the series of the imino derivatives **D**, such as **D1**[94], possessing, among the investigated isoforms, high potency (K_a 1.8 nM) and selectivity for hCA IV, or **D2**, endowed with similar potency (K_a 7 nM) and selectivity toward hCA VII. Other approaches comprise the introduction of substituents directly on the imidazole ring[95] (general structures **E** in **figure 2.9**) or its substitution with pyridinium azoles[96].

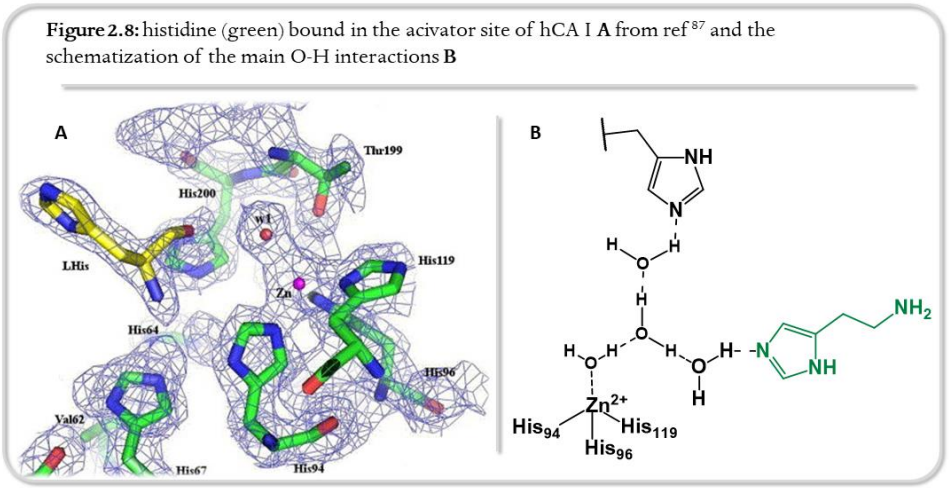

Figure 2.8: histidine (green) bound in the acivator site of hCA I **A** from ref [87] and the schematization of the main O-H interactions **B**

The crystal structures of the adduct of HST with hCA II showed the hydrogen bond network architecture involving the imidazole nitrogen and support the proton shuttling mechanism[86]; a similar pattern of interactions was seen also in the adduct of L-Histidine with hCA II[97]. In general, it has been demonstrated that a pivotal role is played by His 64 (the number refers to hCA II)[15]. Other amino acids such as D and L-phenylalanine, or D-tryptophan bind at the entrance of the cavity stabilizing the active form of the enzyme through a network of H-bonds involving the amino and carboxylic groups[98,99]. In case of L-adrenaline, the H-bond network involves the catechol and alcohol oxygen atoms, showing that a basic nitrogen atom may not be essential[57]. In general, a common structural feature of Carbonic Anhydrase activators is the presence of a flexible tail decorated with protonatable moieties, whose pKa values span between 6 and 8[28]. However, to establish the H-bond network between activator, water molecules and His64 within the binding site, a basic nitrogen is not required, since often oxygen atoms are involved. In addition, there may be isoform specific mode of binding for these activators: for instance, in the X-ray structure of the L-histidine-CA II adduct (**image 4.1B**, discussed in the chapter "results"), the imidazole ring is involved in the H-bond

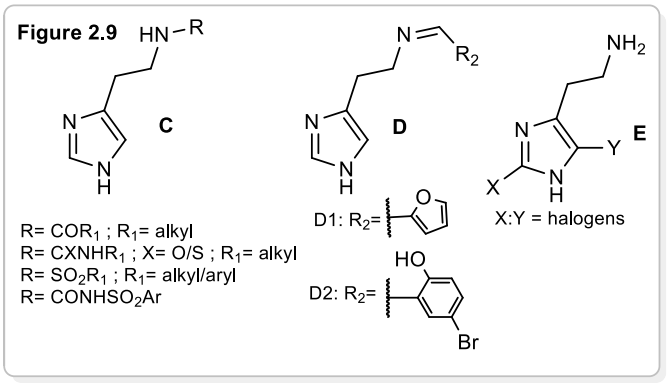

network[97], while in the L-histidine-CA I adduct the same role is played by the carboxylic group[90]. It is difficult to estimate the importance of this difference, but it must be noticed that L-histidine is two orders of magnitude more potent on hCA I than on hCA II[28].

Based on these premises, our work on Carbonic Anhydrase activators started from HST, by searching a suitable 5-membered heterocycle as substitute for the imidazole ring. To this aim we synthesized a series of HST analogues derived from isosteric modifications of the imidazole moiety in order to develop the SAR of this pharmacophore portion (**Figure 2.10**). By variating the heterocycle, we modified the nitrogen number, the basicity and the hydrogen bond donor/acceptor capability of the aromatic portion, aiming to change the proton-shuttling properties.

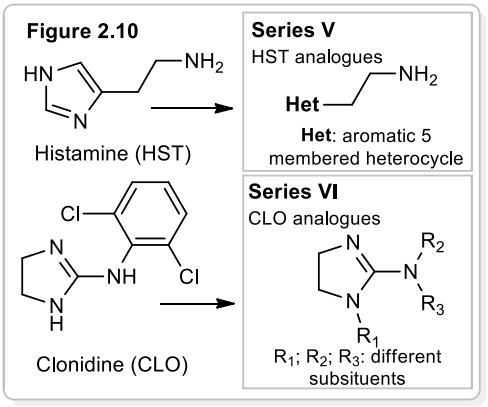

In this search we also reckoned that the imidazoline ring could be a bioisoster of the imidazole ring of HST; therefore, we focused our attention on Clonidine (CLO) (**Figure 2.10**). As a matter of fact, the Supuran group measured enzymatic activation by this small basic molecule (unpublished result) and since the capability of CLO to cross the Blood-Brain Barrier it is a known property[100–102], we thought to use Clonidine as lead compound in the preparation of new derivatives potentially acting in the Central Nervous System (CNS). We indeed aimed to develop new activator tools targeting the CNS expressed Carbonic Anhydrase isoforms, like hCA IV[103] and VII[104]. Thus could be extremely useful to treat some serious cognitive impairments associated with a CA central deficiency and a first confirmation of the positive effects on memory of a CA activator was obtained by Blandina's group[105]. However, we were aware of the multiple biological actions of CLO and other 2-amino-imidazoline derivatives (α2 agonists, IBS1 and IBS2 modulators[106], HCN blockers[107,108]); in case of cellular or in-vivo biological tests, we would need to consider also a possible interaction for these additional biological targets.

Finally, we also tested a series of piperazines, starting from the observation that 2-(Piperazin-1-yl)ethan-1-Amine (PEA, **Figure 2.11**), structurally similar to histamine (the imidazole has been replaced with a piperazine ring), has been reported to be an effective, low micromolar activator for several CA isoforms[109110]. The tested piperazines (series **VII**) were either commercially available or synthesized in our laboratory for other research projects.

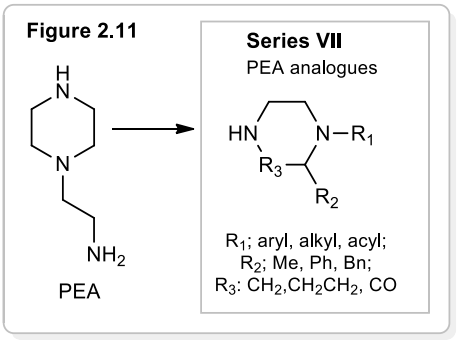

3. Chemistry

3.1 Synthesis of Piperazine and Aminopiperidine derivatives

Several different synthetic methods have been developed to prepare the piperazine ring and nowadays many strategies could be pursued[111], especially when a stereo or enantioselective synthesis is needed. A particular approach is based on the analogy among the two-carbon backbone of a α-amino acid and a "half piperazine" (**Figure 3.1**). The amino acids, useful bifunctional molecules, can represent an ideal starting material for the preparation of piperazines and their enantiopure availability could lead to chiral molecules.

Figure 3.1

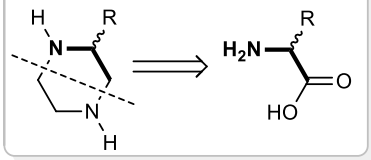

The synthetic method we chose is reported in **scheme 3.1**[112]. L or D phenylalanine was esterified in acidic conditions obtaining the hydrochloric salt **1** that reacted with the intermediate **2**, representing the other half of the heterocycle, built in three subsequent steps (**b-d**) from benzylamine and ethyl bromoacetate. The coupling reaction among the unprotected carboxy and amino moieties of these two fragments gave the dipeptide-analogue **3** that, once cleaved from the Boc-protection, cyclized spontaneously in an ammonium hydroxide / methanol solution, affording the piperazindione **4.** The reduction of the two lactams with $LiAlH_4$ gave the desired 1,3-dibenzylpiperazine **5**.

Scheme 3.1

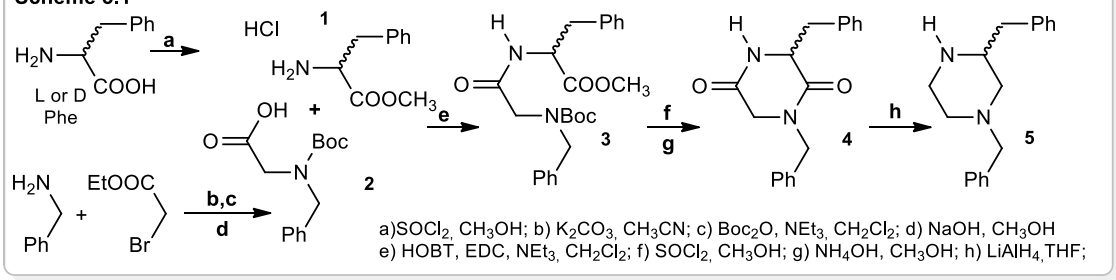

We applied a similar strategy[113] in the preparation of the N-unsubstituted piperazine **9** (**scheme 3.2**). This time the amino function of L or D phenylalanine was protected with the Boc group (intermediate **6**) and the coupling reaction was performed with the hydrochloric salt of glycine methyl ester. We therefore "inverted" the C-N direction as respect to the previous approach obtaining the dipeptide **7**. The intermediate **7** followed afterwards the same synthetic route of its N-benzyl analogue leading to the 2-benzylpiperazine **9.**

Scheme 3.2

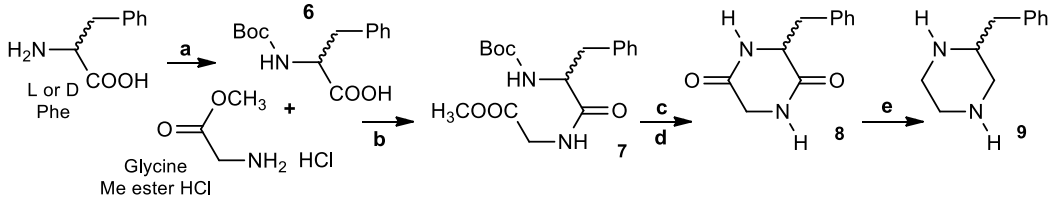

a) Boc_2O, THF, H_2O; b) HOBT, EDC, NEt_3, CH_2Cl_2; c) $SOCl_2$, CH_3OH; d) NH_4OH, CH_3OH;e) $LiAlH_4$,THF;

We then started the N-decoration of 1,3-dibenzylpiperazine **5**. According to our optimized strategy, reported in **scheme 3.3**, the N-amidation with the zinc binding group was performed with 4-sulfamoylbenzoyl chloride[114]. We needed some attempts to find the best conditions, but finally using this activated form of the acid we obtained reaction mixtures from which we easily isolated **IA-1** in good yields. We then moved on to the debenzylation: performing the catalytic hydrogenation in presence of a slightly amount of HCl, we avoided the parasite methylation[115], observed during some of the first attempts. The secondary amine **IA-2** was therefore obtained as HCl salt in good yields, hydrolysed to the corresponding free base and then functionalized on the free nitrogen with different reagents (step **c** in **scheme 3.3**) to obtain the **I-A series** of test-compounds. The conditions and the reactants we used for the various decorations are reported in the experimental part.

Scheme 3.3

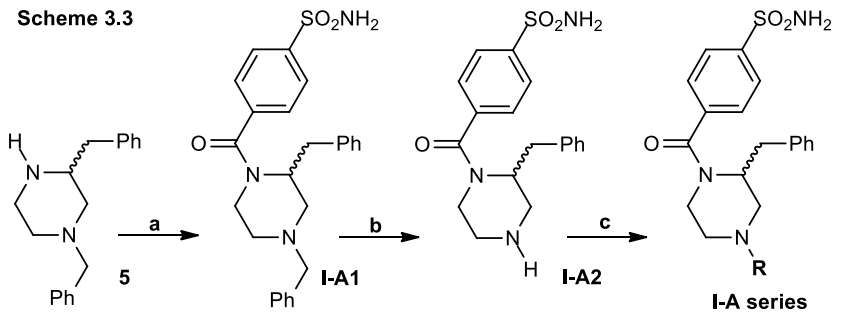

a) 4-sulfamoylbenzoyl chloride, NEt_3,CH_3CN ; (b) CH_3OH/HCl, H_2/Pd/C;
c) R-Z, CH_3CN, base (for the conditions, see the **table 1**)

We additionally used the 1,3-dibenzyl piperazine **5** to prepare the *S*-enantiomer of a product of the **I-B** series too, the compound **I-B3** (**scheme 3.4**). We then applied a classic Eschweiler-Clarke reaction to obtain the methyl derivative *S*-**10** that was then easily cleaved from the benzyl protection and transformed into the desired final product again with the acyl chloride of the 4-sulfamoyl benzoic acid (step **c** in **scheme 3.4**).

Scheme 3.4

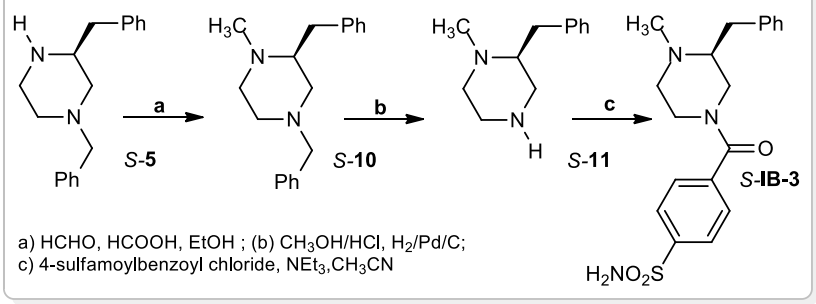

a) HCHO, HCOOH, EtOH ; (b) CH_3OH/HCl, H_2/Pd/C;
c) 4-sulfamoylbenzoyl chloride, NEt_3,CH_3CN

Scheme 3.5

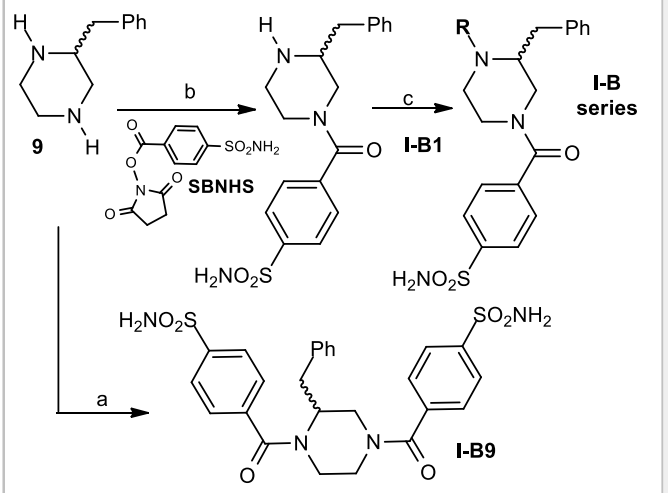

To prepare the **I-B** series we thought to use a slightly diverse approach: avoiding the nitrogen-protection we took advantage of the reactivity difference among the two free amino groups (**scheme 3.5**). Following the idea to first insert on the 2-benzylpiperazine **9** the zinc binding group, we again tried with 4-sulfamoylbenzoyl chloride obtaining almost exclusively the compound **I-B9**. In fact, due to the high reactivity of the acyl chloride was not possible to direct the reaction only on the 4-nitrogen. We therefore prepared a different activated-analogue of the acid: the NHS-activated ester[116] (**Scheme 3.5**, **SBNHS=** 2,5-dioxopyrrolidin-1-yl 4-sulfamoylbenzoate). With this less reactive benzoic acid derivative and carefully modulating the conditions we obtained the desired mono-acylated derivative **IB-1.** We finally obtained the other piperazines belonging to the **I-B** series, as previously done with their isomers **I-A** (conditions reported in experimental part).

To further develop our project, we identified two main paths to pursue: the ring-modification and the side chiral chain variation. The piperazine scaffold could be chemically transformed or replaced in several different ways; as starting point we synthesized the **II-A**, **B** and **C series** of ring-modified compounds (**Figure 3.2**)[82]. We also contemporary moved in a different direction preparing an analogue set of chiral products: the **III-A** and **B series** of basic hydroxyethyl-piperazines (**Figure 3.2**) obtained from a different amino acid, aspartic acid.

Figure 3.2

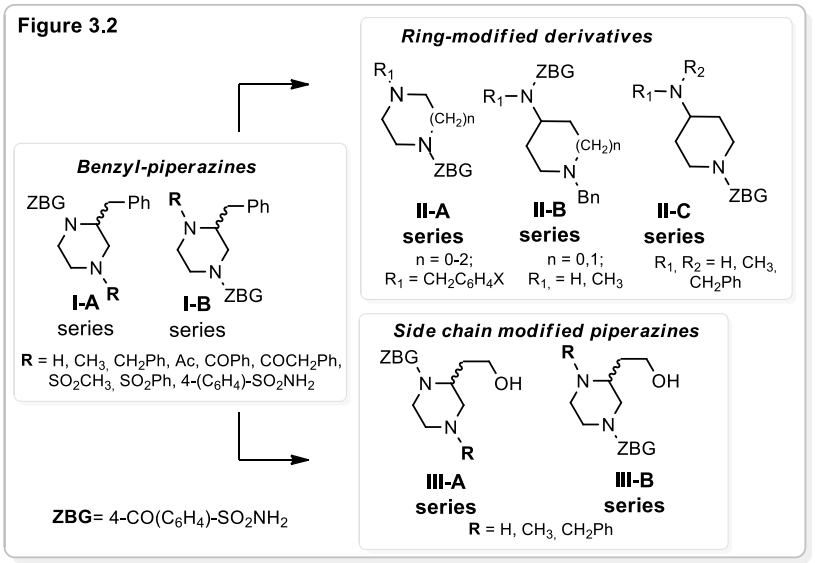

Aiming to generate a wide series of analogues we decided to apply simple synthetic modifications to commercial products, as reported for the **II-A** series in **scheme 3.6.** Inserting the ZBG on the three homologous N-benzyl-imidazoline, piperazine and homopiperazine we obtained the compounds **II-A1**, **II-A2** and **II-A3** respectively. Thanks to availability of several benzyl halides we additionally investigated how different substituents on the benzyl moiety were affecting the activity of the compounds. Through the amine-alkylation of N-Boc piperazine and obtaining **12a-e** as intermediates, we used again 4-sulfamoylbenzoyl chloride to acylate the free nitrogen and isolate the derivatives **II-A4** – **II-A10.** The compounds **II-A4** and **II-A8** are also intermediates in the preparation of **II-A9** and **II-A10**, achieved by means of $SnCl_2$ reduction and catalytic hydrogenation respectively.

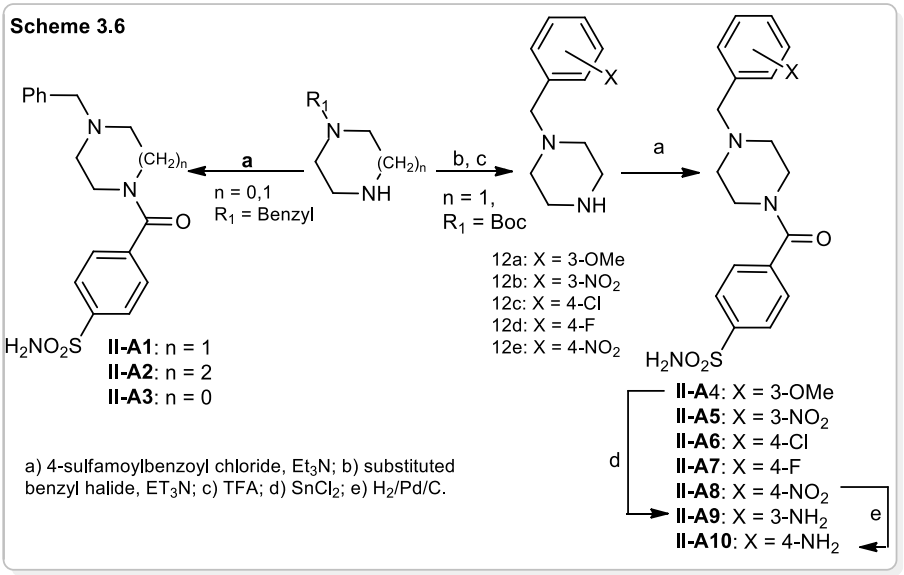

The next scaffold modification we did was the amide-extrusion. Starting simply from 4-aminopiperidines or 3-aminopirrolidines, as write in **scheme 3.7**, we prepared the three **II-B** belonging analogues. In particular, **II-B1**, **II-B2** and **II-B3** derived from, respectively, commercially available 1-benzylpiperidin-4-amine, 1-benzylpirrolidin-3-amine, or with 1-benzyl-N-methylpiperidin-4-amine prepared according to Pryde[117].

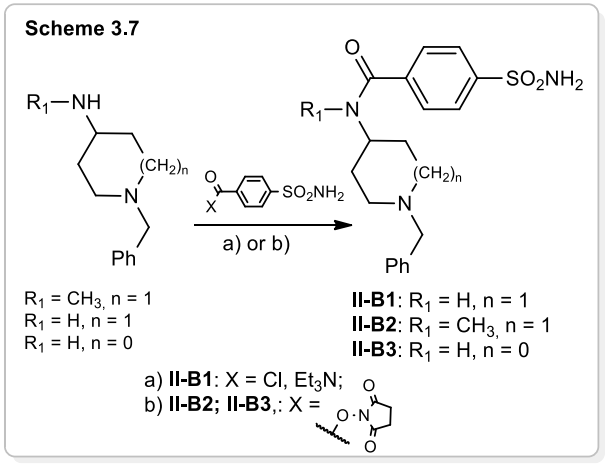

We additionally used two other 4-aminopiperidines to try another slightly different ring-modification: while keeping the amide bond on the endocyclic nitrogen and the basicity of the 4-amino group we inverted the polarity of the molecules with respect to the previous series **II-B**. To obtain the compound **II-C2** and the methyl analogue **II-C3** we thought to start from 4-(Boc-amino)piperidine (upper part of **scheme 3.8**). The ZBG insertion with **SBNHS** and the Boc cleavage were performed without problem but once we tried the 4-N-alkylation the desired benzyl-derivative **II-C2** was isolated only with poor yields. Thanks to the presence of the pharmacophore moiety, we anyway decided to test the 4-NH_2-Boc intermediate **II-C1**. The alternative method we developed made use of 4-(amino)piperidine-1-Boc as starting material. We first performed the exocyclic benzylation followed by Cbz-protection of the same nitrogen and, taking advantage of the orthogonal protections, we cleaved the N-1 from the Boc group. We then added the ZBG on the so obtained piperidine **14** and we removed the Cbz-protection, isolating **II-C2** this time in good yield. With methyl iodide we then prepared the last piperidine derivative: the tertiary amine **II-C3**.

Scheme 3.8

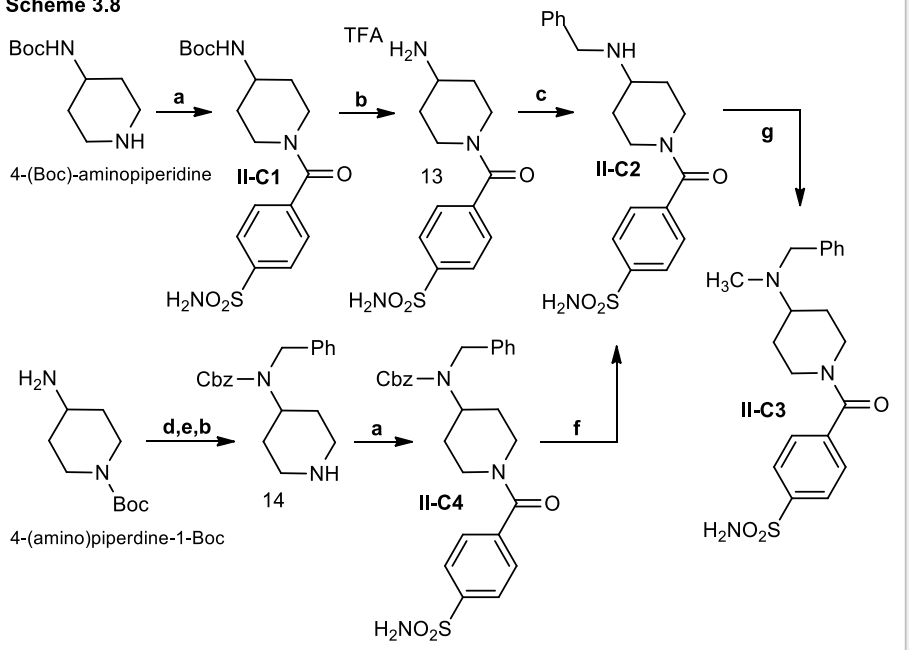

a) SBNHS, CH_3CN; b) TFA; c) $PhCH_2Br$, $NaHCO_3$; d) PhCHO, $NaBH_4$: e) ClCbz, NEt_3; f) HBr, AcOH; g) CH_3I, $NaHCO_3$.

As already pointed out in **figure 3.3**, we contemporary focused our attention on the chiral side chain. This part of the project started during my six-months internship in Germany as a part of the collaboration with Prof. Bernhard Wünsch of the University of Münster, therefore the aim of my internship was to study new chemical approaches to obtain chiral piperazines. Together with Prof. Wünsch, we decided to start from L or D aspartic acid as chiral starting material that would have led to the hydroxyethyl piperazines series (**Figure 3.4**). Our idea was to variate the polarity of the side chain switching from the hydrophobic benzyl moiety to the polar and protic hydroxyethyl group to study

Figure 3.4

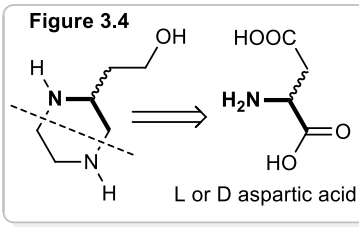

the effects of this portion on the binding mode and to add a new point of possible derivatization.

In analogy with a work already published by the Wünsch group[118], I developed the synthetic chiral pool reported in **scheme 3.9**. With the acid-catalysed double esterification of the desired aspartic acid enantiomer I easily obtained the key intermediate **15** as HCl salt. To insert a nitrogen protective group, I then applied a two-steps reductive amination to obtain the N-benzyl-derivative **16** and the piperazine carbon backbone was completed through the N-amidation with bromoacetyl bromide. Afterwards, I decided to perform the ring-closure of the open derivative **17** with ammonia. Using a methanolic concentrated solution of ammonia the double substitution was slow but I isolated the piperazindione **18** with good yields and I saw only with LC-MS small amounts of the corresponding amide **18a**. To reduce the three carboxylic functions of the piperazinedione **18** I used $LiAlH_4$ in a not-problematic reaction that gave the hydroxyethyl-piperazine **19**.

Scheme 3.9

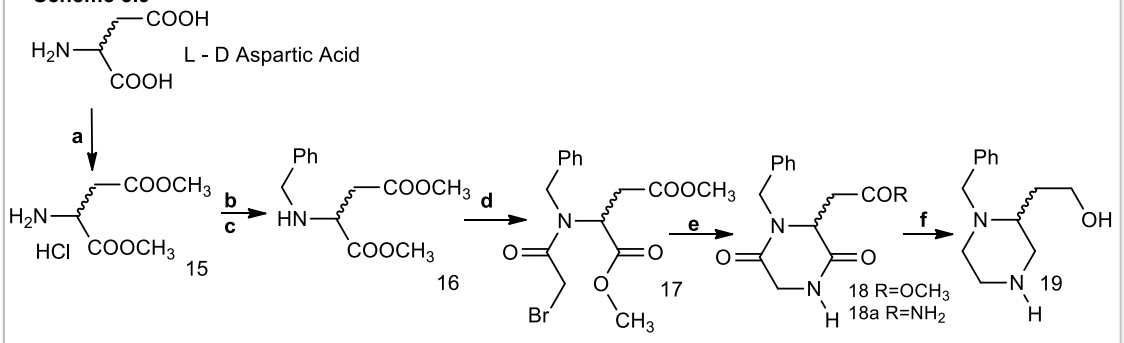

a) $SOCl_2$, CH_3OH; b) PhCHO, NEt_3, CH_3OH; c) $NaBH_4$, CH_3OH; d) $BrCH_2COBr$, NEt_3, CH_2Cl_2; e) NH_3, CH_3OH; f) $LiAlH_4$, THF

The Wünsch group used a slightly different approach[118], summarized in **scheme 3.10**. They performed a three steps procedure (A and B reductive amination; C acylation) without isolation or purification of the reaction intermediates, switching solvent twice and obtaining **17a** in poor yields (from 15% to 49%). I therefore decided to investigate these steps: performing the imine formation and the reduction in CH_3OH (steps **b** and **c**) I initially obtained complex reaction mixtures. Looking for alternatives I found the strategy reported by Faler C. et al.[119] (step **f** in **scheme 3.10**) starting from the free base of aspartic acid dimethyl ester **15a.** I indeed tried to hydrolyse the HCl salt, but every time the extraction was unexpectedly problematic and a lot of compound remained in the basic water phase. I individuated two potential hetero-phase alternatives: using zinc powder as done by Braga C.B. et al.[120] ($2R\text{-}NH_3Cl + Zn \rightarrow 2R\text{-}NH_2 + ZnCl_2 + H_{2(g)}$) I obtained the free base **15a** with a lot of $ZnCl_2$, a deliquescent solid highly soluble in water and organic solvents while, as reported by White K. et al.[121], an ion-exchange resin was more effective and easier removable. With this last method I managed to obtain **15a** but once I tried the reduction

with sodium triacethoxyborohydride[119] (step **f**, **scheme 3.10**) I also isolated high amounts of the N-dibenzbenyl side product **16a.** It was evident that in those conditions the monobenzyl derivative **16** was more reactive than the starting material **15a.** After these attempts I decided to come back again to the initial method and optimizing the reductive amination (step **b,c scheme 3.10**) I obtained a yield around 65%. An additional small difference I implemented was the use of bromoacetyl bromide in step **d** instead of the corresponding chloride to obtain more the reactive intermediate **17** than the analogue **17a** with yields around 80%.

Scheme 3.10

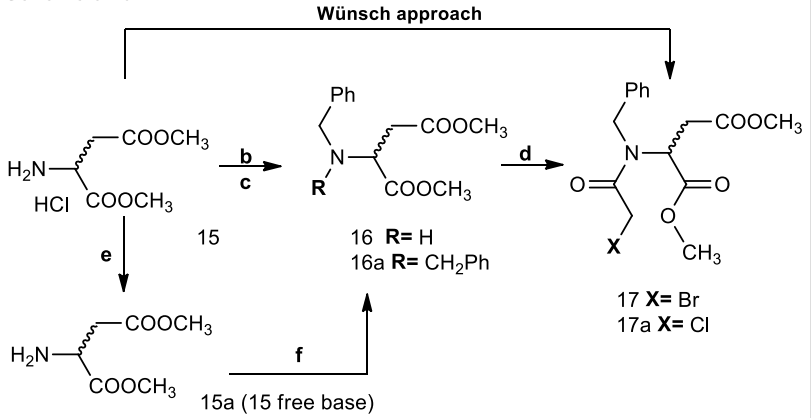

Wünsch approach:
(A) $PhCHO$, NEt_3, Na_2SO_4, CH_2Cl_2
(B) $NaBH_4$, CH_3OH
(C) $ClCH_2COCl$, NEt_3, CH_2Cl_2)

Investigated alternatives:
b) $PhCHO$, NEt_3, CH_3OH;
c) $NaBH_4$, CH_3OH; d) $BrCH_2COBr$, NEt_3, CH_2Cl_2;
e) hydrolis, see the description in the text
f) $PhCHO$, $NaBH(CH_3COO)_3$, CH_2Cl_2 [Faler et al.]

To obtain the other N-benzyl protected piperazine **22** I again started from the dimethyl ester of aspartic acid **15** applying the synthetic pathway shown in **scheme 3.11**. Avoiding the initial reductive amination and performing the acylation directly on **15,** I prepared the opened-intermediate **20** that was then cyclized with 2 equivalents of benzylamine. These conditions led to a slow reaction but the piperazindione **21** was the main product and the formation of the product of double addition **21b** was minimized. In the same way but using CH_3NH_2 I made the methyl analogue **21a;** both compounds were reduced yielding the piperazines **22a** and **22** respectively.

Scheme 3.11

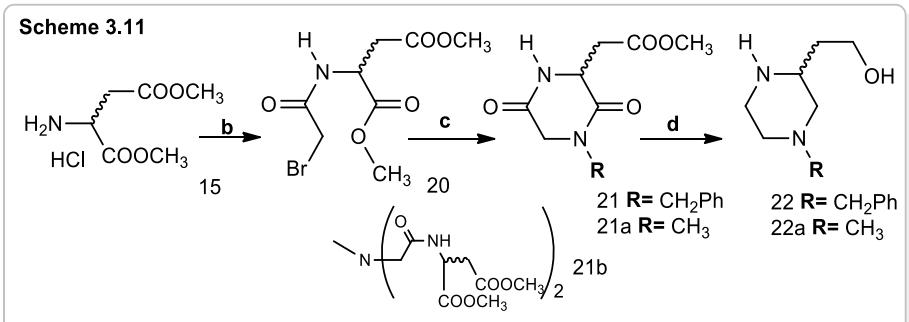

a) $SOCl_2$, CH_3OH; b) $BrCH_2COBr$, NEt_3, CH_2Cl_2; c) **21:** $BnNH_2$, CH_3OH, **21a:** CH_3NH_2, CH_3OH;
d) $LiAlH_4$, THF

To obtain the **III-A** series I started to work directly on the piperazine **22** (**Scheme 3.12**). Again, with the acyl chloride strategy I prepared the two enantiomers of **III-A1** that I this time debenzylated with a different method: the in-situ generation of hydrogen through the Pd-catalysed decomposition of ammonium formate. Performing this step directly in a pressure tube and without any hydrogenator was easier to set up and control the reaction. Initially, the only issue was the reaction-time because a long-lasting reflux was needed. Using the microwaves apparatus, I prepared the derivative **III-A2** in 1 hour instead of the 9 of the first attempts. On the opposite side, I had many troubles in the synthesis of the methyl derivative **III-A3**. My initial strategy was to use the piperazine **22a** (**Scheme 3.11**) but the purification of the reaction mixture was unexpectedly problematic: the obtained product **III-A3** was so polar and basic that I did not manage to remove the NEt_3HCl, not even with flash chromatography. I then tried to perform the N-methylation of the derivative **III-A2** (step **c** in **scheme 3.12**) but this alternative route was also unsuccessful: the reaction was so slow that once I tried to stress the conditions the OH group probably reacted too. Finally, I decided to use a different strategy: modifying the conditions of the debenzylation to perform a contemporary deprotection-reductive amination and go from **III-A1** directly to **III-A3**. I therefore added in the mixture some equivalents of formaldehyde and acetic acid and the attempt was successful giving the desired N-methyl derivative **III-A3**. I further tried to investigate the conditions of this method and I found out that adjusting the equivalents of the aldehyde and the acid is possible to contemporary obtain the debenzyl and the methyl derivatives **III-A2** and **III-A3**.

Scheme 3.12

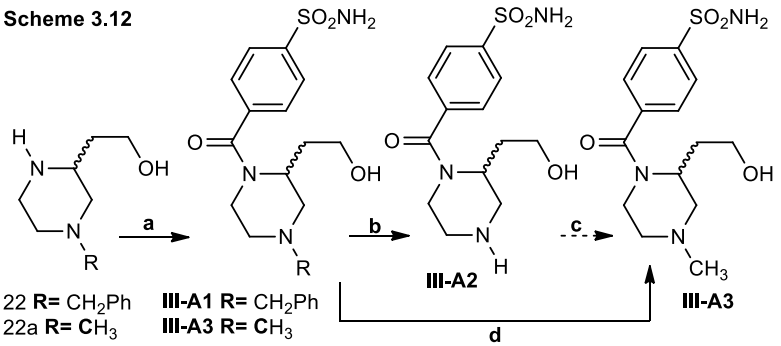

a) 4-sulfamoylbenzoyl chloride, NEt_3, CH_3CN ; b) NH_4HCOO, Pd/C, IPA;
c) CH_3I, $NaHCO_3$, CH_3CN; d) NH_4HCOO, Pd/C, HCHO, CH_3COOH, IPA

The procedure I used to obtain the **III-B** series is similar. To the hydroxyethyl-piperazine **19** I attached the ZBG (**scheme 3.13**) obtaining **III-B1** that I again debenzylated with ammonium formate – Pd/C. I attempted again the methylation of the secondary amine **III-B2** (step **c, scheme 3.13**) but once again the reaction was not working. Due to

Scheme 3.13

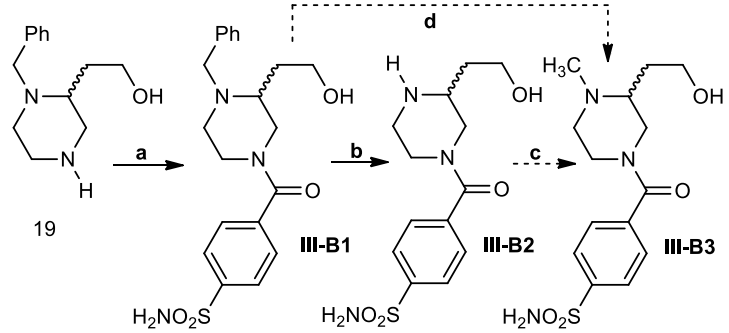

a) 4-sulfamoylbenzoyl chloride, NEt_3, CH_3CN ; b) NH_4HCOO, Pd/C, IPA;
c) CH_3I, $NaHCO_3$, CH_3CN; d) NH_4HCOO, Pd/C, HCHO, CH_3COOH, IPA

another occurred problem that I was in the meanwhile investigating (mentioned in the next paragraph), I haven't had time to apply the method **d** to synthesize **III-B3**, but I hope that the debenzylation-reductive amination approach will work for this compound too.

We contemporary decided to check the enantiomeric purity of the two benzyl-derivatives **III-A1** and **III-B1** (**Figure 3.5**). With chiral HPLC we determined the enantiomeric excess (E.E.) of every benzylated isomer; the results are reported in the table of **figure 3.5**. While the E.E. of the couple of enantiomers **III-A1** is high, the measured values are low and extremely different for both the enantiomers of **III-B1**. Our hypothesis, supported by additional chiral HPLC analysis, is that during the cyclization (see the inset in **figure 3.5** referring to **scheme 3.9**) the acid α-hydrogen of both the intermediates **17** and **18** could be deprotonated by ammonia, leading to the racemization of the stereogenic centre. The different E.E. values could be easily explained by the reaction-time variations. Due to the troubles we found in the separation of the enantiomers and the analysis of some intermediates, the synthesis of the test compounds was extremely slowed down.

Figure 3.5

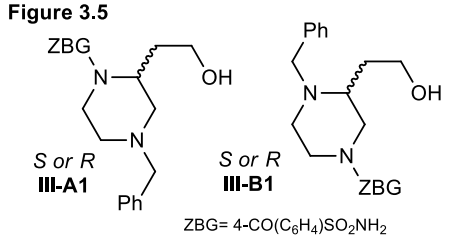

Sample	*S* (%)	*R* (%)	E.E. (%)
***(S)* III-A1**	95	5	90
***(R)* III-A1**	5	95	90
***(S)* III-B1**	83	17	66
***(R)* III-B1**	38	62	24

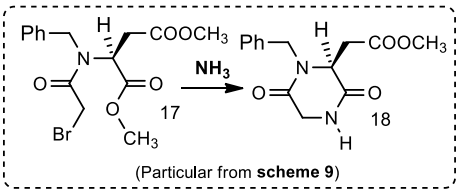

(Particular from **scheme 9**)

In the meantime, I hopefully found a synthetic alternative to perform this step that will be done as soon as possible. As reported by Jida M. et al.[122], using a slightly different opened-intermediate and acetic acid as "cyclizing agent" (**scheme 3.14**) the racemization may be avoided. The attempt I already did was successful but I still have to complete the way to go from ***S*-18** to ***S* III-B1**. Since these piperazines are very polar, a good enantiomeric separation could be obtained only at this level.

Scheme 3.14

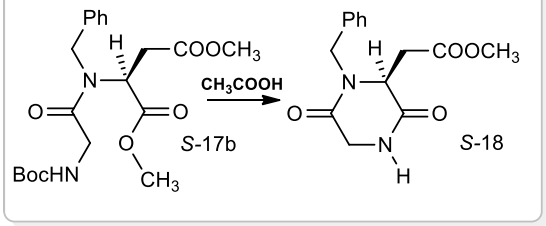

3.2 Synthesis of CA-HDAC hybrids

The synthetic strategy we developed for the preparation of the hybrids is reported in **scheme 3.15.** The first important intermediate we obtained is the 7-O-methylene carboxy coumarin **23**[123]: the useful acetyl linker gave us the possibility to easily exploit the carboxylic group to connect the two portions of the hybrids. We took advantage of the COOH group of **23** to perform a coupling reaction with the SAHA structure-related fragments **24** and **24a** built from p-phenylenediamine and p-aminophenol respectively (step **c**, top of the **scheme 3.15**). The amide **25** and the analogue ester **25a** were immediately characterized by a really poor solubility both in water and organic solvents, the purification was indeed problematic. Moreover, when we tried the hydrolysis of the terminal ester function we had additional troubles. While we managed to prepare the carboxylic acid **26** from **25,** the aromatic ester function of the compound **25a** broke up in those mild conditions and we observed the re-formation of the two fragments **23** and **24a.** As already verified for the ester precursor, the purification of **26** was complicated by the annoying poor solubility and, moreover, when we analysed through LC-MS the collected sample we discovered that an amount of the ester and some other side products where still present. These troubles and the poor solubility properties ushered us to abandon these types of products, so we focused our attention on different linkers. We therefore came back to the intermediate **23** and we decided to connect the alkyl chain directly to this molecule (step **e**). The stability problem of the ester **25a** advised us to generate amide derivatives so we selected two long alkyl-amines: methyl 8-aminooctanoate **26a** and ethyl 7-(benzylamine)heptanoate **26b**, obtaining, respectively **27** and **28**. We afterwards transformed their ester functions into the hydroxamates **IV-1** and **IV-2** in three steps: a first saponification followed by a coupling with the O-THP (O-tetrahydropyranyl)-protected hydroxylamine and a final deprotection in acidic conditions (these steps are summarized as **f,** right part of **scheme 3.15**). To prepare the last structure-related hydroxamate **IV-3** we used a slightly different approach: we transformed the intermediate **23** into the corresponding NHS-activated ester **30** that we reacted with 7-aminoheptanoic acid **26c** without coupling-activator agents (step **h**), obtaining **29**. We then converted it into the hydroxamate **IV-3** by again repeating the COOH activation with NHS and using then a hydroxylamine solution to obtain the hydroxamate **IV-3** (**steps g** and **h**). Since we needed some additional quantity of the product and the already done synthetic method was low-yielding, we decided to prepare the hydroxamate **IV-2** also with a different procedure. Starting again from the activated ester **23**, we separately built the alkyl-portion **31** from 7-aminoheptanoic acid (reported in the bottom part of **scheme 3.15** and described at the end of this paragraph). The coupling among **23** and **31** gave **28b** that we converted into the hybrid **IV-2** hydrolysing the O-THP function (3rd part of **step f**). In a diverse way we prepared the hydroxamate **IV-4**: with the nucleophilic substitution of the 7-hydroxycoumarin on ethyl 7-bromoheptanoate we prepared the ether derivative **32** in which the alkyl chain was directly connected to the coumarin moiety.

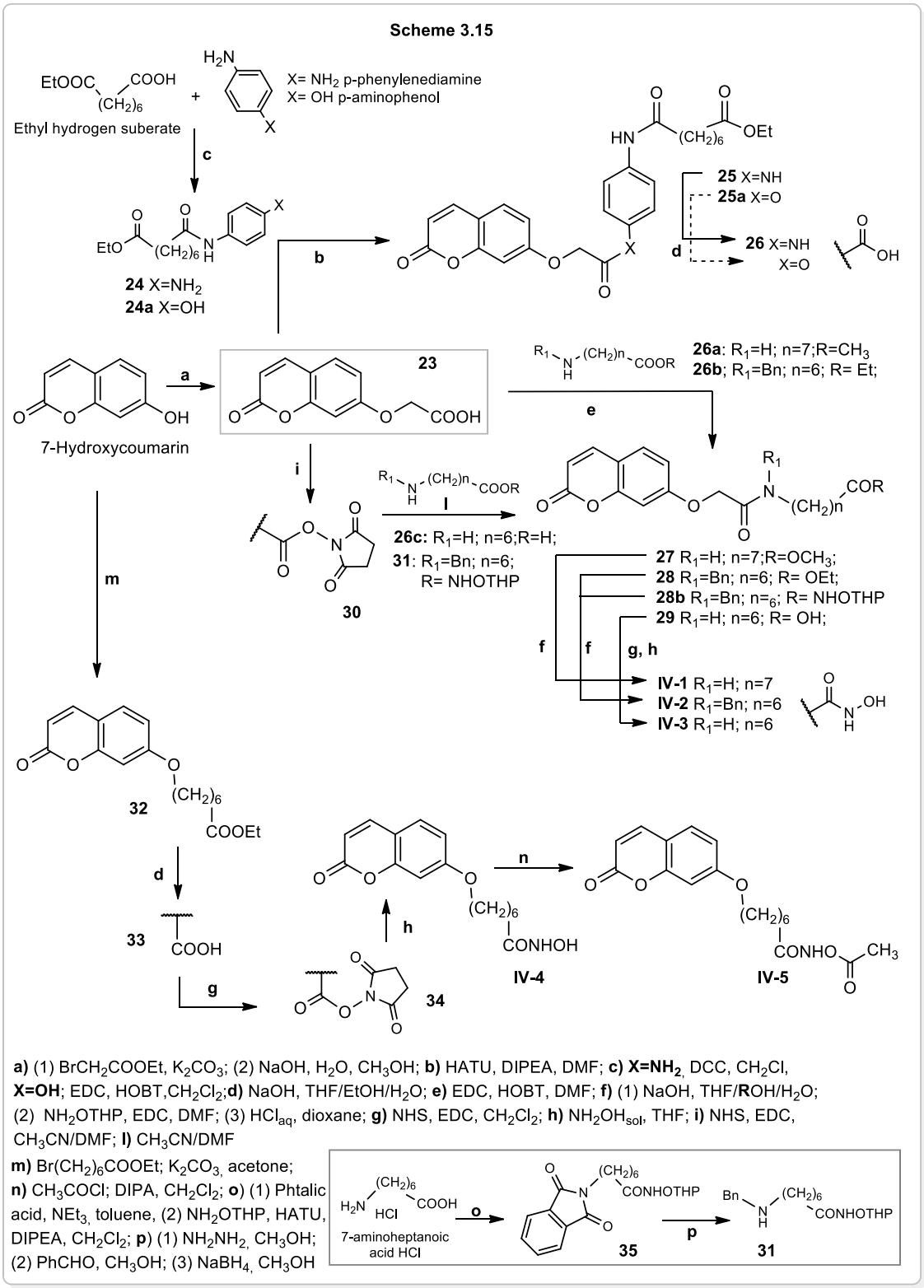

We then hydrolysed the ester function and we activated the carboxylic acid with NHS (intermediates ***33*** and ***34*** respectively). By using a concentrated solution of hydroxylamine in water we directly converted the NHS-ester into the corresponding hydroxamate **IV-4.** In order to understand which moiety, between the coumarin and the hydroxamate, was the real Zn-binding group, we decided to masque the hydroxamate function of **IV-4** with an acetyl moiety[124], obtaining the O-acetyl-hydroxamate **IV-5.** As mentioned before, we

prepared the fragment **31** for the alternative route to obtain **IV-2**. We started from the HCl salt of 7-aminoheptanoic acid that we transformed into the corresponding phtalimide to selectively perform the coupling reaction among its carboxylic group and O-THP hydroxylamine, obtaining the contemporary double protected intermediate **35.** We then cleaved the phtalimide protection and we alkylated the so obtained primary amine with the two-steps reductive amination that gave us to **31**.

3.3 Synthesis of CA Activators

Our work on Carbonic Anhydrase activators started from the evidence that histamine (HST)[88] and Clonidine (CLO), two small basic product, were reported to have activator properties on the enzyme[97]. The crystallographic studies performed on HST[89] determined that the cyclic portion of this molecule is essential for the activator effect while the aminoethyl chain seems not interacting with the enzyme. This evidence prompted us to synthesize a series of HST analogues derived from isosteric modifications of the imidazole moiety in order to develop the SAR of the pharmacophore portion (**Figure 3.6**). By variating the heterocycle, we modified the nitrogen number, the basicity and the hydrogen bond donor/acceptor capability of the aromatic portion, aiming to change the proton-shuttling properties. We contemporary worked on Clonidine structure too, variating some structural motifs to determine their effect on the binding mode (**Figure 3.6**).

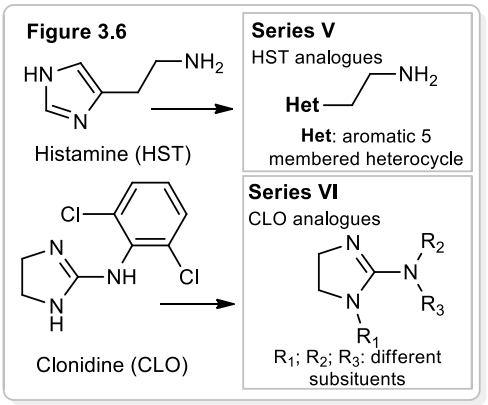

The series **V** of HST analogues were synthesized as reported in **scheme 3.16.** We first "turned" the imidazole group into the pyrazole **V-1** by opening the 4H-pyran-4-one cycle with hydrazine and reducing the intermediate hydrazone **36**, obtaining **V-1**[125]. With the same chemical approach we then prepared the two related compounds **V-2**[126] and **V-3**[127]: the aminoethyl chain was connected to imidazole and 1,2,4-triazole using N-(2-bromoethyl) phtalimide and removing afterwards the protection with hydrazine (intermediates **37** and **38**).

Scheme 3.16

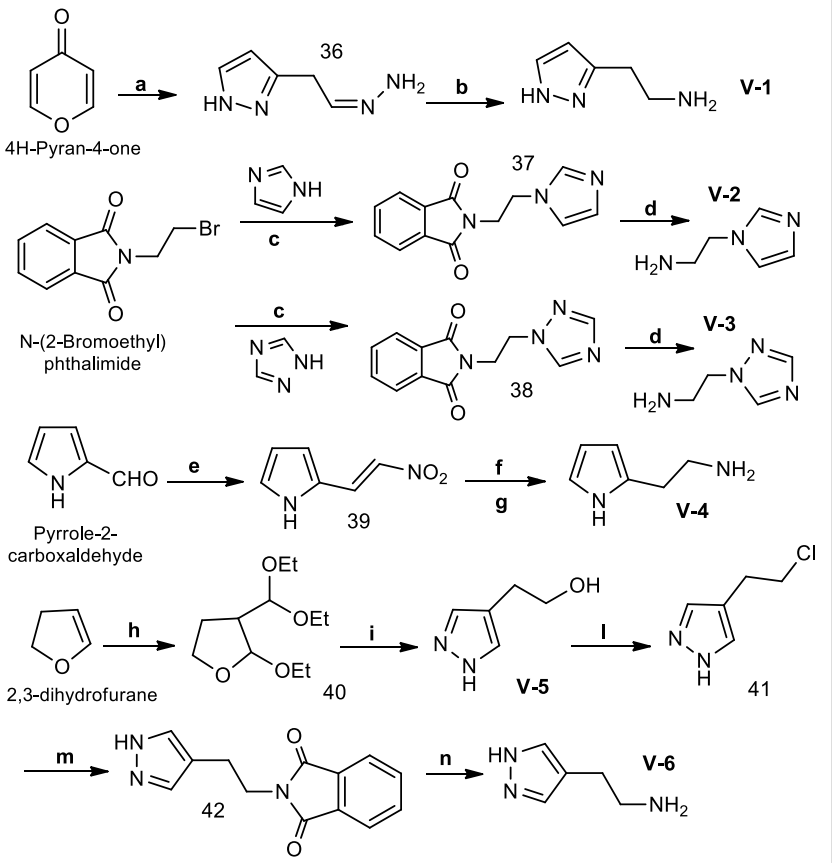

In particular, the product **V-2** represent a direct isomer of HST where the side chain is connected to one of the imidazole nitrogen atoms. With nitromethane we also elongated the chain of pyrrole-2-carboxaldehyde and we then reduced in two steps the conjugated nitro intermediate **39** (**39a** is the saturated analogue), isolating the pyrrole analogue **V-4**[128]. We followed a different pathway to obtain **V-6**[125]. We took advantage of the reactivity of the double bond of dihydrofurane to prepare the intermediate **40**, the analogue of a protected di-aldehyde. The $FeCl_3$-catalysed addition of triethyl orthoformate was initially problematic to perform but after several attempts we isolated the desired furane **40** with fractional distillation. The masked aldehydes reacted then with hydrazine giving the hydroxyethyl pyrazole **V-5**[125]. Thanks to its similarity to HST, we decide to test the potential activator property of this intermediate too. We then transformed the OH group into a chlorine and through the Gabriel synthesis of primary amine we finally obtained the pyrazole **V-6**[125].

Again from the evidence that the activator properties of HST are expressed by the hetorocycle, we also prepared the two slightly modified derivatives **V-7** and **V-8** possessing an oxadiazole ring. (**Scheme 3.17**) We built the 1,3,4-oxadiazole scaffold of **V-7** from N-Boc-β-alanine and acetic hydrazide[129], cyclizing the intermediate **43** with PPh_3 and I_2.

Scheme 3.17

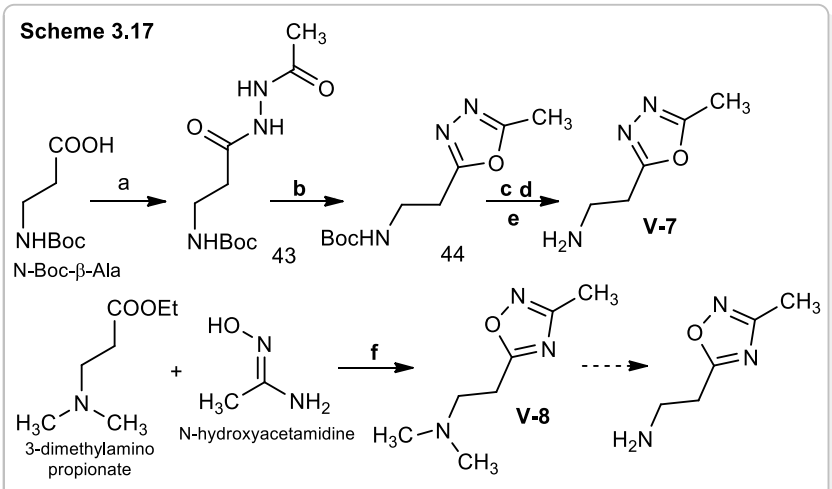

a) EDC, $CH_3CONHNH_2$. CH_3CN **b)** PPh_3, I_2, NEt_3, CH_2Cl_2; **c)** TFA, CH_2Cl_2; **d)** $NaOH_{sol}$; **e)** Oxalic acid, AcOEt; **f)** NaH, THF

We afterward cleaved the Boc protection of **44** and we isolated **V-7** as oxalate salt. We instead synthesize the 1,2,4-oxadiazole **V-8** with a one-pot reaction among 3-dimethylamino propionate and N-hydroxyacetamidine (step **f**, **scheme 3.17**). Our purpose was also the preparation of the primary amine analogue of **V-8**, which is described in the literature starting from this compound. Unfortunately, all our attempts were unsuccessful.

The preparation of the series **VI** of CLO analogues is reported in **scheme 3.18**. We prepared most of the derivatives from the two key-intermediates **VI-2** and **47**. Our synthetic procedure started from imidazolidine-2-thione, we therefore decided to also prepare a small set of thio-imidazoline to investigate the effect of the substitution of the exocyclic amino group with a mercapto one. Treating the starting material with benzyl bromide we obtained its analogue **VI-1** while with CH_3I we made the corresponding S-methyl derivative **VI-2**[130], the first key-intermediate. Just before the reaction to prepare the imidazolines we decided to acylate the endocyclic sp^3 nitrogen with acetic anhydride, isolating **VI-3**, which could serve also as intermediate for the synthesis of **VI-13**. We then used the procedure reported by Aoyagi N. et al.[131] to convert the thio-derivative **VI-2** into the different amino-imidazolines. Heating **VI-2** together with the desired amine the nucleophilic substitution of the methylthio group with the amino one occurred. Depending on the amines, we observed different reactivity properties: while we did not have any problem to prepare **VI-4 – 6**, the situation was different for some of the other products. We synthesize **VI-7** and **VI-8** boiling **VI-2** directly into, respectively, *(S)* or *(R)*-α-methylbenzylamine. When we used secondary amines the reaction was slower and we isolated **VI-9**[131] and **VI-10** only in low yields. Additionally, when we performed the reaction with dibenzylamine we did not observed the formation of the predicted imidazoline but we only isolated the product **VI-11** (inset in the upper part of

scheme 18), derived from the combination of two molecules of starting material **VI-2** and one of the amine; a similar product (**VI-11a**) was also observed in the reaction of *(S)*-α-methylbenzylamine and **VI-2** in THF.

We also did several attempts to react aniline with **VI-2** or with **VI-3**[30] but without success. Since the methylation of the the endocyclic sp^3 nitrogen of **VI-2** (step **e**) was another failure, we therefore decided to investigate an alternative route to obtain these two products. By boiling guanidine directly into ethylenediamine we first prepared the imidazoline **VI-12**[132] but we also used this diamine and its N-methyl-analogue to prepare the intermediates **45a** and **45b**: from **45a** and p-toulensulfonyl chloride (**step h**) we succeeded to obtain the N-phenyl imidazoline **VI-13**[133] while we directly cyclized **45b** to prepare the 2-thione **46** that we finally transformed into **47**[134]. We afterwards used the already described approach to obtain the other imidazolines **VI-14 – VI-24**. The only difference was that we mostly suspended **47** directly into the amine, thus avoided the solvent and generally increased the yields.

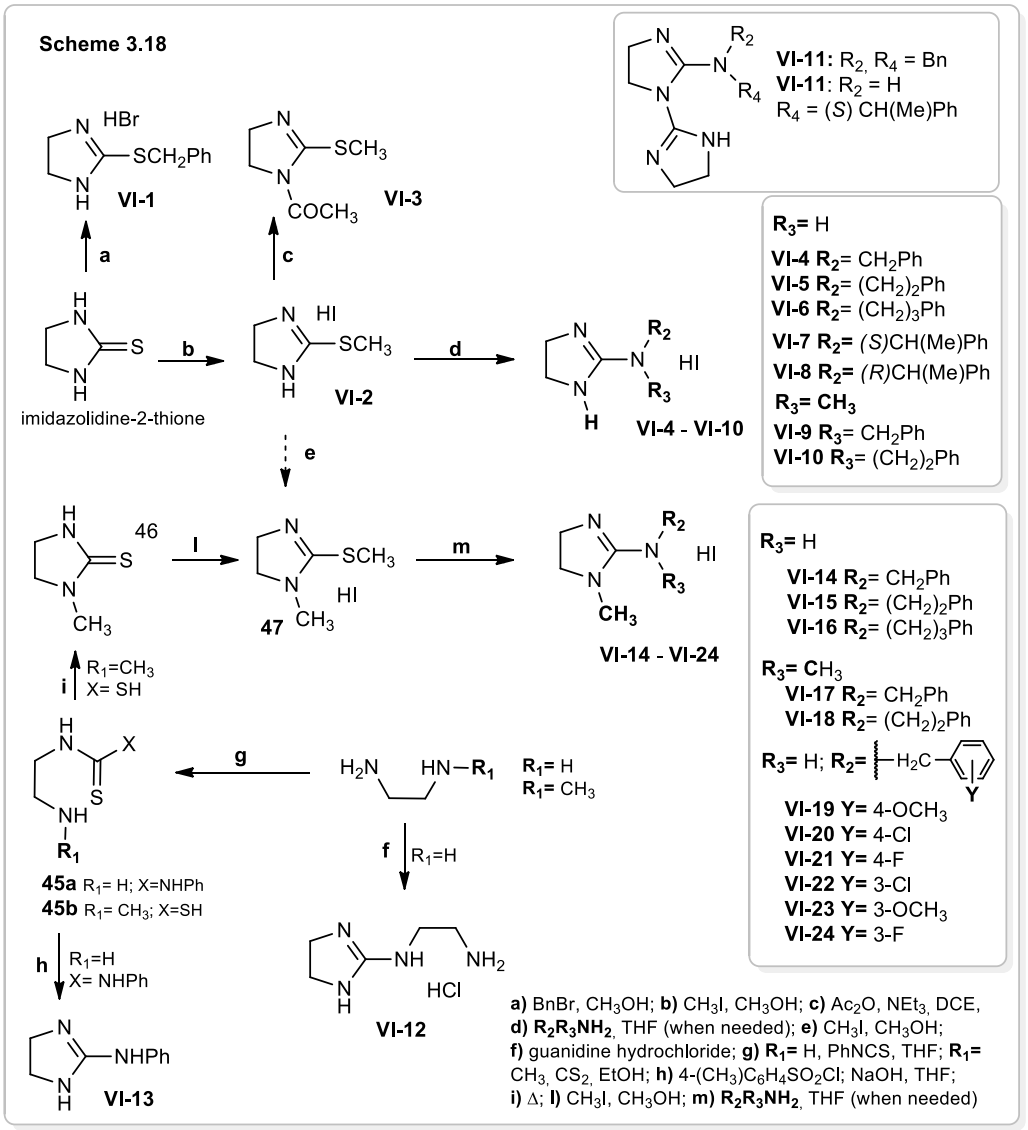

4. Results

The enzymatic tests on Carbonic Anhydrases isoforms have been performed by the group of Prof. Supuran at the Department of Neurosciences, Psychology, Drug Research and Child Health at the University of Florence.

4.1 Carbonic Anhydrase Inhibition

4.1.1 Benzylpiperazines, I-A and I-B series

The inhibitory activity of the compounds belonging to the **I-A, I-B, II-A**, **II-B**, **II-C** , **III-A, III-B** series were assessed on hCAs isoforms using a stopped flow CO_2 hydrase assay[7]. The ubiquitous cytosolic hCA I and hCA II, the membrane-anchored hCA IV, and the transmembrane, tumor-associated hCA IX were chosen for biological testing. Results are reported in **Table 4.1**, **4.2** and **4.3**; the standard sulfonamide inhibitor acetazolamide (AAZ) was used as reference compound.

All the synthesized compounds were able to inhibit the four hCA isoforms, with K_i values ranging from nanomolar to micromolar. The **I-A** and **I-B** series differ for the position of the ZBG, which in the **I-A** series is on the proximal N atom, close to the stereogenic centre, while in the **I-B** series is placed on the distal N atom. The first important information we gained is related to the ZBG: the position of the pharmacophore was not clearly influencing the activity since the compounds belonging to both **I-A** and **I-B** series were potent inhibitors, without any activity preeminence of a series on the other one.

All the inserted substituents were well tolerated but their presence was not essential for the activity on hCA I, II and IV since both the NH derivatives **I-A2** and **I-B1** displayed potency in the low nanomolar range against these isozymes. Also the other derivatives of both the series were potent inhibitors of these isoforms while, on the contrary, most of them showed a poor activity against hCA IX. Nevertheless, even if it was difficult to see a clear-cut influence of the characteristics of the N-substituents (alkyl *vs* acyl/sulphonyl, aromatic *vs* aliphatic, or size) on activity, the R_1 and R_2 groups were able to effectively modulate potency and selectivity, combined with the proper absolute configuration of the piperazine stereogenic centre.

To evaluate the effect of the stereogenic centre we calculated the Eudismic Ratio (ER, defined in **Table 4.1** as the ratio between the K_i of the *S*-enantiomer divided by the K_i of the *R*-one). A wide range of values can be appreciated, going from 0.011 [hCA-IX, (*S*) **I-A1**/(*R*) **I-A1**] to 146 [hCA-I, (*S*) **I-B3**/(*R*) **I-B3**]. Trying to interpret the complicated structure-activity relationships (SAR), we noticed that hCA-I and II do not show a clear *S*/*R* preference while some preferences could be found on hCA IV and hCA IX for, respectively, the *R* and *S* absolute configuration.

By closely looking to the activity of compounds on each isoform, we inferred the following SAR:

hCA I) Several compounds are potent inhibitor of this isoform, with K_i values < 10 nM: (*R*) **I-A6** (K_i 2.9 nM), (*R*) **I-A8** (K_i 3.6 nM), and (*R*) **I-B3** (K_i 3.9 nM) were the most potent. As mentioned before, the absolute configuration was not clearly influencing the of activity but for some compounds we anyway observed high ER values: **I-A2** (R_2 = H, ER 48), **I-A8** (R_2 = $PhSO_2$, ER 92), **I-B3** (R_1 = CH_3, ER 146) and **I-B6** (R_1 = $PhCH_2CO$, ER 82), the eutomer being the *R*-enantiomer for all of them. Lower enantioselectivity was associated to compounds such as **I-B2** and **I-B9** (0.06 and 0.11, respectively) for which the eutomer was the *S*-enantiomer. Regarding the bis-sulfonamide **I-B9**, we could notice that the second SO_2NH_2 group increased activity on the *S*-isomer of compounds **I-A5** and **I-B5** (14 and 5 times, respectively) while it left the *R*-one unaffected.

hCA II) On this isoform the most potent derivative was the bis-sulfonamide (*S*) **I-B9** (K_i 2 nM), which was 6-times more potent than acetazolamide (K_i 12 nM); several other compounds had K_i values ≤ 10 nM, showing a potency in the same range as the reference inhibitor. We again noticed the lack of a clear dependence of activity from the absolute configuration: only the N-methyl derivatives **I-A3** (ER = 48) and **I-B3** (ER = 61) and the NH analogue **I-A2** (ER = 33) possessed relevant ER values. A second sulfonamide group increased activity on both N-benzoyl analogues (compare **I-B9** with **I-A5** and **I-B5**); taking into consideration the S isomer *(S)* **I-B9**, K_i = 2 nM), the effect was more evident on the compound bearing a distal N-benzoyl group [*(S)* **I-A5**, K_i = 61.3] than on the other one [*(S)* **I-B5**, K_i = 15 nM] .

hCA IV) On this isoform all *R*-enantiomers were more active than the *S*-ones, apart for compound **I-A5** (ER= 0.06). Here we derived high ER values for both the *N*-methyl derivatives **I-A3** and **I-B3** again (95 and 86, respectively), the phenylacetate compound **I-B6** (ER = 143) and the methanesulfonyl amide **I-A7** (ER = 36). On this isoform, the most potent was is the *N*-methyl derivative (*R*) **I-B3** with a K_i of 1.7 nM. Interestingly, almost all the *R*-isomer of the various derivatives displayed K_i values in the low nM range, showing a much higher potency than the reference compound acetazolamide. We could therefore assume that the *R*-isomers are better accomodated on hCA IV binding site. Two compounds belonging to the **I-A** series, (*R*) **I-A1** (K_i 66.9 nM) and (*R*) **I-A5** (K_i 133.4 nM) are the two less potent *R*-isomers.

hCA IX) Compared to the others, this isoform is less sensitive to the activity of the benzylpiperazines. Only few of them showed potency in the same range as acetazolamide [(*S*) **I-A1** (K_i = 27.9 nM); (*S*) **I-A7** (K_i = 31.6 nM); **AAZ** (K_i = 25 nM)] while the others were from 3 to 105 times less potent. On this isoform all the *S*-enantiomers are inhibitors equally or more effective than the *R*-ones (ER ≤ 1), with the exception of the phenylsulfonyl amide **I-B8** (ER = 4). We also measured a high enantioselectivity for the *N*-benzyl derivative **I-A1**, for which the *S*-enantiomer was 91 times more potent than the R-one. The methanesulfonyl

group was the best substituent in both **I-A** and **I-B** series [(*S*) **I-A7** (Ki=31.6 nM) and (*S*) **I-B7** (K_i= 74.4 nM)]. The introduction of a second sulfonamide group on (*R*) **I-A5** causes a 10-fold reduction of potency, while the effect on (*R*) **I-B5**, (*S*) **I-B5** and (*S*) **I-A5** was marginal.

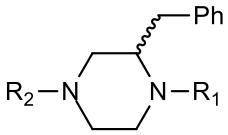

Table 4.1: Inhibitory activity of the enantiomers of the compounds belonging to **I-A** and **I-B** series on the human CAs isoforms I, II, IV and IX. The standard sulfonamide inhibitor acetazolamide (AAZ) was used as reference compound.

			K_i[c] nM							
N	**R_1** [a)]	**R_2** [a)]	**hCA I**	ER[b)]	**hCA II**	ER[b)]	**hCA IV**	ER[b)]	**hCA IX**	ER[b]
(S) I-A1	ZBG	CH_2Ph	88.9	0.20	46.0	0.26	79.3	1	27.9	0.01
(R) I-A1			455.7		176		66.9		2639.1	1
(S) I-A2	ZBG	H	421.9	48	264.5	33	75.4	13	93.0	0.06
(R) I-A2			8.7		8.1		5.6		1442	
(S) I-A3	ZBG	CH_3	707.0	19	358.6	48	342.5	95	1431.9	1
(R) I-A3			37.7		7.6		3.6		1206.9	
(S) I-A4	ZBG	CH_3CO	9.6	0.44	7.7	0.20	6.0	2	170	1
(R) I-A4			21.8		38.9		2.9		197.8	
(S) I-A5	ZBG	PhCO	82.8	2	61.3	2	7.8	0.06	227	1
(R) I-A5			44.3		33.4		133.4		205.0	
(S) I-A6	ZBG	$PhCH_2CO$	29.5	10	6.8	1	5.4	2	191	1
(R) I-A6			2.9		4.8		2.3		166.1	
(S) I-A7	ZBG	CH_3SO_2	186	6	161	21	72.5	36	31.6	0.14
(R) I-A7			29.0		7.5		2.0		232.3	
(S) I-A8	ZBG	$PhSO_2$	330.3	92	59.3	8	7.8	2	83.0	0.07
(R) I-A8			3.6		7.6		3.6		1206.9	
(S) I-B1	H	ZBG	60.7	1	83.4	5	29.3	6	225.1	0.13
(R) I-B1			49.4		15.4		4.6		1717.9	
(S) I-B2	CH_2Ph	ZBG	22.1	0.06	8.3	0.14	73.3	32	249.2	0.59
(R) I-B2			380.2		60.7		2.3		418.5	
(S) I-B3	CH_3	ZBG	568.6	146	327.8	61	146	86	1716.3	1
(R) I-B3			3.9		5.4		1.7		1811.1	
(S) I-B4	CH_3CO	ZBG	8.8	0.16	7.6	0.24	66.8	20	83.7	0.37
(R) I-B4			55.6		32.0		3.3		227.3	
(S) I-B5	PhCO	ZBG	30.7	0.57	15.0	0.29	68.0	17	245	0.15
(R) I-B5			53.9		52.5		4.0		1659.0	
(S) I-B6	$PhCH_2CO$	ZBG	542.6	82	92.7	13	371.0	143	177	0.12
(R) I-B6			6.6		7.0		2.6		1520.4	
(S) I-B7	CH_3SO_2	ZBG	7.9	0.26	6.0	0.19	79.7	4	74.4	0.41
(R) I-B7			30.6		32.3		19.0		181.1	
(S) I-B8	$PhSO_2$	ZBG	245	5	95.1	15	62.2	7	1589.1	4
(R) I-B8			51.6		6.2		8.7		359.6	
(S) I-B9	ZBG	ZBG	6.1	0.11	2.0	0.25	139	27	104	0.04
(R) I-B9			57.2		7.9		5.1		2625.5	
AAZ	-	-	250	-	12	-	74	-	25	-

[a)]ZBG (Zinc Binding Group): $COC_6H_4SO_2NH_2$; [b)]ER(eudismic ratio): Ki (S-enantiomer)/Ki (R-enantiomer); [c]Errors in the range of ±5-10 % of the reported values (data not shown) from three different assays;

As far as isoform selectivity is concerned, some compounds showed some selectivity for the hCA IV, isoform mainly associated to ocular diseases, cancer cell proliferation but also other pathologic conditions[135–137]. Importantly, (*R*) **I-B2** showed an interesting profile against this isoform displaying an activity 165-, 26- and 182-fold higher than on hCA-I, II and IX, respectively. A similar profile was also expressed by (*R*) **I-B5**, showing a 13-fold selectivity for CA-IV *vs* hCA-I and II, and 414-fold *vs* hCA-IX.

Since both hCA-II and IV have been proposed as drug targets for glaucoma, and also hCA-I may have a role in ocular pathologies, we selected compounds (*R*) **I-A2** and (*R*) **I-B3** for in vivo tests (discussed in the last section of this chapter). As a matter of fact, they were equipotent on the hCA I, II and IV isoforms while their activity was respectively 165 and 335 times lower on hCA-IX.

4.1.2 Piperazine and aminopiperidine, II-A, II-B and II-C series

The results are reported in **Table 4.2**. Together with acetazolamide (AAZ), both the enantiomers of the closely related **I-A1** and **I-B2** were also taken as reference compounds.

We thought that the activity of the unsubstituted piperazine **II-A1**, already published for hCA I, II and IX[138], could help us to understand the contribution of the C-benzyl moiety of compounds **I-A1** and **I-B2**. We therefore measured its inhibition profile also on hCA IV, finding that it was almost equipotent with (*R*) **I-A1** but less selective with respect to the other tested isoforms.

To check the importance of ring size the piperazine moiety, we expanded the scaffolds to diazepane (**II-A2**) or contracted to imidazolidine (**II-A3**). These modifications led to a substantial reduction of potency on hCA IV (about 12-15 times) and on CA IX (12-23 times). The activity on hCA I and II was not modified by ring expansion while it was improved by ring contraction, since imidazolidine **II-A3** was, respectively, 8 and 5 times more potent than piperazine **II-A1**. Therefore, these modifications introduced in **II-A2** and **II-A3** some selectivity toward hCA I and II.

We then focused the attention on the N-benzyl moiety, preparing the compounds **II-A5 – 10** that carry different substituents in position 3 and 4 on the aromatic ring. Our aim was indeed to investigate the effect of aromatic substitution on potency or selectivity.

On **hCA I** only the 4-Cl and the 4-NO_2 group moieties were able to influence the potency. In fact, **II-A6** (4-Cl) was **11** times less active than **II-A1** while **II-A8** (4-NO_2) is 3 times more active. On **hCA IV**, only 4-NO_2 and 4-NH_2 groups were tolerated, since **II-A8** and **II-A10** were only twice less potent than **II-A1** whilst all the other substituents decreased the activity from 11 to 53 times. On **hCA IX**, the aromatic substitution did not substantially modify the activity. The only exception is the 3-OMe group (**II-A4**) which decreased 23 times the activity of **II-A1**.

On **hCA II** the aromatic substitution slightly influenced the activity. We only observed 3-4 times increase or decrease of K_i with compounds **II-A4** (3-OMe) and **II-A8** (4-NO_2) that show subnanomolar Ki values, similarly to the already described **II-7A**.
We can conclude that the aromatic substitution, irrespective of the position and electronic characteristics of the group, influence the activity profile of **II-A1.** The compounds **II-A4 - 10** were indeed more active on hCA I and II with respect to hCA IV and IX and the derivative **II-A4** (3-OMe) showed the best selectivity ratios, being 8, 248 and 769 times more active on hCA II than on hCA I, IV and IX, respectively.

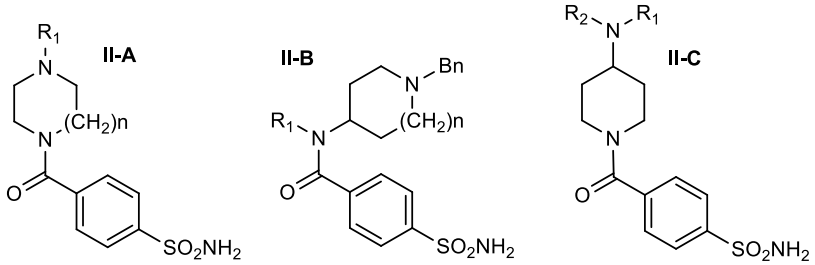

Table 4.2. Inhibitory activity of compounds belonging to the **II-A, B** and **C** series on hCA isoforms I, II, IV and IX. The standard sulfonamide inhibitor acetazolamide (AAZ), **I-A1** and **I-B2** were used as reference compounds.[a]

N	R_1	R_2	n	K_I[a] (nM)			
				hCA I	hCA II	hCA IV	hCA IX
(R) I-A1				380.2	60.7	2.3	418.5
(S) I-A1				22.1	8.3	73.3	249.2
(R) I-B2				455.7	176	66.9	2639
(S) I-B2				88.9	46.0	79.3	27.9
II-A1[b]	Bn	-	1	6.8[c]	3.0[c]	4.2	33.1[c]
II-A2	Bn	-	2	7.7	2.3	52.9	407.6
II-A3	Bn	-	0	0.8	0.6	63.9	750.7
II-A4	3-OMe-Bn	-	1	7.2	0.9	224.9	761.4
II-A5	3-NO_2-Bn	-	1	6.4	9.5	48.7	40.4
II-A6	4-Cl-Bn	-	1	54.8	13.3	89.4	48.4
II-A7[b]	4-F-Bn	-	1	0.69[c]	0.50[c]	68.4	45.1[c]
II-A8	4-NO_2-Bn	-	1	2.4	0.77	9.7	52.3
II-A9	3-NH_2-Bn	-	1	7.4	6.9	74.9	36.3
II-A10	4-NH_2-Bn	-	1	5.8	3.5	9.1	40.2
II-B1	H	-	1	0.9	0.5	17.5	19.7
II-B2	Me	-	1	7.9	7.9	272.0	353.7
II-B3	H	-	0	36.2	4.4	25.3	21.6
II-C1	H	Boc	-	6.5	3.3	42.4	75.7
II-C2	H	Bn	-	39.9	44.5	92.2	38.4
II-C3	Me	Bn	-	9.3	8.9	37.4	129.6
II-C4	Cbz	Bn	-	56.1	86.4	632.5	421.4
AAZ		-	-	250.0	12.0	74.0	25.07

[a]Errors in the range of ±5-10 % of the reported values (data not shown) from three different assays;
[b] From ref[138]

We then tested the effect of moving one nitrogen atom of **II-A1** outside the ring by studying the 4-aminopiperidine derivatives **II-B1-3** and **II-C1-4**.

By shifting the sulfamoylbenzamide group outside the six-membered ring we obtained compound **II-B1**, which showed subnanomolar potency on hCA I and II and 2-digit nanomolar activity on hCA IV and IX. Its N-methyl derivative **II-B2** show a similar selectivity profile but a decreased potency on hCA IV and IX. We supposed that this effect may derive from the removal of a H-bond donor group or to steric hindrance. Decreasing ring size was not productive, since **II-B3** was less potent than **II-B1** and show only a slight preference for hCA II (5-8 times) over the other tested isoforms.
Finally, an exocyclic N-benzyl group was detrimental for activity on hCA I, II and IV. In fact, the activity on these isoforms of **II-C2** was respectively 6, 15 and 22 times less potent when compared to **II-A1**, resulting in a loss of selectivity. When a Me group was added on the NH moiety of **II-C2** to give **II-C3,** the potency was restored on hCA I and II. We therefore assumed that the addition of a NMe group improves the activity on hCA I, II and IV (but not hCA IX) by increasing lipophilic interactions. We also tested the synthetic intermediates **II-C1** and **II-C4.** The good activity of **II-C1** suggested that a basic N atom in this part of the molecule was not required, at least on hCA I and II, but a Cbz group may have been too large thus producing steric hindrance on all the four isoforms. The structure-activity relationships are summarized in **figure 4.1**.

Figure 4.1: SAR of the II-A. B and C series

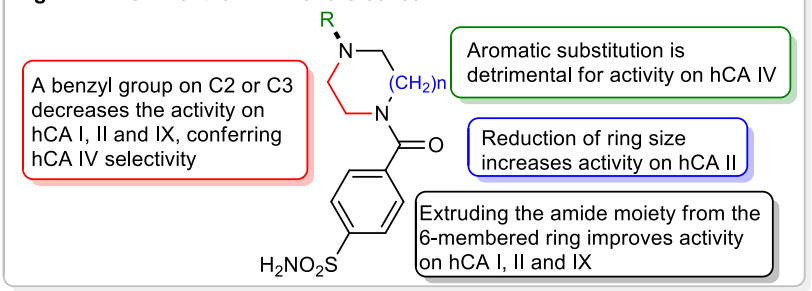

4.1.3 Hydroxyethylpiperazines, III-A and III-B series

The results of the **III-A** and **III-B** series of hydroxyethylpiperazine are reported in **table 4.3.** As already mentioned in the chemical part of this thesis, these compounds derived from the side chain modification of the benzylpiperazine series **I-A** and **I-B**. Thanks to the promising results of the amines *(R)* **I-A1** and *(R)* **I-B3** as Intra Ocular Pressure (IOP) reducing agents (discussed at the end of this chapter), we decided to limit the series to the basic N-derivatives (-H, -CH_3, -CH_2Bn) in order to prepare water-soluble HCl salts.

Even if not yet completed (both enantiomers of **III-B3** still need to be synthesized), the **III-A** and **III-B** series already showed some new interesting peculiar characteristics and the results are discussed in comparison with the basic derivatives **I-A1 – I-A3** and **I-B1 – I-B3.**

On **hCA I** the hydroxyethylpiperazines had K_i values similar to Acetazolamide; only (S) **III-B1** was about 3 times more active than the reference. In general the compounds are also less

potent than the parent benzyl analogues: as a matter of fact, while in the **I** series the K_i values ranged from 8.7 nM (*R* **I-A2**) to 707 (*S* **I-A3**), almost all the hydroxyethyl piperazines displayed only three-digits nanomolar K_i values. Since the hCA I is widespread in the body and many side effects could derive from its off-target inhibition, this may represent a positive peculiarity of the **III-A** and **III-B** series.
As already verified for the previous series of chiral piperazines, on **hCA II** only few compounds are more active than acetazolamide. The exception is **III-B1** whose enantiomers showed low nanomolar potency (*S* 3.9 nM; *R* 8.9 nM). All other compounds have K_i values 3-10 times higher than the reference compound. A close look to isomers **III-A1** and **III-B1** shows that compound *(S)* **III-B1** (K_i= 3.9 nM) was 17 times more active that its correspondent positional isomer *(S)* **III-A1** (K_i= 65.9 nM). This finding suggests that the best structural arrangement is with the ZBG placed on the N-atom away from the stereogenic center; this is more evident when the stereogenic centre is in the *S* configuration.

On **hCA IV** all the hydroxyethylpiperazines are more potent than acetazolamide and several of them have K_i values lower than 10 nM. This inhibitory profile confirms that this isoform is the most sensitive to our piperazine-based CAIs. The activity seems not to be modulated by the nature or the position of the substituents since all the derivatives of **III-A** and **III-B** series display high activity with K_i values in the low nanomolar range.

The substitution of the benzyl moiety with the hydroxyethyl chain led to a strong increase of activity on **hCA-IX**, suggesting that a hydrophilic group as side pendant could be favourable to target this isoform. In fact, while both **I-A3** enantiomers were almost inactive on this isozyme (**Table 4.1**) the replacement of the side chain to obtain **III-A3** increased the potency, 52 times for the *R*-isomer and 82 for the *S*-one (*R* **III-A3** K_i=17.1 nM; *S* **III-A3** K_i=23.3 nM). This may imply that to target the cancer-associated isoform hCA IX the chiral side chain should be hydrophilic, endowed with a high degree of flexibility and have some H-donor/acceptor groups.

As far as chirality is concerned, only partial information can be derived from these biological results. In fact, the **III-B** series suffers from low enantiomeric excess (**figure 5**, chapter 3), therefore the low eudismic ratios are not surprising. On the contrary, **III-A1** has a 90% enantiomeric excess, and the same is for its hydrogenated derivative **III-A2**, since this reaction does not involve racemization; however, both compounds have ER values close to unity. This suggests that the flexible and hydrophilic hydroxyethyl chain can be easily accommodated into the binding pocket, more easily than a bulky benzyl moiety, reducing the importance of the stereogenic center. To verify this hypothesis, it will be important to solve the enantiomers of the compounds belonging to the **III-B** series.
As far as selectivity is concerned, the replacement of the benzyl side chain with a hydroxyethyl moiety changed the selectivity profile of the piperazine derivatives: compounds belonging to the **III-A** and **III-B** series are in general more active on hCA IV and IX with respect to hCA I and II. Among the new compounds, (*R*)-**III-B2** shows the most

interesting selectivity ratios, being a low nanomolar hCA IV inhibitor (K_i 4.8 nM) 59, 27 and 21 times more potent on this isoform than on hCA I, II and IX, respectively.

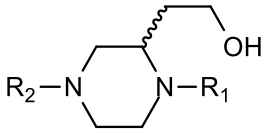

Table 4.3: Inhibitory activity of the enantiomers of the compounds belonging to **III-A** and **III-B** series on the human CAs isoforms I, II, IV and IX. The standard sulfonamide inhibitor acetazolamide (AAZ) was used as reference compound.

			K_i[c] (nM)							
N	R_1	R_2	hCA I	ER[b]	hCA II	ER[b]	hCA IV	ER[b]	hCA IX	ER[b]
(S) **III-A1**	ZBG[a]	CH_2Ph	348.5	1.41	65.9	1.96	18.5	0.76	25.3	1.83
(R) **III-A1**			246.9		33.6		24.2		13.8	
(S) **III-A2**	ZBG[a]	H	124.6	0.61	79.6	0.83	9.0	0.60	34.5	0.73
(R) **III-A2**			203.0		96.4		15.1		47.3	
(S) **III-A3**	ZBG[a]	CH_3	164.7	1.20	68.0	1.23	17.0	0.70	17.1	0.73
(R) **III-A3**			137.0		55.5		24.2		23.3	
(S) **III-B1**	CH_2Ph	ZBG[a]	89.2	0.72	3.9	0.44	6.8	1.55	65.8	0.78
(R) **III-B1**			123.1		8.9		4.4		87.3	
(S) **III-B2**	H	ZBG[a]	216.6	0.77	88.5	0.69	5.2	1.08	101.5	1.01
(R) **III-B2**			281.6		128.6		4.8		100.3	
AAZ	-	-	250	-	12	-	74	-	25	-

[a)]ZBG (Zinc Binding Group): $COC_6H_4SO_2NH_2$; [b)]ER(eudismic ratio): Ki (S-enantiomer)/Ki (R-enantiomer);
[c]Errors in the range of ±5-10 % of the reported values (data not shown) from three different assays;

4.1.4 CA-HDAC hybrids

The stopped-flow method[7] was used to determine the inhibitory potency of the synthesized hybrids on carbonic anhydrase IX and XII, which are overexpressed in hypoxic tumors; the ubiquitous I and II isoforms were taken as comparison to assess selectivity. Acetazolamide was taken as reference compound; SAHA is reported to be devoid of activity on hCA II[139]. At the moment, we don't have the result on HDAC inhibition because the biological tests need to be completed.

The results for CA inhibitions are shown in **table 4.4**. Since all molecules are coumarin derivatives, the compounds were incubated for 6h. In fact, as stated in the introduction, coumarins block carbonic anhydrases activity after the enzyme has hydrolyzed the ester function, owing to its esterase activity; the hydrolysis is usually complete after this time.

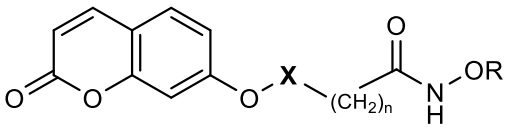

Table 4.4: Inhibition data of hCA I, hCA II, hCA IX and hCA XII with compounds **IV-1-IV-5** and the standard sulfonamide inhibitor acetazolamide (AAZ). Unless otherwise stated, compounds were incubated for 6h with the enzyme.

Cmp	X	n	R	[a]Ki (nM)			
				hCA I	hCA II	hCA IX	hCA XII
IV-1	CH_2CONH	7	H	216.7	>10000	31.5	55.3
IV-2	CH_2CONBn	6	H	3624.0	>10000	30.8	75.0
IV-3	CH_2CONH	6	H	709.5	>10000	29.0	68.4
IV-4	-	6	H	670.1	>10000	108.5	46.7
IV-5	-	6	$COCH_3$	181.7	>10000	23.6	36.9
				295.1[b]	>10000[b]	153.3[b]	274.4[b]
AAZ				250	12	25	5.7

[a]Errors in the range of ±5-10 % of the reported values (data not shown) from three different assays;
[b]After 15 min incubation

All the tested compounds did not show activity on the physiologically dominant cytosolic isoform **hCA II**, confirming the inactivity of SAHA on this isozyme. On the contrary, on the widely distributed **hCA I** the compounds behaved as weak inhibitors, with K_i values ranging from 181.7 to 3624 nM, thus being equally (**IV-1**, **IV-5**) or 2-14 times less active (**IV-2** - **IV-4**) than the reference compound acetazolamide. As expected, the compounds were much more potent on the transmembrane hCA IX and XII isoforms, which are known to be very sensitive to coumarin derivatives[140]. On **hCA IX**, the compounds were equipotent with AAZ, with the exception of **IV-4,** whose K_i value was 4 times higher. On **hCA XII** all compounds showed two-digits nM K_i values, being 6-13 times less potent than AAZ. Compounds **IV** generally showed similar potency on both hCA IX and XII isoforms, thus displaying some selectivity for these isozymes over hCA I and II: the most interesting compound was **IV-2**, which showed one of the lowest K_i value on hCA IX (Ki 30.8 nM) while being 2, 118 and >324 times less potent on hCA XII, I and II, respectively. Therefore, as far as the CA inhibitory activity is concerned, the compound which could be advanced to further studies, based on its selectivity profile, is **IV-2**; the biological tests on HDAC will tell us the real potential of this compound.

As said before, the synthesized molecules have been tested on CA isoforms with a 6 h incubation time reasoning that the inhibitory activity on CA IX and XII could be delivered by the coumarin moiety. However, these derivatives possess also another Zn binding group, the hydroxamate moiety, which is known to coordinate the CA metal ion[141]. Several hydroxamate CA inhibitors are known from the literature, but usually they also contain a sulfonamide moiety which is a more effective Zn-binding group for CA isozymes[142,143]. We tried to address the problem on which, in our molecule, could be the pharmacophore for CA inhibition by preparing the O-acetyl-hydroxamate **IV-5**. The $COCH_3$ group should

change the coordinating and H-bond donor/acceptor properties of the terminal OH, possibly introducing some differences in the inhibitory activity. This moiety was reported in a patent describing some HDAC inhibitors[124], which were found to be extremely potent despite the theoretical reduction of the coordinating ability of the hydroxamate moiety within the HDAC binding site[68]. After 6 h incubation, the potency on hCA I and hCA IX was about 4 times higher than the unsubstituted **IV-4** but remained unchanged on hCA XII. When the compound was incubated with the enzyme for a much shorter time (15 min) activity was decreased, only slightly on hCA I but in a more evident way on hCA IX and XII, on which the K_i values were 6-7 times higher than with 6 h incubation. These data seem to point to a different mechanism of inhibition according to the isoform: on hCA I the hydroxamate moiety should be involved in the metal coordination, because Ki values are similar after 15 min or 6 h incubation time, and not so different from the parent **IV-4** derivative. On the contrary, as expected, on hCA IX and XII there is a larger variation of activity at different incubation times, suggesting that after few minutes the hydrolysis of the pharmacophoric coumarin moiety is not complete. However, the picture is complicated by the fact that the esterase activity of these isoform could have also the O-acetylhydroxamate moiety as substrate. Moreover, the X-ray structure of the adduct between hCA II[144] and trifluoroacetohydroxamic acid showed that such a small molecule bound the Zn ion by means of the N atom, and for this reason should not be negatively affected by the presence of the O-acetyl moiety; however, a larger molecule such as those reported in this thesis may find a different coordination mode within the binding site. Therefore, the modification of the hydroxamate moiety did not cast light on the binding mode of the new substances, and probably only an X-ray study could tell which is the pharmacophore for CA inhibition. Attempts to crystalize hCA IX with **IV-2** will be performed soon.

4.2 Carbonic Anhydrases Activation

A stopped-flow method[7] has been used for assaying the CO_2 hydration activity catalyzed by different CA isoforms (I, II, IV, VA, VII and XIII); the results are expressed as K_A (activation constant, μM) and are reported in **Tables 4.5 - 4.8.** The mitochondrial hCA VA has been selected since it is the isoform, together with hCA XIV, most sensitive to HST[109,145]; while the cytosolic hCA IV and VII isoform have been selected because they are predominantly expressed in the brain. hCA I, II and XIII, all cytosolic and widely expressed, have been taken as comparison.

4.2.1 Histamine analogues

In **Table 4.5** the results of the **V** series of compounds (histamine analogues) on hCA I, II, VA, VII and XIII are reported. Differently from the reference compound, none of the compounds was active on hCA II and on hCA XIII; on the former also **HST** had low potency (K_A 125

μM) while on the latter **HST** showed a K_A value in the low μM range. On the other tested isoforms, most of the new compounds showed activity in the low-medium μM range.

The tested compounds displayed the highest potency on hCA I, with the exception of the oxygenated heterocyclic derivatives **V-7** and **V-8**, which resulted inactive up to a 150 μM concentration; compound **V-4** was equipotent with **HST** while the others were 6-13 times less potent than the reference molecule. As mentioned in the previous sections, the terminal amino group seems not essential for activity: indeed, on hCA I the alcohol **V-5** resulted 13 times more potent than the amino derivative **V-6**.

The X-ray structures of imidazole compounds binding to hCA II suggest that the imidazole nitrogen atoms can serve as H-bond acceptor (**HST**, **figure 4.1a**) or donor (L-histidine, **figure 4.1b**), in both cases the atom involved being Nτ (tele). Pyrazoles **V-1** and **V-6** carry a N atom in a position equivalent to the Nτ, and as well as the imidazole counterpart can tautomerize, they were 5 and 13 times less potent than **HST**. Also azoles **V-2** and **V-3** have a H-bond acceptor N in the equivalent position, and were 5 and 6 times less active, respectively, than **HST**. Pyrrole **V-4** can be only H-bond donor, and its N atom is in a position equivalent to Nπ (pros); this compound was equipotent with **HST**. These observations are difficult to rationalize in terms of Structure-Activity Relationships, but we must keep in mind that such small molecules can be accommodated in different ways within the binding site, and only a crystallographic study could cast some light on their binding mode. However, so far the attempts made to crystallize compound **V-4** with hCA I failed, the only species actually seen in the binding site being the oxalate salt interacting with the Zinc atom (*Andrea Angeli, personal communication*). It is possible that compounds with higher potency are needed for crystallization studies.

The K_A values of compounds **V-1**-**V-8** on hCA VA fell in the range 21.7-78.5 μM, therefore these analogues were >3 orders of magnitude less potent that the reference; the structural modification made on these molecules did not affect substantially the activity, since the potency varied only 2-3 times. On the contrary, on hCA VII the compounds showed K_A values in the same range as **HST**. On this isoform, the most potent compound was the dimethylamino derivative **V-8**, 3 times more potent than **HST**, and twice more potent than the other oxadiazole derivative **V-7**. It is difficult to understand if this difference is due to the diverse heterocycle or to the presence of the tertiary amino group; unfortunately, the synthesis of the NH_2 analogue of **V-8** failed, due to the instability of the oxadiazole derivatives (*Caterina Biliotti, personal communication*). Compounds **V-1**-**V-5** are roughly equipotent on hCA VII, while alcohol **V-5** shows the highest K_A value (120 μM). Contrary to what happened on hCA I, on hCA VII the amino derivative **V-6** was found to be more potent (5 times) than alcohol **V-5**.

As far as isoform selectivity is concerned, compounds **V-4** and **V-5** show some preference for hCA I, being more potent on this isoform than on hCA VA (14 and 36 times, respectively) and hCA VII (20 and 55 times, respectively), while they did not show activity on hCA II and

hCA XIII. These compounds could represent lead molecules whose optimization could possibly give a hCA I selective activation; owing to the wide distribution of this isoform, such a molecule could be useful as tool to study the physio-pathological role of this isoform.

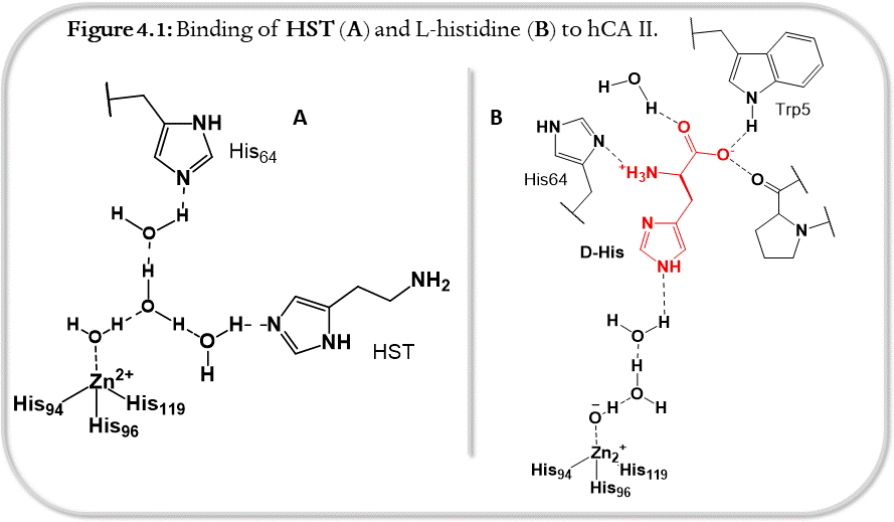

Figure 4.1: Binding of **HST** (**A**) and L-histidine (**B**) to hCA II.

Table 4.5: CA activation of isoforms hCA I, II, VA, VII and XIII with series V compounds, by a stopped-flow CO_2 hydrase assay. Histamine (HST) was used as standard activator.

Cmp (salt)	Structure	[a]K_A (μM)				
		hCA I	hCA II	hCA VA	hCA VII	hCA XIII
V-1 (oxa)	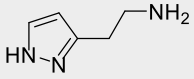	11.6	>150	37.9	32.8	>100
V-2	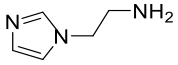	13.5	>150	42.7	25.4	>100
V-3	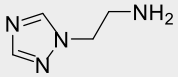	9.84	>150	24.6	35.5	>100
V-4 (oxa)	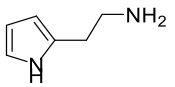	2.16	>150	29.8	44.6	>100
V-5	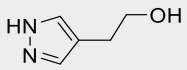	2.19	>150	78.5	120	>100
V-6	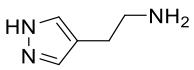	28.4	>150	51.0	23.7	>100
V-7(oxa)	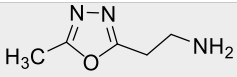	>150	>150	21.7	23.0	>100
V-8 (HCl)	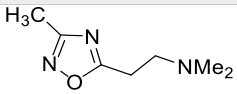	>150	>150	28.6	12.1	>100
HST	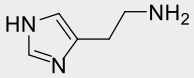	2.10	125	0.010	37.5	4.6

[a]Errors in the range of ±5-10 % of the reported values (data not shown) from three different assays

4.2.2 Clonidine analogues

In **Table 4.6** the K_A values of the **VI** series of compounds (clonidine analogues) on hCA I, II, VA, VII and XIII are reported. All compounds have been tested as hydroiodide salts, with the exception of **VI-1** (as HBr salt), **VI-12** (oxalate), clonidine (as HCl salt) and compounds **VI-3** and **VI-13** (free bases). In addition to the isoforms reported in Table 3, Clonidine HCl has been tested also on hCA IV, IX and XII, on which K_A values of 132 μM, 54.1 μM and 126 μM, respectively, were determined. From these studies we can see that CLO is a CA activator with low μM potency on hCA VII and XIII, showing some preference for these two isoforms over hCA I (10 times), II (>25 times), IV (17 times), IX (7 times) and XII (16 times).

As CLO, none of the compounds was active on hCA II at the highest tested concentration, while on the other isoforms the compounds showed K_A values mainly in the low-medium range, allowing to derive the following structure-activity relationships.

hCA I) The K_A value on this isoform CLO was 76.3 μM. Removal of both chlorine atoms abolished activity, since **VI-13** (R_2 = Ph) was inactive when tested up to a 150 μM concentration. On the contrary, inserting a CH_2 unit between the exocyclic N atom and the Ph ring of **VI-13** improved activity, **VI-4** (K_A 4.18 μM) being 18 times more potent than CLO. The elongation of the methylene chain gave compounds less active than **VI-4**; interestingly, a chain formed by 3 CH_2 units was tolerated (**VI-6**, K_A 36.7 μM) while a CH_2CH_2 chain was not (**VI-5**, K_A >150 μM). Side-chain branching abolished activity (**VI-7, VI-8**: K_A >150 μM). Methylation of the exocyclic $N\alpha$ atom was tolerated when R_2 is a phenethyl group (**VI-10**: K_A 68.6 μM) but not when R_2 is a benzyl moiety (**VI-9**: K_A >150 μM). On the contrary, methylation of the endocyclic N_1 atom gave interesting results, since compounds **VI-15**-**VI-18** are 2-5 times more active than their non-methylated analogues **VI-5**, **VI-6**, **VI-9**, **VI-10**, and when R_2 = benzyl the 4-fold decrease of activity gave **VI-14**, a fairly potent compound (K_A 16.9 μM). When R_2 = benzyl, the replacement of $N\alpha H$ (**VI-4**, K_A 4.18 μM) with S abolished activity (**VI-1**, K_A > 150 μM). As far as the sulfur analogues **VI-1**-**VI-3** are concerned, only a small methyl group seems tolerated, while the basicity of the amidine moiety seems to be not crucial, since the NH and the N-acetyl derivatives (**VI-2** and **VI-3**, respectively) are equipotent.

hCA VA) The K_A value on this isoform CLO was 42.6 μM. The removal of both chlorine atoms did not affect activity, since **VI-13** (R_2 = Ph, K_A 52.7 μM) was almost equipotent with CLO. Also the insertion of a CH_2 unit between the exocyclic N atom and the Ph ring of **VI-13** did not substantially modified potency (**VI-4**, K_A 45.7 μM). On this isoform, the majority of the compounds showed good activating properties: the K_A values of **VI-1**, **VI-3**, **VI-5**-**VI-8**, **VI-10**, **VI-14**-**VI-16** and **VI-18** were in the range 3.7-17.2 μM. The most potent compound was **VI-17** (K_A 0.9 μM), a benzyl derivative carrying a methyl group on both N_1 and $N\alpha$

atoms; this compound is 47 times more active than CLO. The removal of the exocyclic Nα-Me group decreased 4 times the activity (**VI-14**, K_A 3.7 μM), while the removal of the N_1-methyl group was more detrimental: as a matter of fact, compounds **VI-9** (K_A 40.5 μM) and **VI-4** (K_A 45.5 μM) were about 40 times less potent than **VI-17** (K_A 0.9 μM). On the contrary, the degree of methylation did not substantially affect potency of the phenylethyl and phenyl propyl derivatives, as compounds **VI-5**, **VI-6**, **VI-10**, **VI-15** and **VI-16** have K_A values in the range 9.9-17.2 μM. Side-chain branching (compounds **VI-7, VI-8**) was not detrimental for activity on this isoform, and a small enantioselectivity was observed: the *R*-enantiomer **VI-8** was twice more potent as the *S*-isomer **VI-7**. As far as the sulfur derivatives are concerned, the replacement of the NαH moiety of **VI-4** (K_A 45.5 μM) with S (**VI-1**, K_A 11.1 μM) brought a 4-fold improvement in activity. Acetylation of the N1 nitrogen was also favorable, as **VI-3** is twice more potent than **VI-2**.

hCA VII) The K_A value on this isoform CLO was 8.4 μM. All tested compounds showed activation properties on this isoform, with K_A values between 0.9 and 91.6 μM, the less potent being the primary amine **VI-12**. The removal of chlorine atoms of CLO reduced 4 times the activity (**VI-13**, R_2 = Ph, K_A 32.6 μM) while the separation of the phenyl and NαH moieties by means of a CH_2 unit did not substantially modified potency (**VI-4**, K_A 35.2 μM). On the contrary, the potency increased by elongating the chain from 1 to 3 CH_2 units (**VI-4**, K_A 35.2 μM; **VI-6**, K_A 11.4 μM) and by adding a methyl group on the NαH moiety: with the latter modification the potency of **VI-5** (K_A 16.7 μM) and of **VI-4** (K_A 35.2 μM) were increased 4 (**VI-10**, K_A 2.4 μM) and 3 times (**VI-10**, K_A 2.4 μM), respectively. Side-chain branching did not substantially affect activity, since **VI-7** and **VI-8** were equipotent with **VI-4**, while methylation on the endocyclic N_1 atom was the most effective modification in this set of molecules: as a matter of fact, with this structural change the K_A value of **VI-4** (K_A 35.2 μM) is reduced 39 times (**VI-14**, K_A 0.9 μM). Also the activity of the phenylpropyl derivative **VI-6** (K_A 11.4 μM) was increased 4 times (**VI-16**, K_A 3.1 μM). A double methylation on the N_1 and Nα atoms gave potent compounds (**VI-17**, K_A 6.5 μM and **VI-18**, K_A 2.6 μM) even if the K_A values are, respectively, 7 and 3 times lower thanthat of **VI-14**. The K_A values sulfur analogues **VI-1**-**VI-3** were in the range 30.9-46.7 μM, not better that the other tested 2-aminoimidazoline derivatives. Attempts to crystallize adducts of **VI-10**, **VI-14** and **VI-16** with hCA VII are ongoing.

hCA XIII) This is the isoform most sensitive to CLO among those studied (K_A 7.8 μM). As it happened on the hCA I isoform, the removal of both chlorine atoms, to give **VI-13**, abolished activity. Several other compounds resulted inactive when tested at concentrations up to 100 μM, i.e. the sulfur analogues **VI1**-**VI-3**, the polar aminoethyl derivative **VI-12**, and all the compounds having both the N_1 and Nα atoms as secondary amines, with the exception of the lipophilic phenylpropyl derivative **VI-6** (K_A 24.3 μM). Methylation on the Nα atom restored activity on the phenethyl analogue **VI-5**, giving **VI-10** with potency (K_A 6.5 μM) in the low micromolar range. Methylation on the endocyclic N_1 atom gave compounds **VI-14**-

VI-16 whose potency ranged from 10.9 to 31.0 μM, the most potent being the derivative carrying a phenylpropylamino side chain (**VI-16**). Methylation on both N_1 and N_α atoms did not improve activity.

As far as selectivity is concerned, the two compounds showing submicromolar K_A values displayed also interesting selectivity profles: **VI-14** showed a preference for hCA VII over hCA I (19 times), II (>100 times), VA (4 times), and XII (21 times) while **VI-17** was more active on hCA VA with respect to hCA I (33 times), II (>100 times), VII (7 times), and XIII (19 times).

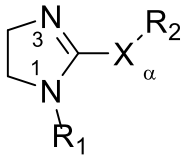

Table 4.5: Activation constant of compounds **VI-1-VI-18** on hCA I, II, VA, VII and XIII determined by means of a stopped-flow CO_2 hydrase assay. Clonidine (CLO) is taken as reference compound.

Compound[a]	R_1	X	R_1	K_A (μM)[b]				
				hCA I	hCA II	hCA VA	hCA VII	hCA XIII
VI-1	H	S	-CH_2Ph	>150	>150	11.1	46.7	>100
VI-2	H	S	-CH_3	9.61	>150	38.3	41.9	>100
VI-3	$COCH_3$	S	-CH_3	12.7	>150	15.0	30.9	>100
VI-4	H	NH	-CH_2Ph	4.18	>150	45.7	35.2	>100
VI-5	H	NH	-$(CH_2)_2$Ph	>150	>150	16.7	18.9	>100
VI-6	H	NH	-$(CH_2)_3$Ph	36.7	>100	9.9	11.4	24.3
VI-7	H	NH	(*S*) -CH(Me)Ph	>150	>150	12.4	31.5	>100
VI-8	H	NH	(*R*) -CH(Me)Ph	>150	>150	4.92	24.2	>100
VI-9	H	NMe	-CH_2Ph	>150	>150	40.5	11.0	>100
VI-10	H	NMe	-$(CH_2)_2$Ph	68.6	>100	14.9	2.4	6.5
VI-12	H	NH	-$CH_2CH_2NH_2$	3.87	>150	31.2	91.6	>100
VI-13	H	NH	-Ph	>150	>150	52.7	32.6	>100
VI-14	CH_3	NH	-CH_2Ph	16.9	>100	3.7	0.9	19.1
VI-15	CH_3	NH	-$(CH_2)_2$Ph	95.4	>100	14.6	16.2	31.0
VI-16	CH_3	NH	-$(CH_2)_3$Ph	10.9	>100	17.2	3.1	10.9
VI-17	CH_3	NMe	-CH_2Ph	30.2	>100	0.9	6.5	17.4
VI-18	CH_3	NMe	-$(CH_2)_2$Ph	20.2	>100	14.9	2.6	36.9
CLO	H	NH	(2,6-dichloro)Ph	76.3	>200	42.6	8.4	7.8

[a] All compounds have been tested as HI salts, with the exception of **VI-1** (as HBr salt), **VI-12** (oxalate), clonidine (as HCl salt) and compounds **VI-3** and **VI-13** (free bases). [b] Errors in the range of ±5-10 % of the reported values (data not shown) from three different assays.

4.2.3 Piperazine derivatives

A library of analogues 4-aminoethylpiperazine (PEA) have been tested for their activating properties against four CA isoforms, hCA I, II, IV and VII, by means of the stopped-flow technique; the results are reported in **table 4.6**[146].

The results let us to delineate the following structure-activity relationship.

hCA I) Although unsubstituted piperazine was inactive as a CA activator (K_As > 150 μM against all investigated enzymes), the substituted-piperazines **VII1- VII 24** showed CA activating properties against hCA I (except compounds **VII-1, VII-10**, **VII-11** and **VII-15**, which had K_As > 150 μM) with activation constants ranging between 32.6 and 131 μM, being thus moderate – weak activators. Indeed, the leads **PEA** and **HST** were much more potent, low micromolar activators of this isoform, with K_As of 2.3 – 7.4 μM (**table 4.6**) [109,110] The best hCA I activators in the series of investigated compounds were **VII-4, VII-19, VII-21** and **VII-24** (K_As of 32.6 – 48.6 μM), and they belong to variously substituted piperazines. Small variations on the core structure of these compounds generally led to a diminution of the activity. For example, **VII-19**, the best hCA I activator, carries a propionyl group on the piperazine ring and a benzyl moiety in the 2 position. Its deacylated analog, **VII-18**, was almost two times a less effective hCA I activator, with a K_A of 73.7 μM, compared to **VII-9**.

hCA II) The physiologically dominant cytosolic isoform hCA II was more sensitive to activation with piperazines **VII-1- VII-24** investigated here compared to hCA I (Table 1). Thus, only **VII-22** was inactive (K_A > 150 μM), and the range of activation constants for the remaining derivatives was of 16.2 – 116 μM. A number of compounds showed K_As in the range of 16.2 – 50.1 μM, among which **VII-2, VII-4, VII-14, VII-19, VII-21, VII-23** and **VII-24**. They belong to various chemical classes and incorporated different substituents, which demonstrates that it might be possible to design much more efficient CA activators incorporating this interesting ring. However, the simple lead compound **PEA** was a much more potent hCA II activator compared to the other piperazines investigated here, whereas histamine was a very inefficient hCA II activator with a K_A of 125 μM (**table 4.4**). Amazingly, the best hCA II activator was **VII-14**, which has two basic rings that may potentially participate in the proton shuttling processes.

hCA IV) Surprisingly, the membrane-bound isoform hCA IV was not activated significantly by any of the piperazines investigated here, although the leads **PEA** and **HST** showed medium potency with K_As of 24.9 - 25.3 μM.

hCA VII) The brain cytosolic isoform hCA VII was not activated by piperazines **VII-5**, **VII-7** and **VII-16** (K_A > 150 μM), whereas the remaining derivatives showed a profile of medium – weak activator, with K_A values in the range of 17.1 – 131 μM (**table 4.6**). The best hCA VII activators were **VII-2, VII-17, VII-18, VII-20** and **VII-22** (K_As in the range of 17.1 – 48.5 μM). For this isoform, the SAR of the couple **VII-18/ VII-19** is completely different compared to what mentioned above for the activation of hCA I. In this case, the deacylatyed derivative

VII-18 was 4.9 times a better hCA VII activator compared to the propionyl derivative **VII-19**. Thus, small changes in the scaffold lead to a very different activation profile in this series of piperazines and their derivatives.

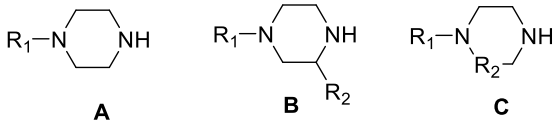

Table 4.6. CA activation of isoforms hCA I, II, and VII (cytosolic) and IV (membrane-associated) with compounds **VII-1** – **VII-24**, by a stopped-flow CO_2 hydrase assay. 4-Aminoethyl-piperazine (PEA) and histamine (HST) have been used as standard activators.

Compound	structure	R_1	R_2	K_A[a] (μM)			
				hCA I	hCA II	hCA IV	hCA VII
PEA[b]	A	$CH_2CH_2NH_2$	H	7.4	2.3	24.9	32.5
HST[b]	-	-	-	2.1	125	25.3	37.5
piperazine	A	H	H	>150	>150	>150	>150
1	A	phenyl	-	>150	74.9	>150	121
2	A	4-F-phenyl	-	88.2	38.7	>150	47.8
3	A	4-Cl-phenyl	-	104	110	>150	126
4	A	4-MeO-phenyl	-	48.6	50.1	>150	80.4
5	A	4-COMe-phenyl	-	83.7	97.9	>150	>150
6	A	3-Cl-phenyl	-	95.2	82.7	>150	104
7	A	3-MeO-phenyl	-	119	80.1	>150	>150
8	A	3-CF_3-phenyl	-	110	77.6	>150	114
9	A	2-pyridyl	-	131	75.2	>150	95.2
10	A	methyl	-	>150	78.4	>150	97.0
11	A	benzyl	-	>150	85.3	>150	98.4
12	A	acetyl	-	127	109	>150	96.4
13	A	CH_2CH_2OH	-	102	91.6	>150	124
14	A	2-piperidinyl	-	62.5	16.2	>150	49.2
15	B	H	methyl	>150	84.0	>150	131
16[c]	B	H	phenyl	80.3	49.7	>150	>150
17[c]	B	benzoyl	phenyl	75.2	84.5	>150	35.2
18[c]	B	H	benzyl	73.7	116	>150	17.1
19[c]	B	acetyl	benzyl	32.6	36.1	>150	84.0
20[c]	B	benzoyl	benzyl	85.2	82.4	>150	48.5
21	B	H	COOH	47.9	46.8	>150	93.6
22	C	H	CO	115	>150	>150	37.1
23	C	H	CH_2CH_2	79.4	44.6	>150	98.5
24	C	benzyl	CH_2CH_2	48.1	33.2	>150	127

[a] Errors in the range of ±5-10 % of the reported values (data not shown) from three different assays. [b] Data for PEA and **HST** from ref.[109,110],[c] Prepared as described in ref[76].

4.3 Pharmacological Results

In vivo IOP testing

The enzymatic tests on Carbonic Anhydrases isoforms have been performed by the group of Prof. Supuran at the Department of Neurosciences, Psychology, Drug Research and Child Health at the University of Florence. The compounds, used as hydrochloride salts, were formulated as 1% eye drops. High IOP was induced to rabbits by injection of 0.1 mL of hypertonic saline solution (5% in pyrogen free sterile 0.9% NaCl solution) into the vitreous of both eyes. Results, reported in **figure 4.2**, were compared to dorzolamide hydrochloride (1% solution) as reference inhibitor. The two compounds were able to reduce IOP after 60 min from administration, reaching the maximum activity at 120 min, lowering the pressure of about 10 mmHg. Potency and efficacy were similar to the reference drug dorzolamide.
The compound (*R*) **I-A2** was tested also in a stable model of glaucoma, obtained through the injection of 0.1 mL of 0.25% carbomer, which induced a sustained ocular hypertension in all tested eyes. Dorzolamide was again used as reference drug. The administration of compound (*R*) **I-A2** significantly reduced the IOP ($p<0.001$) at 24, 48, 72 and 96 hours in comparison to vehicle (**Figure 4.2B**). The effect of both dorzolamide and (*R*) **I-A2** slightly increased from the first to the fourth day of observation, (*R*) **I-A2** being significantly more potent than the reference compound Dorzolamide. As a matter of fact, the ΔIOP value produced by (*R*) **I-A2** was roughly two-fold higher than that produced by the same dose of DRZ.

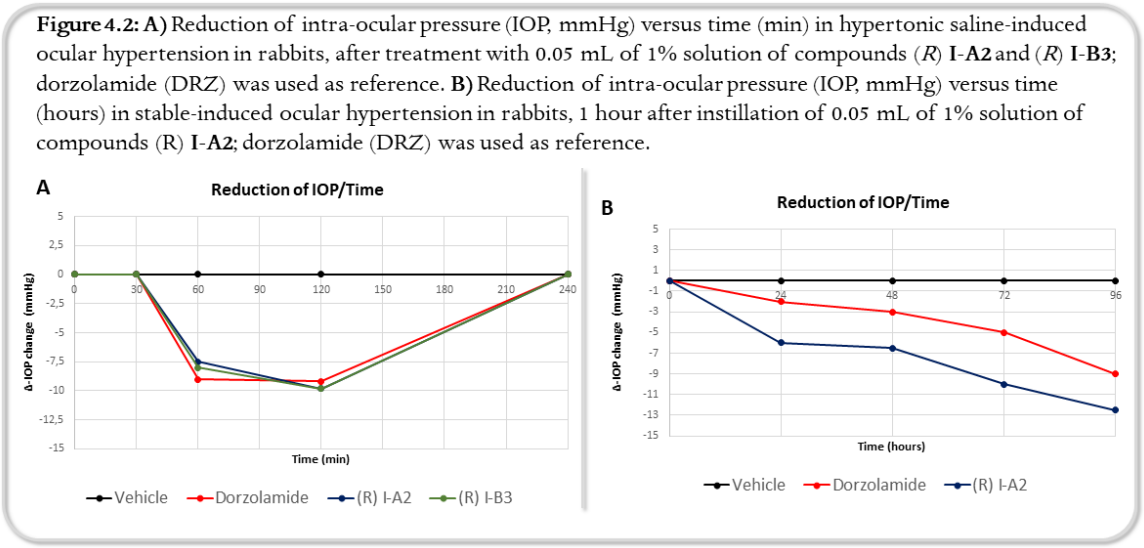

Figure 4.2: A) Reduction of intra-ocular pressure (IOP, mmHg) versus time (min) in hypertonic saline-induced ocular hypertension in rabbits, after treatment with 0.05 mL of 1% solution of compounds (*R*) **I-A2** and (*R*) **I-B3**; dorzolamide (DRZ) was used as reference. **B)** Reduction of intra-ocular pressure (IOP, mmHg) versus time (hours) in stable-induced ocular hypertension in rabbits, 1 hour after instillation of 0.05 mL of 1% solution of compounds (R) **I-A2**; dorzolamide (DRZ) was used as reference.

5. Computational and X-Ray Analysis

5.1 X-ray analysis, I-A and I-B series

The crystallographic experiments for both the **I** and **III** series were performed by Dr. Ferraroni M. (Department of Chemistry, University of Florence) and by Dr. Angeli A., Department of Neurosciences, Psychology, Drug Research and Child Health, University of Florence).

To understand the interaction mode of the benzylpiperazine derivatives with the enzyme, the X-ray structure of the complex of (*S*) **I-A9** and (*S*) **I-B4** bound to hCA I were solved at 1.5 and 1.6 Å resolution, respectively. Compound (*S*) **I-A9** was selected in order to see which arylsulfonamide group was going to coordinate the Zn ion, and (*S*) **I-B4**, carrying a small acetyl group, was selected for comparison. Crystal parameters and refinement data are summarized in table 5.1. Surprisingly, while the electron density maps unambiguously showed the inhibitor molecules, electron density was almost absent for the second N^4 -sulfamoylbenzoyl moiety of (*S*) **I-A9**, which therefore was not introduced in the model. It should be noted that very few adducts of hCA I with bound inhibitors were reported up until now[31], and this is the reason why we concentrated on this isoform for the compounds reported here.

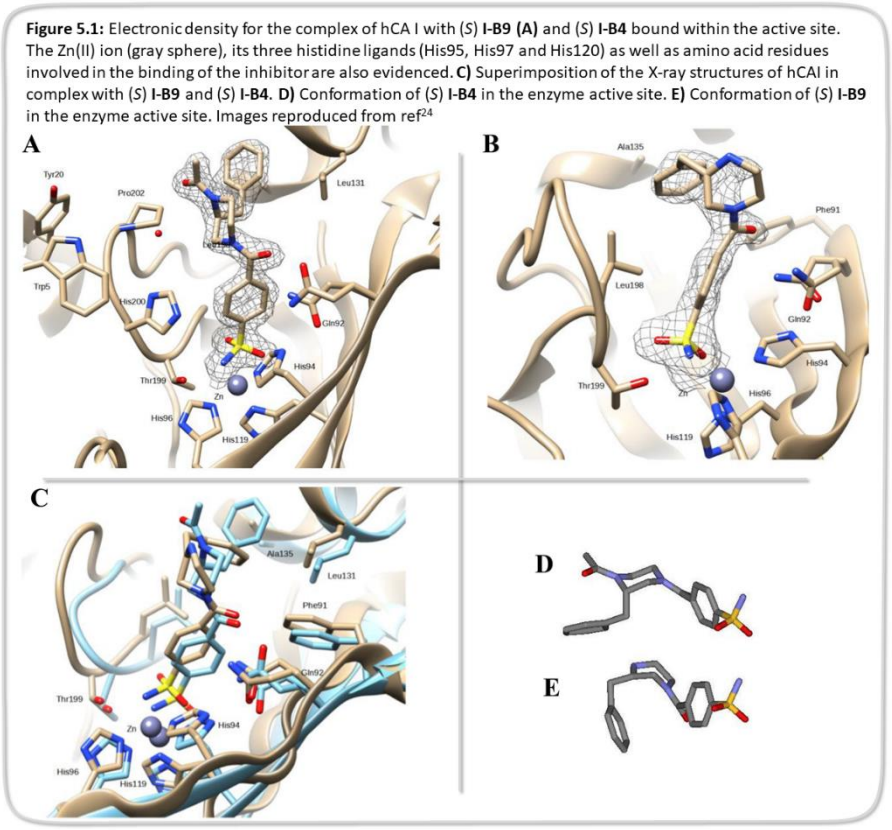

Figure 5.1: Electronic density for the complex of hCA I with (*S*) **I-B9 (A)** and (*S*) **I-B4** bound within the active site. The Zn(II) ion (gray sphere), its three histidine ligands (His95, His97 and His120) as well as amino acid residues involved in the binding of the inhibitor are also evidenced. **C)** Superimposition of the X-ray structures of hCAI in complex with (*S*) **I-B9** and (*S*) **I-B4**. **D)** Conformation of (*S*) **I-B4** in the enzyme active site. **E)** Conformation of (*S*) **I-B9** in the enzyme active site. Images reproduced from ref[24]

Both inhibitors place their sulfamoylbenzoyl moiety in a superimposable position and orientation, coordinating the Zn(II) ion by means of the deprotonated sulfonamide moiety

(**Figure 5.1**). The sulfonamide nitrogen atoms also make a strong H-bond with the OH of Thr199, while one of the sulfonamide oxygen is engaged in a hydrogen bond with the amide nitrogen of Thr199. These are the usual interactions made by the solfonamide group within the binding site[21]. In addition, the benzoyl rings make contacts with His94 and Leu198, and another H-bond is established between the carbonyl oxygen atoms and Asn92. While the sulfamoylbenzamide moieties of both inhibitors are placed in the same orientation and equivalent position (**Figure 5.1C**), the piperazine rings adopted quite different conformations: a chair for (*S*) **I-B4** (**figure 5.1D**), and a twisted boat for (*S*) **I-A9** (**Figure 5.1E**). These different shapes place the benzyl substituent in a pseudoequatorial arrangement for (*S*) **I-A9** and in an axial position for (*S*) **I-B4**. Despite this difference, the benzyl groups are oriented, albeit in slightly different ways, toward the hydrophobic cavity aligned by residues Phe91, Leu131, Ala135, Leu141 and 198, and Pro202 (**Figure 5.1C**). The benzyl moiety of (*S*) **I-B4**, which is more deeply inserted into the hydrophobic cavity, establishes Van der Waals contacts with Ala135 and Leu131; in addition to these interactions, (*S*) **I-A9** is able to interact also with Leu141.

Table 5.1: Summary of Data Collection and Atomic Model Refinement Statistics[a]

	HCA-I + (S)I-B4	*HCA-I + (S)I-A9*
PDB ID	6EVR	6EX1
Wavelength (Å)	0.966	0.966
Space Group	P212121	P212121
Unit cell (a,b,c) (Å)	62.12, 71.06, 122.12	62.98, 71.47, 120.94
Limiting resolution (Å)	28.5 - 1.5	1.6
Unique reflections	87056 (13980)	72418 (11109)
Rsym (%)	4.9 (65.4)	7.2 (140.5)
Rmeas (%)	5.5 (74.6)	8.6 (169.8)
Redundancy	4.41 (4.42)	3.16 (3.06)
Completeness overall (%)	99.4 (98.0)	98.4 (95.0)
<I/(I)>	13.93 (2.04)	7.27(0.69)
CC (1/2)	99.9 (81.3)	99.1 (51.9)
Refinement statistics		
Resolution range (Å)	20.0 – 1.5	20.0-1.6
Unique reflections, working/free	82483/4378	67693/3617
Rfactor (%)	18.43	21.39
Rfree(%)	22.27	24.64
No. of protein atoms	4043	4038
No. of water molecules	453	320
No. of heterogen atoms	72	64
r.m.s.d. bonds(Å)	0.023	0.006
r.m.s.d. angles (°)	2.151	1.156
Ramachandran statistics (%)		
Most favored	97.3	97.3
additionally allowed	2.7	2.7
outlier regions	0	0
Average B factor (Å²)		
All atoms	27.31	36.69
inhibitors	25.37	45.52
solvent	38.66	44.34

[a] Values in parentheses are for the highest resolution shell.

5.2 Computational studies, I-A and I-B series

The docking simulation were done by Prof. Gratteri's research group at the Department of Neurosciences, Psychology, Drug Research and Child Health, University of Florence.
The binding mode of the benzylpiperazine series on hCA II and IV, the isoforms mainly involved in the pathogenesis of glaucoma, was also predicted by docking simulations. A small array of regio- and stereo-isomers, namely the N-benzyl derivatives (*S*) **I-A1**, (*R*) **I-A1**, (*S*)**I-B2** and (*R*)**I-B2**, and *N*-benzoyl amide-bearing (*S*) **I-A5**, (*R*) **I-A5**, (*S*) **I-B5** and (*R*) **I-B5**, were chosen as representative to evaluate the influence on the key interactions taking place within hCA II and hCA IV binding pockets. Despite the similar overall fold of CA II and CA IV, some unique structural features mark the differences between the two isozymes which, however, do not involve the catalytic Zn ion region. The polypeptide segment Val131-Asp136 in CA IV arranges in an extended loop conformation rich of charged residues extending to the outside. The corresponding amino acids in CA II, comprising Phe131, are folded as a short α-helix and constitutes part of the well-known lipophilic region of hCA-II binding cavity[147]. These marked differences did not prevent the benzenesulfonamide moieties of the selected ligands to orient deeply within the active site region of both the isozymes, where the negatively charged nitrogen atom replaced the zinc-bound nucleophile, the NH is at H-bond distance with Thr199 OG1 and one oxygen atom of the ZBG accepts a hydrogen bond by the backbone NH of the same residue. Additionally, the aromatic ring showed π-alkyl interactions with Val121, Val135, His94 and Leu198. This wide set of interactions is consistent with the biological results, being all the screened derivatives strong inhibitors of both hCA II and IV with K_i values spanning in the low-medium nanomolar range, and confirms the pattern of interactions found in the crystal structures of (*S*)**I-A9** and (*S*)**I-B4** with hCA I.

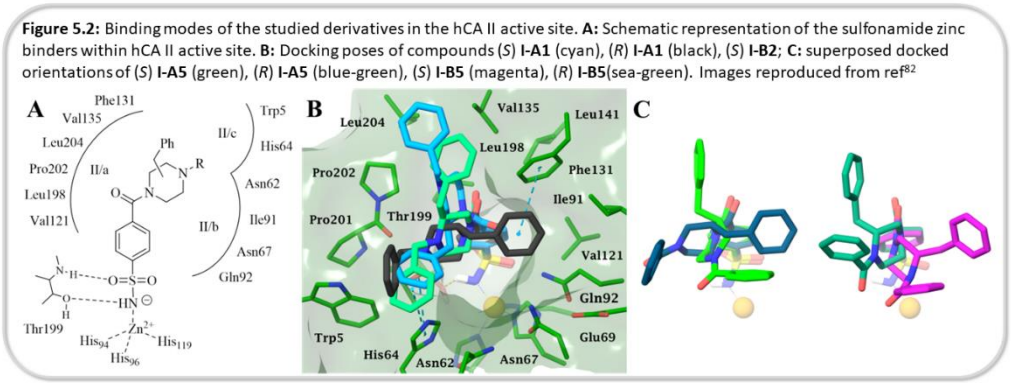

Figure 5.2: Binding modes of the studied derivatives in the hCA II active site. **A:** Schematic representation of the sulfonamide zinc binders within hCA II active site. **B:** Docking poses of compounds (*S*) **I-A1** (cyan), (*R*) **I-A1** (black), (*S*) **I-B2**; **C:** superposed docked orientations of (*S*) **I-A5** (green), (*R*) **I-A5** (blue-green), (*S*) **I-B5** (magenta), (*R*) **I-B5**(sea-green). Images reproduced from ref[82]

The arrangement of the benzylpiperazinyl tails within the binding clefts remarks the distinct nature of the residues at the outer rim of hCA II and IV enzymatic cavities. As a result, the two benzylic moieties of derivatives (*S*) **I-A1**, (*R*) **I-A1**, (*S*) **I-B2** and (*R*) **I-B2** as well as the benzylic and *N*-benzoylic portions of (*S*) **I-A5**, (*R*) **I-A5**, (*S*) **I-B5** and (*R*) **I-B5** were found to lie within three possible area of hCA-II active site, defined by Phe131, Val135, Leu204,

Pro202 (region II/a), Ile91, Gln92, Asn67, Asn62 (region II/b) and Asn62, His64, Trp5 (region II/c), with which form lipophilic and dipole-dipole interactions (**Figure 5.2**).

In the hCA IV binding site, the lipophilic portions of most compounds seek to deviate from the charged residues loop, preferentially pointing towards regions formed by residues Gln92, Met67, Gln60, Asn62, His64 (**Figure 5.3**), with the *N*-benzoyl and/or benzyl groups of (*S*) **I-B5,** (*S*) **I-A5**, (*R*) **I-A1**, (*R*) **I-A5**, and (*R*) **I-B5**, (*R*) **I-B2** forming wide sets of hydrophobic and/or dipole-dipole interactions. Moreover, the CO of the benzoyl groups acted as acceptor in the H-bond contact with His64 (**Figure 5.3**).

Conversely, the analysis of poses for compounds (*S*)**I-A1** and (*S*) **I-B2** showed that the N-benzyl piperazine moieties oriented towards residues Glu123 and Lys206 forming a charged H-bond involving the protonated piperazine nitrogen and the negatively charged carboxy group of Glu123. In addition, a π-cation interaction with NZ atom of Lys206 stabilized the pose.

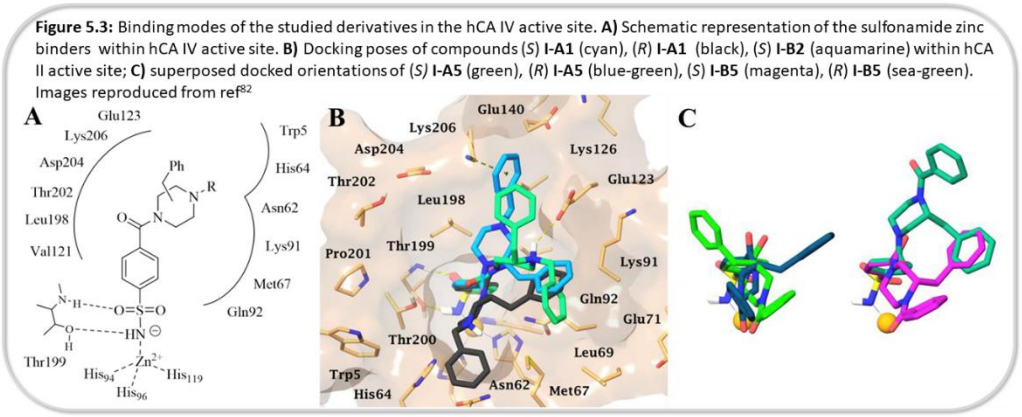

Figure 5.3: Binding modes of the studied derivatives in the hCA IV active site. **A)** Schematic representation of the sulfonamide zinc binders within hCA IV active site. **B)** Docking poses of compounds (*S*) **I-A1** (cyan), (*R*) **I-A1** (black), (*S*) **I-B2** (aquamarine) within hCA II active site; **C)** superposed docked orientations of (*S*) **I-A5** (green), (*R*) **I-A5** (blue-green), (*S*) **I-B5** (magenta), (*R*) **I-B5** (sea-green). Images reproduced from ref[82]

It is interesting to note how the stereocentre configuration as well as the positioning of the benzyl moieties on the C2/C3 piperazine carbon atoms differently influenced the orientation of the tails within both binding sites, eliciting varied sets of contacts with the cleft residues, which were comparable as the scoring function values are concerned. At a greater extent, the influence of the stereocenter configuration is evident in case of hCA IV, within whose binding site the orientations of couples of enantiomers, i.e. (*S*)/(R) **I-A1**, (*S*)/(R) **I-B2**, (*S*)/(R) **I-A5** and (*S*)/(R) **I-B5** almost crossed each other leading to variable trends of non-bonded interactions.

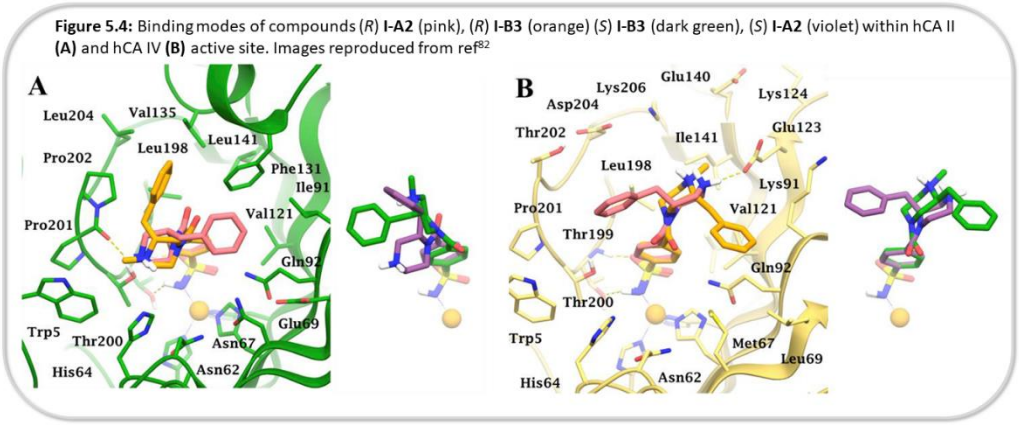

Figure 5.4: Binding modes of compounds (*R*) **I-A2** (pink), (*R*) **I-B3** (orange) (*S*) **I-B3** (dark green), (*S*) **I-A2** (violet) within hCA II **(A)** and hCA IV **(B)** active site. Images reproduced from ref[82]

The inspection of the docking results of both (*R*) **I-A2** and (*R*) **I-B3**, evaluated as anti-glaucoma agents, and their enantiomers (S) **I-A2** and (S) **I-B3** suggested a key role played by Glu123 in defining the orientations of the benzyl piperazine within hCA IV binding cavity (**Figure 5.3B**). Indeed, the absence of a second bulky substituent at the piperazine *N*-atom allowed the charge mediated interaction between $NH_2^+/NH(CH_3)^+$ group of the heterocycle, regardless the configuration or position of the benzyl moieties (regio-isomers). In hCA II, due to the presence of a lipophilic region in place of the hCA IV charged residues, a wide set of hydrophobic ligand/target contacts are present (**Figure 5.4A**) and H-bonds are established between Pro201 backbone CO and the positively charged NH group of piperazine.

Docking scores were not predictive of the activity trends for the computationally investigated derivatives which all exhibit identical coordination geometry of the sulfonamide group to the Zn ion as well as an extended and equipotent sets of interactions within the binding cavities. The accuracy of the used docking protocol was assessed evaluating the ability of the docking in reproducing the geometry of the cocrystallized ligand (S) **I-B4** within hCA I.

5.3 X-ray analysis, series II

To study the differences in binding mode between the derivative belonging to the **II-A**, **II-B** and **II-C** series and the previously synthesized 2-benzylpiperazine analogues, the compounds **II-A2**, **II-A3**, (*R*) **I-A1** and (*R*) **I-B2** were crystallized with hCA II. Compounds (*R*) **I-A1** and (*R*) **I-B2** were chosen among those having higher potency on this isoform (K_i 5.4 nM and 8.1 nM, respectively[24]). Crystal parameters and refinement data of the four complexes are summarized in **table 5.2**.

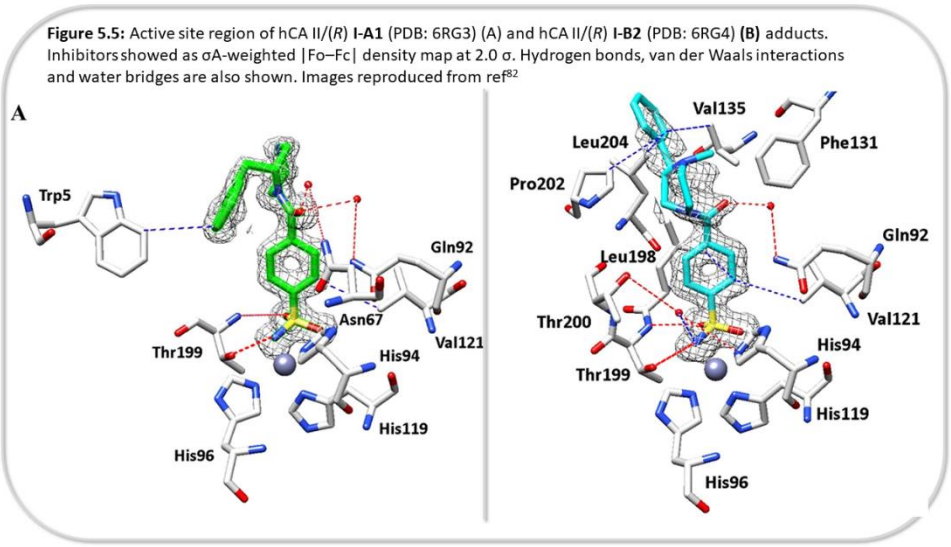

Figure 5.5: Active site region of hCA II/(*R*) **I-A1** (PDB: 6RG3) (A) and hCA II/(*R*) **I-B2** (PDB: 6RG4) **(B)** adducts. Inhibitors showed as σA-weighted |Fo–Fc| density map at 2.0 σ. Hydrogen bonds, van der Waals interactions and water bridges are also shown. Images reproduced from ref[82]

In all the four complexes, the sulfonamide moiety was directly bound to the zinc ion in the active-site. Two additional hydrogen bond interactions, evidenced in **figures 5.5** and **5.6**, between the sulfonamide and Thr199 contributed to stabilize the complexes (NH^- with the OH in the side chain and the sulfonamide oxygen with the peptide nitrogen). These interactions are typical of this zinc binding group[148,149]. The binding of (*R*) **I-A1** and (*R*) **I-B2** was further stabilized through a water molecule bridging the benzoate carbonyl group and Gln92; a second water bridge was observed between the carbonyl moiety of (*R*) **I-B2** and the NH_2 group of Asn67. On the contrary, compound (*R*) **I-A1** showed an additional water molecule linking the hydroxyl portion of the side chain of Thr200 with the NH of the sulfonamide group (**Figure 5.5**). The tail portion of (*R*) **I-B2** showed limited interaction with hCA II active site and, in particular, only a hydrophobic interaction of the benzyl group with residues Trp5 was observed (**Figure 5.5A**). On the other hand, compound (*R*) **I-A1** showed different hydrophobic interactions with hCA II arranging the benzyl portion in a different pocket of the active-site *via* interactions with Val135, Pro202, and Leu204 (**Figure 5.5B**).

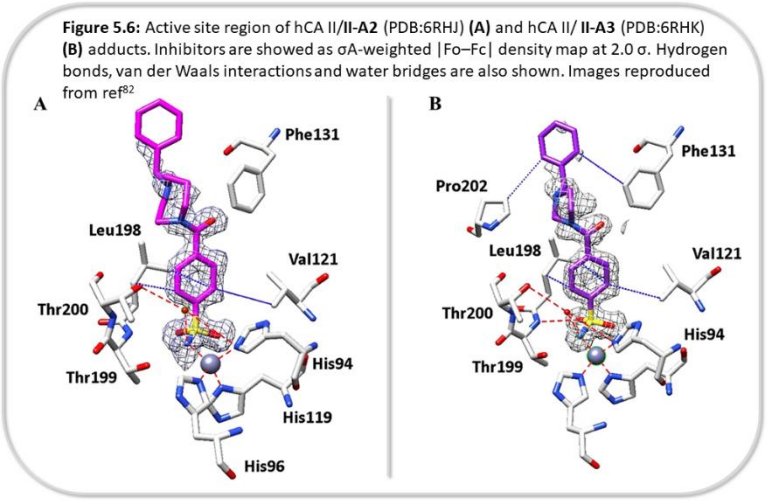

Figure 5.6: Active site region of hCA II/**II-A2** (PDB:6RHJ) **(A)** and hCA II/ **II-A3** (PDB:6RHK) **(B)** adducts. Inhibitors are showed as σA-weighted |Fo–Fc| density map at 2.0 σ. Hydrogen bonds, van der Waals interactions and water bridges are also shown. Images reproduced from ref[82]

The benzyl portion located on the N atom of diazepane **II-A2** or imidazolidine **II-A3** scaffolds moved to the opposite side of the cavity with respect to (*R*) **I-B2**; the higher potency of compounds **II-A2** and **II-A3** (K_i 2.3 and 0.6 nM, respectively, **table 4.2**) for hCA II could result from this different orientation. Both **II-A2** and **II-A3** showed a water bridge linking Thr200 and the sulfonamide NH group (**Figure 5.6A** and **5.6B**) as found for compound (*R*) **I-A1** (**Figure 5.5B**). Moreover, the size of the heterocyclic ring could influence the hydrophobic interactions made by the benzyl group. In fact, a bulkier scaffold such as the diazepane ring pushed the benzyl portion away from the hydrophobic region delimited by residues Phe131, Val135, Leu198, and Pro202 (**Figure 5.6A**). On the contrary, the less bulky imidazolidine scaffold of **II-A3** allowed its N-benzyl moiety to form stronger hydrophobic interactions with residues Phe131 and Pro202 (**Figure 5.6B**). Unfortunately, the poor electron density for the benzyl groups of both inhibitors made their orientation not easily inferable. Interestingly, comparison of the binding modes of compounds (*R*) **I-B2** and (*R*) **I-A1** (**Figure 5.7A**) showed that the presence of a methyl group on the piperazine nitrogen atom of (*R*) **I-A1** led to a different ring conformation which shifted the carbonyl moiety of 1.8 Å (**Figure 5.7B**) and placed the benzyl group in the opposite side of the cavity with respect to (*R*) **I-A1**. This orientation was different also with respect to the position of the 4-fluorobenzyl moiety in the structure of the complex hCA II/**8b**[138]. As previously discussed for **II-A3** and **II-A2**, these substantial differences prove the importance of the inhibitor tail in order to modulate its potency.

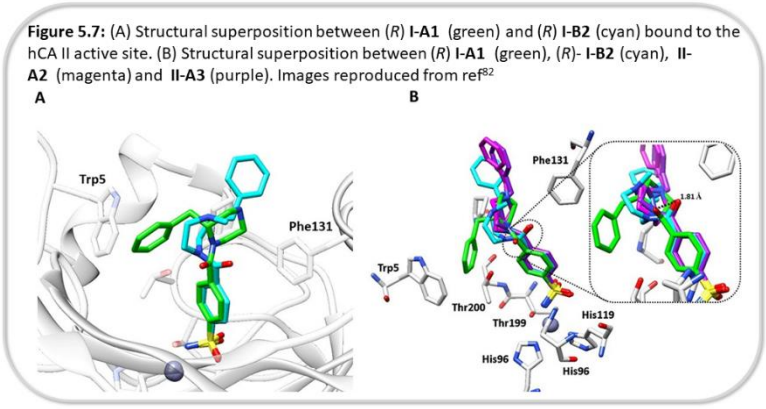

Figure 5.7: (A) Structural superposition between (*R*) **I-A1** (green) and (*R*) **I-B2** (cyan) bound to the hCA II active site. (B) Structural superposition between (*R*) **I-A1** (green), (*R*)- **I-B2** (cyan), **II-A2** (magenta) and **II-A3** (purple). Images reproduced from ref[82]

Table 5.2 Summary of Data Collection and Atomic Model Refinement Statistics

	HCAII + I-A1	HCAII + I-B2	HCAII + II-A2	HCAII + II-A3
PDB ID	6RG4	6RG3	6RHJ	6RHK
Wavelength (Å)	0.827	0.827	1.000	1.000
Space Group	P21	P21	P21	P21
Unit cell (a, b, c, α, β, γ) (Å,°)	42.37, 41.30, 71.93 90.0, 104.4, 90.0	42.36, 41.26, 71.92 90.0, 104.3, 90.0	42.37, 41.37, 71.76 90.0, 104.4 90.0	42.60, 41.63, 72.35 90.0, 104.54, 90.0
Limiting resolution (Å)	41.07-1.25 (1.25-1.33)	41.08-1.32 (1.41-1.32)	69.49-1.44 (1.44-1.47)	70.03-1.44 (1.44-1.47)
Unique reflections	66753 (11257)	188539 (10131)	43292 (2186)	44092 (2184)
Rsym (%)	5.8 (99.2)	4.7 (77.4)	7.6 (18.5)	5.8 (19.4)
Rmeas (%)	6.9 (118.9)	5.5 (92.1)	9.5 (28.2)	7.1 (24.4)
Redundancy	3.3 (3.2)	3.3 (3.3)	2.7 (2.3)	2.9 (2.4)
Completeness overall (%)	99.1 (99.1)	99.2 (98.7)	99.4 (99.0)	99.3 (98.8)
<I/σ(I)>	9.39 (0.79)	12.39 (1.24)	7.2 (2.2)	10.0 (3.4)
CC (1/2)	99.8 (54.1)	99.9 (64.3)	98.9 (82.9)	99.6 (93.1)
Refinement statistics				
Resolution range (Å)	41.07-1.25	41.08-1.32	50.0-1.44	50.0-1.44
Unique reflections, working/free	62531/3239	53621/2719	41141/2125	41791/2061
Rfactor (%)	15.5	17.7	17.6	15.4
Rfree(%)	20.0	19.7	20.0	17.5
r.m.s.d. bonds(Å)	0.015	0.0127	0.0126	0.0134
r.m.s.d. angles (°)	2.008	1.427	1.8699	1.9184
Ramachandran statistics (%)				
Most favored	97.3	96.9	96.9	97.3
additionally allowed	2.7	2.7	3.1	2.7
outlier regions	0.0	0.4	0.0	0.0
Average B factor (Å²)				
All atoms	18.16	17.60	13.53	13.36
inhibitors	34.36	17.68	28.17	32.19
solvent	30.31	28.91	21.90	23.29

6. Conclusions

6.1 Piperazine and Aminopiperdine derivatives

Our data show that the three series of piperazine-based CAIs we developed have good modulator properties on the enzyme. To explore the SAR of these inhibitors, we manipulated the chemical structure of the **I-A** and **I-B** series synthesizing the two other generations of analogues (**II-A**, **II-B**, **II-C** / **III-A**, **III-B**), which were tested on four different hCA isoforms (I, II, IV and IX). We also investigated the interaction of the **I-A** and **I-B** series with human CA through computational methods and we performed x-rays studies on some derivatives of series **I** and **II**, achieving an important snapshot of their binding mode in the hCA active site. In vivo pharmacological tests provided promising information too, being compounds *(R)* **I-A2** and *(R)* **I-B3** potent IOP reducing agents. Besides completing the series of **III-B** analogues, possibly obtaining enantiopure compounds, we are already planning to expand these encouraging set of substances. The future approaches will be aimed to inspect further the role of the chirality, the importance of the nature of the ZBG and the function of the substituents.

6.2 CAIs-HDACs Hybrids

Through a poly-pharmacology approach we developed the **IV** series of hybrids that, for the moment, were only tested against the hCAs. Even though the results are still preliminary, a compound showing selectivity toward the cancer-related CA isoform has been obtained. Together with the investigation of the binding mode on hCA, we need to complete the characterization of this set of hybrids performing HDAC inhibition tests. These experiments will be fundamental to understand if the development of this series could be further pursued or a modification in our strategy will be needed.

6.3 Carbonic Anhydrase Activators

Our approach on the CA activation was based on the rational modification of the histamine (HST) and clonidine (CLO) scaffolds in order to investigate their unknown SAR. We developed the HST analogues from the isosteric substitutions of imidazole scaffold while the CLO based derivatives were mainly obtained through the functionalization of the exocyclic amine. With this strategy, we prepared a library of basic small compounds endowed with hCAs activators properties. Although all the K_a values are in the micromolar range, this first screening was important to infer some preliminary SAR that will be further investigated.

7. Experimental Part

General remarks and instrumentation. All melting points were taken on a Büchi apparatus and are uncorrected. When reactions were performed under anhydrous conditions, the mixtures were maintained under nitrogen. NMR spectra were recorded on a Brucker Avance 400 spectrometer (400 MHz for ^{1}H NMR, 100 MHz for ^{13}C). Chromatographic separations were performed on a silica gel column by gravity chromatography (Kieselgel 40, 0.063- 0.200 mm; Merck) or flash chromatography (Kieselgel 40, 0.040-0.063 mm; Merck). Yields are given after purification, unless differently stated. The purity of the tested compounds has been assessed by means of LC-DAD analyses, carried out on an Agilent 1200 system (Agilent, Palo Alto CA, USA). High resolution mass spectrometry (HR-MS) analysis was performed with a Thermo Finnigan LTQ Orbitrap mass spectrometer equipped with an electrospray ionization source (ESI). The analysis was carried out in positive ion mode monitoring protonated molecules, $[M+H]^+$ species, and it was used a proper dwell time acquisition to achieve 60,000 units of resolution at Full Width at Half Maximum (FWHM). Elemental composition of compounds was calculated on the basis of their measured accurate masses, accepting only results with an attribution error less than 5 ppm and a not integer RDB (double bond/ring equivalents) value, in order to consider only the protonated species[150]. Compounds were named following IUPAC rules by means of MarvinSketch 18.1.

General remarks and instrumentation for the part of the project performed at the **University of Münster**. (**III series**) Oxygen and moisture sensitive reactions were carried out under nitrogen, dried with silica gel with moisture indicator (orange gel, VWR, Darmstadt, Germany) and in dry glassware (Schlenk flask or Schlenk tube). All solvents were of analytical or technical grade quality. Demineralized water was used. CH_2Cl_2 was distilled from CaH_2; THF was distilled from sodium/benzophenone; MeOH was distilled from magnesium methanolate. Thin layer chromatography (tlc): tlc silica gel 60 F_{254} on aluminum sheets (VWR). Flash chromatography (fc): Silica gel 60, 40–63 μm (VWR); parentheses include: diameter of the column (ø), length of the stationary phase (h) and eluent. MS: MAT GCQ (Thermo-Finnigan): EI, MAT LCQ(Thermo Finnigan): ESI, MicroTOF-QII (Bruker Daltonics): APCI. IR: IR spectrophotometer 480Plus FT-ATR-IR (Jasco) or FT/IR Prestige 21 (Shimadzu).

7.1 Benzylpiperazines, I-A and I-B Series

The synthetic procedures of the series **I** and **III** are reported for one enantiomer of each product. If not clearly indicated, the procedure was also applied to the corresponding enantiomer and their properties are the same.

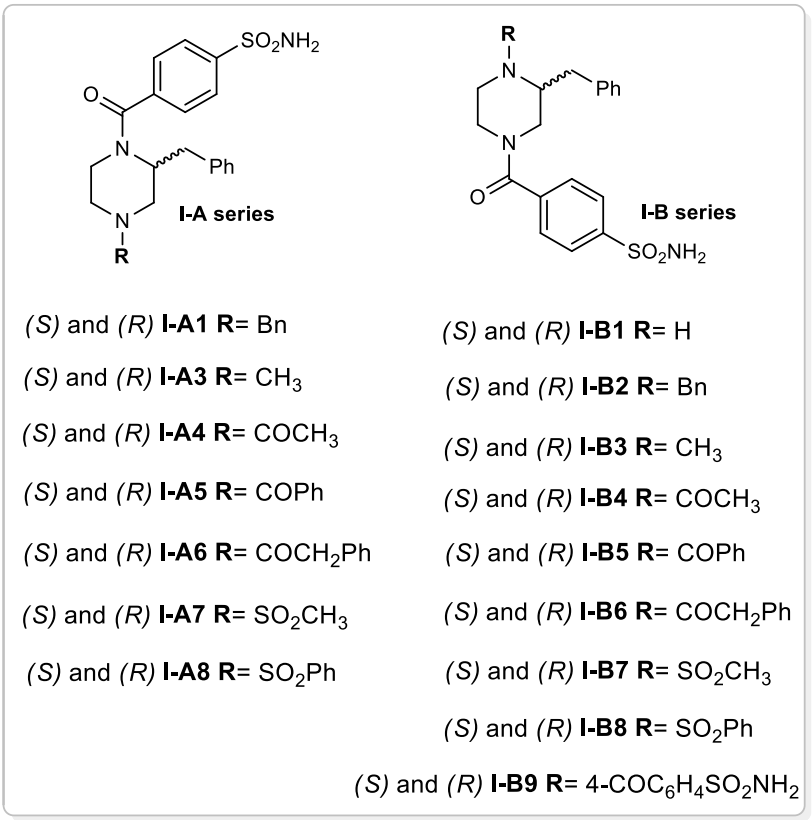

(S) and *(R)* **I-A1 R**= Bn

(S) and *(R)* **I-A3 R**= CH_3

(S) and *(R)* **I-A4 R**= $COCH_3$

(S) and *(R)* **I-A5 R**= COPh

(S) and *(R)* **I-A6 R**= $COCH_2Ph$

(S) and *(R)* **I-A7 R**= SO_2CH_3

(S) and *(R)* **I-A8 R**= SO_2Ph

(S) and *(R)* **I-B1 R**= H

(S) and *(R)* **I-B2 R**= Bn

(S) and *(R)* **I-B3 R**= CH_3

(S) and *(R)* **I-B4 R**= $COCH_3$

(S) and *(R)* **I-B5 R**= COPh

(S) and *(R)* **I-B6 R**= $COCH_2Ph$

(S) and *(R)* **I-B7 R**= SO_2CH_3

(S) and *(R)* **I-B8 R**= SO_2Ph

(S) and *(R)* **I-B9 R**= 4-$COC_6H_4SO_2NH_2$

General procedure 1. Synthesis of the alkyl, acyl or sulfonyl derivatives **I-A1 - A8** and **I-B1 - B9:**

To a solution of the suitable starting material in 5-20 mL of anhydrous acetonitrile, the suitable reactant was added with a base, when needed. The mixture was kept under stirring for 2 hours, then the solvent was removed under vacuum and the residue was purified with flash chromatography to give the corresponding compound. Synthetic details are reported in **table 8.1**. By means of this procedure, the compounds below have been prepared.

(S) and *(R)* **I-A1** (S) and (R)-4-(2,4-dibenzylpiperazine-1-carbonyl)benzenesulfonamide

[^{1}H]-NMR (**DMSO**, mixture of conformers) δ: 1.91-2.20 (m, 2H); 2.57-2.74 (dd, 1H, J= 13.2, 10.2z); 2.76-2.92 (m, 1H); 2.94-3.14 (m, 2H); 3.19-3.37 (m, 2H); 3.38-3.49 (m, 0.5H); 3.51-3.63 (m, 1.5H); 4.27-4.35 (m, 0.5H); 4.65-4.74 (bs, 0.5H, CH); 6.67-6.76 (bs, 1H, Ar); 6.94-7.04 (bs, 1H, Ar); 7.05-7.20 (m, 4H, Ar); 7.20-7.43 (m, 6H, Ar), 7.66-7.75 (m, 1H, Ar); 7.76-7.85 (m, 1H, Ar) **ppm**.

[^{13}C]-NMR (**DMSO**, mixture of conformers) δ: 35.9 (CH_2Ph); 36.4 (CH_2Ph); 37.9 (C_6); 44.0 (C_6); 50.9 (C_2); 53.4 (C_5); 53.7 (C_5 + C_3); 55.3 (C_3); 57.4 (C_2); 62.3 (NCH_2Ph); 126.0 (CH_{Ar}); 126.3 (CH_{Ar}); 126.6 (CH_{Ar}); 126.8 (CH_{Ar}); 127.2 (CH_{Ar}); 127.6 (CH_{Ar}); 127.7 (CH_{Ar}); 128.7 (CH_{Ar}); 129.4 (CH_{Ar}); 129.7 (CH_{Ar}); 138.4 (C_{Ar}); 138.8 (C_{Ar}); 139.1 (C_{Ar}); 139.8 (C_{Ar}); 144.9 (C_{Ar}); 145.1 (C_{Ar}); 168.2 (CO); 168.9 (CO) **ppm**.

ESI-MS (*m/z*): 450.2 (M+1) **ESI-HRMS (*m/z*)** $[M+H]^+$: calculated for $C_{25}H_{28}N_3O_3S$ 450.1846; found 450.1848 for (*S*)-**I-A1** and 450.1843 for (*R*)- **I-A1**

(S) and *(R)* **I-A3** (S) and (R)-4-(2-benzyl-4-methylpiperazine-1-carbonyl)benzenesulfonamide

[^{1}H]-NMR (**DMSO**, mixture of conformers) δ: 1.78-2.12 (m, 2H); 2.20 (s, 3H, CH_3); 2.61-2.97 (m, 3H); 3.05-3.24 (m, 2H); 3.35-3.48 (m, 0.5H); 3.57-3.68 (m, 0.5H); 4.27-4.38 (m, 0.5H); 4.78-4.89 (m, 0.5H); 6.83-7.02 (m, 2H, Ar); 7.18-7.38 (m, 5H, Ar); 7.43 (s, 2H, SO_2NH_2); 7.64-7.87 (m, 2H, Ar) **ppm**.

ESI-HRMS (*m/z*) $[M+H]^+$: calculated for $C_{19}H_{24}N_3O_3S$ 374.1533; found 374.1529 for (*S*)-**3** and 374.1526 for (*R*)- **I-A3**.

(S) and *(R)* **I-A4** (S) and (R) 4-(4-acetyl-2-benzylpiperazine-1-carbonyl)benzenesulfonamide

[^{1}H]-NMR (**$CDCl_3$**, mixture of conformers) δ: 1.56 (s, 1.5H, CH_3); 2.08 (s, 1.5H, CH_3); 2.13-29 (m, 1H); 2.55-3.18 (m, 3H); 3.20-3.42 (m, 2H); 3.63-4.03 (m, 1H); 4.46-4.72 (m, 1H); 4.73-5.01 (m, 2.5H, SO_2NH_2 + 0.5H); 5.12-5.27 (m, 0.5H); 6.78-6.95 (m, 2H, Ar); 7.07-7.39 (m, 5H); 7.72-7.93 (m, 2H, Ar) **ppm**.

ESI-HRMS (*m/z*) $[M+H]^+$: calculated for $C_{20}H_{24}N_3O_4S$ 402.1482; found 402.1478 for (*S*)- **I-A4** and 402.1483 for (*R*)- **I-A4**.

(S) and *(R)* **I-A5** (S) and (R) 4-(4-benzoyl-2-benzylpiperazine-1-carbonyl)benzenesulfonamide

[^{1}H]-NMR (**DMSO**, mixture of conformers) δ: 2.62-2.85 (m, 0.5H); 2.86-3.15 (m, 3.5H); 3.35-3.63 (m, 2H); 3.64-3.83 (m, 1H); 4.25-4.55 (m, 1.5H); 4.60-5.03 (m, 0.5H); 6.68-7.04 (m, 2H, Ar); 7.05-7.59 (m, 12H, SO_2NH_2 + Ar); 7.60-7.87 (m, 2H, Ar) **ppm**.

ESI-HRMS (*m/z*) $[M+H]^+$: calculated $C_{25}H_{26}N_3O_4S$ 464.1639; found 464.1632 for (*S*)-**I-A5** and 464.1639 for (*R*)- **I-A5**.

(S) and *(R)* **I-A6** (S) and (R) 4-(2-benzyl-4-(2-phenylacetyl)piperazine-1-carbonyl) benzenesulfonamide

[^{1}H]-NMR (DMSO, mixture of conformers) δ: 2.53-2.64 (m, 1H); 2.65-2.97 (m, 3H); 2.98-3.31 (m, 1.5H); 3.61-3.96 (m, 3H); 4.08-4.43 (m, 2H); 4.48-4.54 (m, 0.2H); 4.73-4.94 (m, 0.3H); 6.68-6.88 (m, 1.5H, Ar); 6.89-7.00 (m, 0.5H, Ar); 7.11-7.33 (m, 10H, Ar); 7.38 (s, 2H, SO_2NH_2); 7.55-7.84 (m, 2H, Ar) **ppm**.

ESI-HRMS (*m/z*) $[M+H]^+$: calculated for $C_{26}H_{28}N_3O_4S$ 478.1795; found 478.1789 for (*S*) **I-A6** and 478.1800 for (*R*)- **I-A6**.

(S) and *(R)* **I-A7** (S) and (R) 4-(2-benzyl-4-(methylsulfonyl)piperazine-1-carbonyl) benzenesulfonamide

[^{1}H]-NMR (**DMSO**, mixture of conformers) δ: 2.62-3.15 (m, 8H); 3.35-3.78 (m, 3.5H); 4.37-4.48 (m, 0.25H); 4.87-4.98 (m, 0.25H); 6.83-7.02 (m, 2H, Ar); 7.05-7.58 (m, 7H, Ar + SO_2NH_2); 7.60-7.88 (m, 2H, Ar) **ppm**.

[^{13}C]-NMR (**DMSO**, mixture of conformers) δ: 34.5 (SO_2CH_3); 35.2 (CH_2); 36.9 (CH_2); 43.1 (CH_2); 45.9 (CH_2); 47.4 (CH_2); 48.6 (CH_2); 49.8 (CH); 56.5 (CH); 126.0 (CH_{Ar}); 126.3 (CH_{Ar}); 127.0 (CH_{Ar}); 127.3 (CH_{Ar}); 127.7 (CH_{Ar}); 128.9 (CH_{Ar}); 130.0 (CH_{Ar}); 138.3 (C_{Ar}); 139.3 (C_{Ar}); 145.1 (C_{Ar}); 168.5 (CO); 169.1 (CO) **ppm**.

ESI-HRMS (*m/z*) $[M+H]^+$: calculated for $C_{19}H_{24}N_3O_5S_2$ 438.1152; found 438.1153 for (*S*)- **I-A7** and 438.1150 for (*R*)- **I-A7**.

(S) and *(R)* **I-A8** (S) and (R) 4-(2-benzyl-4-(phenylsulfonyl)piperazine-1-carbonyl)benzenesulfonamide

[^{1}H]-NMR (**DMSO**, mixture of conformers) δ: 2.23-2.62 (m, 2H); 2.78-2.93 (m,0.5 H); 2.94-3.14 (m, 1.5H); 3.31-3.43 (m, 1H); 3.43-3.67 (m, 2H); 3.68-3.88 (m, 1H); 4.35-4.48 (m, 0.5H); 4.86-4.93 (m, 0.5H); 6.85-7.04 (m, 2H, Ar); 7.17-7.37 (m, 5H, Ar); 7.41 (s, 2H, SO_2NH_2); 7.58-7.87 (m, 7H, Ar) **ppm**. **[^{13}C]-NMR** (**DMSO**, mixture of conformers) δ: 35.1 ($PhCH_2$); 35.4 ($PhCH_2$); 36.9 (CH_2); 42.9 (CH_2); 46.1 (CH_2); 47.8 (CH_2); 48.9 (CH_2); 49.7 (CH); 56.4 (CH); 125.8 (CH_{Ar}); 126.2 (CH_{Ar}); 127.0 (CH_{Ar}); 127.4 (CH_{Ar}); 127.8 (CH_{Ar}); 128.0 (CH_{Ar}); 128.9 (CH_{Ar}); 133.9 (CH_{Ar}); 135.4 (C_{Ar}); 135.7 (C_{Ar}); 138.2 (C_{Ar}); 139.2 (C_{Ar}); 145.0 (C_{Ar} 145.2 (C_{Ar}); 168.5 (CO); 169.1 (CO) **ppm**.

ESI-HRMS (*m/z*) $[M+H]^+$: calculated for $C_{24}H_{26}N_3O_5S_2$ 500.1308; found 500.1312 for (*S*)- **I-A8** and 500.1304 for (*R*)- **I-A8**.

(S) and *(R)* **I-B1 (S) and (R) 4-(3-benzylpiperazine-1-carbonyl)benzenesulfonamide**

[^{1}H]-NMR (**DMSO**, mixture of conformers) δ: 2.52-2.83 (m, 6H); 2.90-3.05 (m, 1H); 3.22-3.30 (m, 1H); 4.17-4.29 (m, 1H); 7.03-7.36 (m, 5H, Ar); 7.44 (s, 2H, Ar); 7.47-

7.53 (d, J = 7.2 Hz, 1H, Ar); 7.71-7.77 (m, 0.5H, Ar); 7.78-7.85 (d, J = 6.4 Hz, 0.5 H, Ar) **ppm**.

ESI-HRMS (*m/z*) $[M+H]^+$: calculated for $C_{18}H_{22}N_3O_3S$ 360.1376; found 360.1379 for (*S*)-**I-B1** and 360.1373 for (*R*)- **I-B1**.

(S) and *(R)* **I-B2** (S) and (R) 4-(3,4-dibenzylpiperazine-1-carbonyl)benzenesulfonamide

[^{1}H]-NMR (**$CDCl_3$**, mixture of conformers) δ: 2.27-2.46 (m, 1H); 2.59-2.64 (m, 2H); 2.83-2.96 (m, 1H); 2.97-3.18 (m, 1.5H); 3.22-3.39 (m, 1.5H); 3.42-3.63 (m, 2H); 3.72-3.82 (m, 0.5H); 3.85-3.97 (m, 0.5H); 3.98-4.18 (m, 1H); 5.53-5.71 (m, 2H, SO_2NH_2); 6.78-6.88 (m, 1H, Ar); 7.03-7.15 (m, 1H, Ar); 7.16-7.49 (m, 9H, Ar); 7.44-7.58 (m, 1H, Ar); 7.62-7.73 (m, 1H, Ar); 7.83-7.91 (m, 1H, Ar) **ppm**.

[^{13}C]-NMR (**$CDCl_3$**, mixture of conformers) δ: 32.5 (CH_2Ph); 33.9 (CH_2Ph); 42.1 (C_2); 44.9 (C_2); 47.5 (C_6); 48.6 (C_6); 49.3 (C_5); 50.5 (C_5); 58.0 (NCH_2Ph); 58.3 (NCH_2Ph); 60.4 (C_3); 61.8 (C_3); 126.3 (CH_{Ar}); 126.6 (CH_{Ar}); 127.4 (CH_{Ar}); 127.5 (CH_{Ar}); 128.0 (CH_{Ar}); 128.5 (CH_{Ar}); 128.6 (CH_{Ar}); 128.8 (CH_{Ar}); 128.9 (CH_{Ar}); 129.3 (CH_{Ar}); 129.6 (CH_{Ar}); 137.9 (C_{Ar}); 138.2 (C_{Ar}); 138.8 (C_{Ar}); 139.0 (C_{Ar}); 139.6 (C_{Ar}); 143.3 (C_{Ar}); 143.5 (C_{Ar}); 168.7 (CO); 138.9 (CO) **ppm**.

ESI-HRMS (*m/z*) $[M+H]^+$: calculated for $C_{25}H_{28}N_3O_3S$ 450.1846; found 450.1839 for (*S*)-**I-B2** and 450.1847 for (*R*)-**I-B2**.

(S) and *(R)* **I-B3** (S) and (R) 4-(3-benzyl-4-methylpiperazine-1-carbonyl)benzenesulfonamide

[^{1}H]-NMR (**DMSO**, mixture of conformers) δ: 2.13-2.41 (m, 5.5H, NCH_3+piperazine protons); 2.63-2.97 (m, 2.5H); 2.98-3.32 (m, 3H); 3.77-3.87 (m, 0.5H); 4.03-4.14 (m, 0.5H); 6.93-7.02 (m, 1H, Ar); 7.04-7.17 (m, 1H, Ar); 7.18-7.39 (m, 4H); 7.44 (s, 2H, SO_2NH_2); 7.47-7.58 (m, 1H, Ar); 7.61-7.73 (m, 1H, Ar); 7.80-7.91 (m, 1H, Ar) **ppm**.

ESI-HRMS (*m/z*) $[M+H]^+$:calculated for $C_{19}H_{24}N_3O_3S$ 374.1533; found 374.1532 for (*S*)-**I-B3** and 374.1531 for (*R*)-**I-B3.**

(S) and *(R)* **I-B4** (S) and (R) 4-(4-acetyl-3-benzylpiperazine-1-carbonyl)benzenesulfonamide

[^{1}H]-NMR (**$CDCl_3$**, mixture of conformers) δ: 1.43-1.56 (bs, 0.5H, CH_3); 1.57-1.72 (bs, 1H, CH_3); 2.02 (s, 1.5H, CH_3); 2.42-2.63 (m, 0.5H); 2.71-3.18 (m, 3.5H); 3.20-3.73 (m, 2H); 3.81-3.93 (bs, 0.5H); 4.02-4.12 (bs, 0.5H); 4.40-4.97 (m, 2H); 5.88 (bs, 2H, SO_2NH_2); 6.83-6.97 (m, 1H, Ar); 7.00-7.38 (m, 4H, Ar); 7.42-7.57 (m, 2H, Ar); 7.78-7.94 (m, 2H, Ar) **ppm**.

[^{13}C]-NMR (**$CDCl_3$**) δ: 20.8 (CH_3); 21.7 (CH_3); 35.2 (CH_2); 35.9 (CH_2); 36.3 (CH_2); 36.7 (CH_2); 41.4 (CH_2); 42.3 (CH_2); 45.0 (CH_2); 47.3 (CH_2); 50.2 (CH); 56.4 (CH); 126.8 (CH_{Ar}); 127.2 (CH_{Ar}); 127.8 (CH_{Ar}); 128.5 (CH_{Ar}); 128.9 (CH_{Ar}); 129.3 (CH_{Ar}); 136.6 (C_{Ar}); 137.2 (C_{Ar}); 138.9 (C_{Ar}); 144.0 (C_{Ar}); 169.6 (CO); 170.0 (CO) **ppm**.

ESI-HRMS (*m/z*) $[M+H]^+$: calculated for $C_{20}H_{24}N_3O_4S$ 402.1482; found 402.1488 for (*S*)-**I-B4** and 402.1474 for (*R*)-**I-B4**.

(S) and *(R)* **I-B5** (S) and (R) 4-(4-benzoyl-3-benzylpiperazine-1-carbonyl)benzenesulfonamide

[^{1}H]-NMR (**DMSO**, mixture of conformer) δ: 2.82-3.08 (m, 4H); 3.36-3.62 (m, 1.5H); 3.63-3.93 (m, 1H); 4.15-4.52 (m, 2H); 4.72-5.02 (m, 0.5H); 6.58-6.96 (m, 2H, Ar); 6.97-7.39 (m, 8H, Ar); 7.46 (s, 2H, SO_2NH_2); 7.53-7.77 (m, 2H, Ar); 7.78-7.93 (m, 2H, Ar) **ppm**.

ESI-HRMS (*m/z*) $[M+H]^+$: calculated for $C_{25}H_{26}N_3O_4S$ 464.1639; found 464.1633 for (*S*)-**I-B5** and 464.1642 for (*R*)-**I-B5**.

(S) and *(R)* **I-B6** (S) and (R) 4-(3-benzyl-4-(2-phenylacetyl)piperazine-1-carbonyl) benzenesulfonamide

[^{1}H]-NMR (**DMSO**, mixture of conformers) δ: 2.51-2.62 (m, 0.5H); 2.65-3.12 (m, 6H); 3.35-3.52 (m, 1H); 3.53-3.67 (m, 1H); 4.05-4.53 (m, 2H); 4.55-4.85 (m, 0.5H); 6.72-6.95 (m, 1H, Ar); 6.96-7.03 (m, 1H, Ar); 7.05-7.33 (m, 8H, Ar); 7.42 (s, 2H, SO_2NH_2); 7.52-7.72 (bs, 2H, Ar); 7.78-7.93 (m, 2H, Ar) **ppm**.

ESI-HRMS (*m/z*) $[M+H]^+$: calculated for $C_{26}H_{28}N_3O_4S$ 478.1795; found 478.1786 for (S)-**I-B6** and 478.1802 for (*R*)-**I-B6**.

(S) and *(R)* **I-B7** (S) and (R) 4-(3-benzyl-4-(methylsulfonyl)piperazine -1-carbonyl) benzenesulfonamide

[^{1}H]-NMR (**CD_3OD**, mixture of conformers) δ: 2.37-2.72 (m, 3H); 2.93-3.13 (m, 2H); 3.37-3.73 (m, 5H); 4.12-4.23 (m, 0.5H, CH); 4.25-4.47 (m, 0.5H, CH); 4.51-4.68 (m, 1H); 7.02-7.41 (m, 5H, Ar); 7.54-7.68 (m, 2H, Ar); 7.93-8.08 (m, 2H, Ar) **ppm**.

ESI-HRMS (*m/z*) $[M+H]^+$: calculated for $C_{19}H_{24}N_3O_5S_2$ 438.1152; found 438.1148 for (*S*)-**I-B7** and 438.1160 for (*R*)-**I-B7**.

(S) and *(R)* **I-B8** (S) and (R) 4-(3-benzyl-4-(phenylsulfonyl)piperazine-1-carbonyl) benzenesulfonamide

[^{1}H]-NMR (**DMSO**, mixture of conformers) δ: 2.53-2.66 (m, 1H); 2.68-2.83 (m, 1.5H); 2.84-2.91 (m, 0.5H), 2.92-3.08 (m, 0.5H); 3.11-3.29 (m, 2H), 3.40-3.53 (m, 0.5H); 3.55-3.74 (m, 1H); 4.09-4.47 (m, 2H); 6.86-7.02 (bs, 0.5H, Ar); 7.05-7.38 (m, 3.5H, Ar); 7.42-7.79 (m, 10H, Ar +SO_2NH_2); 7.80-7.95 (m, 2H, Ar) **ppm**.

ESI-HRMS (*m/z*) $[M+H]^+$: calculated for $C_{24}H_{26}N_3O_5S_2$ 500.1308; found 500.1310 for (*S*)-**I-B8** and 500.1304 for (*R*)-**I-B8**.

(S) and *(R)* **I-B9** (S) and (R) 4,4'-(2-benzylpiperazine-1,4-dicarbonyl)dibenzenesulfonamide

[^{1}H]-NMR (**DMSO**, mixture of conformers) δ: 2.57-2.89 (m, 1H); 2.90-3.21 (m, 2.5H); 3.30-3.88 (m, 3.5H); 4.22-4.53 (m, 1.5H); 4.58-5.02 (m, 0.5H); 6.73-7.05 (m, 2H, Ar); 7.08-7.40 (m, 5.5H, Ar); 7.45 (bs, 4H, SO_2NH_2); 7.58-7.98 (m, 5.5H, Ar) **ppm**.

ESI-HRMS (*m/z*) $[M+H]^+$: calculated for $C_{25}H_{27}N_4O_6S_2$ 543.1367; found 543.1360 for (*S*)-**I-B9** and 543.11363 for (*R*)-**I-B9**.

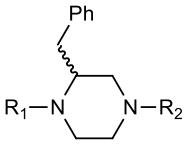

Table 7.1. Details Related to the General Synthetic Procedure 1

N	R_1	R_2	S.M.[A] (mmol)	R-Z (eq)	BASE (eq)	YIELD %	E.[B]	M.P. (°C)
(*S*)I-A1	ZBG	CH_2Ph	(*S*)-**5** (1)	ZBG-Cl	NEt_3	79		118-122
(*R*) I-A1			(*R*)-**5** (1)	(1)	(1.2)	72		120-122
(*S*) I-A3	ZBG	CH_3	(*S*) **I-A2** (0.1)	CH_3I	-	32	A	> 260
(*R*) I-A3			(*R*) **I-A2** (0.1)	(0.5)		41		> 260
(*S*) I-A4	ZBG	CH_3CO	(*S*) **I-A2** (0.1)	Ac_2O (5)	-	98	B	202-205
(*R*) I-A4			(*R*) **I-A2** (0.1)			99		200-204
(*S*) I-A5	ZBG	PhCO	(*S*) **I-A2** (0.1)	PhCOCl	NEt_3 (2)	68	B	> 260
(*R*) I-A5			(*R*) **I-A2** (0.1)	(2)		92		> 260
(*S*) I-A6	ZBG	$PhCH_2CO$	(*S*) **I-A2** (0.1)	$PhCH_2C$	-	87	B	180-182
(*R*) I-A6			(*R*) **I-A2** (0.1)	O-NHS[b] (3)		68		185-188
(*S*) I-A7	ZBG	CH_3SO_2	(*S*) **I-A2** (0.1)	CH_3SO_2C	NEt_3	78	C	> 260
(*R*) I-A7			(*R*) **I-A2** (0.1)	l (2)	(1.2)	91		> 260
(*S*) I-A8	ZBG	$PhSO_2$	(*S*) **I-** (0.1)	$PhSO_2Cl$	NEt_3	75	B	> 260
(*R*) I-A8			(*R*) **I-A2** (0.1)	(2)	(1.2)	98		> 260
(*S*)I-B1	H	ZBG	(*S*)-**9** (0.7)	ZBG-NHS (0.7) [c]	-	70	A	190 (d)
(*R*) I-B1			(*R*)-**9** (0.8)			74		195 (d)
(*S*) I-B2	CH_2Ph	ZBG	(*S*) **I-B1** (0.1)	$PhCH_2Br$	$NaHCO_3$	69	B	160-162
(*R*) I-B2			(*R*) **I-B1** (0.1)	(1.5)	(10)	57		156-159
(*S*) I-B3	CH_3	ZBG	(*S*)-**11** (0.15)	ZBG-Cl (1.5)	NEt_3 (1.2)	35	A	197-199
(*R*) I-B3			(*R*) **I-B1** (0.2)	CH_3I (0.5)	-	40		201-203
(*S*)- I-B4	CH_3CO	ZBG	(*S*) **I-B1** (0.1)	Ac_2O (5)	-	85	B	202-205
(*R*) I-B4			(*R*) **I-B1** (0.1)			95		201-204
(*S*) I-B5	PhCO	ZBG	(*S*) **I-B1** (0.1)	PhCOCl	NEt_3 (3)	80	B	228-231
(*R*) I-B5			(*R*) **I-B1** (0.1)	(2)		85		230-232
(*S*) I-B6	$PhCH_2CO$	ZBG	(*S*) **I-B1** (0.1)	$PhCH_2C$	-	38	C	178-180
(*R*)I-B6			(*R*) **I-B1** (0.1)	O-NHS[d] (2)		72		170-173
(*S*) I-B7	CH_3SO_2	ZBG	(*S*) **I-B1** (0.1)	CH_3SO_2C	NEt_3	82	C	189-192
(*R*) I-B7			(*R*) **I-B1** (0.1)	l (1)	(1.2)	78		195-197
(*S*) I-B8	$PhSO_2$	ZBG	(*S*) **I-B1** (0.1)	$PhSO_2Cl$	NEt_3 (3)	82	B	203-206
(*R*) I-B8			(*R*) **I-B1** (0.1)	(2)		91		210-212
(*S*) I-B9	ZBG	ZBG	(*S*)-**9** (0.16)	ZBG-Cl	NEt_3 (3)	99	B	>260
(*R*) I-B9			(*R*)-**9** (0.16)	(2)		99		> 260

[A]: Starting Material[a]B: Eluent: DCM/MeOH/NH_3 95:5:0.5; **B:** DCM/MeOH 95:5; **C:** DCM/MeOH 93:7. [b] Prepared as reported in ref[151]

[c]Addition performed at 0°C. [d] Prepared as reported in ref[152]. **ZBG:** $COC_6H_4SO_2NH_2$; **ZBG-NHS:** 2,5-dioxopyrrolidin-1-yl 4-sulfamoylbenzoate; **$PhCH_2CO$-NHS:** 2,5-dioxopyrrolidin-1-yl 2-phenylacetate.

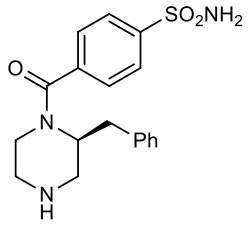

(*S*) **I-A2** (S)-4-(2-benzylpiperazine -1-carbonyl) benzenesulfonamide
A solution of acetyl chloride (0.163 mL; 2.28 mmol) in MeOH (10 mL) was added to a suspension of (S)-**I-A1** (514 mg; 1.14 mmol) in MeOH (10 mL). The resulting solution was hydrogenated at 75 psi over Pd 10%/C (200 mg) for 24 h, then the catalyst was filtered off. Diethyl ether was slowly added to the solution, producing the precipitation of a white solid, which was filtered and treated with a saturated solution of $NaHCO_3$ and extracted three times with ethyl acetate. The organic phase was dried (Na_2SO_4) and the solvent was removed under vacuum to give the title compounds as a white solid.

Yield= 100%; **M.P.**= 212-216°C

[^{1}H]-NMR (**DMSO**, mixture of conformers) δ: 2.57-2.88 (m, 4H); 2.90-3.20 (m, 3.5H); 3.44-3.55 (bs, 0.5H); 4.16-4.27 (m, 0.5H); 4.67-4.74 (bs, 0.5 H); 6.82-6.95 (m, 2H, Ar); 7.14-7.33 (m, 5H, Ar); 7.35-7.44 (s, 2H, SO_2NH_2); 7.63-7.85 (m, 2H, Ar) **ppm**.

[^{13}C]-NMR (**DMSO**, mixture of conformers) δ: 34.7 (CH_2Ph); 35.2 (CH_2Ph); 39.1 (CH_2); 44.1 (CH_2); 45.6 (CH_2); 47.0 (CH_2); 48.3 (CH_2); 49.9 (CH); 57.0 (CH); 125.9 (CH_{Ar}); 126.7 (CH_{Ar}); 127.0 (CH_{Ar}); 127.4 (CH_{Ar}); 128.7 (CH_{Ar}); 129.6 (CH_{Ar}); 129.7 (CH_{Ar}); 138.9 (C_{Ar}); 139.8 (C_{Ar}); 144.7 (C_{Ar}); 168.3 (CO); 169.1 (CO) ppm.

ESI-HRMS (*m/z*) $[M+H]^+$: calculated for $C_{18}H_{22}N_3O_3S$ 360.1376; found 360.1374 for (*S*)-**I-A2** and 360.1373 for (*R*)-**I-A2**.

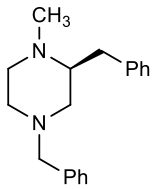

(*S*)-**10** (S)-2,4-dibenzyl-1-methylpiperazine
To a stirring solution of (*S*)-**5**[112] (0.115 mg; 0.43 mmol) in absolute EtOH (5 mL), formaldehyde (0.06 mL; 2.2 mmol) and formic acid (0.28 mL; 7.3 mmol) were added. The mixture was then heated at 80°C for 6 hours, then the solvent was removed and the residue was partitioned between DCM and a solution of $NaHCO_3$. Dehydration (Na_2SO_4) and removal of the solvent gave (*S*)-**10** as a yellow oil.

Yield= 99%

[^{1}H]-NMR (**$CDCl_3$**) δ: 2.0-2.1 (m, 1H); 2.21-2.29 (m, 1H); 2.32-2.41 (m, 1H); 2.43 (s, 3H, NCH_3); 2.44-2.62 (m, 4H); 2.75-2.8 (dt, J= 11.6 Hz, 3.6 Hz, 1H); 3.06-3.09 (d, J = 11.6 Hz, 1H); 3.24-3.28 (d, J= 13.0 Hz,1H); 3.51-3.55 (d, J= 13.0 Hz, 1H); 7.1-7.33 (m, 10H, Ar) **ppm**.

ESI-MS (*m/z*): 281.1 $[M+H]^+$.

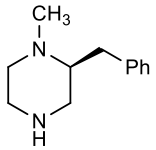

(*S*)-**11**(S)-2-benzyl-1-methylpiperazine
To a solution of (*S*)-**10** (120 mg; 0.43 mmol) in MeOH (10 mL) a solution of acetyl chloride (0.061 ml; 0.86 mmol) in MeOH (10 mL) was added. The resulting mixture was hydrogenated at 75 psi over Pd 10%/C for 24 hours, then the catalyst was filtered off. The solvent was removed under vacuum and the residue was treated with a saturated solution of $NaHCO_3$ and extracted three times with DCM. The organic phase was dried (Na_2SO_4) and the solvent was removed under vacuum. The residue was purified with flash chromatography (DCM/MeOH/NH_3 90:10:1) to give (*S*)-**11**[153] as a yellow oil.

Yield= 40% **ESI-MS (*m/z*):** 191.1 $[M+H]^+$.
[^{1}H]-NMR (**$CDCl_3$**) δ: 1.62 (bs, 1H, NH); 2.20-2.29 (m, 2H, H_2 + H_6); 2.37-2.48 (m, 5H, CH_3 + H_3+ C*H*HPh); 2.69-2.75 (dd, J= 12.4, 2.4 Hz; 1H, H_3); 2.78–2.83 (dt, J= 11.6, 2.8 Hz, 1H, H_6); 2.87-2.92 (m, 2H, H_5); 3.13-3.19 (dd, J= 13.2, 4.0 Hz, 1H, CH*H*Ph); 7.12-7.29 (m, 5H, Ar) **ppm**.
[^{13}C]-NMR (**$CDCl_3$**) δ: 36.9 (CH_2Ph); 43.5 (CH_3); 46.1 (C_5); 50.4 (C_3); 56.6 (C_6); 64.9 (C_2); 126.1 ($C_{4'}$); 128.3 ($C_{2'}$ + $C_{6'}$); 19.3 ($C_{3'}$+$C_{5'}$); 139.1 ($C_{1'}$) **ppm**.

7.2 Piperazines and Aminopiperidine II-A, II-B and II-C Series

General procedure 2: Insertion of the *Z*inc Binding Group to prepare the derivatives of series **II:**

To a solution of the suitable amine (30-100 mg) in anhydrous CH_3CN (5-30 mL), stirred at room T, Et_3N (2 eq) and 4-sulfamoylbenzoyl chloride (1.5 eq) were sequentially added (Method A); alternatively, (Method B), the amine was treated with 2,5-dioxopyrrolidin-1-yl 4-sulfamoylbenzoate [24]. The mixture was left stirring at room T for 6-20 hrs. After removal of the solvent under vacuum, the residue was partitioned between ethyl acetate and sat. aqueous $NaHCO_3$; drying and removal of the solvent gave a residue which was purified by flash chromatography, when necessary (if done, the eluent is reported in the description of the product). In this way the following listed compounds were prepared.

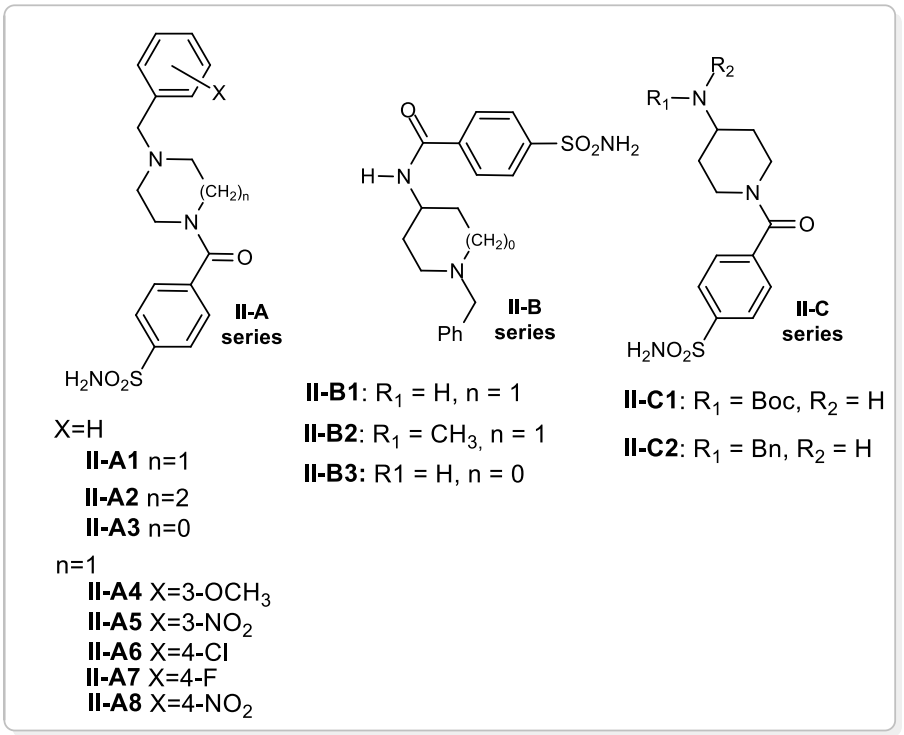

S.M.= starting material

II-A1[138] 4-(4-benzylpiperazine-1-carbonyl)benzenesulfonamide
(Method A); **S.M.=** *N*-benzylpiperazine; White solid; **Yield=** 60%; **M.P.=** 204-5 °C

[^{1}H-NMR] (DMSO) δ: 7.84 (d, J=8.2 Hz, 2H, Ar), 7.54 (d, J=8.2 Hz, 2H, Ar), 7.44 (s, 2H, SO_2NH_2), 7.36-7.20 (m, 5H, Ar), 3.61 (bs, 2H), 3.48 (s, 2H, CH_2Ph), 3.40-3.20 (m, 2H+water), 2.41 (bs, 2H), 2.32 (bs, 2H) **ppm**.

II-A2 4-(4-benzyl-1,4-diazepane-1-carbonyl)benzenesulfonamide
(Method A): **S.M.=** *N*-benzyl-homopiperazine; White solid; **Yield=** 41%; **M.P.=** 175°C (d),
[^{1}H-NMR] (DMSO) δ: 7.94-7.82 (m, 2H, Ar), 7.64-7.51 (m, 2H, Ar), 7.45 (s, 2H, NH_2), 7.35-7.23 (m, 5H, Ar), 3.72-3.54 (m, 4H), 3.32 (s, 2H+water), 2.78-2.69 (m, 1H), 2.67-2.53 (m, 3H), 1.89-1.78 (m, 1H), 1.72-1.62 (m, 1H) **ppm**.
[^{13}C NMR] (DMSO, mixture of conformers) **δ**: 169.57 (CO), 169.50 (CO), 144.88 (C_{Ar}), 140.72 (C_{Ar}), 139.48 (C_{Ar}), 129.03 (CH_{Ar}), 128.90 (CH_{Ar}), 128.67 (CH_{Ar}), 128.64 (CH_{Ar}), 127.53 (CH_{Ar}), 127.43 (CH_{Ar}), 127.35 (CH_{Ar}), 126.29 (CH_{Ar}), 126.26 (CH_{Ar}), 61.57 (CH_2Ph), 61.37 (CH_2Ph), 55.53 (CH_2), 55.19 (CH_2), 54.43 (CH2), 53.84 (CH_2), 49.55 (CH_2), 48.50 (CH_2), 45.70 (CH_2), 45.00 (CH_2), 28.56 (CH_2), 26.99 (CH_2) **ppm**.
ESI-HRMS (*m/z*) $[M+H]^+$: calculated for $C_{19}H_{24}N_3O_3S$ 374.1533; found 374.1532.

II-A3 4-(4-benzylpiperazine-1-carbonyl)benzenesulfonamide
(Method A) **S.M.=** N-benzylimidazolidine[154], **Eluent:** DCM/MeOH 90:10; White solid, **Yield=** 10%; **M.P.=** 175 °C (d);
[^{1}H-NMR] (DMSO, mixture of conformers) **δ**: 7.85-7.79 (m, 2H, Ar), 7.71 (d, *J*=8.0 Hz, 1H, Ar), 7.65 (d, *J* = 8.0 Hz, 1H, Ar), 7.43 (s, 1H, SO_2NH_2), 7.41 (s, 1H, SO_2NH_2), 7.34-7.20 (m, 5H, Ar), 4.10 (s, 1H), 3.97 (s, 1H), 3.66 (s, 1H), 3.55 (s, 1H), 3.52 (t, *J* = 6.4 Hz, 1H), 3.44 (t, *J* = 6.0 Hz, 1H), 2.86 (t, *J* = 6.4 Hz, 1H), 2.80 (t, *J* = 6.4 Hz, 1H) **ppm**.
[^{13}C-NMR] (DMSO, mixture of conformers) **δ**: 167.16 (CO), 166.86 (CO), 145.91 (C_{Ar}), 145.79 (C_{Ar}), 139.80 (C_{Ar}), 139.58 (C_{Ar}), 138.64 (C_{Ar}), 138.53 (C_{Ar}), 129.12 (CH_{Ar}), 128.94 (CH_{Ar}), 128.81 (CH_{Ar}), 128.78 (CH_{Ar}), 128.32 (CH_{Ar}), 128.10 (CH_{Ar}), 127.67 (CH_{Ar}), 126.25 (CH_{Ar}), 126.13 (CH_{Ar}), 70.27 (CH_2), 68.52 (CH_2), 57.43 (CH_2), 56.98 (CH_2), 52.87 (CH_2), 51.31 (CH_2), 47.00 (CH_2), 44.34 (CH_2) **ppm**.
ESI-HRMS (*m/z*) $[M+H]^+$: calculated for $C_{17}H_{20}N_3O_3S$ 346.1220; found 346.1222.

II-A4[155] 4-(4-(3-methoxybenzyl)piperazine-1-carbonyl)benzenesulfonamide
(Method A): **S.M.= 12a**[155] **Eluent:** DCM/MeOH 90:10; White solid, **Yield=** 47%; **M.P.=** 186°C (d).
[^{1}H-NMR] (DMSO) δ: 7.82 (d, *J* = 8.2 Hz, 2H, Ar), 7.52 (d, *J* = 8.2 Hz, 2H, Ar), 7.41 (s, 2H, SO_2NH_2), 7.19 (m, 1H, Ar), 6.87-6.70 (m, 3H, Ar), 3.69 (s, 3H, OCH_3), 3.65-3.55 (m, 2H), 3.43 (s, 2H, CH_2-Ar), 3.30-3.20 (m, 2H+water), 2.45-2.26 (m, 4H) **ppm**.
[^{13}C-NMR] (DMSO) δ: 168.18 (CO), 159.74 (C_{Ar}), 145.22 (C_{Ar}), 139.88 (C_{Ar}), 139.58 (C_{Ar}), 129.73 (CH_{Ar}), 127.95 (CH_{Ar}), 126.31 (CH_{Ar}), 121.52 (CH_{Ar}), 114.81 (CH_{Ar}), 112.90 (CH_{Ar}), 62.19 (CH_2-Ar), 55.41 (OCH_3), 53.13 (CH_2), 52.59 (CH_2), 47.55 (CH_2), 42.07 (CH_2) **ppm**.
ESI-HRMS (*m/z*) $[M+H]^+$: calculated for $C_{19}H_{24}N_3O_4S$ 390.1482 found 390.1480

II-A5 4-(4-(3-nitrobenzyl)piperazine-1-carbonyl)benzenesulfonamide
(Method A): **S.M.= 12b**[156] **Eluent:** DCM/MeOH/NH_3 85:15:1.5; White solid, **Yield=** 73%; **M.P.=** 176°C (d)

[^{1}H-NMR] (DMSO) δ: 8.15 (s, 1H, Ar), 8.11 (d, *J* = 8.0 Hz, 1H, Ar), 7.85 (d, *J* = 8.4 Hz, 2H, Ar), 7.77 (d, *J* = 7.6 Hz, 1H, Ar), 7.62 (t, *J* = 8.0 Hz, 1H, Ar), 7.56 (d, *J* = 8.4 Hz, 2H, Ar), 7.42 (s, 2H, NH_2), 3.64 (bs, 4H), 3.30-3.20 (bs, 2H+water), 2.50-2.40 (bs, 2H+DMSO), 2.40-2.30 (m, 2H) **ppm**.
[^{13}C-NMR] (DMSO) δ: 168.19 (CO), 148.37 (C_{Ar}), 145.26 (C_{Ar}), 140.95 (C_{Ar}), 139.55 (C_{Ar}), 135.95 (CH_{Ar}), 130.24 (CH_{Ar}), 127.94 (CH_{Ar}), 126.30 (CH_{Ar}), 123.63 (CH_{Ar}), 122.56 (CH_{Ar}), 60.99 (CH_2-Ar), 53.04 (CH_2), 52.49 (CH_2), 47.54 (CH_2), 42.01 (CH_2) **ppm**.
ESI-HRMS (*m/z*) $[M+H]^+$: calculated for $C_{18}H_{21}N_4O_5S$ 405.1227 found 405.1230.

II-A6 4-(4-(4-chlorobenzyl)piperazine-1-carbonyl)benzenesulfonamide
(Method A): **S.M.= 14c**[157] **Eluent:** DCM/MeOH/NH_3 90:10:1; White soli; **Yield=** 46%; **M.P.=** 253°C (d);
[^{1}H NMR] (DMSO) δ: 7.82 (d, *J* = 8.4 Hz, 2H, Ar), 7.52 (d, *J* = 8.4 Hz, 2H, Ar), 7.40 (s, 2H, SO_2NH_2), 7.34 (d, *J* = 8.4 Hz, 2H, Ar), 7.28 (d, *J* = 8.4 Hz, 2H, Ar), 3.65-3.50 (m, 2H), 3.45 (s, 2H, CH_2Ar), 3.30-3.20 (m, 2H+water), 2.42-2.25 (m, 4H) **ppm**.
[^{13}C-NMR] (DMSO) δ: 168.17 (CO), 145.22 (C_{Ar}), 139.55 (C_{Ar}), 137.35 (C_{Ar}), 132.04 (C_{Ar}), 131.12 (CH_{Ar}), 128.67 (CH_{Ar}), 127.95 (CH_{Ar}), 126.30 (CH_{Ar}), 61.30 (CH_2-Ar), 53.07 (CH_2), 52.48 (CH_2), 47.55 (CH_2), 42.02 (CH_2) **ppm**.
ESI-HRMS (*m/z*) $[M+H]^+$: calculated for $C_{18}H_{21}ClN_3O_3S$ 394.0987 found 394.0987.

II-A7[138] 4-(4-(4-fluorobenzyl)piperazine-1-carbonyl)benzenesulfonamide
(Method A): **S.M.= 12d**[158]**; Eluent:** DCM/MeOH 90:10; White solid; **Yield=** 41%; **M.P.=** 209 °C (d)
[^{1}H-NMR] (DMSO) δ: 7.84 (d, *J* = 8.4 Hz, 2H, Ar), 7.54 (d, *J* = 8.4 Hz, 2H, Ar), 7.44 (s, 2H, SO_2NH_2), 7.32 (dd, J = 8.3 Hz, 5.8 Hz, 2H, Ar), 7.12 (t, J=8.8 Hz, 2H, Ar), 3.70-3.55 (m, 2H), 3.47 (s, 2H, CH_2Ar), 3.28-3.22 (m, 2H), 2.46-2.28 (m, 4H) **ppm**.

II-A8 4-(4-(4-nitrobenzyl)piperazine-1-carbonyl)benzenesulfonamide
(method A): **S.M.= 12e**[159] **Eluent:** DCM/MeOH/NH_3 92:8:0.8; White solid; **Yield=** 65%; **M.P.=** 226 °C (d);
[^{1}H NMR] (DMSO) δ: 8.18 (d, *J* = 8.8 Hz, 2H, Ar), 7.85 (d, *J* = 8.4 Hz, 2H, Ar), 7.59 (d, *J* = 8.8 Hz, 2H, Ar), 7.55 (d, *J* = 8.4 Hz, 2H, Ar), 7.42 (s, 2H, SO_2NH_2), 3.66 (bs, 4H), 3.30-3.20 (m, 2H+water), 2.50-2.31 (m, 4H) **ppm**.
[^{13}C-NMR] (DMSO) δ: 168.19 (CO), 147.13 (C_{Ar}), 146.75 (C_{Ar}), 145.24 (C_{Ar}), 139.51 (C_{Ar}), 130.25 (CH_{Ar}), 127.96 (CH_{Ar}), 126.30 (CH_{Ar}), 123.87 (CH_{Ar}), 61.21 (CH_2-Ar), 53.15 (CH_2), 52.59 (CH_2), 47.55 (CH_2), 42.02 (CH_2) **ppm**.
ESI-HRMS (*m/z*) $[M+H]^+$: calculated for $C_{18}H_{21}N_4O_5S$ 405.1227 found 405.1225.

II-B1 N-(1-benzylpiperidin-4-yl)-4-sulfamoylbenzamide
(Method A): **S.M.=** 1-benzylpiperidinyl-4-amine **Eluent:** DCM/MeOH/NH_3 90:10:1; White solid; **Yield=** 19% **M.P.=** 220 °C (d);
[^{1}H] NMR (DMSO) δ: 8.40 (d, *J* = 7.6 Hz, 1H, NH) 7.92 (d, *J* = 8.4 Hz, 2H, Ar), 7.83 (d, *J* = 8.4 Hz, 2H, Ar), 7.44 (s, 2H, SO_2NH_2), 7.36-7.19 (m, 5H, Ph), 3.80-3.68 (m, 1H), 3.49 (s, 2H, CH_2Ph), 2.77 (d, *J* = 11.3 Hz, 2H), 2.06-1.88 (m, 1H), 1.74 (d, *J* = 11.6 Hz, 2H), 1.65-1.45 (m, 2H) **ppm**.
[^{13}C] NMR (DMSO) δ: 165.12 (CO), 146.62 (C_{Ar}), 138.09 (C_{Ar}), 129.29 (CH-Ar), 128.26 (CH_{Ar}), 128.39 (CH_{Ar}), 127.42 (CH_{Ar}), 125.98 (CH_{Ar}), 62.46 (CH_2), 52.58 (CH_2), 47.52 (CH), 31.76 (CH_2) **ppm**.
ESI-HRMS (*m/z*) $[M+H]^+$: calculated for $C_{19}H_{24}N_3O_3S$ 374.1533, found 374.1531.

II-B2[117] N-(1-benzylpiperidin-4-yl)-N-methyl-4-sulfamoylbenzamide

(Method B): **S.M.=** 1-benzyl-*N*-methylpiperidin-4-amine **Eluent:** DCM/MeOH/NH_3 90:10:1; White solid; **Yield=** 38%; **M.P.=** 207 °C (d);. **[^{1}H-NMR] ($CDCl_3$,** mixture of conformers) **δ**: 7.92-7.80 (m, 2H, Ar), 7.50-7.35 (m, 2H, Ar), 7.35-7.15 (m, 5H, Ar), 5.27-5.05 (m, 2H, SO_2NH_2), 4.60-4.43 (m, 0.5 H), 3.58-3.43 (bs, 1H), 3.43-3.37 (bs, 1H), 3.37-3.21 (m, 0.5 H), 3.10-2.90 (m, 2.5 H), 2.90-2.80 (m, 1H), 2.75 (s, 1.5 H), 2.23-2.06 (m, 1H), 1.99-1.62 (m, 4H), 1.62-1.48 (m, 1H) **ppm**.

[^{13}C-NMR] (DMSO, mixture of conformers) **δ:** 169.72 (CO), 144.92 (C_{Ar}), 140.75 (C_{Ar}), 138.98 (C_{Ar}), 138.71 (C_{Ar}), 129.95 (CH_{Ar}), 128.61 (CH_{Ar}), 127.75 (CH_{Ar}), 127.36 (CH_{Ar}), 127.12 (CH_{Ar}), 126.34 (CH_{Ar}), 62.44 (CH_2), 62.11 (CH_2), 57.01 (CH), 52.90 (CH_2), 52.50 (CH_2), 51.83 (CH), 32.31 (CH_3), 29.57 (CH_2), 28.56 (CH_2), 27.64 (CH_3) **ppm**. **ESI-HRMS (*m/z*)** $[M+H]^+$: calculated for $C_{20}H_{26}N_3O_3S$ 388.1689, found 388.1692.

II-B3 N-(1-benzylpiperidin-4-yl)-4-sulfamoylbenzamide

(Method B): **S.M:** 1-benzylpirrolidin-3-amine **Eluent:** DCM/MeOH/NH_3 90:10:1; White solid, **Yield=** 54% **M.P.=** 174-178 °C;

[^{1}H-NMR] (MeOD) δ: 7.98-7.86 (m, 4H, Ar), 7.38-7.20 (m, 5H, Ar), 4.60-4.49 (m, 1H), 3.72-3.60 (m, 2H), 2.94- 2.85 (m, 1H), 2.85-2.77 (m, 1H), 2.65-2.50 (m, 2H), 2.41-2.27 (m, 1H), 1.90-1.76 (m, 1H) **ppm**.

[^{13}C NMR] (DMSO) δ: 165.56 (CO), 146.61 (C_{Ar}), 139.41 (C_{Ar}), 137.79 (C_{Ar}), 129.04 (CH_{Ar}), 128.60 (CH_{Ar}), 128.46 (CH_{Ar}), 127.28 (CH_{Ar}), 125.96 (CH_{Ar}), 60.22 (CH_2), 59.86 (CH_2Ph), 52.96 (CH_2), 49.42 (CH_2), 31.12 (CH_2) **ppm**.

ESI-HRMS (*m/z*) $[M+H]^+$: calculated for $C_{18}H_{22}N_3O_3S$ 360.1376, found 360.1377.

II-C1 tert-butyl (1-(4-sulfamoylbenzoyl)piperidin-4-yl)carbamate

(Method B): **S.M.=** *tert*-butyl piperidin-4-ylcarbamate **Eluent:** AcOEt; White solid, **Yield=** 65%; **M.P.=** 229 °C (d);

[^{1}H-NMR] (DMSO) δ: 7.83 (d, J = 8.0 Hz, 2H, Ar), 7.49 (d, J = 8.0 Hz, 2H, Ar), 7.40 (s, 2H, SO_2NH_2), 6.90-6.84 (m, 1H, NH), 4.32-4.21 (m, 1H), 3.52-3.31 (m, 2H), 3.11-2.98 (m, 1H), 2.98-2.83 (m, 1H), 1.82-1.50 (m, 2H), 1.33 (s, 9H, $C(CH_3)_3$), 1.28-1.25 (m, 2H) **ppm**.

[^{13}C-NMR] (DMSO) δ: 168.17 (CO), 155.29 (CO), 145.19 (C_{Ar}), 139.93 (C_{Ar}), 127.63 (CH_{Ar}), 126.37 (CH_{Ar}), 78.16 (CMe_3), 47.53 (CH), 46.33 (CH_2), 32.66 (CH_2), 31.79 (CH_2), 28.71 (CH_3) **ppm**.

ESI-HRMS (*m/z*) $[M+H]^+$: calculated for $C_{17}H_{26}N_3O_5S$ 384.1588, found 384.1586.

II-C4[155] 4-(4-(benzyl(methyl)amino)piperidine-1-carbonyl)benzenesulfonamide

(Method B): **S.M.= 14; Eluent:** DCM/MeOH/NH_3 90:10:1; White solid; **Yield=** 98%; **M.P.=**. 206-209 °C;

[^{1}H-NMR] (DMSO) δ: 7.83 (d, J = 8.0 Hz, 2H, Ar), 7.60-7.09 (m, 14 H, Ar + SO_2NH_2), 5.06 (bs, 2H, OCH_2Ph), 4.60-4.40 (m, 3H, NCH_2Ph + 1H), 4.23-4.05 (m, 1H), 3.30-3.20 (m, 1H+water), 3.14-2.98 (m, 1H), 2.82-2.65 (m, 1H), 1.76-1.60 (m, 3H), 1.59-1.47 (m, 1H) **ppm**.

[^{13}C-NMR] (DMSO) δ: 168.10 (CO), 145.07 (C_{Ar}), 140.04 (C_{Ar}), 138.86 (C_{Ar}), 137.25 (C_{Ar}), 130.34 (CH-Ar), 128.73 (CH_{Ar}), 128.24 (CH_{Ar}), 127.92 (CH_{Ar}), 127.60 (CH_{Ar}), 127.13 (CH_{Ar}), 126.95 CH_{Ar}), 126.27 (CH_{Ar}), 66.82 (OCH_2Ph), 54.88 (CH), 46.91 (NCH_2), 41.43 (CH_2) **ppm**.

ESI-HRMS (*m/z*) $[M+H]^+$: calculated for $C_{27}H_{30}N_3O_5S$ 508.1901, found 508.1903.

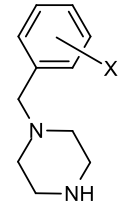

12a X=3-OCH_3
12b X=3-NO_2
12c X=4-Cl
12d X=4-F
12e X=4-NO_2

General procedure 3: Obtainment of compounds **12a-e**:
N-Boc-piperazine and NEt_3 (1.2 eq) were dissolved in anhydrous CH_2Cl_2, and the suitable benzyl bromide (1 eq) was added dropwise at room T. After completion of the reaction (TLC), the mixture was partitioned between CH_2Cl_2 and water. Drying and removal of the solvent gave an oily residue used in the following step without further purification: it was dissolved in CH_2Cl_2 (5 mL) and trifluoroacetic acid (10 eq) was added. After 6 hrs stirring at room T, the solvent was removed and the residue was partitioned between ethyl acetate and sat. aqueous Na_2CO_3; drying and removal of the solvent gave a residue which was purified by flash chromatography if necessary.

12a[155] 1-(3-methoxybenzyl)piperazine
Yellow oil, **Yield=** 98%.
[^{1}H-NMR] ($CDCl_3$) δ: 7.08 (t, *J* = 8.0 Hz, 1H, Ar), 6.93-6.85 (m, 2H, Ar), 6.66 (d, *J* = 8.0 Hz, 1H, Ar), 3.66 (s, 3H, OCH_3), 3.33 (s, 2H, CH_2Ar), 2.87-2.70 (m, 4H), 2.45-2.20 (m, 4H), 1.90 (bs, 1H, NH) **ppm**.

12b[156] 1-(3-nitrobenzyl)piperazine
Eluent: DCM/MeOH/NH_3 90:10:1; Yellow oil; **Yield=** 96%
[^{1}H-NMR] (DMSO) δ: 8.09 (s, 1H, Ar), 8.07 (d, *J* = 8.0 Hz, 1H, Ar), 7.71 (d, *J* = 7.6 Hz, 1H, Ar), 7.57 (t, *J* = 8.0 Hz, 1H, Ar), 3.51 (s, 2H, CH_2Ar), 2.78-2.53 (m, 4H), 2.40-2.17 (m, 4H) **ppm**.

12c[157] 1-(4-chlorobenzyl)piperazine
Yellow oil, **Yield=** 75% yields.
[^{1}H-NMR] (DMSO) δ: 7.31 (d, *J* = 8.4 Hz, 2H, Ar), 7.25 (d, *J* = 8.4 Hz, 2H, Ar), 3.35 (s, 2H, CH_2Ar), 2.66-2.57 (m, 4H), 2.25-2.15 (m, 4H) **ppm**.

12d[158] 1-(4-fluorobenzyl)piperazine
Oil, **Yield=** 70% yields
[^{1}H-NMR] ($CDCl_3$) δ: 7.41-7.25 (m, 2H, Ar), 6.99 (t, *J* = 8.8 Hz, 2H, Ar), 3.49 (s, 2H, CH_2Ar), 3.00-2.88 (m, 4H), 2.50-2.83 (m, 4H), 2.08 (bs, 1H, NH) **ppm**.

12e[159] 1-(4-nitrobenzyl)piperazine
Oil; **Yield=** 92%
[^{1}H-NMR] (DMSO) δ: 8.16 (d, *J* = 8.8 Hz, 2H), 7.56 (d, *J* = 8.8 Hz, 2H), 3.30-3.20 (m, 2H, $ArCH_2$), 2.73-2.60 (m, 4H), 2.33-2.20 (m, 4H) **ppm**.

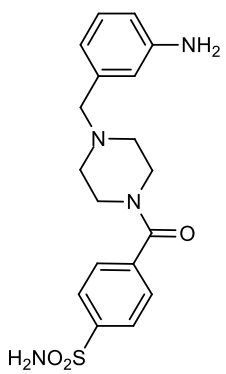

II-A9 4-(4-(3-nitrobenzyl)piperazine-1-carbonyl)benzenesulfonamide
Compound **II-A5** (0.075 g, 0.186 mmol) was dissolved in absolut EtOH (25 mL); the solution was heated at 75°C, then $SnCl_2 \cdot 2H_2O$ (0.29 g, 1.29 mmol) was added. The mixture was stirred at 80°C for 3 hrs. After cooling, the mixture was concentrated and treated with a saturated solution of Na_2CO_3, producing a white precipitate which was filtered off through celite. The solution was partitioned between H_2O and CH_2Cl_2. Drying (Na_2SO_4) and removal of the solvent gave a residue which was purified by flash chromatography using DCM/MeOH/NH_3 85:15:1.5 as eluent, obtaining the title product.

White solid; **Yield=** 59%; **M.P.=** 204 °C (d)

[^{1}H-NMR] (MeOD) δ: 7.94 (d, *J* = 8.4 Hz, 2H, Ar), 7.53 (d, *J* = 8.4 Hz, 2H, Ar), 7.01 (t, *J* = 7.6 Hz, 1H, Ar), 6.68 (s, 1H, Ar), 6.67-6.57 (m, 2H, Ar), 3.80-3.70 (m, 2H), 3.42 (s, 2H, CH_2Ar), 3.40-3.34 (m, 2H), 2.60-2.46 (m, 2H), 2.45-2.34 (m, 2H) **ppm**.

[^{13}C-NMR] (DMSO) δ: 168.15 (CO), 149.03 (C_{Ar}), 145.22 (C_{Ar}), 139.61 (C_{Ar}), 138.73 (C_{Ar}), 129.08 (CH_{Ar}), 127.95 (CH_{Ar}), 126.30 (CH_{Ar}), 116.96 (CH_{Ar}), 114.85 (CH_{Ar}), 113.27 (CH_{Ar}), 62.81 (CH_2-Ar), 53.26 (CH_2), 52.66 (CH_2), 47.60 (CH_2), 42.08 (CH_2) **ppm.**

ESI-HRMS (*m/z*) $[M+H]^+$: calculated for $C_{18}H_{23}N_4O_3S$ 375.1485, found 375.1486.

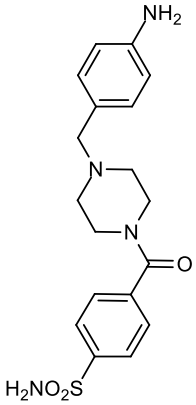

II-A10 4-(4-(4-aminobenzyl)piperazine-1-carbonyl)benzenesulfonamide
Compound **II-A8** (0.03 g, 0.0743 mmol) was dissolved in AcOEt (20 mL) and hydrogenated in a Parr apparatus at 30 psi for 4 hrs, using Pd/C (10 mg) as catalyst. Filtration and removal of the solvent under vacuum gave a residue which was purified by flash chromatography using DCM/MeOH/NH_3 85:15:1.5 as eluent, obtaining the title product as a white solid.

Yield= 72% **M.P.=** 180°C (d).
[^{1}H-NMR] (MeOD) δ: 7.96 (d, *J* = 7.5 Hz, 2H, Ar), 7.55 (d, *J* = 7.4 Hz, 2H, Ar), 7.05 (d, *J* = 7.4 Hz, 2H, Ar), 6.67 (d, *J* = 7.4 Hz, 2H, Ar), 3.77 (bs, 2H, CH_2), 3.45 (s, 2H, CH_2Ar), 3.39 (bs, 2H, CH_2), 2.55 (bs, 2H, CH_2), 2.41 (bs, 2H, CH_2) **ppm**.

[^{13}C-NMR] (DMSO) δ: 168.14 (CO), 148.18 (C_{Ar}), 145.19 (C_{Ar}), 139.59 (C_{Ar}), 130.36 (CH_{Ar}), 127.94 (CH_{Ar}), 126.29 (CH_{Ar}), 114.09 (CH_{Ar}), 62.15 (CH_2-Ar), 52.88 (CH_2), 52.39 (CH_2), 47.52 (CH_2), 41.99 (CH_2) **ppm**.

ESI-HRMS (*m/z*) $[M+H]^+$: calculated for $C_{18}H_{23}N_4O_3S$ 375.1485, found 375.1488.

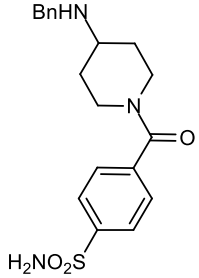

II-C2 4-(4-(benzylamino)piperidine-1-carbonyl)benzenesulfonamide
Compound **13** (0.030 g, 0.0592 mmol) was suspended in glacial acetic acid (5 mL) and, at 0 °C, treated with HBr (33% solution in acetic acid, 0.32 mL). The mixture was left stirring at room T for 24 hrs, cooled in ice bath, made alkaline (pH 9) with ammonium hydroxide, and extracted with AcOEt. Drying (Na_2SO_4) and removal of the solvent under vacuum gave a residue which was purified by

means of flash chromatography (DCM/MeOH/NH_3 90:10:1), obtaining the title compound.

Yield= 91%; **M.P.=** 190°C (d).
[^{1}H NMR] ($CDCl_3$) δ: 7.80 (d, *J* = 8.0 Hz, 2H, Ar), 7.35 (d, *J* = 8.0 Hz, 2H, Ar), 7.30-7.16 (m, 5H, Ar), 4.5-4.37 (m, 1H), 3.77 (s, 2H, CH_2 Ph), 3.60-3.42 (m, 1H), 3.05-2.87 (m, 2H), 2.04-1.85 (m, 1H), 1.82-1.70 (m, 1H), 1.50-1.37 (m, 1H), 1.36-1.20 (m, 1H) **ppm**.
[^{13}C] NMR (DMSO) δ: 168.08 (CO), 145.06 (C_{Ar}), 141.48 (C_{Ar}), 140.13 (C_{Ar}), 128.55 (CH_{Ar}), 128.38 (CH_{Ar}), 127.62 (CH_{Ar}), 126.96 (CH_{Ar}), 126.32 (CH_{Ar}), 53.41 (CH), 50.18 (CH_2 Ph), 46.03 (CH_2), 32.58 (CH_2), 31.87 (CH_2) **ppm**.
ESI-HRMS (*m/z*) $[M+H]^+$: calculated for $C_{19}H_{24}N_3O_3S$ 374.1533, found 374.1531.

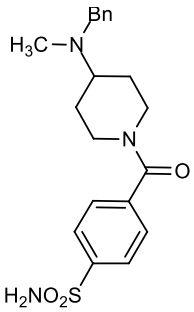

II-C3 4-(4-(benzyl(methyl)amino)piperidine-1-carbonyl)benzenesulfonamide
Compound **II-C2** (0.030 g, 0.08 mmol), dissolved in CH_3CN, was treated with Et_3N (0.01 mL, 0.08 mmol) and CH_3I (0.01 mL, 0.16 mmol). After stirring at room T for 3 days the solvent was removed under vacuum and the residue purified by means of flash chromatography (DCM/MeOH 91:9).

White solid; **Yield=** 46%; **M.P.=** 164 °C (d)
[^{1}H NMR] (CD_3OD) δ: 7.98 (d, *J* = 8.0 Hz, 2H, Ar), 7.57 (d, *J* = 8.0 Hz, 2H, Ar), 7.33-7.20 (m, 5H, Ar), 4.75-4.66 (m, 1H), 3.75-3.64 (m, 1H), 3.63 (s, 2H, CH_2 Ph), 3.20-3.06 (m, 1H), 2.92-2.71 (m, 2H), 2.22 (s, 3H, NCH_3), 2.10-1.99 (m, 1H), 1,90-1.80 (m, 1H), 1.75-1.50 (m, 2H) **ppm**.
[^{13}C] NMR (MeOD) δ: 169.40 (CO), 144.94 (C_{Ar}), 139.24 (C_{Ar}), 137.33 (C_{Ar}), 129.24 (CH_{Ar}), 128-13 (CH_{Ar}), 127.30 (CH_{Ar}), 127.09 (CH_{Ar}), 126.18 (CH_{Ar}), 60.44 (CH), 57.44 (CH_2 Ph), 41.34 (CH_2), 36.36 (CH_3), 27.28 (CH_2), 26.99 (CH_2) **ppm**.
ESI-HRMS (*m/z*) $[M+H]^+$: calculated for $C_{20}H_{26}N_3O_3S$ 388.1689, found 388.1685.

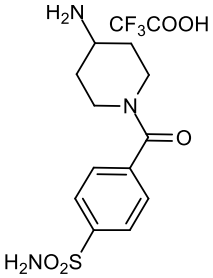

13 4-(4-aminopiperidine-1-carbonyl)benzenesulfonamide trifluoroacetate
Compound **II-C1** (125 mg, 0.33 mmol) was dissolved in trifluoroacetic acid (3 mL) and left strring at room T for 20 hrs. Removal of the solvent under vacuum gave a residue which was crushed with Et_2O.

Low melting solid; **Yield=** 82%
[^{1}H-NMR] (DMSO) δ: 7.94 (s, 2H, SO_2NH_2), 7.84 (d, *J*=6.8 Hz, 2H, Ar), 7.50 (d, *J*=6.8 Hz, 2H, Ar), 4.42 (bs, 1H), 3.51-3.40 (m, 2H), 3.20-3.00 (m, 1H), 2.95-2.80 (m, 1H), 2.08-1.87 (m, 1H), 1.86-1.77 (m, 1H), 1.60-1.30 (m, 2H) **ppm**.

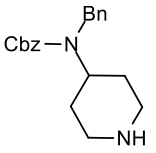

14 Benzyl-N-benzylN-(piperidin-4-yl)carbamate
This compound was prepared following the procedure reported by Lee[155] for a fluorinated analogue.
Yellow oil; **Yield=** 94%
[^{1}H NMR] ($CDCl_3$) δ: 7.42-7.04 (m, 10H, Ar), 5.25-5.03 (m, 2H, OCH_2), 4.46 (s, 2H, NCH_2), 4.22-4.04 (m, 2H), 3.10-2.98 (m, 2H), 2.70-2.49 (m, 2H), 1.99-1.86 (m, 2H), 1.70-1.50 (m, 4H) **ppm**.

7.3 Hydroxyethylpiperazines, III-A and III-B Series

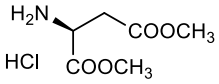

(S)-**15** (S) Aspartic acid dimethyl ester hydrochloride

Under ice-cooling, thionyl chloride (2.74 mL, 37.57 mmol) was added dropwise to a suspension of aspartic acid (1 g, 7.51 mmol) in dry methanol. The resulting solution was refluxed for 2 hours and the stirred at room temperature for 15 hours. The solvent was removed under vacuum and residue was washed three times with diethyl ether affording the 1.48 g of product as a white solid.

Yield: 99% **M.P.** 114-117 °C

[^{1}H] NMR (D_2O) δ: 3.00-3.11 (m, 2H, CH_2); 3.63 (s, 3H, CH_3); 3.72 (s, 3H, CH_3); 4.37-4.39 (m, 1H, CH); 8.65-8.80 (bs ,2H, NH_3); **ppm.**

[^{13}C] NMR (D_2O) δ: 36.21 (CH_2); 57.13 (CH); 55.54 (CH_3); 56.51 (CH_3); 171.95 (CO); 174.22 (CO); **ppm.**

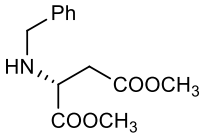

(R)-**16** (R) Dimethyl 2-(benzylamino)succinate

Under nitrogen flux, *(R)*-**15** (0.43 g, 2.18 mmol) was solubilized in 10 mL of anhydrous CH_2Cl_2. Anhydrous Na_2SO_4 and benzaldehyde (0.24 mL, 2.4 mmol) were then added and the resulting suspension was stirred at room temperature under inert atmosphere for 16 hours. The mixture was then filtered and the solvent removed under vacuum. In a schlenk tube, the oily residue was dissolved in 10 mL of anhydrous methanol and cooled down to 0 °C with an ice-bath. $NaBH_4$ was portionwise added and the resulting stirred at 0 °C for 30 minutes. The solvent was then evaporated and the residue partitioned between CH_2Cl_2 and water. The organic phase was washed two more times with water and one with brine, dried (Na_2SO_4) and then evaporated. The resulting colourless was used in the following step without further purifications.

[^{1}H] NMR ($CDCl_3$) δ: 2.67-2.77 (m ,2H, CH_2COOCH_3); 3.65-3.67 (m ,1H, CH); 3.68 (s, 3H, CH_3); 3.73-3.74 (m ,4H, CH_3 + 1 CH_2Ph); 3.88 (d, 1H, J=8 Hz, 1H CH_2Ph); 7.22-7.34 (m ,5H, Ar); **ppm.**

[^{13}C] NMR ($CDCl_3$) δ: 40.58 (CH_2COOCH_3); 54.51 (CH_3); 54.64 (CH_2Ph); 54.81 (CH_3); 59.52 (CH); 129.84 (CH Ar); 130.91 (CH Ar); 131.05 (CH Ar); 142.04 (C_{IV} Ar); 173.93 (CO); 176.66 (CO); **ppm.**

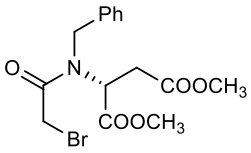

(R)-**17** (R)-dimethyl 2-(N-benzyl-2-bromoacetamido)succinate

To a solution of *(R)*-**16** (0.13 g; 0.52 mmol) in anhydrous CH_2Cl_2 (5mL) NEt_3 (0.11 mL; 0.78 mmol) was added. The mixture was the cooled down to 0°C and a solution of bromoacetyl bromide (0.054 mL; 0.62 mmmol) in 3 mL of dry CH_2Cl_2 was added dropwise. One hour after the dropping completion, the brown solution was washed two times with 1M HCl solution, two times with a saturated $NaHCO_3$ solution and once with brine. The organic phase was dried over Na_2SO_4 and then evaporated. The brown oily residue was purified with flash chromatography (CHX/Acetone/NH_3, 3:1:0.02; h= 17 cm, ø= 2 cm) to afford 0.17 g of product as a light-yellow oil.

Yield: 88%;

APCI-LCMS (m/z) $[M+H]^+$: 372.04

[^{1}H] NMR ($CDCl_3$) δ: 2.72 (dd, 1H, CH_2COOCH_3, J= 17.1, 6.6 Hz); 3.27 (dd, 1H, CH_2COOCH_3, J=17.1, 6.6 Hz); 3.64 (s, 3H, $COOCH_3$); 3.67 (s, 3H, $COOCH_3$); 3.84 (q, 2H, CH_2Br, J= 10.9 Hz); 4.51 (t, 1H, CH, J= 6.6 Hz); 4.71 (q, 2H, CH_2Ph, J=16.7 Hz); 7.29-7.47 (m, 5H, Ar); **ppm.**

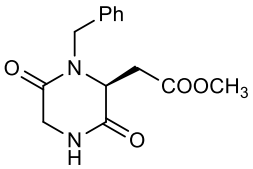

(S)-**18** (S) Methyl 2-(1-benzyl-3,6-dioxopiperazin-2-yl)acetate

The intermediate *(S)*-**17** (1.5 g, 4 mmol) was dissolved in CH_3OH (5 mL), 1.5 mL of a 7M solution of NH_3 in CH_3OH was then added and the mixture was stirred at RT for 7 hours. The solvent was then removed and the residue was purified with flash chromatography (CH_2Cl_2/CH_3OH, 97:3; h= 16 cm; ø= 4 cm) to afford 0.73 g of *(S)*-**18** as a white solid. The preparation of the *(R)*-enantiomer was also reported by Belyankin et Al.[160]

Yield: 65% **M.P.=** 96-98°C

APCI-LCMS (m/z) $[M+H]^+$: 277.12

[^{1}H] NMR ($CDCl_3$) δ: 2.82 (dd, 1H, CH_2COOCH_3, J= 17.4, 5.0 Hz); 3.02 (dd, 1H, CH_2COOCH_3, J= 17.4, 3.5 Hz); 3.63 (s, 3H, $COOCH_3$); 3.97-4.09 (m, 2H, CH + 1 CH_2Ph); 4.18 (d, 1H, CH_2Br, J= 15.1 Hz); 4.36 (d, 1H, CH_2Ph, J= 16.9 Hz); 5.12 (d, 1H, CH_2Br, J= 15.1 Hz); 7.21-7.36 (m, 5H, Ar); **ppm.**

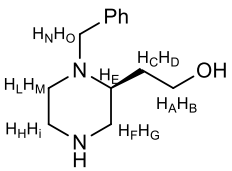

(S)-**19** (S) 2-(1-benzylpiperazin-2-yl)ethanol

To a stirring solution of *(S)*-**18** (0.94 g, 3.4 mmol) in 20 mL of dry THF cooled down to 0°C through an ice bath, $LiAlH_4$ (0.78 g, 20.4 mmol) was slowly added. The resulting suspension was kept at 0°C for 10 min and then refluxed for 1h and 30 min. The reaction was then cooled down and some ice was added directly in the mixture until liberation of H_2 was finished. The suspension was stirred at 0 °C for 10 min, heated to reflux for 15 min and them cooled down to room temperature. The mixture was filtered under vacuum and the solvent removed. The residue was purified with flash chromatography (eluent CH_2Cl_2/CH_3OH/NH_4OH 75:25:2.5, h=14 cm, ø= 4 cm), giving 0.56 g of the desired product as a light orange oil. The preparation of the *(R)*-enantiomer was also reported by Belyankin et Al.[160]

Yield 80%

APCI-LCMS (m/z) $[M+H]^+$: 221.17

[^{1}H] NMR ($CDCl_3$) δ: 1.82 (ddt, 1H, H_C, J= 14.8, 6.2, 4.8 Hz); 2.04 (ddt, 1H, H_D, J= 14.8, 7.7, 5.4 Hz); 2.16 (dt, 1H, H_F, J= 11.2, 4.9 Hz); 2.61-2.68 (m, 1H, H_E); 2.69-2.92 (m, 4H, H_g, H_H, H_I, H_L); 3.02 (ddd, 1H, H_M, J=12.3, 3.4, 0.7 Hz); 3.32 (d, 1H, H_N, J= 13.0 Hz); 3.69-3.80 (m, 1H, H_a); 3.87 (ddd, 1H, H_a, J= 11.2, 7.7, 4.9 Hz); 4.19 (d, 1H, H_O, J= 13.0 Hz); 7.20-7.34 (m, 5H, Ar); **ppm.**

[^{13}C] NMR ($CDCl_3$) δ: 33.2 (C_{CD}); 47.4 (C_{HI}); 51.4 (C_{LM}), 53.3; (C_{FG}) 60.9 (C_{ND}); 61.6 (C_E); 63.4 (C_{AB}); 129.8 (C_{Ar}); 131.0 (C_{Ar}); 131.7 (C_{Ar}); 140.7 (C_{Ar}); **ppm.**

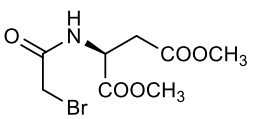

(S)-**20**

(S)-**15** (0.86 g, 4.35 mmol) was dissolved in dry CH_2Cl_2, NEt_3 (1.2 mL, 8.7 mmol) was added and the flask placed into an ice bath. While the

mixture was cooling down, a solution of bromoacetyl bromide (0.42 mL, 4.8 mmol) in 5 mL of anhydrous CH_2Cl_2 was prepared and then dropwise added to the previous one. After the addition completion, the mixture was kept at 0°C for one hour more. The CH_2Cl_2 was then washed two times with a 1M solution of HCl, two times with a saturated solution of $NaHCO_3$ and once with brine. The organic layer was first dried (Na_2SO_4), then evaporated. The brown oily residue was then dissolved in 2mL of AcOEt and eluted over a 6 cm silica layer. The AcOEt was evaporated affording 1.06 g of yellow oil.

Yield= 87%

[^{1}H] NMR ($CDCl_3$) δ: 2.85 (dd, 1H, CH_2COOCH_3, J= 17.3, 4.4 Hz); 3.06 (dd, 1H CH_2COOCH_3, 3.70 (s, 3H, CH_3); 3.77 (s, 3H, CH_3); 3.83-3.96 (m, 2H, CH_2Br); 4.72-4.86 (m, 1H, CH); **ppm.**

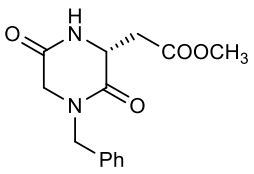

(R)-**21** (R) Methyl 2-(4-benzyl-3,6-dioxopiperazin-2-yl)acetate

To a stirring solution of *(R)*-**20** (0.35 g, 1.25 mmol) in 5 mL of CH_3OH, benzylamine (0.27 mL, 2.5 mmol) was added. After a 36 hours stirring at room T, the solvent was removed under vacuum and the residue purified with flash chromatography (eluent CH_2Cl_2/CH_3OH 95:5, h= 15 cm, ø= 2.2 cm) to give 0.27 g of the desired product as a yellow gummy oil. The *(S)*-enantiomer was also prepared by Schrader T.O. et al.[161] while the *(R)*-one by Aicher T.D. et al.[162]

Yield= 79%

[^{1}H] NMR ($CDCl_3$) δ: 2.83 (dd, 1H, CH_2COOCH_3, J= 17.5, 8.8 Hz); 3.12 (dd, 1H, CH_2COOCH_3, J=17.5, 3.2 Hz); 3.71 (s, 3H, CH_3); 3.88 (q, 2H, NCH_2CO, J= 17.7 Hz); 4.60 (s, 2H, CH_2Ph); 7.13-7.49 (m, 5H, Ar), **ppm.**

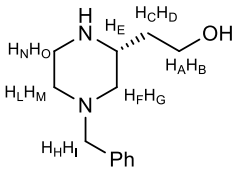

(R)-**22** (R) 2-(4-benzylpiperazin-2-yl)ethanol

The procedure to obtain the compound *(R)*-**22** was the same followed for the derivative *(S)*-**19.** Yellow oil. The *(S)*-enantiomer was also prepared by Williams T.M. et al.[163]

Yield= 74%

[^{1}H] NMR ($CDCl_3$) δ: 1.49-1.59 (m, 1H, H_C); 1.59-1.71 (m, 1H, H_D); 1.90 (t, 1H, H_F, J= 10.6 Hz); 2.07 (td, 1H, H_L, J= 11.3, 2.9 Hz); 2.72 (d, 2H, H_M + H_N , J= 11.4 Hz); 2.81-2.92 (m, 1H, H_E); 2.94-3.09 (m, 32, H_G + H_A); 3.09-3.20 (bs, 1H, OH); 3.10 (s, 2H, H_H + H_I); 3.69-3.83 (m, 2H, H_A + H_B); 7.17-7.36 (m, 5H, Ar); **ppm.**

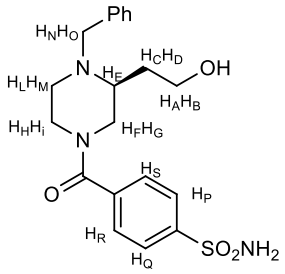

(S) **III-B1** (S) 4-(4-benzyl-3-(2-hydroxyethyl)piperazine-1-carbonyl) benzenesulfonamide

(S)-**19** (0.085 g, 0.41 mmol) was dissolved in anhydrous CH_3CN (5 mL) and NEt_3 (0.073 mL, 0.52 mmol). To this light yellow stirring solution, 4-sulfamoylbenzoyl chloride (0.092 g, 0.45 mmol) was portionwise added. Few seconds after the completion of the addition, the solution turned light orange and after TLC monitoring the reaction was stopped. The solvent was removed under vacuum and the residue purified with flash chromatography (CH_2Cl_2/CH_3OH 92:8, h= 16 cm, ø= 2.5 cm) affording 0.107 g of the product as a white solid.

M.P.= 98-100°C; **Yield=** 69%

APCI-LCMS (m/z) $[M+H]^+$: 404.16

[^{1}H] NMR (DMSO, RT, mixture of conformers) **δ:** 1.41-1.64 (m, 1H), 1.65-1.89 (m, 1H); 2.12-2.30 (m, 1H); 2.52-2.74 (m, 2H); 3.07-3.22 (m, 2H); 3.32-3.73 (m, 4H); 3.76-3.87 (m, 1H): 4.30-4.55 (m, 1H), 7.17-7.25 (m, 1H, Ar); 7.25-7.34 (m, 4H, Ar); 7.40-7.48 (m, SO_2NH_2); 7.54 (d, 2H, H_P + H_Q, J= 8 Hz); 7.85 (d, 2H, H_R + H_S, J= 8 Hz); **ppm.**

[^{13}C] NMR (DMSO, RT, mixture of conformers) **δ:** 30.13 (C_{CD}); 44.86 (C_{FG}); 48.42 (C_{HI}); 48.95 (C_{LM}); 57.13 (C_{NO}); 58.30 (C_{AB}); 58.57 (C_E); 126.24 (CH Ar); 127.33 (CH Ar); 127.91 (CH Ar); 128.66 (CH Ar); 129.05(CH Ar); 139.52 (C Ar); 145.17 (C Ar); 168.3 (CO); **ppm.**

[^{1}H] NMR (DMSO, 100°C) δ: 1.58 (dt, 1H, H_C, J= 13.8, 6.7 Hz); 1.82 (ddd, 1H, H_D, J= 13.8, 10.8, 6.9 Hz), 2.13-2.53 (m, 1H, H_F); 2.57-2.76 (m, 2H, H_G + H_L); 3.28-3.54 (m, 5H, H_A + H_E + H_I+ H_M + H_N); 3.64 (d, 1H, H_B, J=12.4 Hz); 3.87 (d, 1H, H_O, J= 13.9 Hz); 3.96-4.13 (m, 1H, H_H); 7.01-7.17 (bs, 2H, SO_2NH_2); 7.17-7.24 (m, 1H, 7.29 H_4 Bn); 7.29 (m, 4H, CH Bn); 7.52 (d, 2H, CH $PhSO_2NH_2$, J= 8.5 Hz); 7.88 (d, 2H, CH $PhSO_2NH_2$, J= 8.5 Hz); **ppm.**

[^{13}C] NMR (DMSO, 100°C) δ: 31.21 (C_{CD}); 48.93 (C_{FG}); 57.14 (C_{HI} + C_{LM}); 57.28 (C_{NO}); 58.76 (C_E); 126.27 (CH, Ar); 127.16 (CH, Ar); 127.72 (CH, Ar); 128.52 (CH, Ar); 128.92 (CH, Ar); 139.43 (C, Ar); 139.80 (C-CON); 145.44 (C-SO_2NH_2); 168.54 (CO); **ppm.**

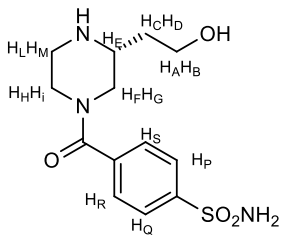

(R) **III-B2** (R) 4-(3-(2-hydroxyethyl)piperazine-1-carbonyl) benzenesulfonamide

In a pressure tube, *(R)* **III-B3** (0.2 g, 0.5 mmol) was dissolved in 5 mL of IPA. Ammonium formate (0.16 g, 2.5 mmol) and Pd/C 10% (0.042 g, 0.05 mmol) were subsequently added. The reaction was refluxed for 16 h, during which time after a TLC monitoring 1 equivalent of both NH_4HCOO and Pd/C were added in two different moments each time. The catalyser was filtered off and the solvent removed. The residue was purified with flash chromatography (eluent CH_2Cl_2/CH_3OH/NH_4OH 4:1:0.1, h= 10 cm, ø= 2 cm), obtaining the compound as a white powder.

Yield= 83%; **M.P. =** 176-178°C

APCI-LCMS (m/z) $[M+H]^+$: 314.12

[^{1}H] NMR (CD_3OD, mixture of conformers) **δ:** 1.36-1.47 8 (m, 0.5H); 1.47-1.62 (m, 0.5H); 1.61-1.77 (m, 1H); 2.54-2.75 (m, 1H); 2.75-3.00 (m, 3H); 3.02-3.11 (m, 0.5H); 3.17 (t, 0.5 H, J= 11.6 Hz); 3.42-

3.61 (m, 2H); 3.65-3.77 (m, 2H); 3.67-3.76 (m, 0.5H); 4.49 (dd, 1H, J= 27.9, 12.6 Hz); 7.57 (d, 2H, Ar, J= 8.5 Hz); 7.97 (d, 2H, Ar, 8.5 Hz); **ppm.**

[^{13}C] NMR (CD_3OD, mixture of conformers) **δ:** 37.22 (C_{CD}); 38.23 (C_{CD}); 44.78 (CH_2); 47.06 (CH_2); 47.63 (CH_2); 49.77 (CH_2); 55.21 (CH_2); 55.52 (CH_2); 55.88 (CH); 60.93 (CH_2OH); 61.12 (CH_2OH); 128.82 (CH Ar); 129.87 (CH Ar); 129.93 (CH Ar); 141.57 (C Ar); 141.67 (C Ar); 147.62 (C Ar); 172.11 (CO); **ppm.**

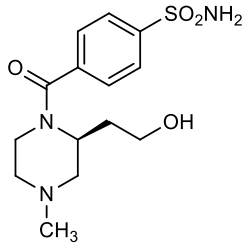

(S) **III-B3** (S) 4-(2-(2-hydroxyethyl)-4-methylpiperazine-1-carbonyl) benzenesulfonamide

In a pressure tube, *(S)* **III-B2** (0.026 g, 0.065 mmol), solid NH_4HCOO (0.02 g, 0.33 mmol), formaldehyde solution (37% in water) (6 µL, 0.08 mmol) and acetic acid (7.4 µL, 0.13 mmol) were dissolved in 3 mL of CH_3OH. Just before the tube closure, Pd/C (0.01 g) was also added and the suspension then refluxed for 16 h. The mixture was cooled down to RT and the catalyser filtered off. The solvent was removed and the residue directly dissolved in water. The pH was adjusted to slightly basic with $NaHCO_3$ solution and extracted several times with AcOEt until the extraction completion (TLC monitored). The organic layer was dried over Na_2SO_4 and then evaporated under vacuum to afford 0.014 g of the methyl derivative NIK-MT05/MT06 as a white solid.

Yield= 66%; **M.P. =** 213-216°C

ESI-LCMS (m/z) [M+H]$^+$: 328.0

[^{1}H] NMR (DMSO, RT, mixture of conformers) **δ:** 1.74-2.09 (m, 4H); 2.17 (s, 3H, CH_3); 2.55-2.88 (m, 2H); 2.89-3.27 (m, 2H); 3.35-3.69 (m, 2H); 4.15-4.52 (m, 1H); 7.38-7.50 (bs, 2H, SO_2NH_2); 7.55 (d, 2H, CH Ar, J= 7.2 Hz); 7.87 (d, 2H, CH Ar, J= 7.2 Hz); **ppm.**

[^{13}C] NMR (DMSO, RT, mixture of conformers) **δ:** 33.3 (CH_2); 46.2 (CH); 55.2 (CH_2); 57.8 (CH_2); 58.7 (CH_2); 74.1 (CH_2); 126.3 (CH Ar); 127.7 (CH Ar); 140.0 (C Ar); 145.0 (C Ar); 168.6 (CO); **ppm.**

[^{1}H] NMR (DMSO, 100°C, mixture of conformers) **δ:** 1.84-2.00 (m, 3H); 2.02-2.13 (m, 1H); 2.20 (s, 3H, CH_3); 2.66-2.80 (m, 2H); 3.18-3.28 (m, 1H); 3.34-3.49 (m, 2H); 3.51-3.91 (bs, 1H); 3.91-4.60 (bs, 1H); 7.16-7.30 (bs, 2H, SO_2NH_2); 7.53 (d, 2H, CH Ar, J= 8 Hz); 7.88 (d, 2H, CH Ar, J= 8 Hz); **ppm.**

[^{13}C] NMR (DMSO, 100°C, mixture of conformers) **δ:** 33.4 (CH_2); 33.6 (CH_2); 46.1 (CH_3); 46.22 (CH_3); 55.2 (CH_2); 57.9 (CH_2); 58.0 (CH_2); 58.7 (CH_2); 126.3 (CH Ar); 127.5 (CH Ar); 127.7 (CH Ar); 140.0 (C Ar); 140.2 (C Ar); 168.6 (CO); **ppm.**

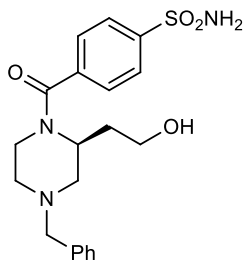

(S) **III-A1** (S) 4-(4-benzyl-2-(2-hydroxyethyl)piperazine-1-carbonyl) benzenesulfonamide

The procedure to obtain compounds *(S)* **III-A1** was the same followed for the derivatives *(S)* **III-B1**. White solid.

Yield= 63%; **M.P. =** 250-253°C

ESI-LCMS (m/z) [M-H]$^-$: 402.0

[^{1}H] NMR (DMSO, RT, mixture of conformers) **δ:** 1.74-2.11 (m, 4H); 2.53-2.90 (m, 2H); 2.90-3.05 (m, 0.5H); 3.05-3.22 (m, 1.5H); 3.31-3.45 (m, 2H); 3.49

(d, 1H, 13.4 Hz); 3.57-3.73 (m, 0.5H); 4.16-4.40 (m, 1H); 4.58-4.73 (m, 0.5H); 7.16-7.31 (m, 5H, Ar, Bn); 7.36-7.45 (bs, 2H, SO_2NH_2); 75 (d, 2H, Ar Ph SO_2NH_2, J= 8.2 Hz); 7.75-7.87 (m, 2H, Ar Ph SO_2NH_2); **ppm.**

[^{13}C] NMR (DMSO, RT, mixture of conformers) **δ:** 33.2 (CH_2); 55.5 (CH_2); 62.2 (CH_2); 126.3 (CH Ar); 127.5 (CH Ar); 127.7 (CH Ar); 128.7 (CH Ar); 129.1 (CH Ar); 138.5 (C Ar); 140.0 (C Ar); 145.1 (C Ar); 168.5 (CO); **ppm.**

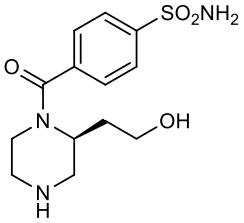

(S) **III-A2** (S) 4-(2-(2-hydroxyethyl)piperazine-1-carbonyl) benzenesulfonamide

*T*he procedure to obtain compounds *(S)* **III-A2** was the same followed for the derivative *(R)* **III-B2**. White solid.

Yield= 70%; **M.P.=** 163-166°C

[^{1}H] NMR (DMSO, RT, mixture of conformers) **δ:** 1.78-2.06 (m, 2H); 2.64-2.79 (m, 2H); 2.79-2.97 (m, 2H); 2.98-3.13 (m, 2H); 3.19-3.63 (m, 2H); 4.12-4.28 (m, 0.5 H); 4.49-4.66 (m, 0.5 H); 7.37-7.5 (bs, 2H, SO_2NH_2); 7.53 (d, 2H, CH Ar, J= 8 Hz); 7.86 (d, 2H, CH Ar, J= 8 Hz); **ppm.**

[^{13}C] NMR (DMSO, RT, mixture of conformers) **δ:** 32.3 (CH_2); 44.5 (CH_2); 46.3 (CH_2); 48.6 (CH_2); 52.8 (CH); 58.11 (CH_2); 58.8 (CH_2); 126.3 (CH Ar); 127.6 (CH Ar); 140.3 (C Ar); 144.9 (C Ar); 168.7 (CO); **ppm.**

[^{1}H] NMR (DMSO, 100°C) δ: 1.83-2.02 (m, 2H); 2.51-2.62 (m, 1H); 2.67-2.89 (m, 4H); 3.32-3.50 (m, 2H); 3.50-3.82 (bs, 1H); 3.86-4.41 (bs, 1H); 6.98-7.41 (bs, , 2H, SO_2NH_2); 7.52 (d, 2H, CH Ar, J= 7.6 Hz); 7.88 (d, 2H, CH Ar, J= 7.6 Hz); **ppm.**

[^{13}C] NMR (DMSO, 100°C) δ: 32.6 (CH_2); 46.2 (CH_2); 48.9 (CH_2); 58.7 (CH_2); 126.3 (CH Ar); 127.5 (CH Ar); 140.5 (C Ar); 145.2 (C Ar); 168.8 (CO); **ppm.**

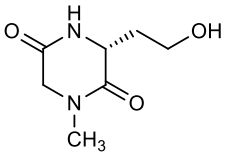

(R)-**21a** (S) 4-(2-(2-hydroxyethyl)piperazine-1-carbonyl) benzenesulfonamide

Using methylamine instead of benzylamine, the procedure to obtain compounds *(R)*-**21a** was the same followed for the derivative *(R)*-**21**. The preparation of the (*S*)-enantiomer was reported by Weber F. et al.[118] Yellow oil.

Yield= 72%

[^{1}H] NMR ($CDCl_3$) δ: 2.79 (dd, 1H, J = 17.6, 9.0 Hz); 3.00 (s, 3H, NC*H*3), 3.08 (dd, 1H, J = 17.6, 3.2 Hz); 3.73 (s, 3H,COOCH3), 3.96 (d, 1H, J = 17.7 Hz); 4.06 (d, 1H, J = 17.7 Hz), 4.35 (d, 1H, J= 8.4 Hz, 1H, C*H*CH2CO2CH3), 6.58 (s, 1H, N*H*); **ppm.**

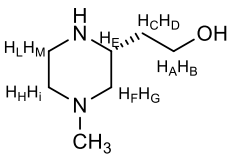

(R)-**22a** (R) 2-(4-methylpiperazin-2-yl)ethanol

Starting from *(R)*-**21a,** the procedure to obtain *(R)*-**22a** is the same described for *(S)*-**19**. The preparation of the (*S*)-enantiomer was reported by Weber F. et al.[118] Yellow oil.

Yield= 92%

[^{1}H] NMR ($CDCl_3$) δ: 1.60 (dqd, 1H, H_CH_D, J= 11.5, 4.0, 1.7 Hz); 1.63-1.71 (m, 1H, H_D), 1.88 (t, 1H, H_H, J= 10.9 Hz); 2.05 (td, 1H, H_F, J= 11.6, 3.0 Hz); 2.25 (s, 3H, CH_3); 2.70-2.75 (m, 2H, $H_G + H_I$); 2.88 (tdd, 1H, H_L,J= 11.6, 3.0, 1.3 Hz); 3.01-3.09 (m, 2H, $H_E + H_M$); 3.70-3.89 (m, 2H, $H_A + H_B$); 4.21-4.44 (bs, 2H, OH + NH); **ppm.**

[^{13}C] NMR ($CDCl_3$) δ: 37.4 (C_{CD}); 47.4 (C_{LM}); 48.9 (CH_3); 57.2 (C_{FG}); 57.7 (C_E); 63.0 (C_{HI}); 63.4 (C_{AB}); **ppm.**

7.4 CAIs-HDACI Hybrids, IV Series

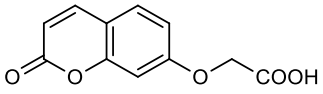

23 2-((2-oxo-2H-chromen-7-yl)oxy)acetic acid
This compound was prepared according to Z. Gao et al[123]

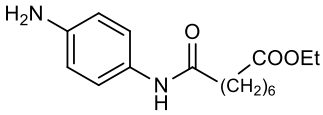

24[164] Ethyl 8-((4-aminophenyl)amino)-8-oxooctanoate
To a stirring solution of ethyl hydrogensuberate (0.44 g, 4 mmol) in 20 mL of anhydrous CH_2Cl_2, at room T, 4-phenylenediamine (0.81 g, 4 mmol) and DCC (1 g; 4.8 mmol) were added. After 24 hours the reaction mixture was cooled to -20°C. The precipitate was then filtered off under vacuum and the solvent collected and evaporated. The residue was purified with flash chromatography (CH_2Cl_2/CH_3OH/NH_4OH 95:5:0.5) to give 0.34 g of the intermediate **24** as a brown solid.

[^{1}H] NMR ($CDCl_3$) δ: 1.25 (t, 3H, CH_3, J= 7.1 Hz); 1.31-1.43 (m, 4H, $2CH_2$); 1.55-1.76 (m, 4H, $2CH_2$); 2.29 (td, 4H, $2CH_2$; J= 7.5, 2.9 Hz); 4.12 (q, 2H, $COOCH_2$, J= 7.1 Hz); 6.64 (d, 2H, CH Ar, J= 8.6 Hz); 7.26 (d, 2H, CH Ar, J= 8.6 Hz); **ppm.**

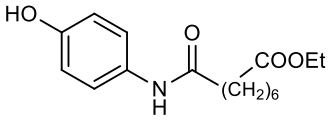

24a Ethyl 8-((4-hydroxyphenyl) amino)-8-oxooctanoate
A suspension of ethyl hydrogensuberate (0.27 g, 1.4 mmol) in 5 mL of anhydrous CH_2Cl_2 turned into solution when NEt_3 (0.6 mL, 4.2 mmol) was added. To the resulting mixture HOBT (0.22 g, 1.6 mmol), EDC (0.31, 1.6 mmol) and 4-aminophenol (0.15 g, 1.4 mmol) were afterwards added and the reaction left at RT for 16 hours. The organic solvent was then washed with a 1M HCl solution, a $NaHCO_3$ saturated solution, brine and then dried on Na_2SO_4. The solvent removal and the residue purification with flash chromatography (eluent CH_2Cl_2/CH_3OH/NH_4OH 95:5:0.5) gave the intermediate **24a** as a pale yellow solid.

[^{1}H] NMR ($CDCl_3$) δ: 1.24 (t, 3H, CH_3, J= 7.1 Hz); 1.28-1.47 (m, 4H, $2CH_2$); 1.50-1.83 (m, 4H, $2CH_2$); 2.28 (t, 4H, $2CH_2$, J= 6.9 Hz); 4.11 (q, 2H, $COOCH_2$, J= 7.1 Hz); 6.74 (d, 2H, CH Ar, J= 8.6 Hz); 7.25 (d, 2H, CH Ar, J= 8.6 Hz); **ppm.**

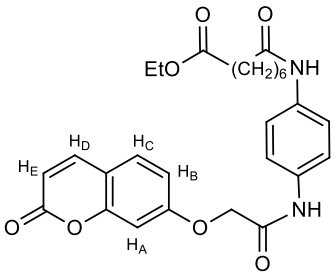

25 Ethyl 8-oxo-8-((4-(2-((2-oxo-2H-chromen-7-yl)oxy)acetamido) phenyl)amino)octanoate

To a stirring solution of **23** (0.064 g, 0.29 mmol), DIPEA (0.1 mL, 0.58 mmol) and HATU (0.17 g, 0.44 mmol) in dry DMF (2 mL), at room T, **24** (0.085 g, 0.29 mmol) and the mixture left for 24 hours. Some ice was then added leading to the formation of a brown precipitate that was collected through filtration under vacuum. The solid was then dissolved in CH_3OH and dropped into water at 0°C where it precipitated again. After filtration and drying, the product was obtained as a pale brown solid.

Yield= 60%

[^{1}H] NMR (DMSO) δ: 1.16 (t, 3H, CH_3, J= 7.1 Hz); 1.21-1.35 (m, 4H, $2CH_2$); 1.45-1.63 (m, 4H, $2CH_2$); 2.27 (t, 4H, $2CH_2$, J= 7.3 Hz); 4.04 (q, 2H, $COOCH_2$, J= 7.1 Hz); 4.81 (s, 2H, OCH_2CO); 6.31 (d, 1H, H_E, J= 9.5 Hz); 6.99-7.08 (m, 2H, H_A + H_B); 7.53 (s, 4H Ar); 7.66 (d, 1H, H_C, J= 9 Hz); 7.96 (d, 1H, H_D, J= 9.5 Hz); **ppm.**

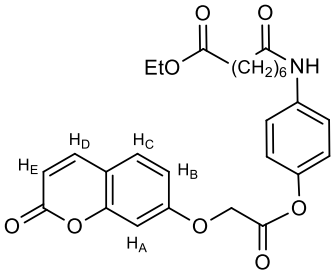

25a Ethyl 8-oxo-8-((4-(2-((2-oxo-2H-chromen-7-yl)oxy)acetoxy) phenyl)amino)octanoate

Starting from **24a**, the procedure to obtain **25a** is the same reported for the related analogue **25**.

Yield= 61%

[^{1}H] NMR (DMSO) δ: 1.16 (t, 3H, CH_3, J= 7.1 Hz); 1.21-1.38 (m, 4H, $2CH_2$); 1.45-1.67 (m, 4H, $2CH_2$); 2.27 (q, 4H, $2CH_2$, J= 7.2 Hz); 4.03 (q, 2H, $COOCH_2$, J= 7.1 Hz); 5.21 (s, 2H, OCH_2CO); 6.32 (d, 1H, H_E, J= 9.5 Hz); 7.06 (d, 1H, H_A, J= 8.8 Hz); 7.09-7.17 (m, 3H, H_B + 2CH Ar); 7.62 (d, 2H, CH Ar); 7.67 (d, 1H, H_C, J= 8.8 Hz) 8.01 (d, 1H, H_D, J= 9.5 Hz); **ppm.**

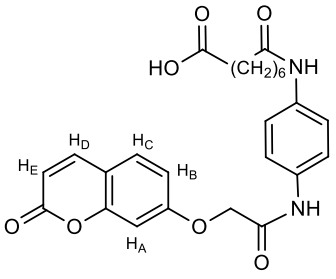

26 8-oxo-8-((4-(2-((2-oxo-2H-chromen-7-yl)oxy)acetamido) phenyl)amino)octanoic acid

The product **25** (0.085 g, 0.17 mmol) was solubilised in 6 mL of a 1:1 THF/CH_3OH mixture. When dissolved, NaOH (0.014 g, 0.34 mmol) in 2 mL of water was dropwise added and the mixture left at RT for 24h. As the reaction was not still over (TLC control), a solution of NaOH (0.034 g, 0.85 mmol) was further dropped inside. The reaction finished in 4 hours, the solvent was afterward removed, the residue dissolved in water and the pH adjusted to acid with a 2M HCl solution. The water layer was then washed three times with AcOEt, the organic phases were collected together, dried (Na_2SO_4) and evaporated. The residue was purified with flash chromatography (eluent CH_2Cl_2/CH_3OH 90:10), obtaining 0.035 g of the desired carboxylic acid as a yellow solid.

Yield= 44%

[^{1}H] NMR (DMSO) δ: 1.23-1.35 (m, 4H, $2CH_2$); 1.43-1.62 (m, 4H, $2CH_2$); 2.22 (dt, 4H, $2CH_2$, J= 37.6, 7.3 Hz); 4.82 (s, 2H, OCH_2CO); 6.31 (d, 1H, H_E, J= 9.5 Hz); 6.98-7.07 (m, 2H, H_A + H_B); 7.53 (s, 4H Ar); 7.66 (d, 1H, H_C, J= 9.2 Hz); 8.00 (d, 1H, H_D, J= 9.5 Hz); 9.85 (s, 1H, CONH); 10.12 (s, 1H, CONH); **ppm.**

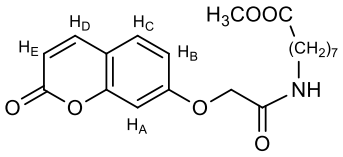

27 Methyl 8-(2-((2-oxo-2H-chromen-7-yl)oxy)acetamido) octanoate

The common intermediate **23** (0.09 g, 0.4 mmol) was solubilized in 1.5 mL of dry DMF and the solution was cooled down to 0°C. HOBT (0.07 g, 0.5 mmol), EDC (0.09 g, 0.5 mmol) and methyl 8-aminooctanoate (0.07 g, 0.4 mmol) prepared from 8-aminooctanoic acid according to L. Gros et al[165]. The reaction was allowed to warm up to RT and stirred for 16 hours. Cold water was then dropped inside leading to a suspension that was poured in a separatory funnel and extracted twice with AcOEt. The organic solvent was afterwards washed one time with $NaHCO_3$ and then brine. Drying (Na_2SO_4) and removal of the solvent afforded the desired intermediate as a white solid.

Yield= 26%

[^{1}H] NMR (DMSO) δ: 1.12-1.27 (m, 6H, $3CH_2$); 1.32-1.54 (m, 4H, $2CH_2$); 2.25 (t, 2H, CH_2COO, J=7.4 Hz); 3.09 (dd, 2H, $CONHCH_2$, J= 12.9, 6.6 Hz) 3.55 (s, 3H, $COOCH_3$); 4.58 (s, 2H, OCH_2CO); 6.29 (d, 1H, H_E, J= 9.5 Hz); 6.91-7.00 (m, 2H, H_A + H_B); 7.63 (d, 2H Ar, J= 8.6 Hz); 7.98 (d, 1H, H_C, J= 8.1 Hz); 8.12 (d, 1H, H_D, J= 9.5 Hz); 9.73 (s, 1H, CONH); **ppm.**

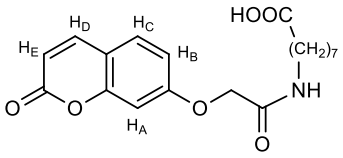

27a 8-(2-((2-oxo-2H-chromen-7-yl)oxy)acetamido)octanoic acid

Starting from **27** and using CH_3OH instead of EtOH, the procedure to obtain the carboxylic derivative **27a** is the same followed for acid **26**.

Yield= 51%

[^{1}H] NMR (DMSO) δ: 1.12-1.30 (m, 6H, $3CH_2$); 1.33-1.54 (m, 4H, $2CH_2$); 2.25 (t, 2H, CH_2COO, J=7.4 Hz); 3.06-3.15 (m, 2H, $CONHCH_2$); 4.60 (s, 2H, OCH_2CO); 6.31 (d, 1H, H_E, J= 9.5 Hz); 6.85-7.04 (m, 2H, H_A + H_B); 7.65 (d, 1H, H_C, J= 8.6 Hz); 8.00 (d, 1H, H_D, J= 9.5 Hz); **ppm.**

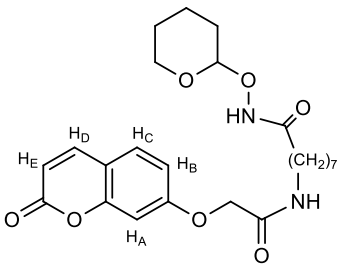

27b 8-(2-((2-oxo-2H-chromen-7-yl)oxy)acetamido)-N-((tetrahydro-2H-pyran-2-yl)oxy)octanamide

To a 0°C stirring solution of **27a** (0.03 g, 0.08 mmol) in 1 mL od anhydrous DMF, HOBT (0.014 g, 0.1 mmol), EDC (0.019 g, 0.1 mmol) and O-(THP)hydroxylamine* (0.015 g, 0.13 mmol) were subsequently added, then the mixture was stirred at RT for 16 hours. The reaction was stopped adding cold water that lead to a suspension that was extracted with AcOEt. The organic solvent was washed three times with water and once with brine, then dried (Na_2SO_4) and evaporated under vacuum. The residue was purified with flash chromatography (eluent CH_2Cl_2/CH_3OH/NH_4OH 90:10:1) that gave the desired compound as a colourless oil.

Yield= 60%

[^{1}H] NMR ($CDCl_3$) δ: 1.20-1.38 (m, 6H); 1.39-1.71 (m, 8H); 1.72-1.88 (m, 3H), 2.03-2.21 (m, 1H); 3.34 (q, 2H, $CONHCH_2$, J= 6.7 Hz); 3.56-3.66 (m, 1H); 3.87-3.99 (m, 1H); 4.54 (s, 2H, OCH_2CO); 4.85-4.97 (bs, 1H);); 6.30 (d, 1H, H_E, J= 9.5 Hz); 6.47-6.52 (bs, 1H); 6.83-6.96 (m, 2H, H_A + H_B); 7.43 (d, 1H, H_C, J= 8.5 Hz); 7.66 (d, 1H, H_D, J= 9.5 Hz); **ppm.**

*O-(Tetrahydro-2H-pyran-2-yl)hydroxylamine 96%

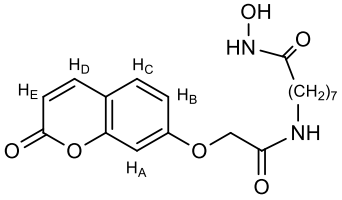

IV-1 N-hydroxy-8-(2-((2-oxo-2H-chromen-7-yl)oxy) acetamido)octanamide

The deprotection of the hydroxamate was performed dissolving **27b** (0.024 g, 0.05 mmol) in dioxane (2mL) and adding 0.5 mL of a 2M HCl solution. The mixture, left at room T for 4 hours, was afterwards concentrated and the white precipitate collected through filtration under vacuum. After drying, the solid afforded the desired compound as a white solid.

Yield= 53%; **M.P.=** 168-171°C ESI-LCMS (m/z) $[M+H]^+$ = 377.3 g/mol

[^{1}H] NMR (CD_3OD) δ: 1.21-1.39 (m, 6H, $3CH_2$); 1.46-1.67 (m, 4H, $2CH_2$); 2.09 (t, 2H, CH_2COO, J=7.4 Hz); 3.29 (t, 2H, $CONHCH_2$, J= 7.0 Hz) 4.64 (s, 2H, OCH_2CO); 6.30 (d, 1H, H_E, J= 9.5 Hz); 6.96-7.00 (m, 1H, H_A); 7.05 (dd, 1H, H_B, J= 8.6, 2.3 Hz); 7.61 (d, 1H, H_C, J= 8.6 Hz); 7.92 (d, 1H, H_D, J= 9.5 Hz); 9.73 (s, 1H, CONH); **ppm.**

[^{13}C] NMR (CD_3OD) δ: 25.2 (CH_2); 26.3 (CH_2); 28.6 (CH_2); 28.7 (CH_2); 28.9 (CH_2); 32.4 (CH_2); 38.7 (CH_2); 67.1 (OCH_2CONH); 101.7 (CH_A Ar); 112.6 (CH_E Ar); 112.8 (CH_B Ar); 113.5 (C Ar); 129.3 (CH_C Ar); 144.2 (CH_D Ar); 155.5 (C Ar); 161.0 (C Ar); 161.7 (CO CUM); 168.6 (CONH); 173.03 (CONHOH); **ppm.**

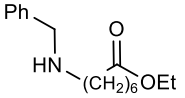

Ethyl 7-(benzylamino)heptanoate[166]

To a solution of Ethyl 7-bromoheptanoate (0.22 g, 0.9 mmol) and benzylamine (0.11 mL, 1.0 mmol) in 5 mL of CH_3CN, potassium iodide (0.30 g, 1.8 mmol) and potassium carbonate (0.25 g, 1.8 mmol) were added.

The resulting suspension was heated to 45°C for 16 hours. The reaction was stopped filtering the solid off, collecting the solution and evaporating the solvent. The oily residue was purified with flash chromatography (eluent: CH_2Cl_2/CH_3OH/NH_4OH 97:3:0.3) and the desired product was collected as a colourless oil.

Yield= 42%

[^{1}H] NMR ($CDCl_3$) δ: 1.24 (t, 3H, CH_3, J= 7.1 Hz); 1.29-1.37 (m, CH, $2CH_2$); 1.43-1.56 (m, 2H, CH_2); 1.56-1.68 (m, 2H, CH_2); 2.28 (t, 2H, CH_2COO, J= 7.5 Hz); 2.62 (t, 2H, $NHCH_2$, J=7.2 Hz); 3.78 (s, 2H, $PhCH_2NH$); 4.11 (q, 2H, $COOCH_2$, J=7.1 Hz); 7.19-7.37 (m, 5H, Ar); **ppm.**

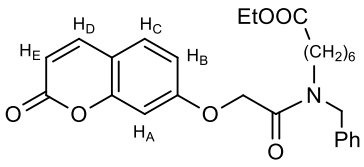

28 Ethyl 8-(N-benzyl-2-((2-oxo-2H-chromen-7-yl)oxy)acetamido) heptanoate

The common intermediate **23** (0.063 g, 0.29 mmol) was initially suspended in 5 mL of anhydrous CH_3CN but then dry DMF was dropwise added until solubilization. The solution was cooled down (0°C, ice bath), then HOBT (0.046 g, 0.34 mmol), EDC (0.065 g, 0.34 mmol) and 7-BnNH-HepEt (0.09 g, 0.34 mmol) were added. When the RT was reached, the reaction was stirred for 16 hours. The solvent was then removed and the residue partitioned among AcOEt/water. The organic phase was afterwards washed every time once with the following solutions: 1M HCl, saturated $NaHCO_3$ and brine. The AcOEt was dried over Na_2SO_4 and then evaporated. Flash chromatography (eluent: hexane/CH_2Cl_2/acetone 8:6:1.5) finally gave the desired compound as a pale-yellow oil.

Yield= 83%; ESI-LCMS (m/z) $[M+H]^+$ = 466.4 g/mol

[^{1}H] NMR ($CDCl_3$, mixture of conformers**) δ:** 1.11-1.38 (m, 7H, CH_3 + $2CH_2$); 1.39-1.68 (m, 4H, $2CH_2$); 2.20 (dt, 2H, CH_2, J= 11.4, 7.4 Hz); 3.06-3.27 (m, 1H); 3.26-3.42 (m, 1H); 3.95-4.14 (m, 2H, $COOCH_2$); 4.54 (s, 1H, $PhCH_2N$); 4.56 (s, 1H, $PhCH_2N$); 4.70 (s, 1H, OCH_2CON); 4.81 (s, 1H, OCH_2CON); 6.17 (t, 1H, H_E, J= 9.1 Hz); 6.53-6.70 (m, 0.5H, Ar); 6.70-6.83 (m, 1H, Ar), 6.83-6.93 (m, 0.5H, Ar); 7.08-7.41 (m, 6H, Ar); 7.57 (t, 1H, Ar, J= 10.3 Hz); **ppm.**

[^{13}C] NMR ($CDCl_3$, mixture of conformers**) δ:** 14.2 (CH_3); 24.6 (CH_2); 24.8 (CH_2); 26.5 (CH_2); 27.1 (CH_2); 28.2 (CH_2); 28.6 (CH_2); 28.7 (CH_2); 34.0 (CH_2); 34.2 (CH_2); 46.3 (CH_2); 46.7 (CH_2); 48.4 (CH_2); 50.4 (CH_2); 60.1 (CH_2); 60.2 (CH_2); 66.8 (CH_2); 67.1 (CH_2); 101.9 (CH Ar); 112.7 (CH Ar), 112.9 (CH Ar); 113.1 (C Ar); 113.2 (C Ar); 113.4 (C Ar); 113.5 (C Ar); 126.3 (CH Ar); 127.6 (CH Ar); 127.9 (CH Ar); 128.1 (CH Ar); 128.6 (CH Ar); 128.9 (CH Ar); 129.0 (CH Ar); 129.1 (CH Ar); 136.2 (C Ar); 136.9 (C Ar); 143.3 (CH Ar); 155.6 (C Ar); 155.7 (C Ar); 160.9 (C Ar); 161.1 (CO); 161.2 (CO); 166.7 (CO); 167.0 (CO); 173.5 (CO); 173.6 (CO); **ppm.**

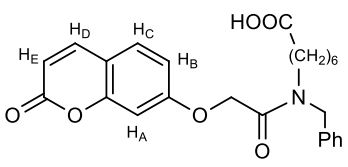

28a 7-(N-benzyl-2-((2-oxo-2H-chromen-7-yl)oxy)acetamido) heptanoic acid

Starting from **28**, the procedure to obtain the carboxylic derivative **28a** is the same followed for **26**. Colourless oil.

Yield= 96%

[^{1}H] NMR ($CDCl_3$, mixture of conformers) **δ:** 1.19-1.39 (m, 4H, $2CH_2$); 1.48-1.65 (m, 4H, $2CH_2$); 2.18-2.39 (m, 2H, CH_2); 3.18-3.27 (m, 1H); 3.37-3.45 (m, 1H); 4.59 (s, 1H, $PhCH_2N$); 4.62 (s, 1H, $PhCH_2N$); 4.74 (s, 1H, OCH_2CON); 4.85 (s, 1H, OCH_2CON); 6.26 (t, 1H, H_E, J= 9.1 Hz); 6.67-6.73 (m, 0.5H, Ar); 6.77-6.85 (m, 1H, Ar), 6.91-6.98 (m, 0.5H, Ar); 7.15-7.46 (m, 6H, Ar); 7.60 (t, 1H, Ar, J= 10.3 Hz); **ppm.**

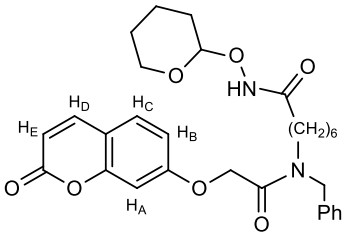

28b 7-(N-benzyl-2-((2-oxo-2H-chromen-7-yl)oxy)acetamido)-N-((tetrahydro-2H-pyran-2-yl)oxy)heptanamide

The coupling-reaction among **28a** (0.1 g, 0.23 mmol) and NH_2OTHP was done according to the method already reported for the related intermediate **27b**. Colourless oil.

Yield= 70%

[^{1}H] NMR ($CDCl_3$, mixture of conformers) **δ:** 1.19-1.39 (m, 4H, $2CH_2$); 1.48-1.65 (m, 8H, $2CH_2$ + $2CH_2$THP); 1.64-1.82 (m, 2H, $2CH_2$ THP); 2.20-2.51 (m, 2H, CH_2); 3.18-3.27 (m, 1H); 3.37-3.45 (m, 1H); 3.58-3.68 (m, 1H THP); 3.89-4.00 (m, 1H THP); 4.59 (s, 1H, $PhCH_2N$); 4.62 (s, 1H, $PhCH_2N$); 4.75 (s, 1H, OCH_2CON); 4.85 (s, 1H, OCH_2CON); 4.91-4.99 (m, 1H THP); 6.27 (t, 1H, H_E, J= 8.7 Hz); 6.66-6.72 (m, 0.5H, Ar); 6.78-6.88 (m, 1H, Ar), 6.93-7.01 (m, 0.5H, Ar); 7.17-7.46 (m, 6H, Ar); 7.59-7.71 (m, 1H, Ar); **ppm.**

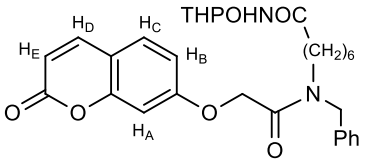

28c 7-(N-benzyl-2-((2-oxo-2H-chromen-7-yl)oxy)acetamido)-N-((tetrahydro-2H-pyran-2-yl)oxy)heptanamide

The ester **30** (0.05 g, 0.16 mmol) and the protected hydroxamate derivative **31** (0.052 g, 0.16 mmol) were dissolved in 5mL of CH_3CN. The solution was stirred at room T for 5 hours, then the solvent was removed and the residue purified with flash chromatography (eluent: AcOEt 100%). The desired compound was afterward isolated as a colourless solid.

Yield= 95%

[^{1}H] NMR ($CDCl_3$) δ: 8.54 (s, 0.40H, NH), 8.40 (s, 0.35H, NH), 7.61 (t, J = 10.1 Hz, 1H,C-4), 7.42 – 7.25 (m, 4H, Ar), 7.19 (m, 2H, Ar), 6.94 (d, J = 8.1 Hz, 0.5H, Ar), 6.85 – 6.73 (m, 2H, Ar), 6.65 (s, 0.5H, Ar), 6.24 (t, J = 8.8 Hz, 1H, C-3), 4.92 (s, 1H, CH-THP), 4.82 (s, 1H, $ArCH_2N$), 4.72 (s, 1H, $ArCH_2N$), 4.59 (s, 1H, $COCH_2O$), 4.56 (s, 1H, $COCH_2O$), 3.92 (m, 1H, CH_2O-THP), 3.59 (m, 1H, CH_2O-THP), 3.47 – 3.32 (m, 1H NCH_2CH_2), 3.23 – 3.13 (m, 1H, NCH_2CH_2), 2.08 (s, 2H, CH_2CH_2CO), 1.87 – 1.68 (m, 3H, $3CH_2$-THP), 1.65 – 1.47 (m, 8H, $CH_2CH_2CH_2CH_2CH_2CH_2$), 1.36 – 1.23 (m, 3H, $3CH_2$-THP); **ppm.**

[^{13}C-NMR] ($CDCl_3$) δ: 167.1 (Cq, CO), 166.7 (Cq, CO), 161.2 (Cq, C-7), 161.0 (Cq, C-2), 155.7 (Cq, C-9), 143.3 (CH, C-4), 136.8 (Cq, Ar), 136.1 (Cq, Ar), 129.1 (CH, Ar), 129.0 (CH, Ar), 128.9 (CH, Ar), 128.7 (CH, Ar), 128.2 (CH, Ar), 128.0 (CH, Ar), 127.6 (CH, Ar), 126.3 (CH, Ar), 113.5 (CH, C-3), 113.2(Cq, C-10), 113.0 (CH, C-6), 102.4 (CH, THP), 101.8 (CH, C-8), 67.1 (CH_2,$COCH_2O$), 66.9

(CH_2,CO*CH_2*O), 62.4 (CH_2,CH_2-THP), 50.4 (CH_2,CH_2N), 48.5 (CH_2,CH_2N), 46.5 (CH_2,CH_2N), 46.2 (CH_2,CH_2N), 28.8 (CH_2), 28.3 (CH_2), 28.0 (CH_2), 27.0 (CH_2), 26.6 (CH_2), 26.4 (CH_2), 25.0 (CH_2,THP), 18.6 (CH_2,THP); **ppm.**

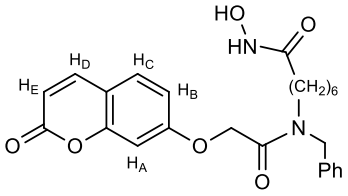

IV-2 7-(N-benzyl-2-((2-oxo-2H-chromen-7-yl)oxy)acetamido) -N-hydroxyheptanamide

The cleavage of the hydroxamate protection of **28b** (0.09 g, 0.16 mmol) was performed in the same way previously reported for the compound **27b**. The purification with flash chromatography was done with eluent: CH_2Cl_2/CH_3OH/NH_4OH 95:5:0.5. Pale-red oil.

Yield= 27%

[^{1}H] NMR ($CDCl_3$, mixture of conformers) **δ:** 1.12-1.38 (m, 4H, 2CH_2); 1.42-1.68 (m, 4H, 2CH_2); 2.01-2.17 (m, 1H); 2.18-2.34 (m, 1H); 3.15-3.24 (m, 1H); 3.34-3.45 (m, 1H); 4.55 (s, 1H, PhCH_2N); 4.59 (s, 1H, PhCH_2N); 4.71 (s, 1H, OCH_2CON); 4.82 (s, 1H, OCH_2CON); 6.23 (t, 1H, H_E, J= 9.0 Hz); 6.62-6.69 (m, 0.5H, Ar); 6.74-6.86 (m, 1H, Ar), 6.89-6.99 (m, 0.5H, Ar); 7.12-7.43 (m, 6H, Ar); 7.55-7.67 (m, 1H, Ar); **ppm.**

[^{13}C] NMR ($CDCl_3$, mixture of conformers) **δ:** 24.6 (CH_2); 24.8 (CH_2); 26.5 (CH_2); 27.1 (CH_2); 28.2 (CH_2); 28.6 (CH_2); 28.7 (CH_2); 34.0 (CH_2); 34.2 (CH_2); 46.3 (CH_2); 46.7 (CH_2); 48.4 (CH_2); 50.4 (CH_2); 60.1 (CH_2); 60.2 (CH_2); 66.8 (CH_2); 67.1 (CH_2); 101.9 (CH Ar); 112.7 (CH Ar), 112.9 (CH Ar); 113.1 (C Ar); 113.2 (C Ar); 113.4 (C Ar); 113.5 (C Ar); 126.3 (CH Ar); 127.6 (CH Ar); 127.9 (CH Ar); 128.1 (CH Ar); 128.6 (CH Ar); 128.9 (CH Ar); 129.0 (CH Ar); 129.1 (CH Ar); 136.2 (C Ar); 136.9 (C Ar); 143.3 (CH Ar); 155.6 (C Ar); 155.7 (C Ar); 160.9 (C Ar); 161.1 (CO); 161.2 (CO); 166.7 (CO); 167.0 (CO); 173.5 (CO); 173.6 (CO); **ppm.**

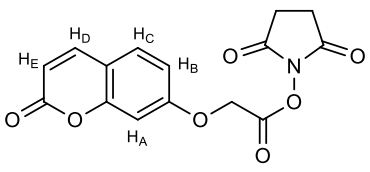

29 2,5-dioxopyrrolidin-1-yl 2-((2-oxo-2H-chromen-7-yl)oxy) acetate

The common intermediate ***23*** (0.21 g; 9.4 mmol) was suspended in 10 mL of anhydrous CH_3CN and dry DMF was then dropped until complete solubilisation. The flask was cooled down through an ice bath, the addition of N-hydroxy succinimide (0.16 g; 1.4 mmol) and EDC (0.22 g; 1.12 mmol) was afterwards carried out. The solution was left at 0°C for 30 minutes and then stirred at RT for 15 hours. The solvent was removed under vacuum and the residue dissolved in EtOAc. The organic layer was subsequently washed with water, $NaHCO_3$ solution, 2M HCl and finally brine. After anhydrification over Na_2SO_4, the AcOEt was evaporated to obtain the desired compound as a white solid. The compound was used as such for the next step.

Yield= 80%; **M.P.=** 180-182°C

[^{1}H] NMR (DMSO) δ: 2.79 (s, 4H, CH_2 NHS); 5.44 (s, 2H, OCH_2COO); 6.29 (d, 1H, H_E, J= 9.5 Hz); 6.83-7.10 (m, 2H, H_A + H_B); 7.63 (d, 1H, H_C, J= 8.6 Hz); 7.96 (d, 1H, H_D, J= 9.5 Hz); **ppm.**

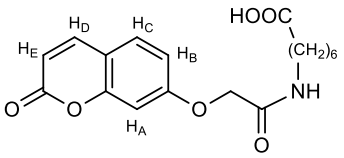

30 7-(2-((2-oxo-2H-chromen-7-yl)oxy)acetamido)heptanoic acid
To a suspension of 7-aminoheptanoic acid (0.026 g, 0.18 mmol) in 5mL of anhydrous CH_3CN, dry DMF was dropped inside until complete dissolution. The latter solution was added to a second one of the ester **30** (0.086 g, 0.27 mmol) in 6 mL of dry CH_3CN and the mixture was heated at 50°C for 1 hour. The solvent was afterwards removed under vacuum and the residue solubilized in water and extracted twice with AcOEt. The organic phase was then washed twice with water, once with $NaHCO_3$ saturated solution and brine. The AcOEt was afterwards dried on Na_2SO_4 and then evaporated. The oily residue was purified with flash chromatography (eluent CH_2Cl_2/CH_3OH 96:4) affording the desired compound as a white gum.

Yield= 48%

[^{1}H] NMR ($CDCl_3$) δ: 1.28-1.49 (m, 4H, $2CH_2$); 1.50-1.66 (m, 2H, CH_2); 1.65-1.79 (m, 2H, $2CH_2$); 2.59 (t, 2H, CH_2, J= 7.3 Hz); 3.36 (dd, 2H, CH_2, J= 13.3, 6.8 Hz); 4.54 (s, 2H, $COCH_2COO$); 6.29 (d, 1H, H_E, J= 9.5 Hz); 6.82-6.90 (m, 2H, H_A + H_B); 7.43 (d, 1H, H_C, J= 8.9 Hz); 7.66 (d, 1H, H_D, J= 9.5 Hz); **ppm.**

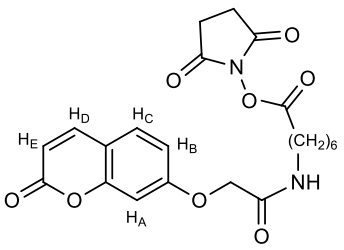

30a 2,5-dioxopyrrolidin-1-yl 7-(2-((2-oxo-2H-chromen-7-yl)oxy) acetamido)heptanoate
Starting from **29** (0.03 g, 0.09 mmol) the corresponding NHS-activated ester **29a** was obtained following the same procedure already reported for 7-AcNHS CUM. White solid.

Yield= 89%

[^{1}H] NMR ($CDCl_3$) δ: 1.28-1.49 (m, 4H, $2CH_2$); 1.50-1.66 (m, 2H, CH_2); 1.65-1.79 (m, 2H, $2CH_2$); 2.59 (t, 2H, CH_2, J= 7.3 Hz); 2.83 (s, 4H, $2CH_2NHS$); 3.36 (dd, 2H, CH_2, J= 13.3, 6.8 Hz); 4.54 (s, 2H, $COCH_2COO$); 6.29 (d, 1H, H_E, J= 9.5 Hz); 6.82-6.90 (m, 2H, H_A + H_B); 7.43 (d, 1H, H_C, J= 8.9 Hz); 7.66 (d, 1H, H_D, J= 9.5 Hz); **ppm.**

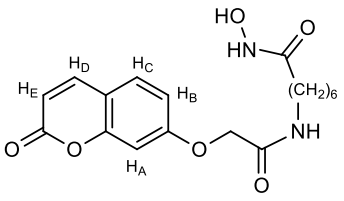

IV-3 N-hydroxy-7-(2-((2-oxo-2H-chromen-7-yl)oxy)acetamido) heptanamide
The protected intermediate **30a** (0.03 g, 0.07 mmol) was dissolved in 2 mL of a 1:1 mixture of CH_3CN/THF and 2 drops of a hydroxylamine solution (50 wt. % in water) were then added. The formation of a white precipitate was almost immediately observed. The reaction was left at RT for 10 minutes then the solvent was removed under vacuum and the residue dissolved in water and extracted three times with AcOEt. Drying (Na_2SO_4) and evaporation of the organic phase afforded the hydroxamate NIK-H33 as a white solid.

Yield= 60%; **M.P.=** 177°C (decomposition)

[^{1}H] NMR (DMSO) δ: 1.12-1.28 (m, 4H, $2CH_2$); 1.31-1.47 (m, 2H, CH_2); 1.65-1.79 (m, 2H, $2CH_2$); 1.90 (t, 2H, $CH_2CONHOH$, J= 7.2 Hz); 3.04-3.13 (m, 2H, $CONHCH_2$); 4.57 (s, 2H, $COCH_2COO$); 6.28 (d, 1H, H_E, J= 9.5 Hz); 6.91-7.02 (m, 2H, H_A + H_B); 7.63 (d, 1H, H_C, J= 8.9 Hz); 7.97 (d, 1H, H_D, J= 9.5 Hz); **ppm.**

[^{13}C] NMR (DMSO) δ: 25.5 (CH_2); 25.7 (CH_2); 26.5 (CH_2); 28.8 (CH_2); 29.4 (CH_2); 32.7 (CH_2); 38.8 ($CONHCH_2$); 102.2 (CH Ar); 113.2 (CH Ar); 113.3 (C Ar); 113.4 (CH Ar); 130.0 (CH Ar); 144.7 (CH Ar); 155.6 (C Ar); 160.7 (C Ar); 161.3 (CO); 167.2 (CO); 169.5 (CO); **ppm.**

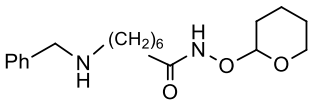

31 7-(benzylamino)-N-((tetrahydro-2H-pyran-2-yl)oxy)heptanamide

The standard deprotection with hydrazine of the intermediate ***35*** as reported by Rodriguez. N. et al.[167], gave the corresponding primary amine (0.460 gr, 1.9 mmol) that was N-benzylated with the two-steps reductive amination already reported for *(R)*-**16**.

Yield= 60%

[^{1}H-NMR] ($CDCl_3$) δ: 7.36 – 7.13 (m, 5H,Ar), 4.89 (s, 1H,CH), 3.90 (s, 1H,CH_2O), 3.74 (s, 2H,CH_2Ar), 3.62 – 3.52 (m, 1H,CH_2O), 2.58 (t, *J* = 7.2 Hz, 2H, NCH_2CH_2), 2.09 (s, 2H, CH_2CO), 1.76 (s, 3H, THP), 1.67 – 1.38 (m, 8H, $CH_2CH_2CH_2CH_2CH_2CH_2$), 1.30 (s, 3H, THP); **ppm.**

[^{13}C-NMR] ($CDCl_3$) δ: 170.4 (Cq,CO), 139.9 (Cq, Ar), 128.4 (CH, Ar), 128.2 (CH, Ar), 127.0 (CH, Ar) , 102.5 (CH, THP), 62.6 (CH_2O, THP), 53.9 (CH_2N), 49.1 (CH_2N), 33.1 (CH_2), 29.6 (CH_2), 28.9 (CH_2), 28.1 (CH_2), 26.8 (CH_2), 25.2 (CH_2), 25.0 (CH_2), 18.7 (CH_2); **ppm.**

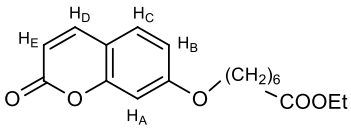

32 Ethyl 7-((2-oxo-2H-chromen-7-yl)oxy)heptanoate

To a suspension of 7-hydroxycoumarin (0.2 g; 1.23 mmol) in 5 mL of acetone, ethyl 7-bromoheptanoate (0.36 mL; 1.85 mmol) and K_2CO_3 (0.34 g; 2.46 mmol) were subsequently added. The mixture was then heated to reflux for 8 hours. The carbonate was filtered off and the yellow solution was evaporated under vacuum. The residue was purified with flash chromatography (eluent CH_2Cl_2/CH_3OH 97:3), obtaining an intermediate fraction that was grinded with Et_2O to further getting rid of the impurities. 0.1 g of the desired product were obtained as a light-yellow solid.

Yield= 25%

[^{1}H] NMR (CD_3OD) δ: 1.25 (t, 3H, CH_3); 1.31-1.58 (m, 4H, $2CH_2$); 1.59-1.72 (m, 2H, CH_2); 1.77-1.89 (m, 2H, CH_2); 2.34 (t, 2H, CH_1COO, J= 7.3 Hz); 4.03-4.17 (m, 4H, OCH_2 + $COOCH_2$); 6.25 (d, 1H, H_E, J= 9.5 Hz); 6.87-6.98 (m, 2H, H_A + H_B); 7.54 (d, 1H, H_C, J= 8.5 Hz); 7.90 (d, 1H, H_D, J= 9.5 Hz); **ppm.**

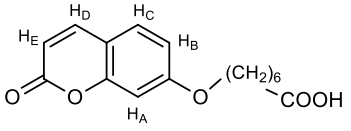

33

Starting from ***32***, the procedure to obtain the carboxylic derivative ***33*** is the same followed for **26**.

Yield= 87 %

[^{1}H] NMR (CD_3OD) δ: 1.31-1.58 (m, 4H, $2CH_2$); 1.59-1.72 (m, 2H, CH_2); 1.77-1.89 (m, 2H, CH_2); 2.24-2.30 (m, 2H, CH_2COO); 4.07 (t, 2H, OCH_2, J=6.4 Hz); 6.23 (d, 1H, H_E, J= 9.5 Hz); 6.82-6.95 (m, 2H, H_A + H_B); 7.52 (d, 1H, H_C, J= 8.6 Hz); 7.88 (d, 1H, H_D, J= 9.5 Hz); **ppm.**

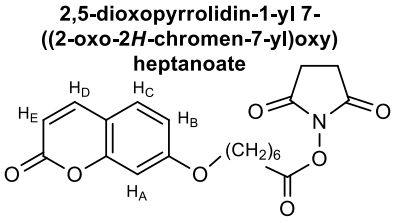

34 7-((2-oxo-2H-chromen-7-yl)oxy)heptanoic acid

The carboxylic acid ***33*** (0.16 g, 0.056 mmol) was solubilised in 5 mL of anhydrous CH_2Cl_2 and the solution was cooled down with an ice bath. NHS (0.13 g, 0.11 mmol) and EDC (0.16 g, 0.084 mmol) were then added and the mixture allowed to reach the RT. After 5 hours the CH_2Cl_2 was directly poured into a separatory funnel and washed subsequently with the following solutions: 2M HCl, saturated $NaHCO_3$ and brine. The organic phase was dried on Na_2SO_4 and evaporated, obtaining a gummy solid that was used for the following step without further purifications.

Yield= 63%

[^{1}H] NMR ($CDCl_3$) δ: 1.36-1.56 (m, 4H, $2CH_2$); 1.58-1.70 (m, 2H, CH_2); 1.72-1.92 (m, 2H, CH_2); 2.62 (dd, 2H, CH_2COO, J= 13.6, 7.3 Hz); 2.83 (s, 4, 2 CH_2 NHS); 4.02 (t, 2H, OCH_2, J= 6.3 Hz); 6.23 (d, 1H, H_E, J= 9.5 Hz); 6.77-6.85 (m, 2H, H_A + H_B); 7.35 (d, 1H, H_C, J= 8.5 Hz); 7.62 (d, 1H, H_D, J= 9.5 Hz); **ppm.**

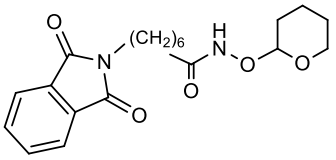

35 7-(1,3-dioxoisoindolin-2-yl)-N-((tetrahydro-2H-pyran-2-yl)oxy) heptanamide

7-aminoheptanoic acid hydrochloride (0.5 g, 2.8 mmol) was suspended in 10 mL of toluene, then phtalic anhydride (0.41 g, 2.8 mmol) and NEt_3 were added and the mixture heated to reflux for 16 hours. The solvent was afterwards removed and the residue dissolved in CH_2Cl_2 and washed twice with a 10% HCl solution and twice with water. The organic phase was dried (Na_2SO_4), filtered and the CH_2Cl_2 removed under vacuum. The oily residue (0.75 g, 2.7 mmol) was then dissolved in anhydrous CH_2Cl_2, and NH_2OTHP (0.32 g, 2.7 mmol), HATU (1.03 g, 2.7 mmol) and DIPEA (0.95 mL, 5.4 mmol) were subsequently added. The solution was stirred at room T for 4 hours, then the solvent was evaporated under vacuum and the residue purified through flash chromatography (eluent: AcOEt/n-hexane 80:20) giving the desired intermediate as a colourless oil.

Yield= 99%

[^{1}H-NMR] ($CDCl_3$) δ: 7.80 (dd, J = 5.4, 3.5 Hz, 2H), 7.73 – 7.60 (dd , 3.5 Hz, 2H), 4.90 (s, 1H, CH), 3.89 (m, 1H,CH_2O), 3.64 (t, J = 7.2 Hz, 2H,CH_2N), 3.61 – 3.54 (m, 1H, CH_2O), 2.07 (s, 2H, CH_2CO), 1.77 (m, 3H, THP), 1.70 – 1.47 (m, 8H, $CH_2CH_2CH_2CH_2CH_2CH_2$), 1.41 – 1.27 (m, 3H, THP); **ppm.**

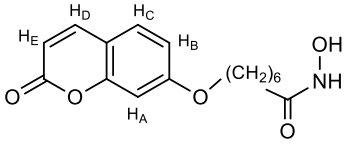

IV N-hydroxy-7-((2-oxo-2H-chromen-7-yl)oxy)heptanamide
The ester **34** (0.03 g; 0.008 mmol) was dissolved in 4 mL of THF. Four drops of a hydroxylamine solution (50 wt. % in water) were slowly added leading to the immediate formation of a white precipitate. The reaction was monitored with TLC after 10 minutes, evidencing the absence of the starting material. The suspension was filtered to remove the precipitate and the solution evaporated. The residue was dissolved in a diluted NaOH solution and this phase was extracted twice with CH_2Cl_2. The water was then acidified to pH≈ 5, then extracted three times again with CH_2Cl_2. The organic fractions were united, dried (Na_2SO_4) and the solvent removed. The desired hydroxamate was therefore isolated as a white solid.

Yield= 71%; **M.P.=** 110-112°C
[^{1}H] NMR (CD_3OD) δ: 1.30-1.57 (m, 4H, $2CH_2$); 1.57-1.72 (m, 2H, CH_2); 1.74-1.90 (m, 2H, CH_2); 2.02-2.15 (m, 2H, CH_2COO); 4.07 (t, 2H, OCH_2, J=6.4 Hz); 6.23 (d, 1H, H_E, J= 9.5 Hz); 6.80-6.99 (m, 2H, H_A + H_B); 7.52 (d, 1H, H_C, J= 8.6 Hz); 7.88 (d, 1H, H_D, J= 9.5 Hz); **ppm.**
[^{13}C] NMR (CD_3OD) δ: 25.3 (CH_2); 25.3 (CH_2); 28.4 (CH_2); 28.6 (CH_2); 32.3 ($CH_2CONHOH$); 68.3 (OCH_2); 100.7 (CH_A), 111.8 (CH_E); 112.5 (C Ar); 112.8 (CH_B); 129.0 (CH_C); 144.4 (CH_D); 155.7 (C Ar); 162.0 (C Ar); 162.7 (CO); 171.6 (CONH); **ppm**

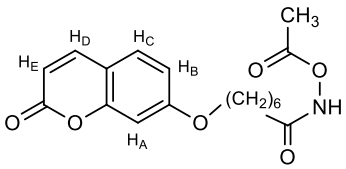

IV-5 N-acetoxy-7-((2-oxo-2H-chromen-7-yl)oxy)heptanamide
The hydroxamate **IV-4** (0.031 g, 0.1 mmol) was suspended in 7 mL of anhydrous CH_2Cl_2, the solution was cooled down to 0°C and acetyl chloride (7 µL, 0.2 mmol) and diisopropylamine 56 µL, 0.4 mmol) were subsequently added. The reaction was then stirred for 15 hours at RT. After a TLC monitoring, the CH_2Cl_2 was poured into a separatory funnel and washed twice with a 1M HCl solution and once with brine. The organic phase was afterwards dried (Na_2SO_4) and evaporated, affording the desired compound as a white solid.

Yield= 78%; **M.P.=** 97-100°C; ESI-LCMS (m/z) $[M+H]^+$ = 348.1 g/mol
[^{1}H] NMR ($CDCl_3$) δ: 1.32-1.53 (m, 4H, $2CH_2$); 1.62-1.88 (m, 4H, CH_2); 2.21 (s, 3H, CH_3); 2.25-2.30 (m, 2H, CH_2); 3.98 (t, 2H, OCH_2, J= 6.4 Hz); 6.23 (d, 1H, H_E, J= 9.5 Hz); 6.76 (s, 1H, H_A) 6.77-6.82 (m, 1H, H_B); 7.36 (d, 1H, H_C, J= 8.6 Hz); 7.62 (d, 1H, H_D, J= 9.5 Hz); **ppm.**
[^{13}C] NMR ($CDCl_3$) δ: 18.33 (CH_3); 24.9 (CH_2); 25.6 (CH_2); 28.7 (CH_2); 28.8 (CH_2); 32.7 ($CH_2CONHOH$); 68.4 (OCH_2); 101.3 (CH_A), 112.4 (C Ar); 112.8 (CH_E); 113.0 (CH_B); 128.8 (CH_C); 143.6 (CH_D); 156.0 (C Ar); 161.4 (C Ar); 162.4 (CO); 168.7 (CONH); **ppm.**

7.5. Carbonic Anhydrase Activators

7.5.1 Histamine Analogues, V Series

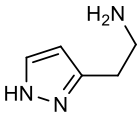

V-1 2-(1H-pyrazol-3-yl)ethanamine
This product was prepared starting from 4H-pyran-4-one according to Jones R. G. et al.[125]

Yield (over two steps) = 25%; **M.P.** (oxalate salt) = 166°C (decomposition)
[^{1}H]-NMR (D_2O) δ: 2.98 (t, J = 7.2 Hz, 2H, CH_2Ar); 3.31 (t, J = 7.2 Hz, 2H, CH_2N); 6.29 (d, J = 2.0 Hz, 1H, H4); 7.65 (d, J = 2.0 Hz, 1H, H5) **ppm.**
[^{13}C]-NMR (D_2O) δ: 22.72 (CH_2Ar); 49.66 (CH_2N); 105.18 (C4); 133.29 (C5); 165.43 (C3) **ppm.**

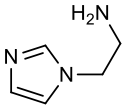

V-2 2-(1H-imidazol-1-yl)ethanamine
The imidazole **V-2** was prepared using imidazole as starting material and following the synthetic pathway described by Buchholz M. et al[126]. Yellow oil.

Yield (over two steps) = 54%; **M.P.** (oxalate salt) = 127°C (decomposition)
[^{1}H]-NMR (CD_3OD) δ: 2.98 (t, J = 6.2 Hz, 2H, CH_2N); 4.07 (t, J = 6.2 Hz, 2H, CH_2Ar); 6.98 (s, 1H, H4); 7.15 (s, 1H, H5); 7.67 (s, 1H, H2); **ppm.**
[^{13}C]-NMR (CD_3OD) δ: 41.83 (CH_2N); 48.82 (CH_2Ar); 119.31 (C5); 127.91 (C4); 137.31 (C2) **ppm.**

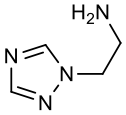

V-3 2-(1H-1,2,4-triazol-1-yl)ethanamine
The triazole-derivative **V-3** was prepared according to Wright W. B. et al[127].

Yield (over two steps) = 46%; **M.P.** (oxalate salt) = 194°C (decomposition)
[^{1}H]-NMR ($CDCl_3$) δ: 1.73 (bs, 2H, NH_2); 3.03 (t, J = 5.6 Hz, 2H, CH_2N); 4.09 (t, J = 5.6 Hz, 2H, CH_2Ar); 7.82 (s, 1H, H3); 8.04 (s, 1H, H5) **ppm.**
[^{13}C]-NMR ($CDCl_3$) δ: 41.29 (CH_2N); 52.55 (CH_2Ar); 143.55 (C5); 151.99 (C3) **ppm.**

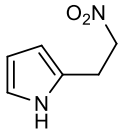

39a 2-(2-nitroethyl)-1H-pyrrole
Starting from Pyrrole-2-carboxaldehyde and following the two-steps procedure reported by J.P. Strachan et al.[128], the compound **39a** was obtained as a red oil.

Yield (over two steps) = 35%
[^{1}H] NMR ($CDCl_3$) δ: 3.29 (t, 2H, CH_2, J= 6.8 Hz); 4.70 (t, 2H, CH_2NO_2, J= 6.8 Hz); 5.98 (s, 1H, CH Ar); 6.08-6.17 (m, 1H, CH, Ar); 6.65-6.72 (m, 1H, CH Ar); 7.98-8.35 (bs, 1H, NH); **ppm.**

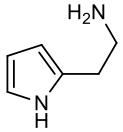

V-4 2-(1H-pyrrol-2-yl)ethanamine
The nitro derivative **39a** (0.071 g, 0.51 mmol) was dissolved in 4 mL of anhydrous CH_3OH, the solution was cooled down to 0°C and $SnCl_2$ (0.15 g, 0.61 mmol) was then suspended inside. $NaBH_4$ (0.29 g, 0.76 mmol) was portionwise added and the reaction kept into the ice-bath for 1 hour. The mixture was then filtered through celite and the solution evaporated under vacuum. The residue was purified with

flash chromatography (eluent $CH_2Cl_2/CH_3OH/NH_4OH$ 80:20:1), leading to the collection of the desired product as a red oil.

Yield= 45%; **M.P.** (oxalate salt) = 144°C (decomposition)
[^{1}H] NMR ($CDCl_3$) δ: 1.63-1.80 (bs, 2H, NH_2); 2.72 (t, 2H, CH_2, J= 6 Hz); 2.95 (t, 2H, CH_2NH_2, J= 6 Hz); 5.91 (s, 1H, CH Ar), 6.08-6.13 (m, 1H, CH Ar); 6.65 (s, 1H, CH Ar); 8.80-9.11 (bs, 1H, NH); **ppm.**
[^{13}C] NMR ($CDCl_3$) δ: 30.7 (CH_2); 42.0 (CH_2NH_2); 105.5 (CH Ar); 108.1 (CH Ar); 116.5 (CH Ar); 130.7 (C Ar); **ppm.**

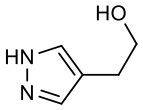

V-5 2-(4H-pyrazol-4-yl)ethanol
Following the synthetic procedures reported by Jones R. G. et al.[125] and starting from dihydrofurane, **V-5** represents an intermediate in the preparation of **V-6**. Colourless oil.

Yield= 45%
[^{1}H]-NMR (CD_3OD) δ: 2.70 (t, J = 6.8 Hz, 2H, CH_2Ar); 3.69 (t, J = 6.8 Hz, 2H, CH_2O); 7.45 (s, 2H, H3 and H5) **ppm.**
[^{13}C]-NMR (CD_3OD) δ: 27.20 (CH_2Ar); 62.50 (CH_2O); 117.30 (C3); 139.50 (C3 and C5) **ppm.**

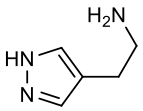

V-6 2-(1H-pyrazol-4-yl)ethanamine
This compound was prepared according to Jones R.G et al.[125] Yellow oil.

Yield (over three steps) = 70%; **M.P.** (oxalate salt) = 173°C (decomposition)
[^{1}H]-NMR (CD_3OD) δ: 2.67 (t, J = 7.2 Hz, 2H, CH_2Ar); 2.86 (t, J = 7.2 Hz, 2H, CH_2N); 7.47 (s, 2H, H3 and H5) **ppm.**
[^{13}C]-NMR (CD_3OD) δ: 26.83 (CH_2Ar); 42.75 (CH_2N); 117.51 (C3); 132.83 (C3 and C5) **ppm.**

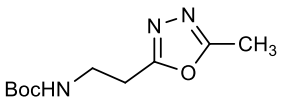

44 Tert-butyl (2-(5-methyl-1,3,4-oxadiazol-2-yl)ethyl)carbamate
Starting from N-Boc-β-alanine and according the two-steps procedure reported by R.A. Ancliff et al[129], the N-Boc-intermediate SUM-21 was prepared, isolated as an orange solid and used for the following synthetic step without purification .

Yield (over two steps) = 70%
[^{1}H]-NMR ($CDCl_3$) δ: 1.39 (s, 9H, tBu); 2.48 (s, 3H, CH_3); 2.96 (t, J = 6.2 Hz, 2H, CH_2); 3.50-3.61 (m, 2H, CH_2); **ppm.**

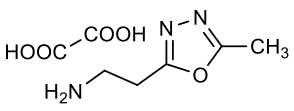

V-7[129] 2-(5-methyl-1,3,4-oxadiazol-2-yl)ethanamine oxalate
0.42 g of the N-Boc-intermediate **44**, prepared as previously described[129], was dissolved in 8 mL of anhydrous CH_2Cl_2. CF_3COOH (1.7 mL, 22 mmol) was then dropwise added and the solution stirred at RT for 2 hours. The solvent was then removed under vacuum and the residue purified with flash chromatography (eluent $CH_2Cl_2/CH_3OH/NH_4OH$ 87:13:1.3). The collected oil was then partitioned among CH_2Cl_2 and a 4M NaOH solution. After dryng (Na_2SO_4); the organic phase was evaporated and the residue treated with a solution of oxalic acid in

AcOEt to give the desired product as the corresponding oxalate. White solid.

Yield= 56%; **M.P.=** 116-119°C

[^{1}H]-NMR (D_2O) δ: 2.42 (s, 3H, CH_3); 3.19 (t, J = 7.0 Hz, 2H, CH_2); 3.36 (t, J = 7.0 Hz, 2H, CH_2); **ppm.**

[^{13}C]-NMR (D_2O) δ: 10.0 (CH_3); 23.0 (CH_2); 35.9 (CH_2); 164.2 (C Ar); 164.7 (CO oxal.); 166.2 (C); **ppm.**

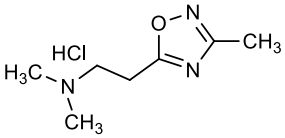

V-8[168] N,N-dimethyl-2-(3-methyl-1,2,4-oxadiazol-5-yl)ethanamine hydrochloride

To a suspension of N-hydroxyacetamidine (0.27 g, 5 mmol) in 10 mL of dry THF, NaH (0.12 g, 5 mmol) was portionwise added in about 30 minutes. After a 1 hour RT stirring, the mixture was heated to 60°C for 15 minutes and then allowed to cool down to RT again. In the meanwhile, ethyl 3-(dimethylamino)propionate (0.38 mL, 2.4 mmol) was dissolved in anhydrous THF (3 mL) and slowly dropped to the acetamidine-suspension. The so obtained mixture was heated to reflux for 20 hours, the solid was then filtered off through celite and the solution evaporated under vacuum. The residue was purified through flash chromatography (eluent CH_2Cl_2/CH_3OH 95:5), giving the desired compound as a colourless oil. A part of the product was afterwards transformed in the corresponding hydrochloric salt, obtained as a white solid.

Yield= 46%; **M.P.** (HCl salt) = 184-186°C

[^{1}H]-NMR ($CDCl_3$) δ: 2.31 (s, 6H, $N(CH_3)_2$); 2.37 (s, 3H, CH_3); 2.81 (t, *J* = 7.4 Hz, 2H, CH_2); 3.04 (t, *J* = 7.4 Hz, 2H, CH_2); **ppm.**

[^{1}H]-NMR (D_2O HCl salt**) δ**: 2.28 (s, 3H, CH_3); 2.67 (s, 6H, $N(CH_3)_2$); 3.24 – 3.31 (m, 2H, CH_2); 3.31-3.39 (m, 2H, CH_2); **ppm.**

7.5.2 Clonidine Analogues, VI Series

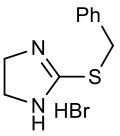

VI-1 2-(benzylthio)-4,5-dihydro-1H-imidazole hydrobromide

2-imidazolidinethione (0.1 g; 0.98 mmol) was suspended in 5 mL of anhydrous CH_3OH, then benzylbromide (0.13 mL; 1.08 mmol) was added dropwise and the mixture heated to reflux (65°C) for two hours. The solvents was afterwards removed under vacuum and the residue washed and grinded three times with Et_2O. After drying, the desired benzyl-derivative was obtained as a pale yellow solid.

Yield= 100%; **M.P.=** 181-183°C; **ESI-LCMS** $[M+H]^+$= 193.1

[^{1}H]-NMR (D_2O) δ: 3.81 (s, 4H, $2CH_2$); 4.35 (s, 2H, SCH_2); 7.28 – 7.39 (m, 2H, Ar); 7.34 – 7.43 (m, 3H, Ar); **ppm.**

[^{13}C]-NMR (D_2O) δ: 35.2 (SCH_2); 45.2 ($2CH_2$); 128.3 (CH Ar); 128.7 (CH Ar); 129.1 (CH Ar); 134.1 (C Ar); 169.7 (C=N); **ppm.**

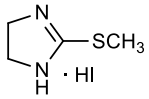

VI-2 2-(methylthio)-4,5-dihydro-1H-imidazole hydroiodide
The compound was prepared following the procedure reported by Gomez-San Juan et. al[130]. White solid.

Yield= 100%; **M.P.** 146-148°C
[^{1}H]-NMR (D_2O) δ: 3.85 (s, 4H, CH_2CH_2), 2.53 (s, 3H, CH_3) **ppm.**

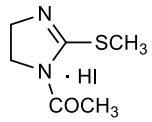

VI-3 1-(2-(methylthio)-4,5-dihydro-1H-imidazol-1-yl)ethanone
The imidazoline **VI-2** was acylated on one imidazoline-nitrogen to obtain **VI-3** as already reported by Gomez-San Juan et. al[130]. Yellow solid.

Yield= 100%; **M.P.=** 107-110°C
[^{1}H]-NMR (D_2O) δ: 2.07 (s, 3H, SCH_3); 2.23 (s, 3H, CH_3); 3.76 (t, J = 8.8 Hz, 2H, CH_2); 3.92 (t, J=8.8 Hz, 2H, CH_2); **ppm.**
[^{13}C]-NMR (D_2O) δ: 14.5 (SCH_3); 23.5 (CH_3); 48.0 ($2CH_2$); 161.5 (C=N); 171.9 (CO); **ppm.**

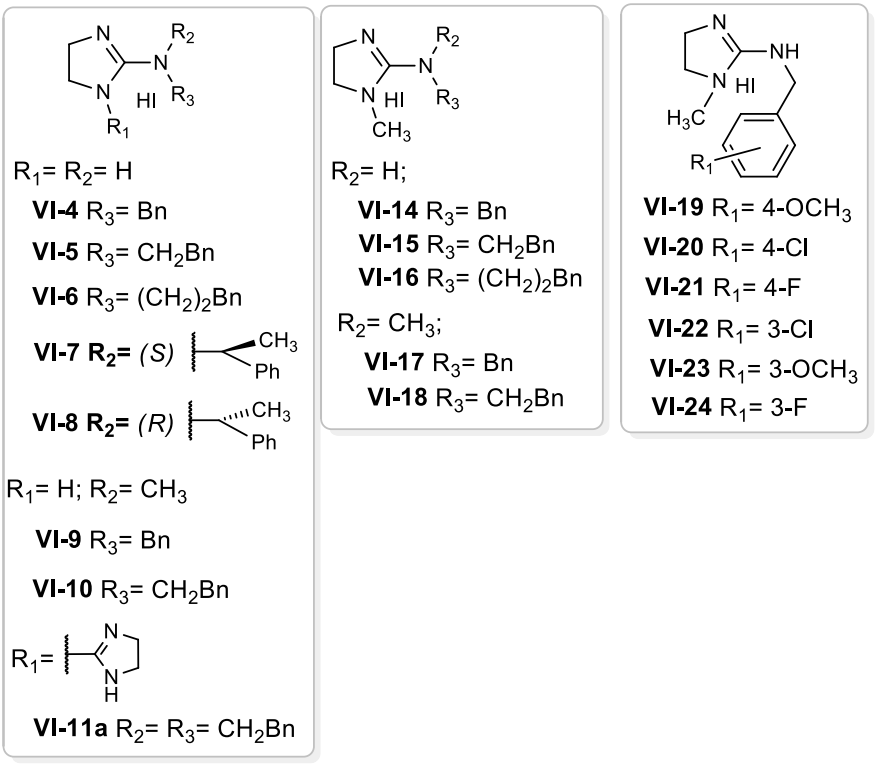

General procedure 4: preparation of the imidazolines **VI-4** – **11** and **VI-14** – **24**.

The appropriate intermediate was suspended in THF or directly in the proper amine and the mixture was heated until reaction completion (TLC monitoring, eluent CH_2Cl_2/CH_3OH/ NH_4OH 90:10:1). The solvent (when present) was evaporated under vacuum and the amine excess removed washing the mixture three times with Et_2O, affording the desired imidazoline-derivative. (For the conditions of each product see the table below.

Product	Reag.	THF (mL)	Temp. (°C)	Amine (eq)
VI-4	**VI-2**	5	40	Benzylamine (1.1)
VI-5	**VI-2**	5	40	2-phenylethanamine (1.1)
VI-6	**VI-2**	-	70	3-phenyl-1-propylamine (5)
VI-7	**VI-2**	-	70	*(S)*-α-methyl-benzylamine (4.5)
VI-8	**VI-2**	-	70	*(R)*-α-methyl-benzylamine (4.5)
VI-9	**VI-2**	5	40	N-benzyl-methylamine (1.1)
VI-10	**VI-2**	-	70	N-methyl-2-phenylethanamine (5)
VI-11	**VI-2**	-	70	Dibenzylamine (5)
VI-14	47	-	70	Benzylamine (5)
VI-15	47	-	70	2-phenylethanamine (5)
VI-16	47	-	70	3-phenylpropylamine (5)
VI-17	47	-	70	N-methyl-1-phenylmethanamine (5)
VI-18	47	-	70	N-methyl-2-phenylethanamine (5)
VI-19	47	5	70	(4-methoxyphenyl)-methanamine (1.5)
VI-20	47	10	70	(4-chlorophenyl)-methanamine (1.5)
VI-21	47	-	70	(4-fluorophenyl)-methanamine (5)
VI-22	47	-	70	(3-chlorophenyl)-methanamine (5)
VI-23	47	-	70	(3-methoxybenzyl)-methanamine (5)
VI-24	47	-	70	(3-fluorobenzyl)-methanamine (5)

VI-4[131] N-benzyl-4,5-dihydro-1H-imidazol-2-aminehydroiodide

White solid; **Yield=** 90%; **M.P. =** 143-146°C **ESI-LCMS** $[M+H]^+$= 176.0
[^{1}H]-NMR (D_2O) δ: 3.56 (s, 4H, CH_2CH_2); 4.31 (s, 2H, CH_2); 7.24- 7.35 (m, 5H, Ar); **ppm.**
[^{13}C]-NMR (D_2O) δ: 42.7 (CH_2Ph); 45.7 ($2CH_2$); 127.0 (CH-Ar); 128.0 (CH-Ar); 129.0 (CH-Ar); 136.2 (C-Ar); 159.91 (C=N); **ppm.**

VI-5[131] N-phenethyl-4,5-dihydro-1H-imidazol-2-aminehydroiodide

White solid; **Yield=** 91%; **M.P.=** 82-83°C; **ESI-LCMS** $[M+H]^+$= 189.7
[^{1}H]-NMR (D_2O) δ: 2.75 (t, J = 6.6 Hz, 2H, CH_2); 3.33 (t, J = 6.6 Hz, 2H, CH_2); 3.43 (s, 4H, CH_2CH_2); 7.14 – 7.31 (m, 5H, Ar); **ppm.**
[^{13}C]-NMR (D_2O) δ: 34.8 (CH_2); 42.6 ($2CH_2$); 43.8 (CH_2); 126.9 (CH-Ar); 127.4 (CH-Ar); 128.8 (CH-Ar); 129.0 (CH-Ar); 129.1 (CH-Ar); 138.5 (C-Ar); 159.4 (C=N); **ppm.**

VI-6 N-(3-phenylpropyl)-4,5-dihydro-1H-imidazol-2-aminehydroiodide

White solid; **Yield=** 88%; **M.P.=** 85-87°C; **ESI-LCMS** $[M+H]^+$= 204.1
[^{1}H]-NMR ($CDCl_3$) δ: 1.96 – 1.82 (m, 2H, CH_2); 2.60 – 2.80 (m, 2H, CH_2); 3.34 (dd, J = 12.7, 6.6 Hz, 2H, NCH_2); 3.60 (s, 4H, CH_2CH_2); 6.96 – 7.32 (m, 5H, Ar); 7.63 (s, 1H, NH); **ppm.**
[^{13}C]-NMR ($CDCl_3$) δ: 30.7 (CH_2); 32.6 (CH_2); 42.6 (CH_2); 43.4 (CH_2); 126.2 (CH Ar); 128.5 (CH Ar); 140.6 (C Ar); 159.7 (C=N); **ppm.**

VI-7 (S) N-(1-phenylethyl)-4,5-dihydro-1H-imidazol-2-amine

Yellow solid **Yield=** 36% **M.P.=** 103-107°C; **ESI-LCMS** $[M+H]^+$= 190.2
[^{1}H]-NMR (D_2O) δ: 1.39 (d, J = 6.9 Hz, 3H, CH_3); 3.47-3.51 (m, 4H, $2CH_2$); 4.53 (q, J = 6.8 Hz, 1H, CH); 7.21-7.33 (m, 5H, Ar); **ppm.**

[^{13}C]-NMR (D_2O) δ: 22.5 (CH_3); 42.6 ($2CH_2$); 52.8 (CH); 125.6 (CH Ar); 125.6 (CH Ar); 128.0 (CH Ar); 129.1 (CH Ar); 142.0 (C Ar); 159.0 (C=N); **ppm.**

VI-8 (R) N-(1-phenylethyl)-4,5-dihydro-1H-imidazol-2-amine

Yield= 75% **M.P.=** 105-109°C; **ESI-LCMS** $[M+H]^+$= 190.2
[^{1}H]-NMR (D_2O) δ: 1.40 (d, J=8Hz, 3H, CH_3); 3.49 (q, J = 4.0 Hz, 4H, $2CH_2$); 4.54 (q, J = 6.9 Hz, 1H, CH); 7.21 – 7.40 (m, 5H, Ar); **ppm.**
[^{13}C]-NMR (D_2O) δ: 22.5 (CH_3); 42.6 ($2CH_2$); 52.8 (CH); 125.6 (CH Ar); 125.6 (CH Ar); 128.0 (CH Ar); 129.1 (CH Ar); 142.0 (C Ar); 159.0 (C=N); **ppm.**

VI-9[131] N-benzyl-N-methyl-4,5-dihydro-1H-imidazol-2-aminehydroiodide

White solid; **Yield=** 32%; **M.P.=** 150-153°C; **ESI-LCMS** $[M+H]^+$= 189.7
[^{1}H]-NMR (D_2O) δ: 2.90 (s, 3H, NCH_3); 3.61 (s, 4H, CH_2CH_2); 4.42 (s, 2H, CH_2Ph); 7.15-7.40 (m, 5H, Ar); **ppm.**
[^{13}C]-NMR (D_2O) δ: 36.4 (CH_3); 43.1 ($2CH_2$); 54.3 (CH_2Ph); 127.1 (CH-Ar); 128.3 (CH-Ar); 129.1 (CH-Ar); 134.7 (C-Ar); 160.5 (C=N); **ppm.**

VI-10 N-methyl-N-phenethyl-4,5-dihydro-1H-imidazol-2-aminehydroiodide

White solid; **Yield=** 89%; **M.P.=** 200-204°C; **ESI-LCMS** $[M+H]^+$= 204.0
[^{1}H]-NMR (D_2O) δ: 2.77 – 2.89 (m, 5H, CH_3 + CH_2); 3.39 (s, 4H, $2CH_2$); 3.42 (dd, J = 11.6, 5.0 Hz, 2H, CH_2); 7.13 – 7.33 (m, 5H, Ar); **ppm.**
[^{13}C]-NMR (D_2O) δ: 32.6 (CH_2Ph); 36.2 (NCH_3); 42.8 (N-CH_2); 52.5 (CH_2CH_2); 127.0 (CH Ar); 128.8 (CH Ar); 129.1 (CH Ar); 136.1 (C Ar); 159.9 (C=N); **ppm.**

VI-11 N,N-dibenzyl-4,4',5,5'-tetrahydro-1'H-[1,2'-biimidazol]-2-amine hydroiodide

Pale yellow gum; **Yield=** 50%; **ESI-LCMS** $[M+H]^+$= 334.2
[^{1}H]-NMR (D_2O) δ: 3.45 (t, J = 8.3 Hz, 2H, CH_2); 3.64 (d, J = 3.7 Hz, 4H, CH_2CH_2); 3.80 (t, J = 8.3 Hz, 2H, CH_2); 4.12 (s, 4H, CH_2); 7.14 – 7.36 (m, 10H, Ar); **ppm.**

VI-14 N-benzyl-1-methyl-4,5-dihydro-1H-imidazol-2-aminehydroiodide

White solid; **Yield=** 81%; **M.P.=** 130-133°C; **ESI-LCMS** $[M+H]^+$= 190.0
[^{1}H]-NMR ($CDCl_3$) δ: 3.16 (s, 3H, CH_3); 3.49-3.74 (m, 4H, CH_2CH_2); 4.67 (d, J = 5.8 Hz, 2H, CH_2Ph); 6.87 (s, 1H, Ar); 7.25-7.38 (m, 2H, Ar); 7.49 (d, J = 7.2 Hz, 2H, Ar); 8.21 (s, 1H, NH); **ppm.**
[^{13}C]-NMR ($CDCl_3$) δ: 33.8 (CH_3); 41.3 (CH_2); 46.9 (CH_2); 50.2 (CH_2); 128.1 (CH Ar); 128.3 (CH-Ar); 129.0 (CH-Ar); 135.6 (C-Ar); 158.4 (C=N); **ppm.**

VI-15 1-methyl-N-phenethyl-4,5-dihydro-1H-imidazol-2-amine hydroiodide

White solid; **Yield=** 86%; **M.P.=** 118-220°C; **ESI-LCMS** $[M+H]^+$= 204.2
[^{1}H]-NMR ($CDCl_3$) δ: 3.01 (d, J = 10.2 Hz, 3H, CH_3); 3.48 (s, 3H, CH_3); 3.65 (dd, J = 13.8, 6.7 Hz, 4H, CH_2CH_2); 6.88 – 7.59 (m, 5H, Ar); **ppm.**
[^{13}C]-NMR ($CDCl_3$) δ: 33.8 (CH_3); 35.5 (CH_2); 41.0 (CH_2); 45.2 (CH_2); 50.1 (CH_2); 126.8 (CH Ar); 128.7 (CH Ar); 129.3 (CH Ar); 137.9 (C Ar); 158.2 (C=N); **ppm.**

VI-16 1-methyl-N-(3-phenylpropyl)-4,5-dihydro-1H-imidazol-2-amine hydroiodide

Orange gum; **Yield=** 45%; **ESI-LCMS** $[M+H]^+$= 218.1
[^{1}H]-NMR ($CDCl_3$) δ: 2.03 (dd, *J* = 14.8, 7.4 Hz, 2H); 2.60 – 2.78 (m, 2H, CH_2); 2.97 (s, 3H, CH_3); 3.41-3.54 (m, 4H, CH_2CH_2); 3.54-3.65 (m, 2H, CH_2); 7.02-7.35 (m, 5H, Ar); **ppm.**
[^{13}C]-NMR ($CDCl_3$) δ: 30.6 (CH_2); 32.9 (CH_2); 33.8 (NCH_3); 41.0 (CH_2); 43.8 (CH_2); 50.1 (CH_2); 128.5 (d, *J* = 13.4 Hz, CH Ar); 141.2 (C-Ar); 154.9 (C=N); **ppm.**

VI-17 N-benzyl-N,1-dimethyl-4,5-dihydro-1H-imidazol-2-amine hydroiodide

Yellow oil; **Yield=** 70%; **ESI-LCMS** $[M+H]^+$= 204.1
[^{1}H]-NMR ($CDCl_3$) δ: 2.82 (s, 3H, CH_3); 2.97 (t, *J* = 6.8 Hz, 2H, NCH_2); 3.13 (s, 3H, CH_3); 3.62 (td, *J* = 16.3, 7.5 Hz, 4H, CH_2CH_2); 3.77 (t, *J* = 6.9 Hz, 2H, CH_2Ph); 7.32 (t, *J* = 7.5 Hz, 5H, Ar); **ppm.**
[^{13}C]-NMR ($CDCl_3$) δ: 37.0 (CH_3); 39.7 (CH_3); 53.1 (CH_2); 56.6 (CH_2); 127.2 (CH-Ar); 128.4 (CH-Ar); 129.3 (d, J = 1.6 Hz); 133.9 (C-Ar); 162.63 (C=N); **ppm.**

VI-18 N,1-dimethyl-N-phenethyl-4,5-dihydro-1H-imidazol-2-amine hydroiodide

White solid; **Yield=** 97%; **M.P.=** 109-110°C; **ESI-LCMS** $[M+H]^+$= 218.2
[^{1}H]-NMR ($CDCl_3$) δ: 2.82 (s, 3H, CH_3); 2.97 (t, *J* = 6.8 Hz, 2H, NCH_2); 3.13 (s, 3H, CH_3); 3.62 (td, *J* = 16.3, 7.5 Hz, 4H, CH_2CH_2); 3.77 (t, *J* = 6.9 Hz, 2H, CH_2Ph); 7.32 (t, *J* = 7.5 Hz, 5H, Ar); **ppm.**
[^{13}C]-NMR ($CDCl_3$) δ: 33.7 (CH_2); 37.0 (CH_3); 39.7 (CH_3); 40.3 (CH_2); 52.9 (CH_2); 54.7 (CH_2); 127.2 (CH-Ar); 128.9 (CH-Ar); 137.0 (C-Ar); 162.5 (C=N); **ppm.**

VI-19 N-(4-methoxybenzyl)-1-methyl-4,5-dihydro-1H-imidazol-2-amine hydroiodide

White solid; **Yield=** 89%; **M.P.=** 167°C; **ESI-LCMS** $[M+H]^+$= 220.3
[^{1}H]-NMR ($CDCl_3$) δ: 3.18 (s, 3H, CH_3); 3.64 (s, 4H, CH_2CH_2); 3.76 (s, 3H, CH_3); 4.58 (d, *J* = 5.7 Hz, 2H, CH_2); 6.38 (s, 1H); 6.85 (d, *J* = 8.5 Hz, 2H, Ar); 7.39 (d, *J* = 8.5 Hz, 2H, Ar); 8.10 (s, 1H); **ppm.**
[^{13}C]-NMR ($CDCl_3$) δ: 33.8 (NCH_3); 41.3 (CH_2); 45.9 (CH_2); 50.1 (CH_2); 55.4 (OCH_3); 114.4 (CH Ar); 127.6 (C Ar); 129.7 (CH-Ar); 158.2 (C-Ar); 159.6 (C=N); **ppm.**

VI-20 N-(4-chlorobenzyl)-1-methyl-4,5-dihydro-1H-imidazol-2-amine hydroiodide

White solid; **Yield=** 97%; **M.P.=** 84-85°C; **ESI-LCMS** $[M+H]^+$= 220.0
[^{1}H]-NMR ($CDCl_3$) δ: 3.21 (s, 3H, CH_3); 3.67 (s, 4H, CH_2CH_2); 4.64 (d, *J* = 5.8 Hz, 2H, CH_2); 7.31 (d, *J* = 8.2 Hz, 2H, Ar); 7.42 (d, *J* = 8.2 Hz, 2H, Ar); 8.32 (s, 1H); **ppm.**
[^{13}C]-NMR (CD_3OD) δ: 30.7 (CH_3); 41.0 (CH_2); 45.4 (CH_2); 50.1 (CH_2); 128.6 (CH Ar); 128.9 (CH Ar); 130.4 (CH Ar); 133.5 (C Ar); 135.0 (C Ar); 158.7 (C=N); **ppm.**

VI-21 N-(4-fluorobenzyl)-1-methyl-4,5-dihydro-1H-imidazol-2-amine hydroiodide

Pale yellow solid; **Yield=** 89%; **M.P.=** 157°C; **ESI-LCMS** $[M+H]^+$= 208.1
[^{1}H]-NMR ($CDCl_3$) δ: 3.17 (s, 3H, CH_3); 3.54-3.76 (m, 4H, CH_2CH_2); 4.66 (d, *J* = 5.3 Hz, 2H, CH_2); 7.00 (t, *J* = 8.5 Hz, 2H, Ar); 7.50 (dd, *J* = 8.5, 5.3 Hz, 2H, Ar); **ppm.**

[^{13}C]-NMR (CD_3OD) δ: 30.6 (CH_3); 41.0 (CH_2); 45.4 (CH_2); 50.1 (CH_2); 125.3 (CH Ar); 126.9 (CH Ar); 127.7 (CH Ar); 130.1 (CH Ar); 134.4 (C Ar); 138.6 (C Ar); 154.1 (C=N);

VI-22 N-(3-chlorobenzyl)-1-methyl-4,5-dihydro-1H-imidazol-2-amine hydroiodide

White solid; **Yield=** 88%; **M.P.=** 190°C; **ESI-LCMS** $[M+H]^+$= 208.1
[^{1}H]-NMR ($CDCl_3$) δ: 3.21 (s, 3H, CH_3); 3.68 (s, 4H, CH_2CH_2); 4.67 (d, J= 5.8 Hz, 2H, CH_2); 7.27 (d, J= 7.0 Hz, 2H, Ar); 7.41 (d, J= 7.0 Hz, 5.8 Hz, 2H, Ar); **ppm.**
[^{13}C]-NMR ($CDCl_3$) δ: 163.70 (d, J = 244 Hz, C-Ar), 158.62 (C-Ar), 132.25 (C-Ar), 129.16 (CH-Ar),115.26 (CH-Ar), 50.11 (CH2), 45.44 (CH2), 40.98 (CH2), 30.81 (CH3) **ppm**.

VI-23 N-(3-methoxybenzyl)-1-methyl-4,5-dihydro-1H-imidazol-2-amine hydroiodide

Pale yellow solid; **Yield=** 92%; **M.P.=** 147°C; **ESI-LCMS** $[M+H]^+$= 220.1
[^{1}H]-NMR ($CDCl_3$) δ: 3.13 (s, 3H, CH_3); 3.61 (s, 4H, CH_2CH_2); 3.76 (s, 3H, OCH_3); 4.59 (s, 2H, CH_2); 6.77 (d, J= 6.4 Hz, 1H, Ar); 6.98-7.31 (m, 3H, Ar);
[^{13}C]-NMR ($CDCl_3$) δ: 33.7 (CH_3); 41.3 (CH_2); 46.2 (CH_2); 50.2 (CH_2); 55.7 (OCH_3); 113.7 (CH-Ar); 114.0 (CH-Ar); 120.3 (CH-Ar); 130.0 (CH Ar); 137.4 (C-Ar); 158.2 (C-Ar); 159.9 (C=N); **ppm.**

VI-24 N-(3-fluorobenzyl)-1-methyl-4,5-dihydro-1H-imidazol-2-amine hydroiodide

Pale yellow solid; **Yield=** 87%; **M.P.=** 195°C; **ESI-LCMS** $[M+H]^+$= 208.1
[^{1}H]-NMR ($CDCl_3$) δ: 3.19 (s, 3H, CH_3); 3.66 (dd, J= 5.4, 3.7 Hz, 4H, CH_2CH_2); 4.68 (s, 2H, CH_2); 6.95 (t, J= 7.7 Hz, 2H, Ar); 7.19-7.33 (m, 2H, Ar); **ppm.**
[^{13}C]-NMR ($CDCl_3$) δ: 33.9 (CH_3); 41.2 (CH_2); 45.4 (CH_2); 50.2 (CH_2); 114.9-115.2 (d, J= 25 Hz, CH-Ar); 123.9 (CH-Ar); 130.4-130.5 (d, J = 8 Hz, CH-Ar); 138.5 (C-Ar); 158.1 (C=N); 161.2-164.0 (d, J= 246 Hz, C-Ar); **ppm.**

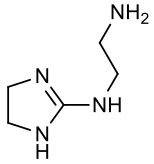

VI-12 N1-(4,5-dihydro-1H-imidazol-2-yl)ethane-1,2-diamine
The compound was prepared following the procedure reported by A. Bucio-Cano et al.[132] Yellow oil, isolated then as oxalate salt.

Yield= 61%; **M.P.** (oxalate salt) = 153-154°C
[^{1}H] NMR (D_2O) δ: 3.10 (t, 2H, CH_2, J= 6 Hz); 3.44 (t, 2H, CH_2, J= 6 Hz); 3.59 (s, 4H, $NHCH_2CH_2NH_2$); **ppm.**
[^{13}C] NMR (D_2O) δ: 38.28 (CH_2); 39.7 (CH_2); 42.8 ($2CH_2$); 159.8 (C); 165.0 (CO Oxalate); **ppm.**

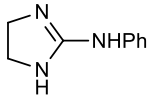

VI-13 N-phenyl-4,5-dihydro-1H-imidazol-2-amine
The compound **VI-13** was prepared according to Heinelt et al[133] and isolated as a was white solid.

Yield= 50%; **M.P.=** 137-140 °C; **ESI-LCMS** $[M+H]^+$= 161.9
[^{1}H]-NMR (D_2O) δ: 3.40 (s, 4H, CH_2CH_2); 6.90 – 6.98 (m, 2H, Ar); 7.23 – 7.32 (m, 2H, Ar), 7.03 (m, 1H, Ar), **ppm.**
[^{13}C]-NMR (D_2O) δ: 42.4 (CH_2); 161.0 (C=N), 123.4 (CH-Ar); 129.6 (C-Ar), 123.55 (CH-Ar); **ppm**.

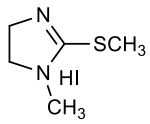

CAB-3

47[134] 1-methyl-2-(methylthio)-4,5-dihydro-1H-imidazole hydroiodide
The imidazoline **44** was prepared according to Zhu Bing Y. et al.[134] White solid.

Yield= 97%; **M.P.=** 99-102°C
[^{1}H]-NMR ($CDCl_3$) δ: 2.95 (s, 3H, CH_3); 3.07 (s, 3H, CH_3); 3.97 – 4.10 (m, 4H, CH_2CH_2); **ppm.**

Abbreviations

CAs: Carbonic Anhydrases
hCAs: human Carbonic Anhydrases
CAIs: Inhibitors
CAAs: Carbonic Anhydrases Activators
HDACs: histone deacetylases
HDACIs: histone deacetylases inhibitors
IOP: intra-ocular pressure
T: temperature
RT: room temperature
E.E. : enantiomeric excess
Glu: glutamic acid
Asp: aspartic acid
Lys: lysine
Thr: threonine
Trp: tryptophan
DCM: dichloromethane
Gln: glutamine
Val: valine
Cys: cysteine
His: histidine
HST: histamine
CLO: clonidine
NHS: N-hydroxysuccinimide
NH_2OTHP: O-(Tetrahydro-2H-pyran-2-yl)hydroxylamine
THP: Tetrahydro-2H-pyrane
EDC: N-(3-Dimethylaminopropyl)-N′-ethylcarbodiimide hydrochloride
HOBT: 1-Hydroxybenzotriazole
DMAP: 4-(dimethylamine)pyridine
DCC: dicycloesylcarbodiimide
DIPA: diisopropylamine
DIPEA: diisopropylethylamine
S.M.: starting material
M.P.: melting point
THF: tetrahydrofurane
AcOEt: ethyl acetate
DMF: dimethylformamide
HPLC: high-performance liquid chromatography
LCMS: liquid chromatography mass spectrometry
SBNHS: 2,5-dioxopyrrolidin-1-yl 4-sulfamoylbenzoate

8. Bibliography

(1) Supuran, C. T.; De Simone, G. Carbonic Anhydrases: An Overview. *Carbon. Anhydrases as Biocatal. From Theory to Med. Ind. Appl.* **2015**, 3–13.

(2) Kupriyanova, E.; Pronina, N.; Los, D. Carbonic Anhydrase — a Universal Enzyme of the Carbon-Based Life. *Photosynthetica* **2017**, *55* (1), 3–19.

(3) Supuran, C. T. Structure and Function of Carbonic Anhydrases. *Biochem. J.* **2016**, *473* (14), 2023–2032.

(4) Del Prete, S.; Vullo, D.; Fisher, G. M.; Andrews, K. T.; Poulsen, S. A.; Capasso, C.; Supuran, C. T. Discovery of a New Family of Carbonic Anhydrases in the Malaria Pathogen Plasmodium Falciparum - The η-Carbonic Anhydrases. *Bioorganic Med. Chem. Lett.* **2014**.

(5) Jensen, E. L.; Clement, R.; Kosta, A.; Maberly, S. C.; Gontero, B. A New Widespread Subclass of Carbonic Anhydrase in Marine Phytoplankton. *ISME J.* **2019**.

(6) Supuran, C. T. Carbonic Anhydrases: Novel Therapeutic Applications for Inhibitors and Activators. *Nat. Rev. Drug Discov.* **2008**, *7* (2), 168–181.

(7) Khalifah, R. G. The Carbon Dioxide Hydration Activity of Carbonic Anhydrase. *J. Biol. Chem.* **1971**, *246* (8), 2561–2573.

(8) Neri, D.; Supuran, C. T. Interfering with PH Regulation in Tumours as a Therapeutic Strategy. *Nat. Rev. Drug Discov.* **2011**, *10* (10), 767–777.

(9) D'Ambrosio, K.; De Simone, G.; Supuran, C. T. Human Carbonic Anhydrases: Catalytic Properties, Structural Features, and Tissue Distribution. *Carbon. Anhydrases as Biocatal. From Theory to Med. Ind. Appl.* **2015**, 17–30.

(10) Supuran, C. Carbonic Anhydrases and Metabolism. *Metabolites* **2018**, *8* (2), 25.

(11) Lindskog, S. Structure and Mechanism of Carbonic Anhydrase. *Pharmacol. Ther.* **1997**, *74* (1), 1–20.

(12) De Simone, G.; Di Fiore, A.; Capasso, C.; Supuran, C. T. The Zinc Coordination Pattern in the η-Carbonic Anhydrase from Plasmodium Falciparum Is Different from All Other Carbonic Anhydrase Genetic Families. *Bioorg. Med. Chem. Lett.* **2015**, *25* (7), 1385–1389.

(13) Kikutani, S.; Nakajima, K.; Nagasato, C.; Tsuji, Y.; Miyatake, A.; Matsuda, Y. Thylakoid Luminal θ-Carbonic Anhydrase Critical for Growth and Photosynthesis in the Marine Diatom <Em>Phaeodactylum Tricornutum</Em> *Proc. Natl. Acad. Sci.* **2016**, *113* (35), 9828 LP – 9833.

(14) Supuran, C. T. Carbonic Anhydrases as Drug Targets: General Presentation. *Drug Design of Zinc-Enzyme Inhibitors*. August 3, 2009, pp 13–38.

(15) Supuran, C. T. Carbonic Anhydrase Activators. *Future Med. Chem.* **2018**, *10* (5), 561–573.

(16) Tu, C.; Silverman, D. N.; Forsman, C.; Jonsson, B. H.; Lindskog, S. Role of Histidine 64 in the Catalytic Mechanism of Human Carbonic Anhydrase II Studied with a Site-Specific Mutant. *Biochemistry* **1989**, *28* (19), 7913–7918.

(17) De Simone, G.; Alterio, V.; Supuran, C. T. Exploiting the Hydrophobic and Hydrophilic Binding Sites for Designing Carbonic Anhydrase Inhibitors. *Expert Opin. Drug Discov.* **2013**, *8* (7), 793–810.

(18) Nocentini, A.; Supuran, C. T. Advances in the Structural Annotation of Human Carbonic Anhydrases and Impact on Future Drug Discovery. *Expert Opin. Drug Discov.* **2019**, *14* (11), 1175–1197.

(19) Christianson, D. W.; Fierke, C. A. Carbonic Anhydrase: Evolution of the Zinc Binding Site by Nature and by Design. *Acc. Chem. Res.* **1996**.

(20) Drugs Originating from the Screening of Dyes. *Drug Discovery*. April 15, 2005, pp 375–402.

(21) Supuran, C. T. How Many Carbonic Anhydrase Inhibition Mechanisms Exist? *Journal of Enzyme Inhibition and Medicinal Chemistry*. 2016, pp 345–360.

(22) Supuran, C. T. Advances in Structure-Based Drug Discovery of Carbonic Anhydrase Inhibitors. *Expert Opin. Drug Discov.* **2017**, *12* (1), 61–88.

(23) Supuran, C. T. Structure-Based Drug Discovery of Carbonic Anhydrase Inhibitors. *Journal of Enzyme Inhibition and Medicinal Chemistry*. 2012, pp 759–772.

(24) Chiaramonte, N.; Bua, S.; Ferraroni, M.; Nocentini, A.; Bonardi, A.; Bartolucci, G.; Durante, M.; Lucarini, L.; Chiapponi, D.; Dei, S.; et al. 2-Benzylpiperazine: A New Scaffold for Potent Human Carbonic Anhydrase Inhibitors. Synthesis, Enzyme Inhibition, Enantioselectivity, Computational and Crystallographic Studies and in Vivo Activity for a New Class of Intraocular Pressure Lowering Agents. *Eur. J. Med. Chem.* **2018**, *151*, 363–375.

(25) Karioti, A.; Carta, F.; Supuran, C. T. Phenols and Polyphenols as Carbonic Anhydrase Inhibitors. *Molecules* **2016**, *21* (12), 12–17.

(26) Maresca, A.; Temperini, C.; Pochet, L.; Masereel, B.; Scozzafava, A.; Supuran, C. T. Deciphering the Mechanism of Carbonic Anhydrase Inhibition with Coumarins and Thiocoumarins. *J. Med. Chem.* **2010**, *53* (1), 335–344.

(27) D'Ambrosio, K.; Carradori, S.; Monti, S. M.; Buonanno, M.; Secci, D.; Vullo, D.; Supuran, C. T.; De Simone, G. Out of the Active Site Binding Pocket for Carbonic Anhydrase Inhibitors. *Chem. Commun.* **2015**, *51* (2).

(28) Bozdag, M.; Altamimi, A. S. A.; Vullo, D.; Carta*, C. T. S. and F. State of the Art on Carbonic Anhydrase Modulators for Biomedical Purposes. *Current Medicinal Chemistry*. 2018, pp 1–15.

(29) Alterio, V.; Di Flore, A.; D'Ambrosio, K.; Supuran, C. T.; De Simone, G. X-Ray Crystallography of Carbonic Anhydrase Inhibitors and Its Importance in Drug Design. *Drug Des.Zinc-Enzyme Inhib.* 2009, pp 73–138.

(30) Winum, J.-Y.; Montero, J.-L.; Scozzafava, A.; Supuran, C. T. Zinc Binding Functions in the Design of Carbonic Anhydrase Inhibitors. *Drug Design of Zinc-Enzyme Inhibitors*. August 3, 2009, pp 39–72.

(31) Alterio, V.; Di Fiore, A.; D'Ambrosio, K.; Supuran, C. T.; De Simone, G. Multiple Binding Modes of Inhibitors to Carbonic Anhydrases: How to Design Specific Drugs Targeting 15 Different Isoforms? *Chemical Reviews*. 2012, pp 4421–4468.

(32) Supuran, C. T.; Casini, A.; Scozzafava, A. Development of Sulfonamide Carbonic Anhydrase Inhibitors. In *Carbonic Anhydrase*; 2004; pp 67–147.

(33) Chiaramonte, N.; Romanelli, M. N.; Teodori, E.; Supuran, C. T. Amino Acids as Building Blocks for Carbonic Anhydrase Inhibitors. *Metabolites* **2018**, *8* (2).

(34) Vu, H.; Pham, N. B.; Quinn, R. J. Direct Screening of Natural Product Extracts Using Mass Spectrometry. *J. Biomol. Screen.* **2008**, *13* (4), 265–275.

(35) Maresca, A.; Temperini, C.; Vu, H.; Pham, N. B.; Poulsen, S.-A.; Scozzafava, A.; Quinn, R. J.; Supuran, C. T. Non-Zinc Mediated Inhibition of Carbonic Anhydrases: Coumarins Are a New Class of Suicide Inhibitors. *J. Am. Chem. Soc.* **2009**, *131* (8), 3057–3062.

(36) Kyllönen, M. S.; Parkkila, S.; Rajaniemi, H.; Waheed, A.; Grubb, J. H.; Shah, G. N.; Sly, W. S.; Kaunisto, K. Localization of Carbonic Anhydrase XII to the Basolateral Membrane of H+-Secreting Cells of Mouse and Rat Kidney. *J. Histochem. Cytochem.* **2003**, *51* (9), 1217–1224.

(37) Splendiani, G.; Condò, S. [Diuretic therapy in heart failure]. *G. Ital. Nefrol.* **2006**, *23 Suppl 3*, S74-6.

(38) Thiry, A.; Dogne, J.-M.; Supuran, C.; Masereel, B. Carbonic Anhydrase Inhibitors as Anticonvulsant Agents. *Curr. Top. Med. Chem.* **2007**.

(39) Woodbury, D. M.; Rollins, L. T.; Gardner, M. D.; Hirschi, W. L.; Hogan, J. R.; Rallison, M. L.; Tanner, G. S.; Brodie, D. A. Effects of Carbon Dioxide on Brain Excitability and Electrolytes. *Am. J. Physiol. Content* **1957**, *192* (1), 79–90.

(40) Cammer, W. B.; Brion, L. P. Carbonic Anhydrase in the Nervous System BT - The Carbonic Anhydrases: New Horizons; Chegwidden, W. R., Carter, N. D., Edwards, Y. H., Eds.; Birkhäuser Basel: Basel, 2000; pp 475–489.

(41) Thöne, J.; Leniger, T.; Splettstösser, F.; Wiemann, M. Antiepileptic Activity of Zonisamide on Hippocampal CA3 Neurons Does Not Depend on Carbonic Anhydrase Inhibition. *Epilepsy Res.* **2008**, *79* (2–3), 105–111.

(42) Supuran, C. T. Antiepileptic Activity of Zonisamide on Hippocampal CA3 Neurons Does Not Depend on Carbonic Anhydrase Inhibition. *Epilepsy Res.* **2008**, *82* (1), 109.

(43) Schmidl, D.; Schmetterer, L.; Garhöfer, G.; Popa-Cherecheanu, A. Pharmacotherapy of Glaucoma. *J. Ocul. Pharmacol. Ther.* **2015**, *31* (2), 63–77.

(44) Supuran, C. T.; Altamimi, A. S. A.; Carta, F. Carbonic Anhydrase Inhibition and the Management of Glaucoma: A Literature and Patent Review 2013-2019. *Expert Opin. Ther. Pat.* **2019**, 1–12.

(45) Schehlein, E. M.; Novack, G.; Robin, A. L. New Pharmacotherapy for the Treatment of Glaucoma. *Expert Opinion on Pharmacotherapy*. 2017.

(46) Li, J.; Zhang, G.; Wang, X.; Li, X. F. Is Carbonic Anhydrase IX a Validated Target for Molecular Imaging of Cancer and Hypoxia? *Future Oncology*. 2015.

(47) Pastorek, J.; Pastorekova, S. Hypoxia-Induced Carbonic Anhydrase IX as a Target for Cancer Therapy: From Biology to Clinical Use. *Seminars in Cancer Biology*. 2015.

(48) Lendahl, U.; Lee, K. L.; Yang, H.; Poellinger, L. Generating Specificity and Diversity in the Transcriptional Response to Hypoxia. *Nat. Rev. Genet.* **2009**, *10* (12), 821–832.

(49) McDonald, P. C.; Dedhar, S. Carbonic Anhydrase IX (CAIX) as a Mediator of Hypoxia-Induced Stress Response in Cancer Cells BT - Carbonic Anhydrase: Mechanism, Regulation, Links to Disease, and Industrial Applications; Frost, S. C., McKenna, R., Eds.; Springer Netherlands: Dordrecht, 2014; pp 255–269.

(50) De Simone, G.; Supuran, C. T. Carbonic Anhydrase IX: Biochemical and Crystallographic Characterization of a Novel Antitumor Target. *Biochimica et Biophysica Acta - Proteins and Proteomics*. 2010.

(51) Supuran, C. T.; Alterio, V.; Di Fiore, A.; D'Ambrosio, K.; Carta, F.; Monti, S. M.; De Simone, G. Inhibition of Carbonic Anhydrase IX Targets Primary Tumors, Metastases, and Cancer Stem Cells: Three for the Price of One. *Med. Res. Rev.* **2018**, No. January, 1–38.

(52) Švastová, E.; Hulíková, A.; Rafajová, M.; Zaťovičová, M.; Gibadulinová, A.; Casini, A.; Cecchi, A.; Scozzafava, A.; Supuran, C. T.; Pastorek, J.; et al. Hypoxia Activates the Capacity of Tumor-Associated Carbonic Anhydrase IX to Acidify Extracellular PH. *FEBS Lett.* **2004**, *577* (3), 439–445.

(53) Nocentini, A.; Supuran, C. T. Carbonic Anhydrase Inhibitors as Antitumor/Antimetastatic Agents: A Patent Review (2008–2018). *Expert Opin. Ther. Pat.* **2018**, *28* (10), 729–740.

(54) Andreucci, E.; Ruzzolini, J.; Peppicelli, S.; Bianchini, F.; Laurenzana, A.; Carta, F.; Supuran, C. T.; Calorini, L. The Carbonic Anhydrase IX Inhibitor SLC-0111 Sensitises Cancer Cells to Conventional Chemotherapy. *J. Enzyme Inhib. Med. Chem.* **2019**, *34* (1), 117–123.

(55) Singh, S.; Lomelino, C.; Mboge, M.; Frost, S.; McKenna, R. Cancer Drug Development of Carbonic Anhydrase Inhibitors beyond the Active Site. *Molecules* **2018**, *23* (5), 1045.

(56) Supuran, C. T.; Scozzafava, A. Activation of Carbonic Anhydrase Isozymes BT - The Carbonic Anhydrases: New Horizons; Chegwidden, W. R., Carter, N. D., Edwards, Y. H., Eds.; Birkhäuser Basel: Basel, 2000; pp 197–219.

(57) Temperini, C.; Innocenti, A.; Scozzafava, A.; Mastrolorenzo, A.; Supuran, C. T. Carbonic Anhydrase Activators: L-Adrenaline Plugs the Active Site Entrance of Isozyme II, Activating Better Isoforms I, IV, VA, VII, and XIV. *Bioorganic Med. Chem. Lett.* **2007**.

(58) Clark, A. M.; Perrin, D. D. A Re-Investigation of the Question of Activators of Carbonic Anhydrase. *Biochem. J.* **1951**, *48* (4), 495 LP – 502.

(59) Nelson 1942-, D. L. (David L. *Lehninger Principles of Biochemistry*; Fourth edition. New York : W.H. Freeman, 2005., 2005.

(60) Mariño-Ramírez, L.; Kann, M. G.; Shoemaker, B. A.; Landsman, D. Histone Structure and Nucleosome Stability. *Expert Rev. Proteomics* **2005**, *2* (5), 719–729.

(61) Luger, K.; Mäder, A. W.; Richmond, R. K.; Sargent, D. F.; Richmond, T. J. Crystal Structure of the Nucleosome Core Particle at 2.8 Å Resolution. *Nature* **1997**, *389* (6648), 251–260.

(62) Mersfelder, E. L.; Parthun, M. R. The Tale beyond the Tail: Histone Core Domain Modifications and the Regulation of Chromatin Structure. *Nucleic Acids Res.* **2006**, *34* (9), 2653–2662.

(63) RUIJTER, A. J. M. de; GENNIP, A. H. van; CARON, H. N.; KEMP, S.; KUILENBURG, A. B. P. van. Histone Deacetylases (HDACs): Characterization of the Classical HDAC Family. *Biochem. J.* **2003**, *370* (3), 737–749.

(64) Ropero, S.; Esteller, M. The Role of Histone Deacetylases (HDACs) in Human Cancer. *Molecular Oncology*. 2007.

(65) Minucci, S.; Pelicci, P. G. Histone Deacetylase Inhibitors and the Promise of Epigenetic (and More) Treatments for Cancer. *Nat. Rev. Cancer* **2006**, *6*, 38.

(66) Hancock, W. W.; Akimova, T.; Beier, U. H.; Liu, Y.; Wang, L. HDAC Inhibitor Therapy in Autoimmunity and Transplantation. *Ann. Rheum. Dis.* **2012**, *71* (Suppl 2), i46 LP-i54.

(67) Valente, S.; Mai, A. Small-Molecule Inhibitors of Histone Deacetylase for the Treatment of Cancer and Non-Cancer Diseases: A Patent Review (2011-2013). *Expert Opinion on Therapeutic Patents*. 2014.

(68) Zhang, L.; Zhang, J.; Jiang, Q.; Zhang, L.; Song, W. Zinc Binding Groups for Histone Deacetylase Inhibitors. *Journal of Enzyme Inhibition and Medicinal Chemistry*. 2018.

(69) Suzuki, T.; Ando, T.; Tsuchiya, K.; Fukazawa, N.; Saito, A.; Mariko, Y.; Yamashita, T.; Nakanishi, O. Synthesis and Histone Deacetylase Inhibitory Activity of New Benzamide Derivatives. *J. Med. Chem.* **1999**.

(70) Liu, L.; Chen, B.; Qin, S.; Li, S.; He, X.; Qiu, S.; Zhao, W.; Zhao, H. A Novel Histone Deacetylase Inhibitor Chidamide Induces Apoptosis of Human Colon Cancer Cells. *Biochem. Biophys. Res. Commun.* **2010**.

(71) Clawson, G. A. Histone Deacetylase Inhibitors as Cancer Therapeutics. *Ann. Transl. Med. Vol 4, No 15 (August 2016) Ann. Transl. Med.* **2016**.

(72) Bieliauskas, A. V.; Pflum, M. K. H. Isoform-Selective Histone Deacetylase Inhibitors. *Chemical Society Reviews*. 2008.

(73) Supuran, C. T.; Winum, J.-Y. Selectivity Issues in the Design of CA Inhibitors. *Drug Design of Zinc-Enzyme Inhibitors*. August 3, 2009, pp 399–413.

(74) Shaquiquzzaman, M.; Verma, G.; Marella, A.; Akhter, M.; Akhtar, W.; Khan, M. F.; Tasneem, S.; Alam, M. M. Piperazine Scaffold: A Remarkable Tool in Generation of Diverse Pharmacological Agents. *Eur. J. Med. Chem.* **2015**, *102*, 487–529.

(75) Martino, M. V.; Guandalini, L.; Di Cesare Mannelli, L.; Menicatti, M.; Bartolucci, G.; Dei, S.; Manetti, D.; Teodori, E.; Ghelardini, C.; Romanelli, M. N. Piperazines as Nootropic Agents: New Derivatives of the Potent Cognition-Enhancer DM235 Carrying Hydrophilic Substituents. *Bioorg.*

Med. Chem. **2017**, *25* (6), 1795–1803.

(76) Guandalini, L.; Martino, M. V.; Di Cesare Mannelli, L.; Bartolucci, G.; Melani, F.; Malik, R.; Dei, S.; Floriddia, E.; Manetti, D.; Orlandi, F.; et al. Substituted Piperazines as Nootropic Agents: 2- or 3-Phenyl Derivatives Structurally Related to the Cognition-Enhancer DM235. *Bioorg. Med. Chem. Lett.* **2015**, *25* (8), 1700–1704.

(77) Guandalini, L.; Martini, E.; Di Cesare Mannelli, L.; Dei, S.; Manetti, D.; Scapecchi, S.; Teodori, E.; Ghelardini, C.; Romanelli, M. N. Influence of Ring Size on the Cognition-Enhancing Activity of DM235 and MN19, Two Potent Nootropic Drugs. *Bioorg. Med. Chem. Lett.* **2012**, *22* (5), 1936–1939.

(78) Sławiński, J.; Szafrański, K.; Vullo, D.; Supuran, C. T. Carbonic Anhydrase Inhibitors. Synthesis of Heterocyclic 4-Substituted Pyridine-3-Sulfonamide Derivatives and Their Inhibition of the Human Cytosolic Isozymes I and II and Transmembrane Tumor-Associated Isozymes IX and XII. *Eur. J. Med. Chem.* **2013**, *69*, 701–710.

(79) Congiu, C.; Onnis, V.; Deplano, A.; Balboni, G.; Dedeoglu, N.; Supuran, C. T. Synthesis of Sulfonamides Incorporating Piperazinyl-Ureido Moieties and Their Carbonic Anhydrase I, II, IX and XII Inhibitory Activity. *Bioorg. Med. Chem. Lett.* **2015**, *25* (18), 3850–3853.

(80) Congiu, C.; Onnis, V.; Deplano, A.; Balboni, G.; Ceruso, M.; Supuran, C. T. Synthesis and Carbonic Anhydrase I, II, IX and XII Inhibitory Activity of Sulfamates Incorporating Piperazinyl-Ureido Moieties. *Bioorg. Med. Chem.* **2015**, *23* (17), 5619–5625.

(81) Havránková, E.; Csöllei, J.; Vullo, D.; Garaj, V.; Pazdera, P.; Supuran, C. T. Novel Sulfonamide Incorporating Piperazine, Aminoalcohol and 1,3,5-Triazine Structural Motifs with Carbonic Anhydrase I, II and IX Inhibitory Action. *Bioorg. Chem.* **2018**, *77*, 25–37.

(82) Chiaramonte, N.; Bua, S.; Angeli, A.; Ferraroni, M.; Picchioni, I.; Bartolucci, G.; Braconi, L.; Dei, S.; Teodori, E.; Supuran, C. T.; et al. Sulfonamides Incorporating Piperazine Bioisosteres as Potent Human Carbonic Anhydrase I, II, IV and IX Inhibitors. *Bioorg. Chem.* **2019**, *91* (June), 103130.

(83) Huang, W. J.; Chen, C. C.; Chao, S. W.; Yu, C. C.; Yang, C. Y.; Guh, J. H.; Lin, Y. C.; Kuo, C. I.; Yang, P.; Chang, C. I. Synthesis and Evaluation of Aliphatic-Chain Hydroxamates Capped with Osthole Derivatives as Histone Deacetylase Inhibitors. *Eur. J. Med. Chem.* **2011**, *46* (9), 4042–4049.

(84) Ledaki, I.; McIntyre, A.; Wigfield, S.; Buffa, F.; McGowan, S.; Baban, D.; Li, J. liang; Harris, A. L. Carbonic Anhydrase IX Induction Defines a Heterogeneous Cancer Cell Response to Hypoxia and Mediates Stem Cell-like Properties and Sensitivity to HDAC Inhibition. *Oncotarget* **2015**.

(85) Bayat Mokhtari, R.; Baluch, N.; Ka Hon Tsui, M.; Kumar, S.; S. Homayouni, T.; Aitken, K.; Das, B.; Baruchel, S.; Yeger, H. Acetazolamide Potentiates the Anti-Tumor Potential of HDACi, MS-275, in Neuroblastoma. *BMC Cancer* **2017**.

(86) Datta, R.; Shah, G. N.; Rubbelke, T. S.; Waheed, A.; Rauchman, M.; Goodman, A. G.; Katze, M. G.; Sly, W. S. Progressive Renal Injury from Transgenic Expression of Human Carbonic Anhydrase IV Folding Mutants Is Enhanced by Deficiency of P58^{IPK} *Proc. Natl. Acad. Sci.* **2010**, *107* (14), 6448 LP – 6452.

(87) Shah, G. N.; Bonapace, G.; Hu, P. Y.; Strisciuglio, P.; Sly, W. S. Carbonic Anhydrase II Deficiency Syndrome (Osteopetrosis with Renal Tubular Acidosis and Brain Calcification): Novel Mutations in CA2 Identified by Direct Sequencing Expand the Opportunity for Genotype-Phenotype Correlation. *Hum. Mutat.* **2004**, *24* (3), 272.

(88) Briganti, F.; Mangani, S.; Orioli, P.; Scozzafava, A.; Vernaglione, G.; Supuran, C. T. Carbonic Anhydrase Activators: X-Ray Crystallographic and Spectroscopic Investigations for the Interaction of Isozymes I and II with Histamine,. *Biochemistry* **1997**, *36* (34), 10384–10392.

(89) Temperini, C.; Scozzafava, A.; Vullo, D.; Supuran, C. T. Carbonic Anhydrase Activators. Activation of Isozymes I, II, IV, VA, VII, and XIV with L- and D-Histidine and Crystallographic Analysis of Their Adducts with Isoform II: Engineering Proton-Transfer Processes within the Active Site of an Enzyme. *Chem. – A Eur. J.* **2006**, *12* (27), 7057–7066.

(90) Temperini, C.; Scozzafava, A.; Supuran, C. T. Carbonic Anhydrase Activators: The First X-Ray Crystallographic Study of an Adduct of Isoform I. *Bioorg. Med. Chem. Lett.* **2006**, *16* (19), 5152–5156.

(91) Scozzafava, A.; Briganti, F.; Mincione, G.; Menabuoni, L.; Mincione, F.; Supuran, C. T. Carbonic Anhydrase Inhibitors: Synthesis of Water-Soluble, Aminoacyl/Dipeptidyl Sulfonamides Possessing Long-Lasting Intraocular Pressure-Lowering Properties via the Topical Route. *J. Med. Chem.* **1999**, *42* (18), 3690–3700.

(92) Scozzafava, A.; Supuran, C. T. Carbonic Anhydrase Activators – Part 21. Novel Activators of Isozymes I, II and IV Incorporating Carboxamido and Ureido Histamine Moieties. *Eur. J. Med. Chem.* **2000**, *35* (1), 31–39.

(93) Briganti, F.; Scozzafava, A.; Supuran, C. T. Novel Carbonic Anhydrase Isozymes I, II and IV Activators Incorporating Sulfonyl-Histamino Moieties. *Bioorg. Med. Chem. Lett.* **1999**, *9* (14), 2043–2048.

(94) Akocak, S.; Lolak, N.; Vullo, D.; Durgun, M.; Supuran, C. T. Synthesis and Biological Evaluation of Histamine Schiff Bases as Carbonic Anhydrase I, II, IV, VII, and IX Activators. *J. Enzyme Inhib. Med. Chem.* **2017**, *32* (1), 1305–1312.

(95) Saada, M.-C.; Vullo, D.; Montero, J.-L.; Scozzafava, A.; Winum, J.-Y.; Supuran, C. T. Carbonic Anhydrase I and II Activation with Mono- and Dihalogenated Histamine Derivatives. *Bioorg. Med. Chem. Lett.* **2011**, *21* (16), 4884–4887.

(96) Ilies, M.; Banciu, M. D.; Ilies, M. A.; Scozzafava, A.; Caproiu, M. T.; Supuran, C. T. Carbonic Anhydrase Activators: Design of High Affinity Isozymes I, II, and IV Activators, Incorporating Tri-/Tetrasubstituted-Pyridinium-Azole Moieties. *J. Med. Chem.* **2002**.

(97) Temperini, C.; Scozzafava, A.; Puccetti, L.; Supuran, C. T. Carbonic Anhydrase Activators: X-Ray Crystal Structure of the Adduct of Human Isozyme II with l-Histidine as a Platform for the Design of Stronger Activators. *Bioorg. Med. Chem. Lett.* **2005**, *15* (23), 5136–5141.

(98) Temperini, C.; Scozzafava, A.; Vullo, D.; Supuran, C. T. Carbonic Anhydrase Activators, Activation of Isoforms I, II, IV, VA, VII, and XIV with L- and D-Phenylalanine and Crystallographic Analysis of Their Adducts with Isozyme II: Stereospecific Recognition within the Active Site of an Enzyme and Its Consequenc. *J. Med. Chem.* **2006**.

(99) Temperini, C.; Innocenti, A.; Scozzafava, A.; Supuran, C. T. Carbonic Anhydrase Activators: Kinetic and X-Ray Crystallographic Study for the Interaction of d- and l-Tryptophan with the Mammalian Isoforms I-XIV. *Bioorganic Med. Chem.* **2008**.

(100) Lipman, J. J.; Spencer, P. S. J. Further Evidence for a Central Site of Action for the Antinociceptive Effect of Clonidine-like Drugs. *Neuropharmacology* **1979**, *18* (8–9), 731–733.

(101) BOUSQUET, P.; GUERTZENSTEIN, P. G. Localization of the Central Cardiovascular Action of Clonidine. *Br. J. Pharmacol.* **1973**, *49* (4), 573–579.

(102) Huwyler, J.; Fricker, G.; Török, M.; Schneider, M.; Drewe, J. Transport of Clonidine Across Cultured Brain Microvessel Endothelial Cells. *J. Pharmacol. Exp. Ther.* **1997**, *282* (1), 81 LP – 85.

(103) Ghandour, M. S.; Langley, O. K.; Zhu, X. L.; Waheed, A.; Sly, W. S. Carbonic Anhydrase IV on Brain Capillary Endothelial Cells: A Marker Associated with the Blood-Brain Barrier. *Proc. Natl. Acad. Sci.* **1992**, *89* (15), 6823 LP – 6827.

(104) De Luca, L.; Ferro, S.; Damiano, F. M.; Supuran, C. T.; Vullo, D.; Chimirri, A.; Gitto, R. Structure-Based Screening for the Discovery of New Carbonic Anhydrase VII Inhibitors. *Eur. J. Med. Chem.* **2014**, *71*, 105–111.

(105) Canto de Souza, L.; Provensi, G.; Vullo, D.; Carta, F.; Scozzafava, A.; Costa, A.; Schmidt, S. D.; Passani, M. B.; Supuran, C. T.; Blandina, P. Carbonic Anhydrase Activation Enhances Object Recognition Memory in Mice through Phosphorylation of the Extracellular Signal-Regulated Kinase in the Cortex and the Hippocampus. *Neuropharmacology* **2017**, *118*, 148–156.

(106) Dardonville, C.; Rozas, I. Imidazoline Binding Sites and Their Ligands: An Overview of the Different Chemical Structures. *Medicinal Research Reviews*. 2004.

(107) Knaus, A.; Zong, X.; Beetz, N.; Jahns, R.; Lohse, M. J.; Biel, M.; Hein, L. Direct Inhibition of Cardiac Hyperpolarization-Activated Cyclic Nucleotide-Gated Pacemaker Channels by Clonidine. *Circulation* **2007**.

(108) Stable, H.; Daniel, H. Chemistry, Pharmacology, and Structure-Activity Relationships with a New Type of Imidazolines Exerting a Specific Bradycardic Action at a Cardiac Site. *J. Med. Chem.* **1980**.

(109) Vullo, D.; Innocenti, A.; Nishimori, I.; Scozzafava, A.; Kaila, K.; Supuran, C. T. Carbonic Anhydrase Activators: Activation of the Human Isoforms VII (Cytosolic) and XIV (Transmembrane) with Amino Acids and Amines. *Bioorganic Med. Chem. Lett.* **2007**.

(110) Vullo, D.; Nishimori, I.; Scozzafava, A.; Supuran, C. T. Carbonic Anhydrase Activators: Activation of the Human Cytosolic Isozyme III and Membrane-Associated Isoform IV with Amino Acids and Amines. *Bioorg. Med. Chem. Lett.* **2008**, *18* (15), 4303–4307.

(111) Gettys, K. E.; Ye, Z.; Dai, M. Recent Advances in Piperazine Synthesis. *Synthesis (Germany)*. Georg Thieme Verlag June 19, 2017, pp 2589–2604.

(112) Gerdes, J. M.; Bolstad, D. B.; Braden, M. R.; Barany, A. W. 1-[(2'substituted)Piperazin-1'-Yl)Isoquinolines as Norepinephrine Transporter Inhibitor Therapeutics and Positron Emission Tomography Imaging Agents. WO2008115593, 2008.

(113) Levy, D. E.; Smyth, M. S.; R.M., S. Piperazine and Homopiperazine Compounds. US2003153556.

(114) ZONGRU, G.; GUIFANG, C.; FENGMING, C. Sulfonyl-Containing 2,3-Diarylindole Compounds, Methods for Making Same, and Methods of Use Thereof. US2004058977 (A1), 2004.

(115) BENOITON, N. L. On the Side-reaction of N-alkylation of Amino Groups during Hydrogenolytic Deprotection in Alcohol-containing Solvents. *International Journal of Peptide and Protein Research*. 1993.

(116) Jain, A.; Huang, S. G.; Whitesides, G. M. Lack of Effect of the Length of Oligoglycine- and Oligo(Ethylene Glycol)-Derived Para-Substituents on the Affinity of Benzenesulfonamides for Carbonic Anhydrase II in Solution. *J. Am. Chem. Soc.* **1994**, *116* (12), 5057–5062.

(117) Pryde, D. C.; Corless, M.; Fenwick, D. R.; Mason, H. J.; Stammen, B. C.; Stephenson, P. T.; Ellis, D.; Bachelor, D.; Gordon, D.; Barber, C. G.; et al. The Design and Discovery of Novel Amide CCR5 Antagonists. *Bioorganic Med. Chem. Lett.* **2009**.

(118) Weber, F.; Brune, S.; Korpis, K.; Bednarski, P. J.; Laurini, E.; Dal Col, V.; Pricl, S.; Schepmann, D.; Wünsch, B. Synthesis, Pharmacological Evaluation, and Σ1 Receptor Interaction Analysis of Hydroxyethyl Substituted Piperazines. *J. Med. Chem.* **2014**, *57* (7), 2884–2894.

(119) Faler, C. A.; Joullié, M. M. Substituted Azabicyclo[3.1.0]Hexan-1-Ols from Aspartic and Glutamic Acid Derivatives via Titanium-Mediated Cyclopropanation. *Tetrahedron Lett.* **2008**, *49* (46), 6512–6513.

(120) Braga, C. B.; Ducati, L. C.; Rittner, R. Experimental and Theoretical Evaluation on the Conformational Behavior of L-Aspartic Acid Dimethyl Ester and Its N-Acetylated Derivative. *RSC Adv.* **2015**, *5* (23), 18013–18024.

(121) White, K. N.; Konopelski, J. P. Facile Synthesis of Highly Functionalized N-Methyl Amino Acid Esters without Side-Chain Protection. *Org. Lett.* **2005**, *7* (19), 4111–4112.

(122) Jida, M.; Ballet, S. An Efficient One-pot Synthesis of Chiral N-protected 3-substituted (Diketo)Piperazines via Ugi-4CR/De-boc/Cyclization Process. *ChemistrySelect* **2018**.

(123) Gao, Z.; Maloney, D. J.; Dedkova, L. M.; Hecht, S. M. Inhibitors of DNA Polymerase β: Activity and Mechanism. *Bioorg. Med. Chem.* **2008**, *16* (8), 4331–4340.

(124) SRINIVAS AKELLA, SATYA SURYA VI KACHHADIA, VIRENDRA MATHIYAZHAGAN, K.; THARA, SATHYA NARAYANA MANIKANDAN, L.; RAJAGOPAL, SRIRAM REDDY, G. O. New HDAC Inhibitors. WO2007113644 (A2), 2007.

(125) Jones, R. G.; Mann, M. J. New Methods of Synthesis of β-Aminoethylpyrazoles. *J. Am. Chem. Soc.* **1953**, *75* (16), 4048–4052.

(126) Buchholz, M.; Heiser, U.; Schilling, S.; Niestroj, A. J.; Zunkel, K.; Demuth, H. U. The First Potent Inhibitors for Human Glutaminyl Cyclase: Synthesis and Structure-Activity Relationship. *J. Med. Chem.* **2006**.

(127) Wright, W. B.; Press, J. B.; Chan, P. S.; Marsico, J. W.; Haug, M. F.; Lucas, J.; Tauber, J.; Tomcufcik, A. S. Thromboxane Synthetase Inhibitors and Antihypertensive Agents. 1. N-[(1H-Imidazol-1-Yl)Alkyl]Aryl Amides and N-[(1H-1,2,4-Triazol-1-Yl)Alkyl]Aryl Amides. *J. Med. Chem.* **1986**, *29* (4), 523–530.

(128) Strachan, J.-P.; O'Shea, D. F.; Balasubramanian, T.; Lindsey, J. S. Rational Synthesis of Meso-Substituted Chlorin Building Blocks. *J. Org. Chem.* **2000**, *65* (10), 3160–3172.

(129) Ancliff, R. A.; et Al. Novel Compounds. WO2003/82861 (A2), 2003.

(130) Gómez-SanJuan, A.; Botija, J. M.; Méndez, A.; Sotomayor, N.; Lete, E. C-N Bond Forming Reactions in the Synthesis of Substituted 2-Aminoimidazole Derivatives. *Arkivoc* **2013**, *2014* (2), 44–56.

(131) Aoyagi, N.; Endo, T. Synthesis of Five- and Six-Membered Cyclic Guanidines by Guanylation with Isothiouronium Iodides and Amines under Mild Conditions. *Synth. Commun.* **2017**, *47* (5), 442–448.

(132) Bucio-Cano, A.; Reyes-Arellano, A.; Correa-Basurto, J.; Bello, M.; Torres-Jaramillo, J.; Salgado-Zamora, H.; Curiel-Quesada, E.; Peralta-Cruz, J.; Avila-Sorrosa, A. Targeting Quorum Sensing by Designing Azoline Derivatives to Inhibit the N-Hexanoyl Homoserine Lactone-Receptor CviR: Synthesis as Well as Biological and Theoretical Evaluations. *Bioorg. Med. Chem.* **2015**, *23* (24), 7565–7577.

(133) Heinelt, U.; Schultheis, D.; Jäger, S.; Lindenmaier, M.; Pollex, A.; Beckmann, H. S. g. A Convenient Method for the Synthesis of 2-Amino Substituted Aza-Heterocycles from N,N′-Disubstituted Thioureas Using TsCl/NaOH. *Tetrahedron* **2004**, *60* (44), 9883–9888.

(134) ZHU BING, Y.; ZHANG, P.; WANG, L. H. W.; GOLDMAN, E. A.; LI, W.; ZUCKETT, J. BENZAMIDES AND RELATED INHIBITORS OF FACTOR XA. US201414175087 20140207.

(135) Waheed, A.; Sly, W. S. Membrane Associated Carbonic Anhydrase IV (CA IV): A Personal and Historical Perspective BT - Carbonic Anhydrase: Mechanism, Regulation, Links to Disease, and Industrial Applications; Frost, S. C., McKenna, R., Eds.; Springer Netherlands: Dordrecht, 2014; pp 157–179.

(136) Zhang, J.; Tsoi, H.; Li, X.; Wang, H.; Gao, J.; Wang, K.; Go, M. Y. Y.; Ng, S. C.; Chan, F. K. L.; Sung, J. J. Y.; et al. <Em>Carbonic Anhydrase IV</Em> Inhibits Colon Cancer Development by Inhibiting the Wnt Signalling Pathway through Targeting the WTAP–WT1–TBL1 Axis. *Gut* **2016**, *65* (9), 1482 LP – 1493.

(137) Barker, H.; Aaltonen, M.; Pan, P.; Vähätupa, M.; Kaipiainen, P.; May, U.; Prince, S.; Uusitalo-Järvinen, H.; Waheed, A.; Pastoreková, S.; et al. Role of Carbonic Anhydrases in Skin Wound Healing. *Exp. Mol. Med.* **2017**, *49* (5), e334–e334.

(138) Buemi, M. R.; Di Fiore, A.; De Luca, L.; Angeli, A.; Mancuso, F.; Ferro, S.; Monti, S. M.; Buonanno, M.; Russo, E.; De Sarro, G.; et al. Exploring Structural Properties of Potent Human Carbonic Anhydrase Inhibitors Bearing a 4-(Cycloalkylamino-1-Carbonyl)Benzenesulfonamide Moiety. *Eur. J. Med. Chem.* **2019**, *163*, 443–452.

(139) Day, J. A.; Cohen, S. M. Investigating the Selectivity of Metalloenzyme Inhibitors. *J. Med. Chem.* **2013**.

(140) Lomelino, C. L.; Supuran, C. T.; McKenna, R. Non-Classical Inhibition of Carbonic Anhydrase. *Int. J.*

Mol. Sci. **2016**, *17* (7).

(141) Di Fiore, A.; Maresca, A.; Supuran, C. T.; De Simone, G. Hydroxamate Represents a Versatile Zinc Binding Group for the Development of New Carbonic Anhydrase Inhibitors. *Chem. Commun.* **2012**.

(142) Marques, S. M.; Nuti, E.; Rossello, A.; Supuran, C. T.; Tuccinardi, T.; Martinelli, A.; Santos, M. A. Dual Inhibitors of Matrix Metalloproteinases and Carbonic Anhydrases: Iminodiacetyl-Based Hydroxamate-Benzenesulfonamide Conjugates. *J. Med. Chem.* **2008**.

(143) Scozzafava, A.; Supuran, C. T. Carbonic Anhydrase and Matrix Metalloproteinase Inhibitors: Sulfonylated Amino Acid Hydroxamates with MMP Inhibitory Properties Act as Efficient Inhibitors of CA Isozymes I, II, and IV, and N-Hydroxysulfonamides Inhibit Both These Zinc Enzymes. *J. Med. Chem.* **2000**, *43* (20), 3677–3687.

(144) Merz, K. M.; Banci, L. Binding of Bicarbonate to Human Carbonic Anhydrase II: A Continuum of Binding States. *J. Am. Chem. Soc.* **1997**.

(145) Vullo, D.; Nishimori, I.; Innocenti, A.; Scozzafava, A.; Supuran, C. T. Carbonic Anhydrase Activators: An Activation Study of the Human Mitochondrial Isoforms VA and VB with Amino Acids and Amines. *Bioorganic Med. Chem. Lett.* **2007**.

(146) Angeli, A.; Chiaramonte, N.; Manetti, D.; Romanelli, M. N.; Supuran, C. T. Investigation of Piperazines as Human Carbonic Anhydrase I, II, IV and VII Activators. *J. Enzyme Inhib. Med. Chem.* **2018**.

(147) Stams, T.; Nair, S. K.; Okuyama, T.; Waheed, A.; Sly, W. S.; Christianson, D. W. Crystal Structure of the Secretory Form of Membrane-Associated Human Carbonic Anhydrase IV at 2.8-Å Resolution. *Proc. Natl. Acad. Sci. U. S. A.* **1996**, *93* (24), 13589–13594.

(148) Angeli, A.; Trallori, E.; Ferraroni, M.; Di Cesare Mannelli, L.; Ghelardini, C.; Supuran, C. T. Discovery of New 2, 5-Disubstituted 1,3-Selenazoles as Selective Human Carbonic Anhydrase IX Inhibitors with Potent Anti-Tumor Activity. *Eur. J. Med. Chem.* **2018**, *157*, 1214–1222.

(149) Angeli, A.; Tanini, D.; Capperucci, A.; Malevolti, G.; Turco, F.; Ferraroni, M.; Supuran, C. T. Synthesis of Different Thio-Scaffolds Bearing Sulfonamide with Subnanomolar Carbonic Anhydrase II and IX Inhibitory Properties and X-Ray Investigations for Their Inhibitory Mechanism. *Bioorg. Chem.* **2018**, *81*, 642–648.

(150) Marshall, A. G.; Hendrickson, C. L. High-Resolution Mass Spectrometers. *Annu. Rev. Anal. Chem.* **2008**, *1* (1), 579–599.

(151) Huang, L.; Kerns, R. J. Diversity-Oriented Chemical Modification of Heparin: Identification of Charge-Reduced N-Acyl Heparin Derivatives Having Increased Selectivity for Heparin-Binding Proteins. *Bioorg. Med. Chem.* **2006**, *14* (7), 2300–2313.

(152) Jain, A.; Huang, S. G.; Whitesides, G. M. Lack of Effect of the Length of Oligoglycine- and Oligo(Ethylene Glycol)-Derived Para-Substituents on the Affinity of Benzenesulfonamides for Carbonic Anhydrase II in Solution. *J. Am. Chem. Soc.* **1994**, *116* (12), 5057–5062.

(153) Chapman, K. T.; Dinnell, K.; Elliott, J. M.; Hollingworth, D.E. Hutchins, G. J.; Shaw, S. M.; Willoughby, C. A. 2-Aryl Indole Derivative as Antagonists of Tachykinins. US6518273 (B1), 2003.

(154) Ashweek, N. J.; Coldham, I.; Haxell, T. F. N.; Howard, S. Preparation of Diamines by Lithiation-Substitution of Imidazolidines and Pyrimidines. *Org. Biomol. Chem.* **2003**.

(155) Lee, H.-Y.; An, K.-M.; Jung, J.; Koo, J.-M.; Kim, J.-G.; Yoon, J.-M.; Lee, M.-J.; Jang, H.; Lee, H.-S.; Park, S.; et al. Identification of Novel Aminopiperidine Derivatives for Antibacterial Activity against Gram-Positive Bacteria. *Bioorg. Med. Chem. Lett.* **2016**, *26* (13), 3148–3152.

(156) Obreque-Balboa, J. E.; Sun, Q.; Bernhardt, G.; König, B.; Buschauer, A. Flavonoid Derivatives as Selective ABCC1 Modulators: Synthesis and Functional Characterization. *Eur. J. Med. Chem.* **2016**, *109*, 124–133.

(157) Flanagan, J. U.; Atwell, G. J.; Heinrich, D. M.; Brooke, D. G.; Silva, S.; Rigoreau, L. J. M.; Trivier, E.; Turnbull, A. P.; Raynham, T.; Jamieson, S. M. F.; et al. Morpholylureas Are a New Class of Potent and Selective Inhibitors of the Type 5 17-β-Hydroxysteroid Dehydrogenase (AKR1C3). *Bioorg. Med. Chem.* **2014**, *22* (3), 967–977.

(158) Perez, M.; Lamothe, M.; Maraval, C.; Mirabel, E.; Loubat, C.; Planty, B.; Horn, C.; Michaux, J.; Marrot, S.; Letienne, R.; et al. Discovery of Novel Protease Activated Receptors 1 Antagonists with Potent Antithrombotic Activity in Vivo. *J. Med. Chem.* **2009**, *52* (19), 5826–5836.

(159) Palimkar, S. S.; More, V. S.; Kumar, P. H.; Srinivasan, K. V. Synthesis of an Indole Containing KDR Kinase Inhibitor by Tandem Sonogashira Coupling-5-Endo-Dig-Cyclization as a Key Step. *Tetrahedron* **2007**.

(160) Belyankin, Andrei V Duplantier, Allen Jacob Zhang, L.; O'Donnell, C. J.; Rogers, B. N.; Vincent, L. A.; Sviridov, S. I. AZABENZOXAZOLES FOR THE TREATMENT OF CNS DISORDERS. WO2006051410.

(161) Schrader, T. O.; Zhu, X.; Kasem, M.; Li, S.; Liu, C.; Ren, A.; Wu, C.; Semple, G. Asymmetric Syntheses of (R)-4-Halo-6,6a,7,8,9,10-Hexahydro-5H-Pyrazino[1,2-a][1,n]Naphthyridines, Important 5-HT2C Agonist Precursors. *Tetrahedron Lett.* **2018**, *59* (21), 2030–2033.

(162) Aicher, Thomas Daniel; Chen, Z.; Chen, Y.; Faul, Margaret Mary; Krushinski, Joseph Herman, J.; Le Huerou, Yvan; Pineiro-Nunez, Marta Maria; Rocco, Vincent Patrick; Ruley, Kevin Michael; Schaus, John Mehnert; Thompson, Dennis Charles; Tupper, D. E. PIPERAZINE SUBSTITUTED ARYL BENZODIAZEPINES AND THEIR USE AS DOPAMINE RECEPTOR ANTAGONISTS FOR THE TREATMENT OF PSYCHOTIC DISORDERS. WO03082877.

(163) Williams, T. M.; Ciccarone, T. M.; MacTough, S. C.; Bock, R. L.; Conner, M. W.; Davide, J. P.; Hamilton, K.; Koblan, K. S.; Kohl, N. E.; Kral, A. M.; et al. 2-Substituted Piperazines as Constrained Amino Acids. Application to the Synthesis of Potent, Non Carboxylic Acid Inhibitors of Farnesyltransferase [1]. *J. Med. Chem.* **1996**.

(164) Chu-Farseeva, Y. yi; Mustafa, N.; Poulsen, A.; Tan, E. C.; Yen, J. J. Y.; Chng, W. J.; Dymock, B. W. Design and Synthesis of Potent Dual Inhibitors of JAK2 and HDAC Based on Fusing the Pharmacophores of XL019 and Vorinostat. *Eur. J. Med. Chem.* **2018**.

(165) Gros, L.; Lorente, S. O.; Jimenez; Yardley, V.; Rattray, L.; Wharton, H.; Little, S.; Croft, S. L.; Ruiz-Perez, L. M.; Gonzalez-Pacanowska, D.; et al. Evaluation of Azasterols as Anti-Parasitics. *J. Med. Chem.* **2006**, *49* (20), 6094–6103.

(166) Ashwell, M. A.; Tandon, M.; Namdew, Nivedita D, Lapierre, J. M.; Liu, Y.; Wu Hui, N. HDAC INHIBITORS. WO2009026446.

(167) Rodrigues, N.; Bennis, K.; Vivier, D.; Pereira, V.; C. Chatelain, F.; Chapuy, E.; Deokar, H.; Busserolles, J.; Lesage, F.; Eschalier, A.; et al. Synthesis and Structure–Activity Relationship Study of Substituted Caffeate Esters as Antinociceptive Agents Modulating the TREK-1 Channel. *Eur. J. Med. Chem.* **2014**, *75*, 391–402.

(168) Macor, J. E.; Ordway, T.; Smith, R. L.; Verhoest, P. R.; Mack, R. A. Synthesis and Use of 5-Vinyl-1,2,4-Oxadiazoles as Michael Acceptors. A Rapid Synthesis of the Potent Muscarinic Agonist L-670,548. *J. Org. Chem.* **1996**, *61* (10), 3228–3229.